

ODEEP



The Japanese Society
of Conservative Dentistry

Operative
Dentistry,
Endodontology
and
Periodontology



Vol.3 No.1
2023 December

ISSN 2436-4975





NEO DENTAL CHEMICAL
PRODUCTS CO., LTD.



カタログ PDF



添付文書 PDF

NEW

覆髄+裏層 2in1

素材の品質も
性能の一部です。

1本で覆髄から裏層まで！

DirectCapping+BaseLiner CAVIOS with MTA

- 1本で直接覆髄から裏層まで
- デンティンブリッジ形成促進
- ALP活性に最適なpH
- HAPによるマイクロシール効果
- ネオホワイトピュア® 配合

ALP：アルカリフォスファターゼ
HAP：ハイドロキシアパタイト



高い操作性を有するキャビオスがMTA系製材として生まれかわりました。スムーズで切れが良く、歯質へのなじみが高いペーストに、MTA系成分「ネオホワイトピュア®」を配合。MTAの効果発現を促す新処方により光重合裏層材としての理工学的性質に加え、直接覆髄材としての性能を獲得しました。1本で覆髄にも裏層にも使える2in1製材です。

MTA系覆髄+裏層材

D-Cavios® MTA

ネオホワイトピュア® 配合

1.5g入シリンジ 1本
先端チップ 15本
標準価格 6,500円

D-キャビオス®MTA

医療機器認証番号 304ADBZX00054000
歯科用覆髄材料(歯科裏層用高分子系材料)
管理医療機器

製造販売業者



ネオ製薬工業株式会社

〒150-0012 東京都渋谷区広尾3丁目1番3号
Tel. 03-3400-3768(代) Fax. 03-3499-0613

「ネオホワイトピュア」は太平洋セメント株式会社の登録商標第 6125963 号です。

Super Low

NEW

1色^{*}で天然歯色に親和するフロアブルCR

※白歯部の場合

Low

High

NEW

クリアフィル[®] マジェスティ[®] ES フロー-

Super Low

Low

High

Universal

なぜ色が親和するのか？物性は？操作性は？詳しい特長は特設サイトへ！ →



単品 クリアフィル[®] マジェスティ[®] ES フロー-

Universal

管理医療機器 歯科充填用コンポジットレジン 医療機器認証番号：224ABBZX00170000

○本品は、袋包装です。

Super Low

- レジン充填材
(Super Low) (U, UD) 各2.7g (1.5mL)
- 付属品 ニードルチップ (N)(5個)
ニードルチップキャップ (5個)



Low

- レジン充填材
(Low) (U, UD, UOP, UW) 各2.7g (1.5mL)
- 付属品 ニードルチップ (N)(5個)
ニードルチップキャップ (5個)



High

- レジン充填材
(High) (U, UD, UOP) 各2.7g (1.5mL)
- 付属品 ニードルチップ (N)(5個)
ニードルチップキャップ (5個)



クラレノリタケ デンタル株式会社

〒100-0004 東京都千代田区大手町2丁目6-4 常盤橋タワー

お問い合わせ | ☎ 0120-330-922 月曜～金曜 10:00～17:00

ホームページ | www.kuraraynoritake.jp

- 仕様及び外観は、製品改良のため予告無く変更することがありますので、予めご了承ください。
- 印刷のため実際の色調と異なる場合があります。
- ご使用に際しましては添付文書を必ずお読みください。

【製造販売元】クラレノリタケデンタル株式会社 【販売元】株式会社モリタ
〒959-2653 新潟県胎内市倉敷町2-28 〒564-8650 大阪府吹田市垂水町3-33-18 お客様相談センター：0800-222-8020 (医療従事者様向窓口)

・「クリアフィル」及び「マジェスティ」は株式会社クラレの登録商標です。

CAD/CAM 活用による 歯冠修復治療

メタルフリーの歴史と展望

詳細は
2次元コードの
リンク先から!

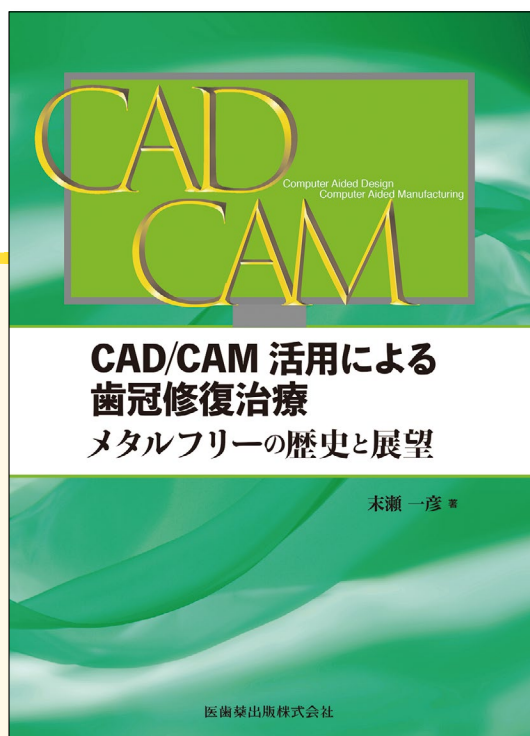


■ B5判/136頁/カラー ■ 定価 8,800円(本体 8,000円+税10%)
■ ISBN978-4-263-44690-4 ■ 注文コード: 446900

末瀬一彦 著

金属修復を脱却して、 メタルフリーの 歯冠修復治療へ

- CAD/CAM 冠の保険導入から9年。保険導入の経緯と臨床適用の現状を紹介するとともに、CAD/CAM 冠の臨床応用上の留意点(支台歯形成、研磨、接着操作など)を網羅的に解説。
- ジルコニア修復についても、その特徴や臨床応用のポイントをわかりやすく示しています。
- その他、歯科における CAD/CAM システムの展望やデジタル化の課題、歯科技工士の将来など、永年にわたって研究・教育・臨床に携わってきた著者の思いの丈がこもった渾身の一冊です。



掲載内容(目次より)

- 01 序論
- 02 金属修復物の課題
- 03 CAD/CAM 冠の保険導入
- 04 CAD/CAM 冠の臨床応用上の留意点
- 05 ジルコニアの歯冠修復への応用
- 06 ファイバーポストの正しい使用方法

- 07 歯科用 CAD/CAM システムの開発・現状・展望
- 08 歯科技工の現状と展望
- 09 これからの歯科医療
～「9028」の実現を目指して～
- 10 おわりにあたって

OPERATIVE DENTISTRY, ENDODONTOLOGY AND PERIODONTOLOGY

Vol. 3, No. 1

DECEMBER 2023

CONTENTS

Original Articles

- Effect of Apical Limit Settings on the Occurrence of Apical Dentinal Microcracks
in Procedures up to Root-end Filling
.....Shuntaro NAKAYAMA, Taro NISHIDA, Miki SEKIYA, Munehiro MAEDA and Masaru IGARASHI (1)
- Differentiation of Murine Enamel Organ-derived Tissue Stem Cells
into Cementoblasts after Transplantation
.....Minoru TAKASE, Naoki MARUO, Kazuhiko OKAMURA, Nanako TSUCHIMUCHI, Hiroaki YAMATO,
Kimiko OHGI, Atsushi NAGAI, Takashi KANEKO, Yasunori YOSHINAGA and Ryuji SAKAGAMI (12)
- Five-year Prognosis and Risk Factor Analysis of Open Flap Debridement for Older People
.....Yukari AOKI-NONAKA, Takahiro HOKARI, Yumi MATSUKAWA, Keisuke SATO, Miki HARA,
Mai TAKEUCHI, Kei TAKAMISAWA, Kyoko YAMAZAKI, Takahiro TSUZUNO, Hikaru TAMURA,
Takumi HIYOSHI, Fumiya MEGURO, Emi HOSHIKAWA, Aoi MATSUGISHI, Chihiro KANEKO,
Shuhei MINEO, Moe YAMASHITA and Koichi TABETA (22)
- Shaping Ability of Controlled Memory Wire Nickel-titanium Files by Minimally Invasive Endodontics
.....Pil Seoung KANG, Takahito TSUKUDA, Kazuhiro ITONAGA,
Masahito YAMANE, Noriko MUTOH and Nobuyuki TANI-ISHII (35)
- Discoloration of Conventional Resin Composite Cements and Self-adhesive
Resin Cements Immersed in Water for 180 Days
.....Ayaka HORI-ISHIKAWA, Yuka OGAWA-UZAWA, Ayako OKADA, Daichi AIZAWA, Nana SAKAEDA-NAITO,
Hiro MATSUMOTO, Kaoru OHMORI, Masao HANABUSA and Takatsugu YAMAMOTO (43)
- Comparison of Shaping Ability between Nickel-titanium Hand Files
and Nickel-titanium Rotary Files during Glide path
.....Masashi YAMADA, Norio KASAHARA, Satoru MATSUNAGA, Tomoyuki INOSE, Hiroki IWASAWA,
Ryo NAKAJIMA, Yoshiki TAMIYA and Masahiro FURUSAWA (52)
- Influence of Additional Insertion after Reaching the Working Length on Root Canal
Transportation and Extrusion of the Gutta-percha Point in Five Ni-Ti Rotary File Systems
with Different Bending Properties
.....Fumiyasu MURAYAMA, Hirokazu SUGITA, Miki SEKIYA, Keisuke SAIGUSA,
Taro NISHIDA, Munehiro MAEDA and Masaru IGARASHI (59)
- Clinical Assessment of Root Caries Treatment Based on the Discoloration
of Silver Diamine Fluoride as a Caries Indicator
.....Yuki MURASE, Hanemi TSURUTA, Tomohiro TAKAGAKI, Shusuke KUSAKABE,
Masaomi IKEDA, Michael F BURROW and Toru NIKAIDO (73)
- The Effects of Dietary pH Changes on Tooth Staining of the Enamel Surface
.....Hiroki SUGITO, Takako EGUCHI, Rika TANAKA, Akiko HARUYAMA and Takashi MURAMATSU (80)
- Evaluation of the Hardness of Infected Root Canal Dentin with Fluorescence Excitation
.....Shuya SHIBANO, Mie MAYERS, Tokuji HASEGAWA, Takashi TAKAKI and Katsuhiko ISATSU (86)

Published
by
THE JAPANESE SOCIETY OF CONSERVATIVE DENTISTRY (JSCD)
c/o Oral Health Association of Japan (Kōkūhoken kyōkai)
1-43-9, Komagome, Toshima-ku, Tokyo 170-0003
Japan

Effect of an MDP-based Cleaner on Adhesion to Dentin Contaminated with a Temporary Luting CementTaiho IDONO, Shojiro SHIMIZU, Tomohiro TAKAGAKI, Michael F. BURROW and Toru NIKAIDO	(95)
Color Evaluation of Porcelain Laminate Veneer Restorations Bonded with a Single-shade Resin CompositeToshinari TOYAMA, Mikihiro KOBAYASHI, Rintaro SUGAI, Yuiko NIIZUMA and Atsufumi MANABE	(104)
Comparison of Root Canal Preparation Ability of Three Gold Wire-based NiTi Rotary File Systems in Simulated Curved Root CanalsMiki SEKIYA, Shuntaro NAKAYAMA, Fumiyasu MURAYAMA, Kentaro FURUTA, Yoshiyuki INUYAMA, Munehiro MAEDA, Kazuo KITAMURA and Masaru IGARASHI	(113)
2-deoxy-D-glucose Inhibits Cell Activity by Inhibiting Intracellular Glucose Metabolism in Human Gingival FibroblastsYoichiro TAGUCHI, Hirohito KATO, Runbo LI, Tsurayuki TAKAHASHI, Daisuke KIMURA, Kosho KASHITANI, Niina MASU, Hitoshi AZUMA, Chizuko OGATA and Makoto UMEDA	(121)
Development and Clinical Evaluation of Anti-Aspiration Gauze Roll Assessment of Water Absorbency and Usability of Gauze Roll—An Exploratory StudyChiharu KAWAMOTO, Ryotaro YAGO, Mai FUKUYAMA, Toru TANAKA, Hidehiko SANO and Atsushi TOMOKIYO	(129)
Three-dimensional Analysis of the Shaping Characteristics and Ability of a Novel Ni-Ti Rotary FileKazuma MATSUMOTO, Haruna HIROSE, Kota ISSHI, Seishiro FUJIMASA, Shingo KANEMARU, Tsukasa YANAGI and Etsuko MATSUZAKI	(137)
Inhibition of Intracellular Glucose Metabolism by 2-deoxyglucose Suppresses Proliferation and Differentiation of Mouse Osteoblast-like CellsHirohito KATO, Yoichiro TAGUCHI, Runbo LI, Chiaki MANDAI, Masahiro NOGUCHI, Kei SHIOMI, Hideki AKIMOTO, Sho MIZUTANI, Tomoko KANDA, Chizuko OGATA and Makoto UMEDA	(144)

Case Report

Risk of an Immediate-type Allergy to Minocycline Hydrochloride OintmentMaki HOSOKI, Yoshifumi OKAMOTO, Toyoko TAJIMA, Mayu MIYAGI, Yoshiaki KUBO, Maiko SOGAWA, Resmi RAJU, Shaista AFROZ and Yoshizo MATSUKA	(152)
---	---------

Editorial Board of Operative Dentistry, Endodontology and Periodontology

Editor-in-Chief

Hideki SHIBA

Graduate School of Biomedical and Health Sciences, Hiroshima University

Associate Editor

Yoshihiro NISHITANI

Kagoshima University Graduate School of Medical and Dental Sciences

Editorial Board

Atsushi KAMEYAMA

Matsumoto Dental University

Motohiro KOMAKI

Kanagawa Dental University Faculty of Dentistry

Keiso TAKAHASHI

Ohu University School of Dentistry

Osamu TAKEICHI

Nihon University School of Dentistry

Mamoru NODA

School of Dentistry, Iwate Medical University

Yasushi FURUICHI

School of Dentistry, Health Sciences University of Hokkaido

Keiichi HOSAKA

Tokushima University Graduate School of Biomedical Sciences

Takahiko MOROTOMI

School of Dentistry, Aichi Gakuin University

Kunihiko YOSHIBA

Niigata University Graduate School of Medical and Dental Sciences

Atsutoshi YOSHIMURA

Nagasaki University Graduate School of Biomedical Sciences

Masahiro YONEDA

Fukuoka Dental College

Editorial Secretary

Katsuhiko TAKEDA

Graduate School of Biomedical and Health Sciences, Hiroshima University

Effect of Apical Limit Settings on the Occurrence of Apical Dentinal Microcracks in Procedures up to Root-end Filling

Shuntaro NAKAYAMA, Taro NISHIDA, Miki SEKIYA, Munehiro MAEDA and Masaru IGARASHI

Department of Endodontics, The Nippon Dental University School of Life Dentistry at Tokyo

Abstract

Purpose: In this study, teeth in which root canal shaping was performed with different apical limit settings were used to clarify the timing of development of apical dentinal microcracks (microcracks). The microcracks occurring during root canal shaping were observed using micro-computed tomography (micro-CT). Root canal obturation of the experimental teeth was followed by root-end resection and cavity preparation for the same teeth, and the occurrence of microcracks on the resected root surfaces was evaluated.

Methods: Nineteen human-extracted mandibular canines and premolars with similar root morphology were used. Root planting models with exposed apex (test piece) were prepared for the teeth. Once a tooth was removed, micro-CT scanning was performed before the procedure. The apical limits were set in three groups (n=6): at the anatomical apical foramen (Af), at 1 mm inner Af (Af-1), and at 1 mm outer Af (Af+1). After root canal shaping with nickel-titanium rotary files under wetting, micro-CT scans were performed, and the presence of a microcrack was evaluated in each image. After root canal obturation, the apex was resected perpendicularly to the tooth axis using carbide burs at 3 mm from the apex. The resected root surfaces were stained with methylene blue solution, and stereomicroscopic observation was performed under light-emitting diode (LED) transillumination to record the occurrence and direction of microcracks. The length of microcracks from the root canal wall was also measured. Following these observations, 3 mm depth root-end cavities were prepared along the root canal axis using an ultrasonic tip. Subsequently, staining and transillumination observations were performed using the preview method, and the occurrence and direction of microcracks on the resected root surface were recorded. The length of microcracks from the wall of the root-end cavity was also measured.

Results: Micro-CT images demonstrated no new microcracks during root canal shaping. After root-end resection, the number and length of microcracks increased in the order of the Af-1, Af and Af+1 groups. After root-end cavity preparation, the detected incomplete cracks ran in the labiolingual direction and the complete crack ran in the mesiodistal direction. Furthermore, the length of microcracks after root-end cavity preparation was significantly greater in the Af+1 group than in the Af-1 group ($p < 0.05$).

Conclusion: The results suggest that root canal shaping with apical limit settings outside the root causes thinning of the dentin and increases the probability of microcracks during ultrasonic root-end cavity preparation.

Key words: apical limit settings, apical dentinal microcrack, root-end cavity preparation

Corresponding author: Shuntaro NAKAYAMA, Department of Endodontics, The Nippon Dental University School of Life Dentistry at Tokyo, 1-9-20, Fujimi, Chiyoda-ku, Tokyo 102-8159, Japan

TEL: +81-3-3261-5698, FAX: +81-3-5216-3718, E-mail: s-nakayama2119004@tky.ndu.ac.jp

Received for Publication: December 9, 2022/Accepted for Publication: January 6, 2023

J-STAGE advance published date: October 12, 2023

DOI: 10.11471/odep.2023-001

Introduction

The aim of root canal treatment is to obtain a proper prognosis through proper root canal shaping, disinfection and obturation¹⁻⁴. Root canal shaping is performed to ensure mechanical cleaning and the provision of proper morphology for root canal obturation⁵. In this case, mechanical root canal shaping with instruments should be limited to apical constriction^{6,7}. It has been reported that if the apical limits are incorrectly set beyond the length of the tooth, excessive instrumentation can occur, leading to the development of microcracks^{8,9}. These microcracks are the starting points of fractures. They gradually develop into vertical root fractures owing to the repeated application of occlusal force during mastication¹⁰⁻¹². A vertical root fracture is the most common cause of tooth extraction; hence, it is important to protect against root fracture¹³. In cases with poor response to nonsurgical root canal treatments, endodontic surgery should be used to remove the cause of the periapical lesions. In particular, root-end resection and filling can reliably remove the lesion and closely seal the root canal at the apex¹⁴⁻¹⁶. In recent years, ultrasonic tips have been used for root-end cavity preparation¹⁷. Compared with the conventional method of using a round bur attached to a micro-motor handpiece, it is possible to prepare root-end cavities along the long axis of the tooth with less risk of perforation^{18,19}. However, microcracks may occur during root-end cavity preparation²⁰.

Previous reports on the occurrence of microcracks at the root apex have been evaluated based on the apical limit settings of the root canal shaping; however, no study has evaluated the effect of root-end resection and ultrasonic root-end cavity preparation on microcracks^{8,21-24}. Therefore, in this study, teeth in which root canal shaping was performed with different apical limit settings were used to clarify the timing of microcrack development. The microcracks occurring during root canal shaping were observed and evaluated nondestructively and longitudinally using micro-computed tomography (micro-CT). The root canal obturation of the experimental tooth was followed by root-end resection and ultrasonic root-end cavity preparation for the same teeth, and the occurrence of microcracks on the resected root surfaces was evaluated.

Materials and Methods

Nineteen human-extracted mandibular canines and premolars with similar root morphology, which had been preserved underwater after extraction, were used in the experiment. The teeth had no caries or restorations in the root region and were not endodontically treated. The use of human-extracted teeth was approved by the Ethical Committee of The Nippon Dental University School of Life Dentistry at Tokyo (NDU-T2021-25).

All endodontic procedures were completed by a dentist (with 5 years of clinical experience).

1. Experiment I : Effect of over-instrumentation on the roots during root canal shaping

1) Preparation of a root planting model with the apex exposed

After removing the calculus and soft tissues on the root surface with a Gracey curette (Hu-Friedy, Chicago, IL, USA), the root surface was covered with a single layer of aluminum foil. An acrylic tube with an inner diameter of 16 mm and a height of 12 mm was filled with auto-polymerizing resin (Ostron II, GC, Tokyo, Japan) and implanted so that the tooth axis was as vertical as possible. After the auto-polymerizing resin had cured, the tooth with the aluminum foil was removed. To ensure the adherence of a soft material corresponding to the periodontal ligament to the tooth when the tooth was reimplanted, an adhesive material (Fusion II adhesive, GC) was applied to the inner surface of the auto-polymerizing resin. After drying, a self-wetting hybrid polysiloxane impression material (Fusion II extra wash type, GC) was filled, and the tooth was immediately reimplanted²⁵. After the impression material was cured, the tooth was removed, and the basal 3 mm of the tube and resin were polished and removed under water cooling using silicon carbide grinding paper (#80 and #400, Buehler, Lake Bluff, IL, USA). After the root planting models (test piece) were prepared to expose 3 mm of the root apex (Fig. 1), the roots of the teeth were cut under water cooling perpendicular to the tooth axis at 12 mm from the root apex using a low-speed saw (Isomet LS, Buehler).

2) Micro-CT scanning before root canal shaping

Each test piece was scanned using a micro-CT (ScanXmate-D100SS270, Comscantecno, Kanagawa,

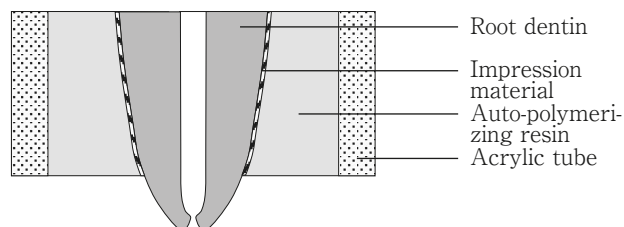


Fig. 1 Cross-sectional image of test piece

Japan), from the root apex to 6 mm under the conditions of $10.332\ \mu\text{m}/\text{pixel}$ at 80 kV and $80\ \mu\text{A}$. The images were used as control images before root canal shaping.

3) Determination of working length

A #10 stainless steel hand K file (MANI, Tochigi, Japan) was inserted into the canal to confirm patency. After confirming patency, a #10 K file was inserted into the canal until the file tip was visible in the anatomical apical foramen and the length from the coronal reference plane to the tip of the file was measured. The experimental teeth were divided into three groups ($n=6$): the apical limits were set at the anatomical apical foramen (Af), at 1 mm inner anatomical apical foramen (Af-1), and at 1 mm outer anatomical apical foramen (Af+1).

4) Root canal shaping

Root canal shaping was performed using nickel-titanium rotary files (ProTaper Gold, Dentsply Sirona, Ballaigues, Switzerland) attached to an endodontic torque control motor (X-Smart IQ, Dentsply Sirona). ProTaper Gold was used because of its improved resistance to cyclic fatigue and flexibility compared to conventional nickel-titanium rotary files^{26,27}. At first, a glide path was created using ProGlider (#16/.02, Dentsply Sirona). Subsequently, the preflaring was done using SX (#19/.04) to the coronal third. Root canal shaping was performed in the following order until the set working length was achieved: S1 (#18/.02), S2 (#20/.04), F1 (#20/.07), F2 (#25/.08), F3 (#30/.09) and F4 (#40/.06). During root canal shaping, a 2.5 ml syringe (Terumo syringe, Terumo, Tokyo, Japan) with a 27 G needle (Jet Needle Straight type, B. S. A. Sakurai, Nagoya, Japan) was used to frequently irrigate the canal with 3% sodium hypochlorite solution (NaClO: ChlorCid, Ultradent, South Jordan, UT, USA) and patency was maintained with a #10 K file. During root canal shaping, the root apex of the test piece was continuously moistened

with water²⁸). Afterwards, an 18% ethylenediaminetetracetic acid solution (Ultradent EDTA 18%, Ultradent) was applied for 1 min. and the canal was irrigated again with NaClO. The root canal was dried with paper points (ProTaper Gold Absorbent Point, Dentsply Sirona). Micro-CT scans were obtained after root canal shaping, under the same conditions as control imaging.

5) Root canal obturation

Root canal sealer (AH Plus Jet, Dentsply Sirona) was placed into the root canal using a #35 K file. A ProTaper Gold F4 gutta-percha point (ProTaper Gold Conform Fit Gutta-Percha, Dentsply Sirona), which matched the geometry of ProTaper Gold F4, was inserted and the root canal was obturated. Subsequently, excess gutta-percha points were cut at the root canal orifice using a heated root canal plugger (Ishizuka, Saitama, Japan), then the gutta-percha points were lightly pressed in the apex direction and stored in an incubator at 37°C with 100% humidity. After confirming complete setting at 24 hr, micro-CT scans were obtained after root canal obturation.

To confirm whether microcracks could be observed on micro-CT scans, root canal shaping was performed on another tooth to F4 under Af-1 conditions. A spreader (Star Dental D11T, DentalEZ, Lancaster, PA, USA) was placed in the root canal to intentionally induce vertical root fracture as a positive control and micro-CT scans were obtained²⁹.

6) Evaluation

Three-dimensional images were reconstructed from tomographic images obtained pre-root canal shaping, post-root canal shaping and post-root canal obturation using image processing software (TRI/3D-BON, Ratoc System Engineering, Tokyo, Japan). The area from the root apex to 6 mm (581 cross-sectional images for each test piece) was defined as the observation site. In each image obtained by micro-CT scanning, a line continuously reaching the external surface of the root from the canal wall was defined as a complete crack and a line extending from the canal wall into the root dentin not reaching the external surface of the root was defined as an incomplete crack²³. In addition, the presence or absence of microcracks was evaluated.

2. Experiment II : Effect of root-end resection on roots in over-instrumented teeth

1) Root-end resection

A straight plain fissure carbide bur (#57, VDW, Munich, Germany) was attached on an electric hand-piece (Ti-Max Z95L, NSK, Tochigi, Japan) and the apical 3 mm was resected to an angle of 90 degrees to the tooth axis under 30,000 rpm water cooling.

2) Evaluation of microcracks on the resected root surfaces after root-end resection

One % methylene blue solution (Muto Pure Chemicals, Tokyo, Japan) was applied with a microbrush (Tokuyama Dental, Tokyo, Japan) for 5 s to the resected root surface following root-end resection, the surface was washed with distilled water, and excess water was removed with water-absorbable paper³⁰⁾. Subsequently, an LED transilluminator (Microlux2, AdDent, Danbury, CT, USA) with a 1-mm-diameter fiber light guide (Endo-Light Guide, AdDent) was used to observe the resected root surface. The irradiation was performed in low power mode (1,500 lux) at a position 1 mm from the external surface of the root and 90 degrees to the tooth axis³¹⁾. Furthermore, the resected root surface was observed and recorded under a stereomicroscope (Leica MZ75, Leica Microsystems, Bensheim, Germany). Microcracks on the resected root surface were evaluated using image analysis software (Leica Application Suite, Leica Microsystems). Similar to experiment I, the occurrence of microcracks in each group was recorded. The running direction of each microcrack was captured and classified into four directions: mesial, distal, labial and lingual. In addition, the length from the canal wall to the end of the microcrack was measured.

3. Experiment III: Effect of ultrasonic root-end cavity preparation on roots in over-instrumented teeth

1) Ultrasonic root-end cavity preparation

The test piece after root-end resection was fixed in a jig (Japan Mecc, Tokyo, Japan). Subsequently, a diamond-coated ultrasonic tip (E32D, NSK) was attached to an ultrasonic unit (Varios 2 Lux, NSK) and the root-end cavity was prepared under water cooling at a power recommended by the manufacturer's instructions (mode E, power 6). The cavity was made 3 mm deep along the root canal axis until the gutta-percha point was removed from the cavity wall.

2) Evaluation of microcracks on the resected root surfaces after root-end cavity preparation

Similar to Experiment II, the resected root surfaces were stained with methylene blue solution and the surfaces were recorded and observed under a stereomicroscope with LED transillumination. A line continuously reaching the external surface of the root from the root-end cavity wall was defined as a complete crack and a line extending from the root-end cavity wall into the root dentin not reaching the external surface of the root was defined as an incomplete crack. Both pre-existing microcracks on the resected root surfaces after root-end resection with a carbide bur and new microcracks generated by ultrasonic root-end cavity preparation were evaluated. The presence, direction and length of the microcracks from the root-end cavity wall to the end of the microcracks were measured.

3) Statistical analysis

IBM SPSS Statistics for Windows, Version 28.0 (IBM Corp, Armonk, NY, USA) was used for statistical analysis, and the significance level was set at 5%. The Kruskal-Wallis multiple comparison test was used to compare the length of each microcrack.

Results

1. Experiment I : Effect of over-instrumentation on roots during root canal shaping

In the positive control with root fracture, micro-CT images clearly demonstrated complete and incomplete cracks (Fig. 2). Overall, 31,374 images taken with 18 test pieces exhibited no new microcracks. There was no microcrack on images at 3 mm from the root apex. Representative images obtained pre-root canal shaping, post-root canal shaping and post-root canal obturation for each group are shown in Fig. 2.

2. Experiment II : Effect of root-end resection on roots in over-instrumented teeth

1) Microcracks after root-end resection

A complete crack was observed in one test piece in the Af+1 group (Table 1). The number of test pieces with microcracks and the number of microcracks increased in the order of Af-1, Af and Af+1 groups.

2) Direction of running of microcracks after root-end resection

All the incomplete cracks ran in the labiolingual direction, and the complete cracks ran in the mesiodis-

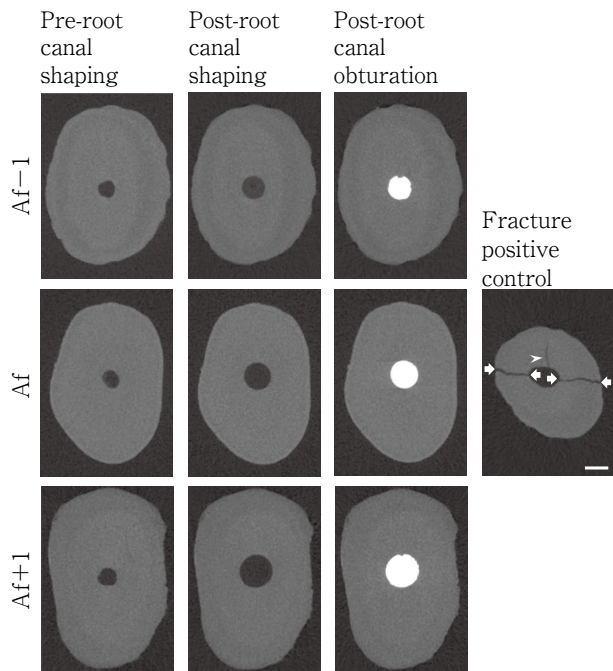


Fig. 2 Representative cross-sectional micro-CT images obtained during root canal treatment in each group

Positive control was an artificially induced vertical root fracture. Arrows : complete cracks, arrowhead : incomplete crack, scale bar=500 μm

tal direction.

3) Length of microcracks after root-end resection

After root-end resection, the length of microcracks increased in the order of Af-1, Af and Af+1 groups, with no statistical difference (Fig. 3).

3. Experiment III: Effect of ultrasonic root-end cavity preparation on roots in over-instrumented teeth

1) Microcracks after ultrasonic root-end cavity preparation

A complete crack was observed in one test piece in the Af+1 group (Table 2). The number of test pieces with microcracks increased in the Af group compared with the Af-1 group. In addition, the number and line with microcracks increased in the Af+1 group compared with the Af-1 group. Furthermore, the number of microcracks increased in the Af+1 group compared with the Af group.

2) Direction of running of microcracks after ultrasonic root-end cavity preparation

94.7% of the incomplete cracks ran in the labiolingual direction. All the complete cracks in the Af+1 group

ran in the mesiodistal direction (Fig. 4).

3) Length of microcracks after ultrasonic root-end cavity preparation

After ultrasonic root-end cavity preparation, the length of microcracks increased in the order of Af-1, Af and Af+1 groups (Fig. 5). The length of microcracks was significantly longer in the Af+1 group than in the Af-1 group ($p < 0.05$).

Discussion

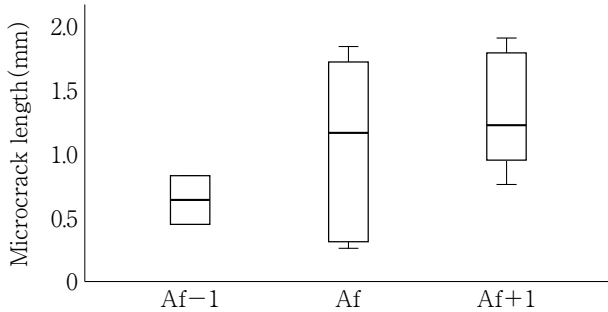
The effect of root canal shaping on the occurrence of root microcracks is often evaluated by the root sectioning method using a low-speed saw and observation of the resected surfaces using a stereomicroscope^{30,32,33}. In a study by Karataş et al., no microcracks occurred in the group without root canal shaping using the root sectioning method. In addition, root canal shaping with a nickel-titanium rotary file caused more microcracks than in the no root canal shaping group (control group)³². Shantiaee et al. evaluated the effect of root canal shaping on the occurrence of microcracks using the root sectioning method. They observed microcracks in the root canal shaping and no shaping groups. Since there was no statistically significant difference in the number of microcracks between the root canal shaping and no root canal shaping groups, it was difficult to determine whether the microcracks identified were caused by root canal shaping³⁴. In the present study, changes in the internal structure of teeth before and after the experiment were evaluated using micro-CT scans. This enables non-destructive, longitudinal and three-dimensional observation of test pieces from various directions on a computer. Micro-CT scans are used in endodontics to evaluate root canal anatomy, root canal shaping and the density of root canal obturation³⁵⁻³⁷. De-Deus et al. evaluated root canal shaping with a nickel-titanium rotary file using micro-CT scans, and reported no new microcracks in the roots after root canal shaping³⁸. In addition, it has been reported that microcracks observed after root canal shaping with a nickel-titanium rotary file were also present before root canal shaping³⁹.

No new microcracks occurred when root canal shaping was performed using nickel-titanium rotary files with different apical limit settings; Af-1, Af and Af+1. Since microcracks were observed in positive controls

Table 1 Number of teeth and lines of microcracks after root-end resection

	Af-1		Af		Af+1	
	Complete	Incomplete	Complete	Incomplete	Complete	Incomplete
Teeth	0 (0%)	1 (16.7%)	0 (0%)	3 (50.0%)	1 (16.7%)	4 (66.7%)
Lines	0	2	0	6	1	7

Complete cracks : Complete, Incomplete cracks : Incomplete

**Fig. 3** Length of microcracks obtained after root-end resection

with obvious root fractures, we can conclude that micro-CT imaging is useful for the non-destructive observation of microcracks in the roots. Previous studies using the root sectioning method have reported an increase in microcracks as the apical limit settings progressed outside the root canal^{8,21,22}. On the other hand, a study similar to the present study that evaluated the occurrence of microcracks in roots due to root canal shaping with a nickel-titanium rotary file using micro-CT reported no new microcracks regardless of the location of apical limit settings^{23,24}. Bier et al. reported that more root dentin could be removed with the 6%-tapered nickel-titanium rotary file that was also used for root canal shaping in this study compared with the 2%-tapered hand file specified for use in the ISO standard⁴⁰. The absence of microcracks during root canal shaping, despite using a nickel-titanium rotary file with a large taper was due to the cutting efficiency of the nickel-titanium rotary file. Deari et al. compared the lateral cutting efficiencies of austenitic and martensite nickel-titanium rotary files of the same geometry on bovine-extracted teeth and observed that the martensite nickel-titanium rotary file demonstrated significantly higher lateral cutting efficiency⁴¹. Under the present experimental conditions, the use of a nickel-titanium rotary file with a martensite phase and high lat-

eral cutting efficiency reduced the load applied to the root dentin. Hence, microcracks did not occur.

In this study, root canal obturation was performed to evaluate the influence of the apical limit settings on endodontic surgery. Micro-CT, similar to cone-beam computed tomography, uses X-rays, so artifacts due to root canal obturation material can be observed, making the detection of microcracks difficult⁴²⁻⁴⁴. It has also been suggested that the lateral condensation method using a spreader and the vertical condensation method using a thermoplasticized gutta-percha point significantly impact the root dentin and may result in microcracks^{45,46}. Therefore, in this study, a matched-taper single-cone technique with gutta-percha points matched to the size and taper of the nickel-titanium rotary file was employed to reduce the impact of root canal obturation on the roots^{47,48}.

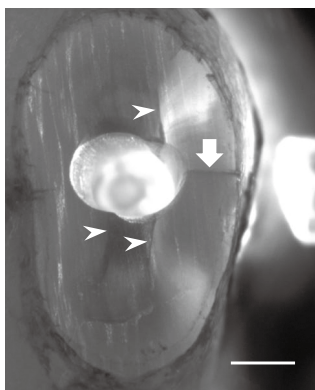
A complete crack was observed on the resected root surface after root-end resection in the Af+1 group. Rose et al. reported that root canal shaping using a nickel-titanium rotary file with a working length of Af-1 and root-end resection using a #57 bur on a premolar implanted in the mandible from pigs demonstrated no complete crack on the resected root surface in the group that had root canal shaping performed using a nickel-titanium rotary file. However, root-end resection was performed on an over-instrumented tooth using a #80 K file, and a complete crack was observed⁴⁹. The present study demonstrated a similar trend to studies involving organisms, suggesting that the root planting model can set up an environment equivalent to the natural periodontal tissue structures.

The number of microcracks increased in the Af+1 group compared with the Af-1 group after root-end cavity preparation with an ultrasonic tip. Sachdeva et al. prepared a root-end cavity for mandibular premolars up to apical size #40 with a working length of Af-0.5 using a diamond-coated ultrasonic tip at a medium

Table 2 Number of teeth and lines of microcracks after ultrasonic root-end cavity preparation

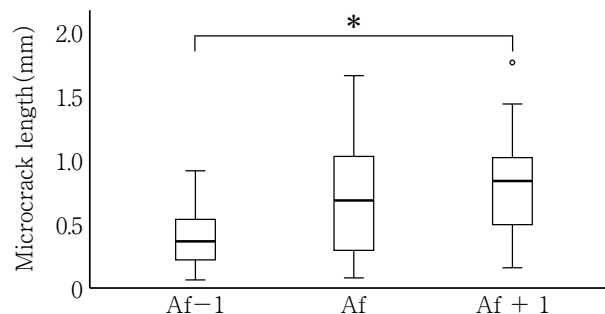
	Af-1		Af		Af+1	
	Complete	Incomplete	Complete	Incomplete	Complete	Incomplete
Teeth	0 (0%)	5 (83.3%)	0 (0%)	6 (100%)	1 (16.7%)	6 (100%)
Lines	0	13	0	11	1	14

Complete cracks : Complete, Incomplete cracks : Incomplete

**Fig. 4** Image of resected root surface obtained after ultrasonic root-end cavity preparation in the Af+1 group

Arrow : complete crack, arrowheads : incomplete cracks, scale bar=1 mm

power setting. The results demonstrated that test pieces with preexisting microcracks occurred and spread more frequently after root-end cavity preparation than those without microcracks⁵⁰). Tawil demonstrated that ultrasonic root-end cavity preparation on intact roots does not induce new microcracks but may spread existing ones⁵¹). In this study, microcracks were observed after ultrasonic root-end cavity preparation in all groups. This may have been due to the power of the ultrasonic unit. Layton et al. compared the effect of ultrasonic unit power on ultrasonic root-end cavity preparation and reported that the number of microcracks per tooth was significantly higher for ultrasonic root-end cavity preparation at the highest power setting than at the lowest⁵²). In addition, Palma et al. performed root canal shaping to #25 with a working length of Af-0.5, followed by root-end resection and root-end cavity preparation. Microcracks were reported after root-end cavity preparation using the same ultrasonic tip and power settings as in the present study⁵³). The

**Fig. 5** Length of microcracks obtained after ultrasonic root-end cavity preparation

* : $p < 0.05$

power setting used in this study (mode E, power 6) is a medium power setting in mode E (maximum power setting: 10) suitable for endodontic treatment. The use of low-power settings in ultrasonic units may be recommended to reduce the occurrence of microcracks during ultrasonic root-end cavity preparation. It is also possible that the size of the ultrasonic tip affected the number of microcracks in the Af-1 group compared with the Af group. Using an ultrasonic tip with a larger diameter than the root canal obturation material might have resulted in more cutting of the healthy root dentin and more force being applied to the dentin. The results suggest the need for an appropriately sized ultrasonic tip according to the diameter of the root canal obturation material to reduce the occurrence of microcracks.

The present study demonstrated that incomplete cracks tend to run in the labiolingual direction after root-end resection and cavity preparation. The results are similar to those of Palma et al., who observed that incomplete cracks occurred in areas with a wide residual dentin width after root-end cavity preparation⁵³). In addition, complete cracks were observed in the mesiodistal directions. These may be related to the root morphology. The mandibular single-root canal teeth

used in this experiment are generally compressed with a smaller mesiodistal diameter compared with the labiolingual diameter⁵⁴). The complete cracks were probably caused by the force applied to the mesial and distal dentin of the thinned compressed root due to root canal shaping. Teeth with narrower mesiodistal diameters are significantly more likely to fracture than those with wider diameters, suggesting that great care should be taken when performing root-end resection and root-end cavity preparation on teeth with narrower mesiodistal diameters⁵⁵).

Few studies that evaluated the effect of endodontic surgery on the occurrence of microcracks mentioned the length of microcracks. Min et al. performed root canal shaping of a molar to apical size #25 with a working length of Af-1, followed by root-end resection with a diamond disc and root-end cavity preparation using an inverted cone bur or an ultrasonic tip with varying power settings of the ultrasonic unit. Confocal microscopy of dentin defects on the resected root surface demonstrated that ultrasonic root-end cavity preparation produced dentin defects ranging from 126.0 to 520.0 μm in length regardless of the power setting of the ultrasonic unit⁵⁶). However, no study has compared the length of microcracks that occurred at different time points during endodontic surgery by changing the apical limit settings until now. In the present study, the length of microcracks increased in the order of Af-1, Af and Af+1 groups after root-end resection and cavity preparation. This may have been because the amount of root canal dentin removed increases in accordance with the taper of the file as the file tip reaches the outer part of the root canal, resulting in the thinning of the dentin⁵⁷⁻⁵⁹). The length of microcracks was significantly longer in the Af+1 group than in the Af-1 group after root-end cavity preparation. The Af-1 group is set at the apical constriction, recommended as the apical limit^{6,7,60}). Bergenholtz et al. reported a significantly lower incidence of periapical lesions in endodontically-treated teeth at the proper apical limit⁶¹). The results demonstrated that the over-instrumentation at Af+1 reduces the success rate of endodontic treatment and may induce microcracks during endodontic surgery, indicating the need for caution in setting the working length during root canal shaping. In addition, while examining an endodontically-treated tooth, it is impossible to determine whether

over-instrumentation was performed during root canal shaping. Therefore, we suggest that all dentists select an appropriately sized ultrasonic tip based on the diameter of the root canal obturation material exposed on the resected root surface and perform root-end cavity preparation without applying excessive force in the setting of the over-instrumentation during endodontic surgery.

Conclusion

From the results of this study, the following conclusions can be drawn.

1. No new microcracks occurred during root canal shaping, regardless of the apical limit settings.
2. The number and length of microcracks on the resected root surface following root-end resection increase in the order of the Af-1, Af and Af+1 groups.
3. The number of microcracks after ultrasonic root-end cavity preparation was the highest in the Af+1 group.
4. The incomplete cracks ran in the labiolingual direction, and the complete cracks ran in the mesiodistal direction after root-end resection and ultrasonic root-end cavity preparation.
5. The length of microcracks after ultrasonic root-end cavity preparation was longer in the order of Af-1, Af and Af+1 groups and was significantly larger in the Af+1 group than in the Af-1 group.

Conflicts of Interest

There are no conflicts of interest to disclose regarding this study.

References

- 1) Siqueira JF Jr, Lima KC, Magalhães FA, Lopes HP, de Uzeda M. Mechanical reduction of the bacterial population in the root canal by three instrumentation techniques. *J Endod* 1999; 25: 332-335.
- 2) Siqueira JF Jr, Rôças IN, Favieri A, Lima KC. Chemomechanical reduction of the bacterial population in the root canal after instrumentation and irrigation with 1%, 2.5%, and 5.25% sodium hypochlorite. *J Endod* 2000; 26: 331-334.
- 3) Delgado RJR, Gasparoto TH, Sipert CR, Pinheiro CR, Moraes IG, Garcia RB, Bramante CM, Campanelli AP,

- Bernardineli N. Antimicrobial effects of calcium hydroxide and chlorhexidine on *Enterococcus faecalis*. J Endod 2010; 36: 1389-1393.
- 4) Nagas E, Altundasar E, Serper A. The effect of master point taper on bond strength and apical sealing ability of different root canal sealers. Oral Surg Oral Med Oral Pathol Oral Radiol Endod 2009; 107: e61-e64.
 - 5) Romania C, Beltes P, Boutsoukis C, Dandakis C. *Ex-vivo* area-metric analysis of root canal obturation using gutta-percha cones of different taper. Int Endod J 2009; 42: 491-498.
 - 6) Wu MK, Wesselink PR, Walton RE. Apical terminus location of root canal treatment procedures. Oral Surg Oral Med Oral Pathol Oral Radiol Endod 2000; 89: 99-103.
 - 7) Ricucci D, Langeland K. Apical limit of root canal instrumentation and obturation, part 2. A histological study. Int Endod J 1998; 31: 394-409.
 - 8) Adorno CG, Yoshioka T, Suda H. Crack initiation on the apical root surface caused by three different nickel-titanium rotary files at different working lengths. J Endod 2011; 37: 522-525.
 - 9) Zhou X, Jiang S, Wang X, Wang S, Zhu X, Zhang C. Comparison of dentinal and apical crack formation caused by four different nickel-titanium rotary and reciprocating systems in large and small canals. Dent Mater J 2015; 34: 903-909.
 - 10) Shemesh H, Bier CAS, Wu MK, Tanomaru-Filho M, Wesselink PR. The effects of canal preparation and filling on the incidence of dentinal defects. Int Endod J 2009; 42: 208-213.
 - 11) Adorno CG, Yoshioka T, Jindan P, Kobayashi C, Suda H. The effect of endodontic procedures on apical crack initiation and propagation *ex vivo*. Int Endod J 2013; 46: 763-768.
 - 12) Chan CP, Tseng SC, Lin CP, Huang CC, Tsai TP, Chen CC. Vertical root fracture in nonendodontically treated teeth—a clinical report of 64 cases in Chinese patients. J Endod 1998; 24: 678-681.
 - 13) Axelsson P, Nyström B, Lindhe J. The long-term effect of a plaque control program on tooth mortality, caries and periodontal disease in adults. Results after 30 years of maintenance. J Clin Periodontol 2004; 31: 749-757.
 - 14) Kim S, Kratchman S. Modern endodontic surgery concepts and practice: A review. J Endod 2006; 32: 601-623.
 - 15) Song M, Shin SJ, Kim E. Outcomes of endodontic micro-resurgery: A prospective clinical study. J Endod 2011; 37: 316-320.
 - 16) Torabinejad M, Higa RK, McKendry DJ, Pitt Ford TR. Dye leakage of four root end filling materials: Effects of blood contamination. J Endod 1994; 20: 159-163.
 - 17) Navarre SW, Steiman HR. Root-end fracture during retro-preparation: A comparison between zirconium nitride-coated and stainless steel microsurgical ultrasonic instruments. J Endod 2002; 28: 330-332.
 - 18) Wuchenich G, Meadows D, Torabinejad M. A comparison between two root end preparation techniques in human cadavers. J Endod 1994; 20: 279-282.
 - 19) Engel TK, Steiman HR. Preliminary investigation of ultrasonic root end preparation. J Endod 1995; 21: 443-445.
 - 20) Saunders WP, Saunders EM, Gutmann JL. Ultrasonic root-end preparation, Part 2. Microleakage of EBA root-end fillings. Int Endod J 1994; 27: 325-329.
 - 21) Adorno CG, Yoshioka T, Suda H. The effect of root preparation technique and instrumentation length on the development of apical root cracks. J Endod 2009; 35: 389-392.
 - 22) Adorno CG, Yoshioka T, Suda H. The effect of working length and root canal preparation technique on crack development in the apical root canal wall. Int Endod J 2010; 43: 321-327.
 - 23) de Oliveira BP, Câmara AC, Duarte DA, Heck RJ, Antonino ACD, Aguiar CM. Micro-computed tomographic analysis of apical microcracks before and after root canal preparation by hand, rotary, and reciprocating instruments at different working lengths. J Endod 2017; 43: 1143-1147.
 - 24) Belladonna FG, Rodrigues LLC, Leal ASM, Oliveira HE, Maciel ACC, Cavalcante DM, Silva EJNL, Valois ÉM, Souza EM, De-Deus G. Is canal overinstrumentation able to produce apical root dentinal microcracks in extracted teeth? Int Endod J 2021; 54: 1647-1652.
 - 25) Liu R, Hou BX, Wesselink PR, Wu MK, Shemesh H. The incidence of root microcracks caused by 3 different single-file systems versus the ProTaper system. J Endod 2013; 39: 1054-1056.
 - 26) Elnaghy AM, Elsaka SE. Mechanical properties of ProTaper Gold nickel-titanium rotary instruments. Int Endod J 2016; 49: 1073-1078.
 - 27) Logsdon J, Dunlap C, Arias A, Scott R, Peters OA. Current trends in use and reuse of nickel-titanium engine-driven instruments: A survey of endodontists in the United States. J Endod 2020; 46: 391-396.
 - 28) Liu R, Kaiwar A, Shemesh H, Wesselink PR, Hou B, Wu MK. Incidence of apical root cracks and apical dentinal detachments after canal preparation with hand and rotary files at different instrumentation lengths. J Endod 2013; 39: 129-132.
 - 29) Shemesh H, van Soest G, Wu MK, Wesselink PR. Diagnosis of vertical root fractures with optical coherence tomography. J Endod 2008; 34: 739-742.
 - 30) Borges ÁH, Damião MS, Pereira TM, Filho GS, Miran-

- da-Pedro FL, Luiz de Oliveira da Rosa W, Piva E, Guedes OA. Influence of cervical preflaring on the incidence of root dentin defects. *J Endod* 2018; 44: 286-291.
- 31) Coelho MS, Card SJ, Tawil PZ. Visualization enhancement of dentinal defects by using light-emitting diode transillumination. *J Endod* 2016; 42: 1110-1113.
 - 32) Karataş E, Gündüz HA, Kırıcı Dö, Arslan H. Incidence of dentinal cracks after root canal preparation with Pro Taper Gold, Profile Vortex, F360, Reciproc and Pro Taper Universal Instruments. *Int Endod J* 2016; 49: 905-910.
 - 33) Capar ID, Arslan H, Akcay M, Uysal B. Effects of ProTaper Universal, ProTaper Next, and HyFlex instruments on crack formation in dentin. *J Endod* 2014; 40: 1482-1484.
 - 34) Shantiaee Y, Dianat O, Mosayebi G, Namdari M, Tordik P. Effect of root canal preparation techniques on crack formation in root dentin. *J Endod* 2019; 45: 447-452.
 - 35) Amoroso-Silva PA, Ordinola-Zapata R, Duarte MAH, Gutmann JL, del Carpio-Perochena A, Bramante CM, de Moraes IG. Micro-computed tomographic analysis of mandibular second molars with C-shaped root canals. *J Endod* 2015; 41: 890-895.
 - 36) Gagliardi J, Versiani MA, de Sousa-Neto MD, Plazas-Garzon A, Basrani B. Evaluation of the shaping characteristics of ProTaper Gold, ProTaper NEXT, and ProTaper Universal in curved canals. *J Endod* 2015; 41: 1718-1724.
 - 37) Roizenblit RN, Soares FO, Lopes RT, Dos Santos BC, Gusman H. Root canal filling quality of mandibular molars with EndoSequence BC and AH Plus sealers: A micro-CT study. *Aust Endod J* 2020; 46: 82-87.
 - 38) De-Deus G, Silva EJNL, Marins J, Souza E, Neves Ade A, Gonçalves Belladonna FG, Alves H, Lopes RT, Versiani MA. Lack of causal relationship between dentinal microcracks and root canal preparation with reciprocation systems. *J Endod* 2014; 40: 1447-1450.
 - 39) Miguéns-Vila R, Martín-Biedma B, De-Deus G, Belladonna FG, Peña-López A, Castelo-Baz P. Micro-computed tomographic evaluation of dentinal microcracks after preparation of curved root canals with ProTaper Gold, WaveOne Gold, and ProTaper Next instruments. *J Endod* 2021; 47: 309-314.
 - 40) Bier CAS, Shemesh H, Tanomaru-Filho M, Wesselink PR, Wu MK. The ability of different nickel-titanium rotary instruments to induce dentinal damage during canal preparation. *J Endod* 2009; 35: 236-238.
 - 41) Deari S, Zehnder M, Al-Jadaa A. Effect of dentine cutting efficiency on the lateral force created by torque-controlled rotary instruments. *Int Endod J* 2020; 53: 1153-1161.
 - 42) Zaslansky P, Fratzl P, Rack A, Wu MK, Wesselink PR, Shemesh H. Identification of root filling interfaces by microscopy and tomography methods. *Int Endod J* 2011; 44: 395-401.
 - 43) Zhang L, Wang T, Cao Y, Wang C, Tan B, Tang X, Tan R, Lin Z. *In vivo* detection of subtle vertical root fracture in endodontically treated teeth by cone-beam computed tomography. *J Endod* 2019; 45: 856-862.
 - 44) Hassan B, Metska ME, Ozok AR, van der Stelt P, Wesselink PR. Detection of vertical root fractures in endodontically treated teeth by a cone beam computed tomography scan. *J Endod* 2009; 35: 719-722.
 - 45) Pitts DL, Matheny HE, Nicholls JL. An *in vitro* study of spreader loads required to cause vertical root fracture during lateral condensation. *J Endod* 1983; 9: 544-550.
 - 46) Saw LH, Messer HH. Root strains associated with different obturation techniques. *J Endod* 1995; 21: 314-320.
 - 47) Krug R, Krastl G, Jahreis M. Technical quality of a matching-taper single-cone filling technique following rotary instrumentation compared with lateral compaction after manual preparation: A retrospective study. *Clin Oral Investig* 2017; 21: 643-652.
 - 48) Capar ID, Saygili G, Ergun H, Gok T, Arslan H, Ertas H. Effects of root canal preparation, various filling techniques and retreatment after filling on vertical root fracture and crack formation. *Dent Traumatol* 2015; 31: 302-307.
 - 49) Rose E, Svec T. An evaluation of apical cracks in teeth undergoing orthograde root canal instrumentation. *J Endod* 2015; 41: 2021-2024.
 - 50) Sachdeva N, Nikhil V, Jha P. Effect of ultrasonic root-end cavity preparation on dentinal microcrack formation: A micro-computed tomography study. *J Conserv Dent* 2019; 22: 362-366.
 - 51) Tawil PZ. Periapical microsurgery: Can ultrasonic root-end preparations clinically create or propagate dentinal defects? *J Endod* 2016; 42: 1472-1475.
 - 52) Layton CA, Marshall JG, Morgan LA, Baumgartner JC. Evaluation of cracks associated with ultrasonic root-end preparation. *J Endod* 1996; 22: 157-160.
 - 53) Palma PJ, Marques JA, Casau M, Santos A, Caramelo F, Falacho RI, Santos JM. Evaluation of root-end preparation with two different endodontic microsurgery ultrasonic tips. *Biomedicine*; doi: 10.3390/biomedicine8100383.
 - 54) Woelfel JB, Scheid RC. *Dental Anatomy Its Relevance to Dentistry*. 6th ed. Lippincott Williams & Wilkins: Philadelphia; 2002. 97.
 - 55) Rosen H, Patida-Rivera M. Iatrogenic fracture of roots reinforced with a cervical collar. *Oper Dent* 1986; 11: 46-50.
 - 56) Min MM, Brown CE Jr, Legan JJ, Kafrawy AH. *In vitro* evaluation of effects of ultrasonic root-end preparation on resected root surfaces. *J Endod* 1997; 23: 624-628.
 - 57) Wilcox LR, Roskelley C, Sutton T. The relationship of

- root canal enlargement to finger-spreader induced vertical root fracture. J Endod 1997; 23: 533-534.
- 58) Zandbiglari T, Davids H, Schäfer E. Influence of instrument taper on the resistance to fracture of endodontically treated roots. Oral Surg Oral Med Oral Pathol Oral Radiol Endod 2006; 101: 126-131.
- 59) Krikeli E, Mikrogeorgis G, Lyroudia K. *In vitro* comparative study of the influence of instrument taper on the fracture resistance of endodontically treated teeth: An integrative approach-based analysis. J Endod 2018; 44: 1407-1411.
- 60) Gutmann JL, Leonard JE. Problem solving in endodontic working-length determination. Compend Contin Educ Dent 1995; 16: 288, 290, 293-294.
- 61) Bergenholtz G, Lekholm U, Milthon R, Engstrom B. Influence of apical overinstrumentation and overfilling on re-treated root canals. J Endod 1979; 5: 310-314.

Differentiation of Murine Enamel Organ-derived Tissue Stem Cells into Cementoblasts after Transplantation

Minoru TAKASE¹, Naoki MARUO¹, Kazuhiko OKAMURA², Nanako TSUCHIMOCHI¹, Hiroaki YAMATO¹, Kimiko OHGI¹, Atsushi NAGAI³, Takashi KANEKO⁴, Yasunori YOSHINAGA^{1,5} and Ryuji SAKAGAMI¹

¹Section of Periodontology, Department of Odontology, Fukuoka Dental College

²Section of Pathology, Department of Morphological Biology, Fukuoka Dental College

³Regional Liaison Center, Fukuoka Dental College

⁴Center for Oral Diseases, Fukuoka Dental College

⁵Oral Medicine Research Center, Fukuoka Dental College

Abstract

Purpose: It has been proposed that some enamel organ-derived cells undergo an epithelial-mesenchymal transition (EMT) during tooth development, differentiate into cementoblasts, and make acellular cementum. The primary purpose of this study was to elucidate the mechanisms of cell differentiation by transplanting apical bud-derived stem cells of the epithelial lineage of tooth embryos into the bony defects around the molars and tracking their dynamics. The secondary purpose of this study was to use those tissue stem cells as a source of cell transplantation for future periodontal tissue regeneration therapy.

Methods: Apical bud cells from GFP-positive mouse incisors were isolated under a microscope, collected, dispersed, and transplanted into bone defects created around the molars of wild-type mice, and their dynamics were observed for three months. Undecalcified cryosections were made by Kawamoto's method, and immunofluorescence staining was made using antibodies against Osteocalcin (OCN), Cementum protein 1 (CEMP1), and Cytokeratin 10 (CK10).

Results: GFP-positive cells were observed to settle in the periodontal tissue after four weeks of transplantation. Most of the GFP-positive cells showed OCN positivity throughout the observation period. In 12 weeks, some transplanted cells were aligned along the surface of the cementum, and HE images showed the development of cement matrix-like structures around the cells. Among the transplanted cells, cells in the periodontal space were mostly CK10-positive and CEMP1-negative, while cells on the cementum and near alveolar bone were mostly CEMP1-positive and CK10-negative.

Conclusion: Our observations revealed that some transplanted cells underwent EMT and became cementoblast-like on the root surface and osteoblast-like, where they were incorporated into the alveolar bone. Both cementoblast-like and osteoblast-like cells were CEMP1-positive. On the other hand, CEMP1-negative and CK10-positive cells were located in the middle of the periodontal ligament space, suggesting that they settled into the tissue as ERM without undergoing EMT. It is interesting to see how the transplanted cells migrate and settle or differentiate under the influence of surrounding cells. These results suggest that enamel organ-derived tissue stem cells may differentiate into osteoblasts and cementoblasts/cementocytes and could be the source of periodontal tissue regeneration.

Key words: cementoblasts, epithelial-mesenchymal transition, Hertwig's epithelial root sheath

Corresponding author: Ryuji SAKAGAMI, Department of Periodontology, Department of Odontology, Fukuoka Dental College, 2-15-1, Tamura, Sawara-ku, Fukuoka 814-0193, Japan

TEL: +81-92-801-0411, FAX: +81-92-871-9494, E-mail: sakagami@fdcnet.ac.jp

Received for Publication: November 29, 2022/Accepted for Publication: January 11, 2023

DOI: 10.11471/odep.2023-002

Introduction

The lifelong elongation of rodents' maxillary and mandibular incisors has a unique anatomical structure, with enamel forming on the labial side and the periodontal ligament starting on the lingual side. The most apical side of the incisors, called the labial cervical loop initially, has been named the apical bud by Harada et al.¹⁾ The apical bud contains a cell population composed of epithelial tissue stem cells corresponding to human enamel organs¹⁻³⁾. Using the apical bud as a grafting material may be a valuable tool for studying cell differentiation.

We have already reported the successful development of a technique in which incisor apical bud cells from GFP-positive transgenic mice were harvested under a microscope and transplanted into the incisor root tips of wild-type mice⁴⁾. The apical bud cells differentiated into ameloblasts/Hertwig's epithelial root sheaths (HERS)/epithelial cell rests of Malassez (ERM). HERS can stimulate and transform mesenchymal cells of the dental follicle into cementoblasts. HERS eventually remains in the periodontal ligament to form ERM, some of which undergo apoptosis^{5,6)}. The functions of the ERM remaining in the periodontal ligament are thought to be diverse, including maintenance of the periodontal space, prevention of root resorption and ankylosis, maintenance of homeostasis of the periodontal ligament, and induction of acellular cementum formation⁷⁾.

Recently, it has been proposed that HERS undergoes an epithelial-mesenchymal transition (EMT) during tooth development and differentiates into cementoblasts⁸⁻¹²⁾. Much circumstantial evidence supports this theory in several *in vitro* experimental systems. However, some studies suggest that there are no or few HERS cells that differentiate into cementoblasts¹³⁻¹⁷⁾.

Especially in externally transplanted HERS, it is unclear whether these cells can generate EMT and whether such cell transplantation can be applied for periodontal tissue regeneration with cementum formation.

The primary purpose of this study was to elucidate the mechanisms of cell differentiation by transplanting apical bud-derived stem cells of the epithelial lineage of tooth embryos and tracking their dynamics. The sec-

ondary purpose of this study was to use those tissue stem cells as a source of cell transplantation for future periodontal tissue regeneration therapy. In this study, apical bud cells from GFP-positive mouse incisors were isolated under a microscope, collected, dispersed, and transplanted into bone defects created in the molars of wild-type mice. Their fate was observed for three months. Cellular characteristics were monitored using antibodies against Osteocalcin (OCN), Cementum protein 1 (CEMP1), and Cytokeratin 10 (CK10) as markers for calcification, cementum, and epithelial cells, individually.

Materials and Methods

1. Experimental animals

This study was approved by the Fukuoka Dental College Animal Experiment Committee, considering animal welfare and in compliance with the Fukuoka Dental College Animal Experiment Guidelines (Fukuoka Dental College Animal Experiment Approval No. 20007). Experimental animals were bred in the SPF Laboratory at the Animal Center of Fukuoka Dental College and kept on a 12-hour light/dark cycle according to the facility's guidelines. Fifty-four 10-day-old C57BL/6-TG (CAG-EGFP) mice (Green Mouse, SLC, Shizuoka, Japan) transfected with the GFP gene were used as donors^{18,19)}. Eighteen 6-week-old male wild-type C57BL/6 mice were used as recipients. Donors were housed with their maternal mice.

2. Cell preparation method from donors

Ten-day-old C57BL/6-TG (CAG-EGFP) mice were euthanized by inhalation of isoflurane anesthesia overdose, the mandible was removed under a stereomicroscope, and the incisor teeth, including the root apex, were extracted from the mandible. The teeth were then treated in 37°C saline containing 1,500 PU/mL of dispase (Dispase, Gibco, Beverly MA, USA) for 20 minutes, and the apical bud portion was isolated from the root apex (Fig. 1). The isolated apical buds were then incubated in 1 mL of cell detachment solution (Accumax, Innovative Cell Technologies, Inc., San Diego, CA, USA) for 10 minutes at room temperature and collected by centrifugation after cell dispersion.

3. Method of transplantation to the recipient

Under general anesthesia with isoflurane, 6-week-old wild-type mice were fitted with a mouth opening

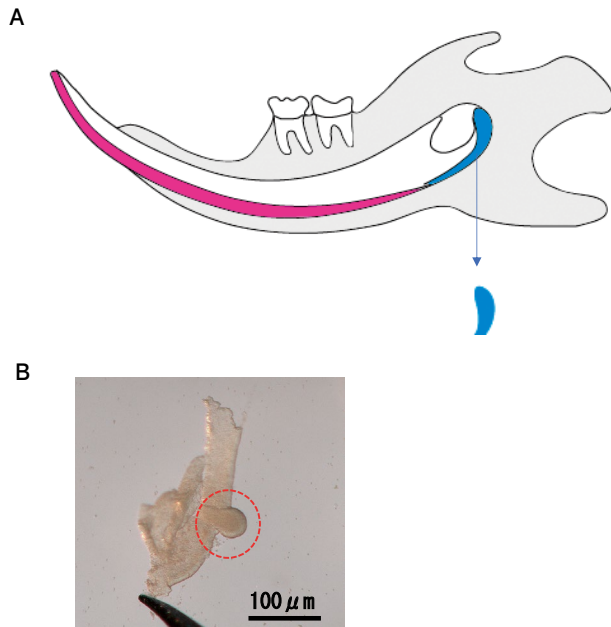


Fig. 1 Schematic illustration of a method for collecting apical buds

A : Sagittal section of mouse mandible. The enamel of the mandibular incisor is shown in red. After removal of the mandibular incisor from the mandible, apical buds and the extending tissue transitioning to enamel epithelium (blue) were harvested.

B : Enamel epithelial tissue containing apical buds collected from the mandibular incisor.

From the tissue fragment shown in the figure, the portion indicated by the dotted circle was separated as an apical bud.

device, and two holes of 0.5 mm in diameter and 1.5 mm in depth were drilled into the periodontal ligament of the maxillary molar using an engine drill without opening periodontal flap (Fig. 2). Compression hemostasis was applied as needed to ensure adequate hemostasis after drilling. The transplantation of cells was performed with a micropipette (Reference 2, Eppendorf, Hamburg, Germany) with a gel loading tip (124-R-204, BIO-BIK, Osaka, Japan). Cell counts were verified on a blood cell counter. An average number of 3.0×10^5 cells were inoculated at one socket. The number of transplanted cells was three μL per defect, and each hole received cells from three donor sites. Dispersed cells were injected into the periodontal ligament and bone defect without carrier materials. No sutures were made after injection. Animals were euthanized at 1, 4, and 12 weeks after transplantation ($n=6$ per week, a total of 18 animals), and the right and left maxillae were

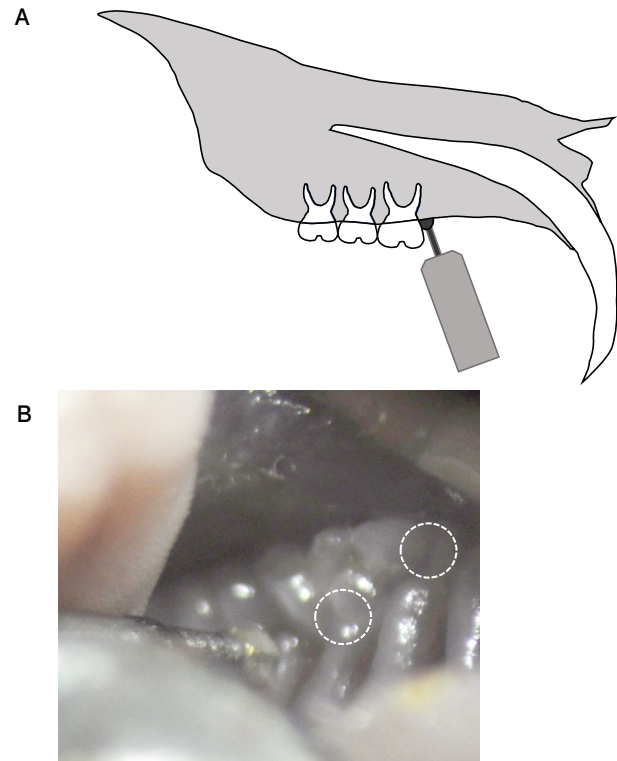


Fig. 2 Schematic illustration of a method for creating bone defects in the recipient

A : Sagittal section model of mouse maxilla. Defects of 0.5 mm in diameter and 1.5 mm in depth were created in two locations on the mesial and palatal sides of the mouse maxillary first molar using a round bar attached to a straight handpiece.

B : The palatal surface of the maxillary first molar undergoing bone defect formation. Drilling was performed at two locations, the mesial surface of the mesial root and the furcation area between the mesial and lingual roots, as indicated by the dotted circles, and cells collected from the donor were carefully injected.

removed and fixed in 4% paraformaldehyde buffer solution.

4. Preparation of pathological specimens

The undecalcified maxillary bone was placed in a $10 \times 10 \times 5$ mm cryomold container (Sakura FineTek Cryomold, Osaka, Japan) with the occlusal surface facing upward and frozen in liquid nitrogen with Cryo-Embedding Medium (SCEM, SectionLab, Hiroshima, Japan). The frozen sections were cut with a tungsten knife at -20°C in a cryostat (CM3050S, Leica, Wetzlar, Germany) at a thickness of $4 \mu\text{m}$ by the Kawamoto's method (film transfer method) using the height of the root furcation of the maxillary first molar as a refer-

ence. The specimens were observed by HE staining and immunofluorescence staining. For immunostaining, an anti-GFP chicken antibody (Abcam, Cambridge, UK) was used as the primary antibody, and an anti-chicken AlexaFluor 488 antibody (Thermo Fisher Scientific Inc., Cambridge, UK) as the secondary antibody to enhance GFP fluorescence. In addition, six samples at one week, six at four weeks, and three at 12 weeks were treated with anti-OCN antibody followed by anti-rabbit Alexafluor568 antibody. In the three 12-week samples, anti-CEMP1 and anti-CK10 rabbit antibodies (Abcam) were used as primary antibodies and anti-rabbit Alexafluor568 antibody (Thermo Fisher Scientific Inc.) as the secondary antibody. All sections were sealed in VectorShield with DAPI (Vector Laboratories, Newark, CA, USA). Tissue sections were observed with a fluorescence microscope (BZ-X710, Keyence, Osaka, Japan).

Results

Representative examples of tissue images from 1 to 12 weeks after transplanting cells collected from donor mice into the first molar area of recipient mice are shown.

1. One week after transplantation

Images at one week after transplantation are shown in Figure 3. The low-magnification HE image showed drilled bone defects on the mesial surface of the maxillary first molar's mesial root and the lingual root's mesial furcation side. The transplanted cells showed green fluorescence over a wide area on the mesial surface of the maxillary first molar's mesial root and the lingual root's mesial furcation. Most transplanted cells strongly expressed OCN one week after surgery, although the HE images did not show calcification. DAPI images showed that some of the transplanted cells were in an aggregated state.

2. Four weeks after transplantation

Four weeks after transplantation, GFP-positive cells were observed in and around the periodontal ligament (Fig. 4). OCN-positive oval-shaped cells were widely distributed on the cementum and alveolar bone surfaces, and some GFP-positive cells showed strong OCN expression. These cells showed cementoblast-like and osteoblast-like morphology on HE images.

3. Twelve weeks after transplantation

Images at 12 weeks after transplantation are shown

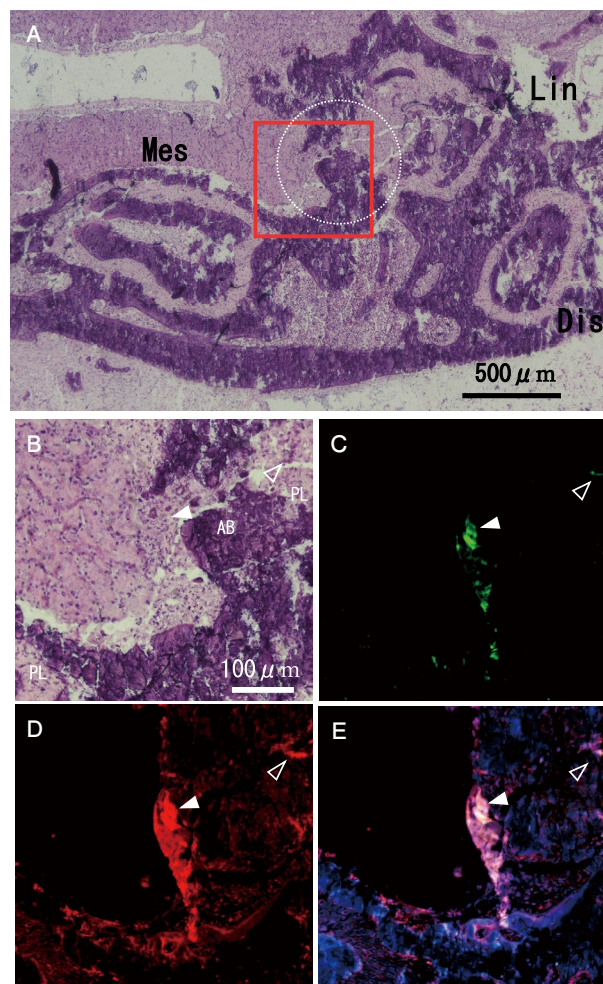


Fig. 3 HE-stained and immunofluorescent-stained images at one week after transplantation

A : HE image of a horizontal section of the maxillary first molar. A magnified image of the red-framed area is shown in B. The area of the created bone defect is shown as a dotted white circle. Mes : mesial root ; Dis : distal root ; Lin : lingual root

B : Magnified HE image of the mesial surface of the lingual root. The arrowhead and outlined arrowhead indicate the transplanted cells. C, D, and E show immunofluorescent-stained images of the same area. AB : alveolar bone ; PL : periodontal ligament

C : GFP-positive cells are mostly found around the alveolar bone (arrowhead) and in the periodontal ligament space (outlined arrowhead).

D : OCN-positive cells are found around the alveolar bone and the periodontal ligament space, overlapping most GFP-positive cells.

E : The merged image of C, D, and DNA stained with DAPI shows that some transplanted cells are in an aggregated state ; most of the GFP-positive cells are OCN-positive.

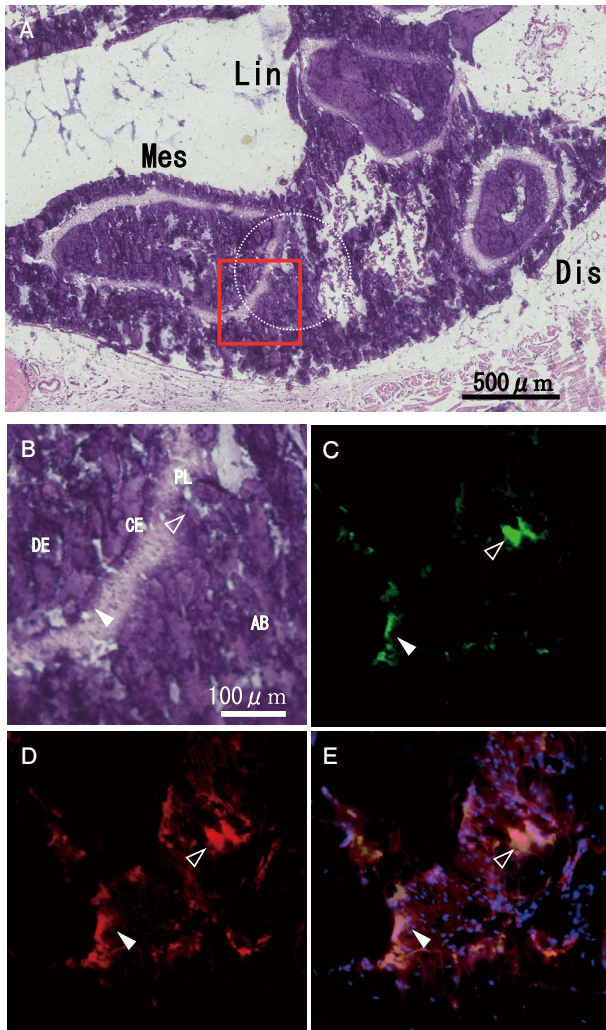


Fig. 4 HE-stained and immunofluorescent-stained images four weeks after transplantation

A : HE image of a horizontal section of the maxillary first molar. A magnified image of the red-framed area is shown in B. The area of the created bone defect is shown as a dotted white circle. Mes : mesial root ; Dis : distal root ; Lin : lingual root

B : Magnified HE image of the distal surface of the mesial root. The arrowhead and outlined arrowhead indicate the transplanted cells. C, D, and E show immunofluorescent-stained images of the same area. AB : alveolar bone ; PL : periodontal ligament ; CE : cementum ; DE : dentin

C : GFP-positive cells are partly aligned along the cementum surface (arrowhead) and partly in the periodontal ligament space close to the alveolar bone (outlined arrowhead).

D : OCN-positive cells are found on the cementum and alveolar bone.

E : Merged image of C, D, and DNA stained with DAPI showing that most of the GFP-positive cells are OCN-positive.

in Figure 5. GFP-positive cells produced cementoblast-like cells in the periodontal ligament and cement matrix-like structures around the partitions on HE images. GFP-positive cells were also found along the cementum surface of the root and on the alveolar bone side across the periodontal ligament, which was OCN-positive. Some GFP-positive cells were also found in the periodontal space, and even though they were OCN-positive, they did not show calcification on the HE images.

4. CEMP1 and CK10-positive cells at 12 weeks after transplantation

Images at 12 weeks after transplantation are shown in Figure 6. Some of the GFP-positive cells migrating into the periodontal ligament were found. In addition, some of the cells were aligned along the surface of the cementum, indicating CEMP1 positivity, and HE images showed the development of cement matrix-like structures around the cells. Cells in the periodontal ligament were mainly CK10-positive and CEMP1-negative, while many CEMP1-positive and CK10-negative cells were found on the cementum and alveolar bone surfaces.

Discussion

In our previous study, we transplanted the apical tissue of the mandibular incisor, including epithelial and mesenchymal cells derived from GFP mice, into wild-type mice and observed the dynamics of the cells by GFP green fluorescence⁴⁾. In the current study, to further limit the number of cells to be transplanted, we performed enzyme treatment on the grafts and transplanted only cells dispersed from the isolated apical buds. With this new approach, we aimed to elucidate the fate of HERS cells after tissue transplantation and to utilize the cells in new cell-based regenerative therapies.

In periodontal tissue regeneration therapy, the cementum, the periodontal ligament, and the alveolar bone are expected to be regenerated. This is because the cementum is calcified periodontal tissue bound to the dentin, and one end of the primary fibers of the periodontal ligament enters the cementum as Sharpy fibers, while the other end joins the alveolar bone to help hold the tooth in place. This study investigated the kinetics of epithelial tissue stem cells after transplantation by tracking GFP fluorescence.

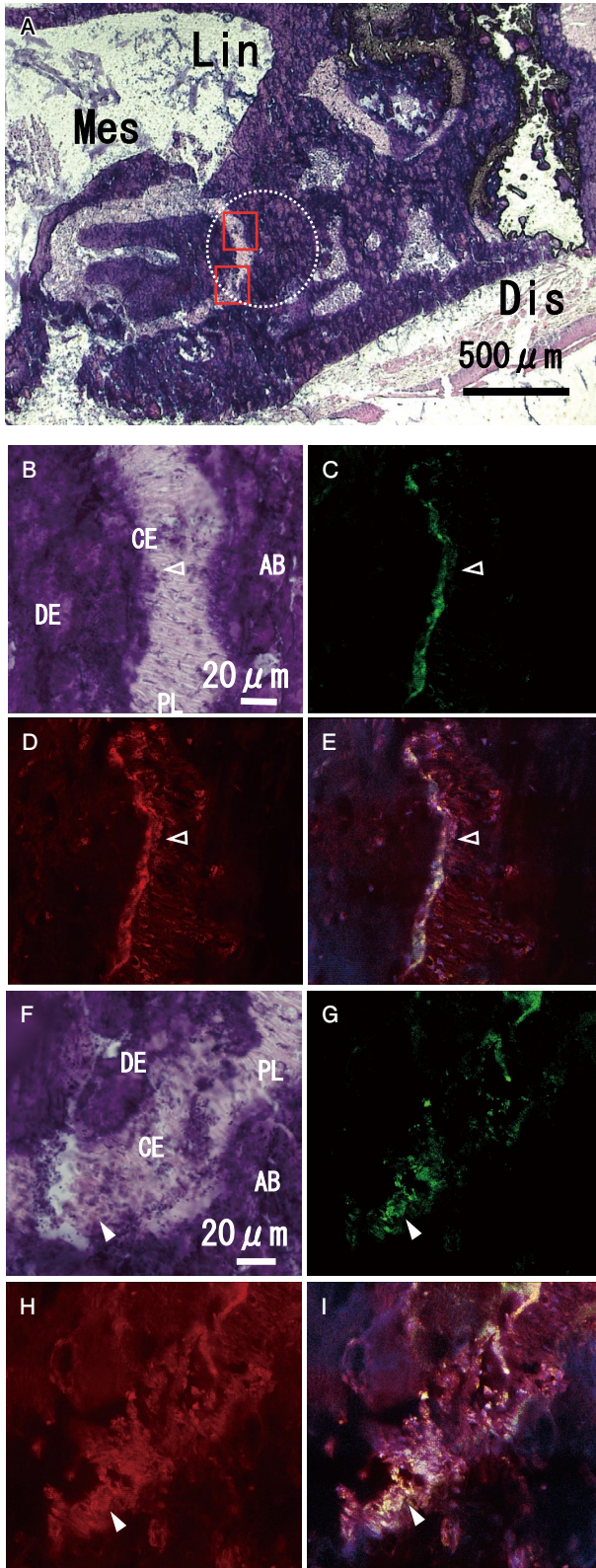


Fig. 5 HE-stained and immunofluorescent-stained images at 12 weeks after transplantation

A : HE image of a horizontal section of the maxillary first molar. Magnified images of the red-framed areas are shown in B and F. The area of the created bone defect is shown as a dotted white circle. Mes : mesial root ; Dis : distal root ; Lin : lingual root

B : Magnified HE image of the distal surface of the mesial root (palatal side). The outlined arrowhead indicates the transplanted cells. C, D, and E show immunofluorescent-stained images of the same area. AB : alveolar bone ; PL : periodontal ligament ; CE : cementum ; DE : dentin

C : GFP-positive cells are aligned along the cementum surface (outlined arrowhead).

D : OCN-positive cells are aligned along the cementum surface (outlined arrowhead).

E : Merged image of C, D, and DNA stained with DAPI showing that most of the GFP-positive cells are OCN-positive.

F : Magnified HE image of the distal surface of the mesial root (buccal side). The arrowhead indicates the transplanted cells. Immunofluorescent-stained images of the same area are shown in G, H, and I. AB : alveolar bone ; PL : periodontal ligament ; CE : cementum ; DE : dentin

G : GFP-positive cells are aligned along the cementum surface ; some are found in the periodontal ligament space (arrowhead).

H : OCN-positive cells are aligned along the cementum surface and in the periodontal ligament space (arrowhead).

I : Merged image of G, H, and DNA stained with DAPI showing that GFP-positive cells in the periodontal ligament space are predominantly OCN-positive.

CEMP1 is explicitly expressed in cementoblasts. It is also weakly expressed in mesenchymal cells such as osteoblasts, osteocytes, cement cells, and fibroblasts^{20,21}.

The results showed that the cells migrated into the periodontal ligament space and differentiated into periodontal and cementoblast-like cells. Some of the cells

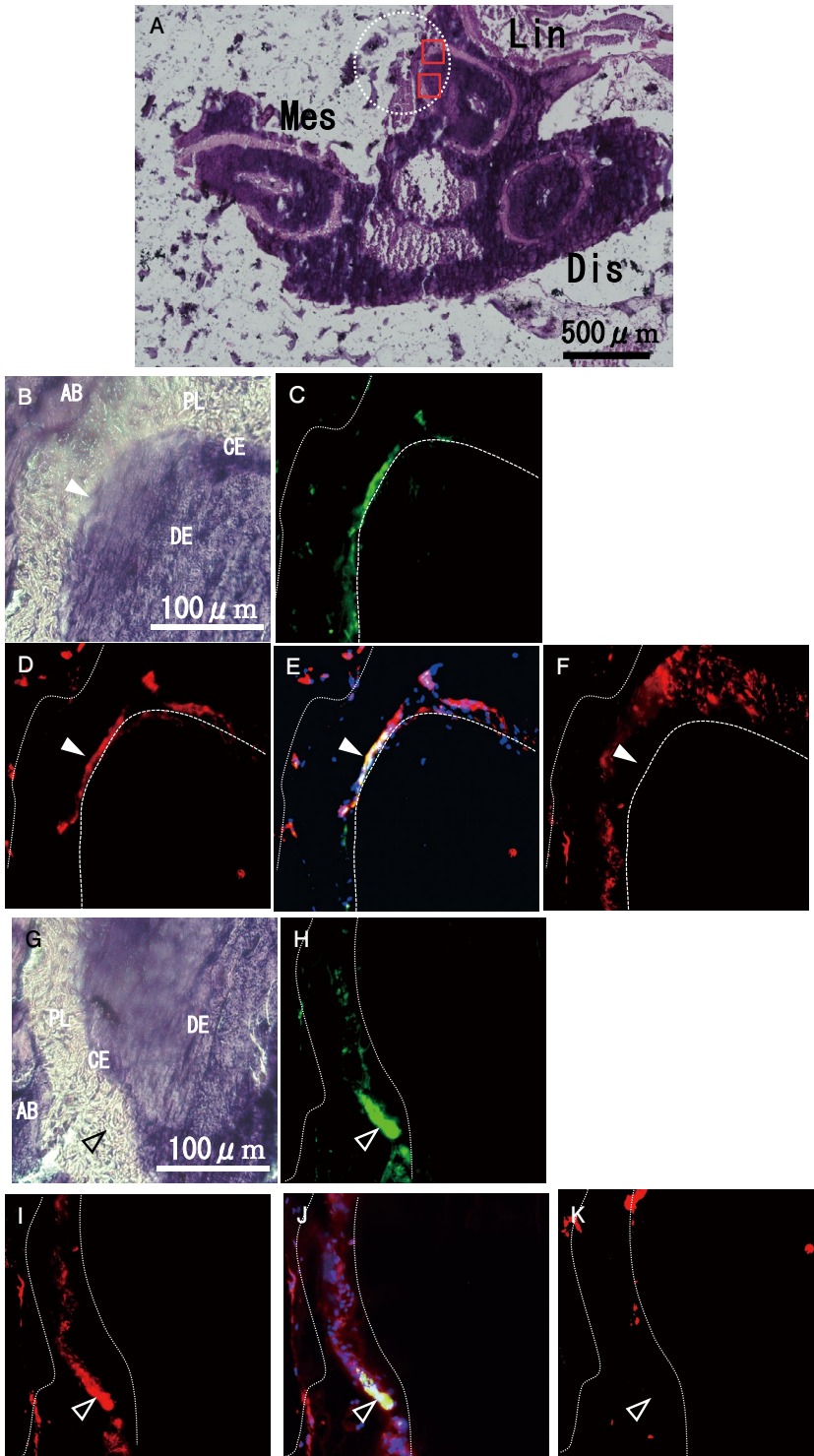


Fig. 6 CEMP1- and CK10-positive cells at 12 weeks after transplantation.

A : HE image of a horizontal section of the maxillary first molar. A magnified image of the red-framed areas is shown in B and G. The location of the created bone defect is shown as a dotted white circle. Mes : mesial root ; Dis : distal root ; Lin : lingual root

B : Magnified HE image of the mesial aspect of the lingual root (palatal side). The arrowhead indicates the transplanted cells. Immunofluorescent-stained images of the same area are shown in C, D, E, and F. AB : alveolar bone ; PL : periodontal ligament ; CE : cementum ; DE : dentin

C : GFP-positive cells are mostly aligned along the cementum surface (arrowhead) and alveolar bone surface.

D : CEMP1-positive cells are found on the cementum and alveolar bone surfaces.

E : Merged image of C, D, and DNA stained with DAPI showing that parts of the GFP-positive cells along the cementum surface are CEMP1-positive.

F : CK10-positive cells are primarily aligned in the periodontal space. CEMP1-positive cells (arrowhead in D) along the cementum surface are found to be CK10-negative in F.

G : Magnified HE image of the mesial aspect of the lingual root (labial side). The outlined arrowhead indicates the transplanted cells. Immunofluorescent-stained images of the same area are shown in H, I, J, and K. AB : alveolar bone ; PL : periodontal ligament ; CE : cementum ; DE : dentin

H : GFP-positive cells are mostly aligned along the cementum surface (outlined arrowhead) and alveolar bone surface.

I : CK10-positive cells are found on the cementum and alveolar bone surfaces.

J : Merged image of H, I, and DNA stained with DAPI showing that among GFP-positive cells, those within the periodontal ligament are predominantly CK10-positive.

K : CEMP1-positive cells are mostly aligned along the cementum surface. CK10-positive cells (outlined arrowhead in I) in the periodontal space are found to be CEMP1-negative in K.

were OCN-positive and CEMP1-positive on the surface of the cementum with cement matrix-like structures.

This experiment observed the healing process in observation periods of 1, 4, and 12 weeks. The transplanted cells were already OCN-positive at one week postoperatively, indicating that a shorter observation period is needed to observe EMT of enamel organ-derived cells. It was deemed necessary to keep the transplanted cells over a long period to determine how they are taken up and function in the tissue.

Our observations revealed that some transplanted cells underwent EMT and became cementoblast-like on the root surface and osteoblast-like, where they were incorporated into the alveolar bone. Both cementoblast-like and osteoblast-like cells were CEMP1-positive. On the other hand, CEMP1-negative and CK10-positive cells were located in the middle of the periodontal ligament space, suggesting that they settled into the tissue as ERM without undergoing EMT. It is interesting to see how the transplanted cells migrate and settle or differentiate under the influence of surrounding cells. These results suggest that enamel organ-derived tissue stem cells can differentiate into osteoblasts and cementoblasts/cementocytes and could be the source of periodontal tissue regeneration.

Numerous *in vitro* and *in vivo* experiments support that HERS undergoes EMT and differentiates into cementoblasts⁸⁻¹². The first report was by Webb et al.⁸ in 1996, who showed immunohistochemical co-localization of keratin and vimentin in cementoblasts during acellular cementum formation in rat molars. They assumed that these were HERS-derived and that acellular cementum could be made by HERS-derived cells.

Zeichner-David et al.⁹ isolated HERS cells from the molars of genetically modified mice and created HERS-derived cell lines. These cells initially secreted enamel-associated proteins such as ameloblastin but gradually changed morphology to secrete an extracellular matrix with calcification that resembled the structure of acellular cementum. Based on this finding, they hypothesized that acellular cementum is formed from HERS-origin cementoblasts and that cellular cementum is formed from neural crest-origin cementoblasts.

Sonoyama et al.¹⁰ immortalized human HERS cells, established them as cell lines, and investigated their properties *in vitro*. They found that HERS cells could differentiate periodontal ligament stem cells to produce

calcified nodules. HERS cells also expressed markers of cementum- and bone-related proteins such as enamel protein, cytokeratin, vimentin, and E-cadherin. Furthermore, TGF- β 1-treated HERS cells activated the PI3K/AKT pathway, resulting in EMT, and subcutaneous transplantation of HERS cells after 48 hours of TGF- β 1 treatment in mice revealed cementum-like calcification.

Akimoto et al.¹¹ examined gene and protein expression *in vitro* using HERS-derived cell lines. The results showed that mesenchymal markers such as vimentin and N-cadherin and epithelial stem cell markers such as cytokeratin14, E-cadherin, and p63 were observed. In addition, stimulation with TGF- β captured many mesenchymal markers and EMT markers such as snail1 and snail2. These results indicate that HERS cells may undergo EMT during root formation.

Huang et al.¹² investigated cementum formation in molars by genetically engineering a mechanism by which keratin14-positive HERS cells maintained β gal positivity after EMT in experiments using K14-Cre; R26R mice. They found numerous β gal-positive cells in the cementum near the root apex and concluded that HERS cells had differentiated into cementoblasts. Huang et al.'s study strongly suggests that acellular cementum may be composed of cells derived from the enamel epithelium.

Thus, many studies have shown that HERS cells may differentiate into cementoblasts. It has also been suggested that different mechanisms by cells of other origins may form cellular cementum and acellular cementum.

Furthermore, when we look at the early stages of root development, there is an intermediate cementum at the interface between the dentin and cementum surfaces, produced by cells derived from the enamel epithelium. This suggests that HERS cells can deposit cemental matrix and are likely to differentiate into cementoblasts.

On the other hand, some studies suggest that HERS cells do not become cementoblasts. Although the involvement of HERS in the odontoblast during root development is widely accepted, it is still controversial that HERS cells undergo EMT and differentiate into cementoblasts. Luan et al.¹³ used cytokeratin14 as a marker of HERS/ERM cells to observe the root surfaces of mouse molars. They found many cytokeratin14-positive epithelial cells in the cementum, which

they attributed to the encapsulation and incorporation of HERS cells into the calcifying cemental matrix rather than their differentiation into cementoblasts. Although most ERM cells remain close to the cemental surface, they are not strongly involved in cementum formation. Their study supports Lester's view that epithelial cells on the root surface may be bound to the cementum¹⁴.

Hirata and Nakamura¹⁵ reported the absence of keratin-osteopontin co-localization or keratin-bone sialoprotein co-localization in cellular cementum formation using mouse molars. Yamamoto and Takahashi¹⁶ also performed immunohistochemical staining on tissue sections of rat molars and found no evidence of keratin-vimentin co-localization or Runx2-keratin co-localization among cementoblasts and no evidence of epithelial cells differentiating into mesenchymal cells or calcifying^{16,17}. The keratin-positive cells in the cementum were not considered cementoblasts/cementocytes, but HERS cells were left behind in the cementum during cementogenesis^{12,13}. They concluded that HERS cells do not differentiate into cementoblasts regardless of whether they are in cellular or acellular cementum and that cells in the dental follicle differentiate into cementoblasts, as has been the conventional theory.

As described above, *in vivo* studies have yet to reach a clear conclusion. This is partly due to the limitations of the research methodology. Most *in vivo* studies are based on observations at a single time and do not employ a method to follow cells over time to identify HERS cells. We can conclude from Huang et al¹², that acellular cementum is produced from HERS cells, at least in mice.

In periodontal tissue regeneration therapy using enamel matrix protein, which is currently used in routine dental practice, the role of enamel organ-derived cells present in the tissue in regeneration is not well understood; Hammaström et al. reported that there is acellular cementum deposition by the combination of enamel matrix proteins in rat molars and monkey anterior teeth^{22,23}. They considered that mesenchymal cells differentiated into cementoblasts and formed acellular cementum by the action of enamel matrix protein. However, it has not yet been demonstrated that mesenchymal cells are responsible for developing acellular cementum in periodontal tissue regeneration therapy. It is also possible that the mesenchymal cells themselves

are observed as fibroblasts in the tissue due to the EMT of enamel organ-derived epithelial cells.

In this study, animal experiments were conducted in mice to elucidate the role of enamel organ-derived cells in periodontal tissues and to apply them to periodontal tissue regeneration therapy by transplanting them directly into wounds. The cells may have a dual function by becoming cementoblasts and as HERS, inducing surrounding mesenchymal cells to become cementoblasts by releasing enamel matrix proteins.

It has been reported that the transcription factor *sox2* regulates apical bud cells²⁴, and HERS cells express genes related to epithelial stem cells and embryonic stem cell markers such as Oct-4, Nanog, and SSEA-4^{25,26}, so there is a possibility that these cells can be used for tissue regeneration. However, there is currently no suitable cell source for clinical use, and seeking such a source from extracted teeth, ES cells, or iPS cells, is a high hurdle. However, periodontal tissues have distinct cell populations, such as ERMs, which are essential in cementum homeostasis and repair. There is potential to develop periodontal tissue regeneration therapy using these cell sources²⁷.

One problem of our study is that the bone defects were too significant compared to those in experimental animals, resulting in excessive invasion. Thus, the results were uneven as a controlled study for tissue regeneration. In the future, we would like to further verify the results by performing cell transplantation with palatal flap formation only, without creating a bone defect.

Conclusion

It was suggested that enamel organ-derived tissue stem cells may differentiate into osteoblasts and cementoblasts/cementocytes and could be the source of periodontal tissue regeneration.

Acknowledgments

We would like to express our deep appreciation to Dr. Hidemitsu Harada, Professor of Iwate Medical University School of Dentistry, who kindly taught us how to collect apical bud cells from the jaws of mice.

Conflict of Interest

We have no conflicts of interest to disclose regarding the present paper.

References

- 1) Harada H, Ohshima H. New perspectives on tooth development and the dental stem cell niche. *Arch Histol Cytol* 2004; 67: 1-11.
- 2) Morotomi T, Kawano S, Toyono T, Kitamura C, Terashita M, Uchida T. *In vitro* differentiation of dental epithelial progenitor cells through epithelial-mesenchymal interactions. *Arch Oral Biol* 2005; 50: 695-705.
- 3) Ohshima H, Nakasone N, Hashimoto E, Sakai H, Nakakura-Ohshima K, Harada H. The eternal tooth germ is formed at the apical end of continuously growing teeth. *Arch Oral Biol* 2005; 50: 153-157.
- 4) Maruo N, Sakagami R, Yoshinaga Y, Okamura K, Sawa Y. Development of an apical bud differentiation model using transgenic mice expressing green fluorescent protein as a donor. *PLoS ONE* 2016; 11: e0150766.
- 5) Wentz FM, Weinmann JP, Schour I. The prevalence, distribution, and morphologic changes of the epithelial remnants in the molar region of the rat. *J Dent Res* 1950; 29: 637-646.
- 6) Kaneko H, Hashimoto S, Enokiya Y, Ogiuchi H, Shimono M. Cell proliferation and death of Hertwig's epithelial root sheath in the rat. *Cell Tissue Res* 1999; 298: 95-103.
- 7) Luan X, Ito Y, Diekwisch TG. Evolution and development of Hertwig's epithelial root sheath. *Dev Dyn* 2006; 235: 1167-1180.
- 8) Webb PP, Moxham BJ, Benjamin M, Ralphs JR. Changing expression of intermediate filaments in fibroblasts and cementoblasts of the developing periodontal ligament of the rat molar teeth. *J Anat* 1996; 188: 529-539.
- 9) Zeichner-David M, Oishi K, Su Z, Zakartchenko V, Chen LS, Arzate H, Bringas P Jr. Role of Hertwig's epithelial root sheath cells in tooth root development. *Dev Dyn* 2003; 228: 651-663.
- 10) Sonoyama W, Seo BM, Yamaza T, Shi S. Human Hertwig's epithelial root sheath cells play crucial roles in cementum formation. *J Dent Res* 2007; 86: 594-599.
- 11) Akimoto T, Fujiwara N, Kagiya T, Otsu K, Ishizeki K, Harada H. Establishment of Hertwig's epithelial root sheath cell line from cells involved in epithelial-mesenchymal transition. *Biochem Biophys Res Commun* 2001; 404: 308-312.
- 12) Huang X, Bringas P Jr, Slavkin HC, Chai Y. Fate of HERS during tooth root development. *Dev Biol* 2009; 334: 22-30.
- 13) Luan X, Ito Y, Diekwisch TG. Evolution and development of Hertwig's epithelial root sheath. *Dev Dyn* 2006; 235: 1167-1180.
- 14) Lester KS. The incorporation of epithelial cells by cementum. *J Ultrastr Res* 1969; 27: 63-87.
- 15) Hirata A, Nakamura H. Localization of perlecan and heparanase in Hertwig's epithelial root sheath during root formation in mouse molars. *J Histochem Cytochem* 2006; 54: 1105-1113.
- 16) Yamamoto T, Takahashi S. Hertwig's epithelial root sheath cells do not transform into cementoblasts in rat molar cementogenesis. *Ann Anat* 2009; 191: 547-555.
- 17) Yamamoto T, Yamamoto T, Yamada T, Hasegawa T, Hongo H, Oda K, Amizuka N. Hertwig's epithelial root sheath cell behavior during initial acellular cementogenesis in rat molars. *Histochem Cell Biol* 2014; 142: 489-496.
- 18) Okabe M, Ikawa M, Kominami K, Nakanishi T, Nishimune Y. 'Green mice' as a source of ubiquitous green cells. *FEBS Lett* 1997; 407: 313-319.
- 19) Ikawa M, Kominami K, Yoshimura Y, Tanaka K, Nishimune Y, Okabe M. Green fluorescent protein as a marker in transgenic mice. *Dev Growth Differ* 1995; 37: 455-459.
- 20) Komaki M, Iwasaki K, Arzate H, Narayanan AS, Izumi Y, Morita I. Cementum protein 1 (CEMP1) induces a cementoblastic phenotype and reduces osteoblastic differentiation in periodontal ligament cells. *J Cell Physiol* 2015; 227: 649-657.
- 21) Arzate H, Jiménez-García LF, Álvarez-Pérez MA, Landa A, Bar-Kana I, Pitaru S. Immunolocalization of a human cementoblastoma-conditioned medium-derived protein. *J Dent Res* 2002; 81: 541-546.
- 22) Hammarström L. Enamel matrix, cementum development and regeneration. *J Clin Periodontol* 1997; 24: 658-668.
- 23) Hammarström L, Heijl L, Gestrelus S. Periodontal regeneration in a buccal dehiscence model in monkeys after application of enamel matrix proteins. *J Clin Periodontol* 1997; 24: 669-677.
- 24) Zhang L, Yuan G, Liu H, Lin H, Wan C, Chen Z. Expression pattern of Sox2 during mouse tooth development. *Gene Expr Patterns* 2012; 12: 273-281.
- 25) Nam H, Kim J, Park J, Park JC, Kim JW, Seo BM, Lee JC. Expression profile of the stem cell markers in human Hertwig's epithelial root sheath/Epithelial rests of Malassez cells. *Mol Cells* 2011; 31: 355-360.
- 26) Nakagawa E, Li Z, Jeong-Oh S, Eun-Jung K, Sung-Won C, Hayato O, Zhi C, Han-Sung J. The novel expression of Oct3/4 and Bmi1 in the root development of mouse molars. *Cell Tissue Res* 2012; 347: 479-484.
- 27) Shinmura Y, Tsuchiya S, Hata K, Honda JM. Quiescent epithelial cell rests of Malassez can differentiate into ameloblast-like cells. *J Cell Physiol* 2008; 217: 728-738.

Five-year Prognosis and Risk Factor Analysis of Open Flap Debridement for Older People

Yukari AOKI-NONAKA, Takahiro HOKARI, Yumi MATSUKAWA, Keisuke SATO, Miki HARA, Mai TAKEUCHI, Kei TAKAMISAWA, Kyoko YAMAZAKI, Takahiro TSUZUNO, Hikaru TAMURA, Takumi HIYOSHI, Fumiya MEGURO, Emi HOSHIKAWA, Aoi MATSUGISHI, Chihiro KANEKO, Shuhei MINEO, Moe YAMASHITA and Koichi TABETA

Division of Periodontology, Faculty of Dentistry & Graduate School of Medical and Dental Sciences, Niigata University

Abstract

Purpose: Examination of the effectiveness of periodontal surgery for older people for which no solid evidence is available is important because the number of healthy, independent older patients is increasing annually. This study aimed to clarify the risk factors associated with the efficacy and prognosis of open flap debridement for older patients.

Methods: Clinical data of 186 patients who underwent open flap debridement and were subsequently followed by supportive periodontal therapy (SPT) or maintenance for >5 years were retrospectively reviewed. Patients were divided into two groups according to age at the time of periodontal surgery: an adult group, aged 20-64 years and an older group, aged ≥ 65 years. Improvement, recurrence, and tooth loss were evaluated, and related risk factors were analyzed by multivariate logistic regression analysis.

Results: The improvement of periodontal disease by open flap debridement in the older group was similar to that in the adult group, and no difference was found in the frequency of tooth loss in the 5 years after the start of SPT. However, the risk of recurrence at 5 years after the start of SPT was three times higher in the older group than in the adult group, suggesting that age is a risk factor for recurrence. In this study, no risk factors were specific to the older group other than age. This suggests that aggressive open flap debridement can be considered even in patients aged ≥ 65 years if there are no underlying diseases or compliance problems. However, the possibility of future hospital visits affected by health status and social background, presence of bleeding during probing, increase in pocket depth of ≥ 6 mm, and changes in the total periodontal inflamed surface area (total PISA), should be fully considered, and regular maintenance should be continued after surgical procedures.

Conclusion: The results of open flap debridement in patients aged ≥ 65 years were comparable to those in patients aged <65 years. In older patients without underlying disease or compliance problems, open flap debridement should be actively considered. However, age is a risk factor for recurrence and regular postoperative management should be continued with attention to changes in clinical parameters.

Key words: older people, open flap debridement, risk factor

Introduction

The population aged ≥ 65 years in Japan was 36.21 million in 2021, with an aging rate of 28.9%, and the aging rate will increase to approximately 40% by 2060¹⁾. The number of remaining teeth among older people has increased markedly, and the proportion of those with ≥ 20 teeth at age 80 years now exceeds 50%. However, the prevalence of periodontal diseases is increasing annually as the number of remaining teeth increases²⁾.

Periodontal disease is a chronic inflammatory disease caused by bacterial biofilm. Periodontal surgical treatment is used when the cause cannot be adequately removed by basic periodontal treatment, and deep periodontal pockets remain.

Many studies have examined bone defect morphology, materials, and surgical techniques as factors involved in the prognosis of periodontal surgical treatment³⁾. However, no solid evidence has been obtained as to whether periodontal surgical treatment can be equally effective in older people. The health status and independent capacity of older people vary widely, and their dental treatment is often limited by their underlying disease. Therefore, the goals of periodontal treatment for older people are unclear, making it difficult to design a study with a large-enough sample size to minimize bias.

Maintenance and supportive periodontal therapy (SPT) are important for maintaining dental and oral function after periodontal surgical treatment, and the lack of compliance is significantly associated with tooth loss^{4,5)}. However, older people often discontinue regular visits because of various psychological, physical, and social reasons. For example, older patients with dementia are less motivated to perform oral hygiene and have more periodontitis⁶⁾, and patients with rheumatoid arthritis and stroke have decreased mobility^{7,8)}. On the contrary, healthy life expectancy exceeds 70 years for both men and women, and many older people lead healthy and independent lives. Thus, the pros and cons of aggressive dental treatment should be considered, including periodontal surgery, considering the health status and compliance of the individual.

Therefore, this study aimed to clarify the factors that influence the efficacy and prognosis of periodontal sur-

gical procedures for older patients by retrospectively examining clinical data in healthy patients without periodontitis-related systemic diseases, with the type of periodontal surgery limited to open flap debridement.

Materials and Methods

1. Participant selection

This study was conducted as a longitudinal case-control study. Data were analyzed retrospectively from medical record information and examination data. The quality rating (Newcastle-Ottawa Scale^{9,10)}) of the observational study methodology was 7 points.

The study participants were 186 patients (77 men and 109 women). At the first visit, the mean (\pm SD) age was 54.3 ± 10.9 years, and the mean (\pm SD) number of remaining teeth was 25.1 ± 3.8 . These patients visited the Division of Periodontics, Niigata University Medical and Dental Hospital between April 1, 1998 and November 30, 2018, underwent open flap debridement, and then ≥ 5 years had elapsed after the start of SPT or maintenance. The participant selection process is shown in Figure 1. In addition, selection criteria were age of ≥ 20 years at the first visit, presence of periodontitis, and absence of systemic diseases related to periodontitis (diabetes and cardiovascular diseases). Of the 85 patients excluded because of having < 5 years of SPT or maintenance, 81 had < 5 years postoperatively as of November 30, 2018, and 4 were excluded because they discontinued treatment during SPT or maintenance.

The open flap debridement was performed after basic periodontal treatment when the probing pocket depth was ≥ 4 mm. The surgeon suggested open flap debridement on the basis of factors, including bone defect morphology. Informed consent from the patients was obtained. Periodontal pocket depths were measured using the 6-point method and probing was performed by a dentist or dental hygienist on our staff. Open flap debridement was performed by a dentist with a minimum of 1 year of clinical experience.

In this study, the older group included participants aged ≥ 65 years, which is the current standard in many developed countries, including Japan, and the World Health Organization¹¹⁾. The participants were divided into two groups according to age at the time of periodontal surgery: the adult group included those aged 20–64 years, and the older group included those aged

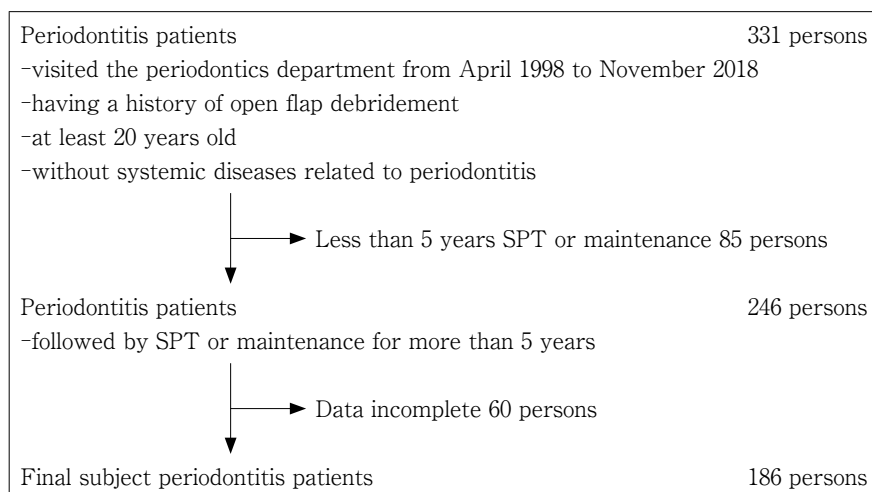


Fig. 1 Process of selecting the participants
Finally, 186 people were targeted in this study.

≥65 years. In this study, 38 participants were aged ≥ 65 years at the time of periodontal surgery, 11 were ≥ 70 years, and the oldest was 79 years of age. In cases with open flap debridement at multiple sites, we ensured that all the applicable surgeries were performed within the same age group.

This study was planned in compliance with the Declaration of Helsinki and was conducted in accordance with the “Ethical Guidelines for Medical and Health Research Involving Human Subjects (MEXT/MHLW, December 22, 2014, partially revised on February 28, 2017).” It was approved by the Niigata University Ethical Review Committee (Date of approval: December 28, 2018; Approval no. 2018-0297).

2. Participant information and clinical parameters

Participant information was examined with regard to the time from the initial diagnosis to the start of SPT (year), recall interval during SPT (times/year), number of patients with smoking habit (smoking, N), number of patients with bruxism (bruxism, N), and number of patients using dentures (use of dentures, N).

Clinical evaluation was performed on the results of four visits: initial visit, after scaling root planing (SRP), beginning of SPT, and after 5 years of SPT. The clinical parameters at the individual level were as follows: number of teeth (N), lost teeth (N), plaque control record (PCR, %), site rate of bleeding on probing (BOP, %), mean probing pocket depth (PD) for intraoral (PD mean, mm), percentage of sites with PD 4-6 mm (PD 4-6 mm,

%), percentage of sites with PD ≥6 mm (PD ≥6 mm, %), total periodontal epithelial surface area (total PESA, mm²), and total periodontal inflamed surface area (total PISA, mm²).

The diagnostic criteria for tooth extraction during the treatment period were based on Hopeless’ criteria¹²⁾.

3. Prognostic evaluation at the tooth level

In the prognostic evaluation at the tooth level where open flap debridement was performed, data on sex, smoking, bruxism, and denture use were matched to the individual level evaluation for each tooth. Compliance with treatment was evaluated based on data on recall intervals and regular visits. Tooth types were classified into molar, premolar, and front teeth. Age was defined as the age at the time of periodontal surgery, and PD was evaluated in terms of the deepest pocket for the target teeth. Changes of the deepest pocket are shown: first visit, end of SRP, start of SPT, and 5 years after the start of SPT.

With reference to the report by Minabe et al.¹⁰⁾, the following three endpoints were defined in this study:

1) Improvement of periodontitis (improvement): A decrease of PD of ≥2 mm at the start of SPT compared with the data after SRP.

2) Recurrence of periodontitis (recurrence): One or more of pocket deepening of ≥3 mm, or periodontal abscess observed after 5 years of SPT compared with the data at the start of SPT.

3) Tooth loss (loss): Extraction or loss of a tooth

Table 1 Participant information

	Total (N=186)	Age<65 (N=148)	Age≥65 (N=38)	p-value
Men (N) ϕ	77 (41.4%)	61	16	>0.999
Women (N) ϕ	109 (58.6%)	87	22	
Smoking status (N) ϕ	14 (7.5%)	13	1	0.472
Bruxism (N) ϕ	16 (8.6%)	11	5	0.176
Use of dentures (N)	11 (5.9%)	7	4	0.119
Time from first visit to start of SPT (year)	3.4±2.4 (Range 0-15)	3.4±2.5	3.3±2.0	0.781
Recall interval (times/year)	4.0±1.4 (Range 0-13)	4.1±1.5	3.9±0.7	0.482

Adult group aged <65 vs. older group aged ≥65. Fisher's exact test was performed for the items indicated as ϕ , and the Mann-Whitney *U* test was performed for other items. Values represent mean±SD, * : p<0.05. SPT, supportive periodontal therapy.

within 5 years after the start of SPT.

4. Statistical analysis

Fisher's exact test and the Mann-Whitney *U* test were used to analyze participant information. For clinical data at the individual level, Tukey's multiple comparisons test was used to analyze changes over time within the same group, and the Mann-Whitney *U* test was used for comparisons between the two groups at the same time point.

The chi-square test and multivariate logistic regression analysis were used to analyze the association between prognostic risk factors and improvement, recurrence, and tooth loss. A statistically significant p value of <0.05 was used. IBM SPSS Statistics for Windows version 26.0 (IBM Corp., Armonk, NY, USA) was used for statistical analysis. Receiver operator characteristic (ROC) curve analysis was used to predict the risk of recurrence of periodontitis using EZR¹³.

A prior analysis of power using G*Power 3 (<http://www.gpower.hhu.de/>) showed a sample size of 32 (chi-square test, effect size 0.5, α error prob 0.05, power (1- β error prob) 0.8, degrees of freedom 1), which is sufficient to examine sample sizes at the patient and tooth levels.

Results

1. Participant information

The participant information is shown in Table 1. Patients were divided into two age groups: 148 were younger than 65 years (adult group) and 38 were 65 years or older (older group) at the time of periodontal

surgery. No significant difference was found in the ratio of male and female participants between the two groups. No differences were found in smoking, bruxism, or denture use. The mean (\pm SD) time from the first visit to the start of SPT was 3.4±2.5 years in the adult group and 3.3±2.0 years in the older group, with no significant difference. The recall intervals during SPT were 4.1±1.5 times/year in the adult group and 3.9±0.7 times/year in the older group, showing no difference between the two groups.

2. Changes in the clinical parameters over time at the individual level

Tables 2-a and 2-b show the changes in clinical parameter values over time at the individual level for the adult group and older group, respectively. When comparing the changes in clinical parameters from the initial visit to those after basic treatment, all values, except for the number of missing teeth, decreased significantly after SRP in both the adult and older groups, in which the number of missing teeth increased significantly in both groups.

A comparison between values after SRP and at the start of SPT, i.e., before and after periodontal surgery, showed no significant decrease in PCR in the adult group or in PCR, BOP, PD 4-6 mm, and total PISA in the older group, but significant changes were noted in other parameters.

In the comparison at each time point between the adult group and older group, no significant difference was noted between the two groups in all items at the first visit, at the end of basic treatment, or at the start of SPT, including PD mean, percentage of sites with PD

Table 2 Changes over time in clinical data at the individual level

a) Age < 65 (N=148)				
	First visit	End of SRP	Start of SPT	5 years after the start of SPT
Number of teeth (N)	25.3±3.8	24.4±4.3 (*<0.0001)	23.7±4.5 (*0.0001)	23.1±4.9 (*<0.0001)
Lost teeth (N)	2.7±3.8	3.6±4.3 (*<0.0001)	4.3±4.5 (*0.0001)	4.9±4.9 (*<0.0001)
PCR (%)	33.0±27.0	9.3±11.6 (*<0.0001)	8.0±13.1 (0.461)	10.4±14.3 (0.218)
BOP (%)	19.3±20.8	6.7±7.9 (*<0.0001)	4.0±6.2 (*<0.0001)	4.6±6.2 (0.897)
PD mean (mm)	3.5±1.1	2.7±0.6 (*<0.0001)	2.3±0.5 (*<0.0001)	2.3±0.5 (0.276)
PD 4-6 mm (%)	28.1±17.7	13.5±13.9 (*<0.0001)	5.9±8.2 (*<0.0001)	6.2±9.0 (0.945)
PD ≥ 6 mm (%)	7.6±11.5	1.8±3.2 (*<0.0001)	0.3±0.7 (*<0.0001)	0.6±1.8 (0.136)
Total PESA (mm ²)	1,849.1±741.8	1,282.7±411.5 (*<0.0001)	1,023.5±297.1 (*<0.0001)	1,024.7±325.6 (0.999)
Total PISA (mm ²)	501.4±604.8	133.5±176.2 (*<0.0001)	58.9±95.2 (*<0.0001)	63.7±87.6 (0.935)
b) Age ≥ 65 (N=38)				
	First visit	End of SRP	Start of SPT	5 years after the start of SPT
Number of teeth (N)	24.4±4.1	23.6±4.5 (*0.002)	23.0±4.4 (*0.046)	22.4±4.7 (*0.025)
Lost teeth (N)	3.5±4.1	4.4±4.5 (*0.002)	5.0±4.5 (*0.046)	5.7±4.7 (*0.025)
PCR (%)	31.1±29.9	9.3±11.7 (*0.001)	8.1±11.5 (0.995)	11.8±14.1 (0.812)
BOP (%)	22.6±26.6	5.2±7.4 (*0.004)	4.5±6.3 (0.997)	9.0±12.6 (0.083) [#]
PD mean (mm)	3.2±0.96	2.7±0.5 (*0.020)	2.2±0.5 (*<0.0001)	2.4±0.4 (0.222)
PD 4-6 mm (%)	26.0±18.6	13.6±13.7 (*0.0002)	6.5±14.0 (0.085)	5.6±7.8 (0.998)
PD ≥ 6 mm (%)	4.8±6.3	1.4±1.9 (*0.003)	0.4±0.7 (*0.012)	1.0±1.6 (0.088) [#]
Total PESA (mm ²)	1,587.6±581.0	1,238.0±332.9 (*0.0004)	946.5±281.9 (*<0.0001)	1,003.7±261.6 (0.518)
Total PISA (mm ²)	530.3±663.6	92.50±134.2 (*0.0009)	66.9±113.3 (0.796)	131.7±177.6 (0.073) [#]

Clinical data at the individual level of (a) the adult group aged <65 and (b) older group aged ≥65. BOP, bleeding on probing ; PCR, plaque control record ; PD, probing depth ; SPT, supportive periodontal therapy ; SRP, scaling root planing ; Total PESA, total periodontal epithelial surface area ; Total PISA, total periodontal inflamed surface area. Values represent mean±SD.

Tukey's multiple comparisons test was performed for the successive changes at the following points within the same group : (1) first visit vs. end of SRP, (2) end of SRP vs. start of SPT, (3) start of SPT vs. 5 years after the start of SPT. * : p<0.05. The Mann-Whitney U test was performed to compare the values between the adult group aged <65 and the older group aged ≥65 at each time point. # : p<0.05

4-6 mm and PD ≥ 6 mm. Differences in the BOP positivity rate (p=0.042), percentage of sites with PD ≥ 6 mm (p=0.026), and total PISA (p=0.033) were found between the two groups at 5 years after the start of SPT.

3. Frequency of improvement, recurrence, and tooth loss

Table 3 shows data on the 520 teeth that underwent open flap debridement. The mean PD was significantly deeper in the adult group, and the number of BOP-positive teeth was also significantly higher in the adult group than in the older group. The mean amount of PD reduction from the end of SRP to the start of SPT was 1.95±1.49 mm, with no significant difference between

the adult and older groups. Moreover, no significant difference in the amount of PD within 5 years of SPT was found between the adult and older groups.

When the postoperative course was classified for each tooth according to the definitions of each item described in Method 3 above, the results were as follows:

1) At the start of SPT, 354 teeth showed periodontitis improvement, and the improvement rate was 68.1% (adult group, 67.4%; older group, 70.5%).

2) At 5 years after SPT, 48 teeth showed periodontitis recurrence, and the recurrence rate was 9.4% (adult group, 7.0%; older group, 18.0%).

3) During the 5 years of SPT, 7 teeth were lost, and

Table 3 Subjective tooth information

	Total (N=520)	Age<65 (N=408)	Age≥65 (N=112)	p-value
Most deep PD (mm)				
First visit	6.46±1.71	6.56±1.74	6.09±1.52	0.014*
End of SRP	5.57±1.27	5.60±1.29	5.46±1.19	0.395
Start of SPT	3.62±1.29	3.64±1.23	3.53±1.48	0.065
5 years after the start of SPT	3.86±1.52	3.89±1.61	4.13±1.94	0.566
BOP positive (N) ϕ	385	317	68	0.001*
Reduction of PD from end of SRP to start of SPT (mm)	1.95±1.49	1.96±1.44	1.93±1.68	0.644
Increase of PD from start of SPT to 5 years later (mm)	0.32±1.66	0.24±1.48	0.59±2.17	0.347

Subjective tooth information of the adult group aged <65 and the older group aged ≥65. Fisher's exact test was performed for the items indicated as ϕ , and the Mann-Whitney *U* test was performed for other items. Values represent mean±SD. * : p<0.05. BOP, bleeding on probing ; PD, probing depth ; SRP, scaling root planing ; SPT, supportive periodontal therapy.

Table 4 Association between the improvement of periodontitis and prognostic risk factors at the tooth level

Variable	Disease category (N=520)		p-value	
	Improve (N=354)	Non-improve (N=166)		
Sex	Men	162 (45.8%)	64 (38.6%)	0.130
	Women	192 (54.2%)	102 (61.4%)	
Age (year)	≥65	79 (22.3%)	33 (19.9%)	0.569
	<65	275 (77.7%)	133 (80.1%)	
Smoking status	Yes	58 (16.4%)	27 (16.3%)	1.000
	No	296 (83.6%)	139 (83.7%)	
Tooth type	Molar	154 (43.5%)	79 (47.6%)	0.202
	Premolar	81 (22.9%)	44 (26.5%)	
	Front teeth	119 (33.6%)	43 (25.9%)	
Compliance	Regular	340 (96.0%)	161 (97.0%)	0.803
	Irregular	14 (4.0%)	5 (3.0%)	
Bruxism	Yes	44 (12.4%)	13 (7.8%)	0.133
	No	310 (87.6%)	153 (92.2%)	
Use of dentures	Yes	19 (5.4%)	3 (1.8%)	0.064
	No	335 (94.6%)	163 (98.2%)	
PD (mm)	≥6	228 (64.4%)	44 (26.5%)	<0.0001*
	<6	126 (35.6%)	122 (73.5%)	

The chi-square test was performed. Values represent the number of samples (percentage). * : p<0.05.

the loss rate was 1.3% (adult group, 1.47%; older group, 0.89%). There were 2, 2, 2, and 1 missing teeth in the groups aged 45-49, 50-54, 60-64, and 70-74 years, respectively.

4. Association between periodontitis improvement and risk factors

Table 4 shows the association between periodontitis

improvement and risk factors after open flap debridement. The results of the chi-square test showed an association between periodontitis improvement and teeth with a PD of ≥6 mm (p<0.0001). Sex, age, smoking, tooth type, compliance, bruxism, and denture use were not significantly associated with periodontitis improvement.

Multivariate logistic regression analysis was performed to identify factors associated with periodontitis improvement; the results are shown in Table 5. A PD of ≥ 6 mm was significantly associated with periodontitis improvement ($p < 0.0001$, odds ratio [OR] = 5.428, confidence interval [CI] = 3.561-9.272). In addition, molars were less likely to improve than the front teeth

Table 5 Multiple logistic analysis of periodontitis improvement and risk factors

Factor		Odds ratio	95% CI	p-value (Prob>ChiSq)
Age (year)	≥ 65	1.203	0.736-1.968	0.461
	< 65	1		
Tooth type	Molar	0.515	0.318-0.834	0.007*
	Premolar	0.630	0.366-1.084	0.095
	Front teeth	1		
Bruxism	Yes	1.404	0.698-2.827	0.342
	No	1		
PD (mm)	≥ 6	5.428	3.561-9.272	< 0.0001 *
	< 6	1		

Multiple logistic regression analysis was performed.

* : $p < 0.05$.

($p = 0.007$, OR = 0.515, CI = 0.318-0.834). Age was not associated with periodontitis improvement.

Figure 2-a shows the results of the ROC curve analysis on the relationship between periodontitis improvement and age at periodontal surgery. Again, no association was found between age and periodontitis improvement (AUC = 0.535, CI = 0.482-0.587, sensitivity 0.946, specificity 0.116).

5. Association of risk factors with periodontitis recurrence

Table 6 shows the association between periodontitis recurrence and risk factors at 5 years after SPT. The results of the chi-square test showed that age ($p = 0.001$), tooth type ($p = 0.013$), and bruxism ($p = 0.028$) were significantly associated with periodontitis recurrence. Sex, smoking, compliance, denture use, and PD showed no significant association. Furthermore, when the same sample was divided into adult and older groups and subjected to the same chi-square test, tooth type and bruxism were not significantly associated with recurrence in the group aged ≥ 65 years (Supplementary Table 1).

The results of the multivariate logistic regression analysis with periodontitis recurrence as the objective

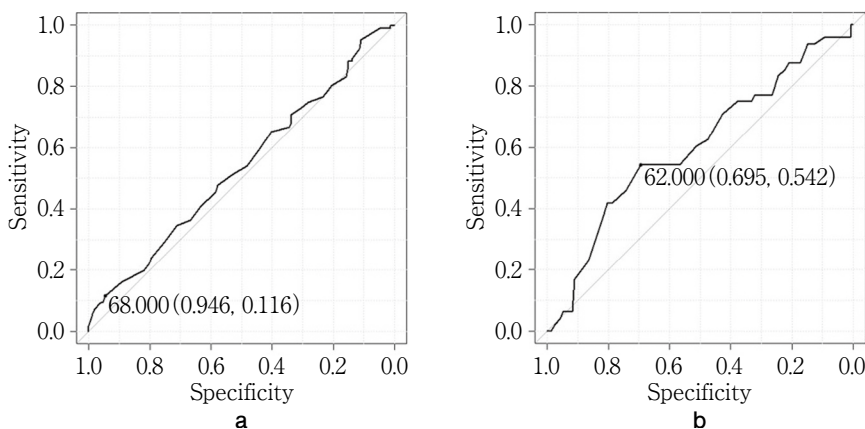


Fig. 2 ROC analysis : A predictive risk analysis of improvement or recurrence of periodontitis

The vertical and horizontal axes indicate sensitivity and specificity, respectively. Age higher than the following cutoff values is considered positive for improvement or recurrence, and false positives are taken as (1 - specificity).

(a) Improvement of periodontitis and age at surgery (AUC = 0.535, CI = 0.482-0.587, sensitivity 0.946, specificity 0.116). Although the cutoff value for age was set at 68.0 years, this graph shows no correlation between age and improvement. (b) Recurrence of periodontitis and age at surgery (AUC = 0.603, CI = 0.515-0.691, sensitivity 0.695, specificity 0.542). The AUC was 0.6, which does not have high predictive power, but the cutoff value for age at increased risk of recurrence was 62.0 years.

Table 6 Association between the recurrence of periodontitis and prognostic risk factors at the tooth level

Variable	Disease category (N=513)		p-value	
	Recurrence (N=48)	Non-recurrence (N=465)		
Sex	Men	16 (33.3%)	205 (44.1%)	0.170
	Women	32 (66.7%)	260 (55.9%)	
Age (year)	≥65	20 (41.7%)	91 (19.6%)	0.001*
	<65	28 (58.3%)	374 (80.4%)	
Smoking status	Yes	11 (22.9%)	73 (15.7%)	0.218
	No	37 (77.1%)	392 (84.3%)	
Tooth type	Molar	31 (64.6%)	197 (42.4%)	0.013*
	Premolar	8 (16.7%)	116 (24.9%)	
	Front teeth	9 (18.8%)	152 (32.7%)	
Compliance	Regular	44 (91.7%)	451 (97.0%)	0.077
	Irregular	4 (8.3%)	14 (3.0%)	
Bruxism	Yes	10 (20.8%)	46 (9.9%)	0.028*
	No	38 (79.2%)	419 (90.1%)	
Use of dentures	Yes	2 (4.2%)	20 (4.3%)	1.000
	No	46 (95.8%)	445 (95.7%)	
PD (mm)	≥6	29 (60.4%)	238 (51.2%)	0.230
	<6	19 (39.6%)	227 (48.8%)	

The chi-square test was performed. Values represent the number of samples (percentage).

* : $p < 0.05$.

Supplementary Table 1 Association between the recurrence of periodontitis and prognostic risk factors at the tooth level by groups

Variable	Disease category (N=111)			Disease category (N=402)			
	Age ≥ 65		p-value	Age < 65		p-value	
	Recurrence (N=20)	Non-recurrence (N=91)		Recurrence (N=28)	Non-recurrence (N=374)		
Sex	Men	7 (35.0%)	34 (37.4%)	1.000	9 (32.1%)	171 (45.7%)	0.175
	Women	13 (65.0%)	57 (62.6%)		19 (67.9%)	203 (54.3%)	
Smoking status	Yes	4 (20.0%)	23 (25.3%)	0.777	7 (25.0%)	50 (13.4%)	0.095
	No	16 (80.0%)	68 (74.7%)		21 (75.0%)	324 (86.6%)	
Tooth type	Molar	12 (60.0%)	36 (39.6%)	0.237	19 (67.9%)	161 (43.0%)	0.039*
	Premolar	4 (20.0%)	24 (26.4%)		4 (14.3%)	92 (24.6%)	
	Front teeth	4 (20.0%)	31 (34.1%)		5 (17.9%)	121 (32.4%)	
Compliance	Regular	17 (85.0%)	86 (94.5%)	0.154	27 (96.4%)	365 (97.6%)	0.518
	Irregular	3 (15.0%)	5 (5.5%)		1 (3.6%)	9 (2.4%)	
Bruxism	Yes	2 (10.0%)	14 (15.4%)	0.732	8 (28.6%)	32 (8.6%)	0.003*
	No	18 (90.0%)	77 (84.6%)		20 (71.4%)	342 (91.4%)	
Use of dentures	Yes	2 (10.0%)	5 (5.5%)	0.607	0 (0.0%)	15 (4.0%)	0.613
	No	18 (90.0%)	86 (94.5%)		28 (100.0%)	359 (96.0%)	
PD (mm)	≥6	12 (60.0%)	44 (48.4%)	0.460	17 (60.7%)	194 (51.9%)	0.435
	<6	8 (40.0%)	47 (51.6%)		11 (39.3%)	180 (48.1%)	

The chi-square test was performed. Values represent the number of samples (percentage). * : $p < 0.05$.

variable are shown in Table 7. Age ≥ 65 years at periodontal surgery ($p=0.001$, OR=3.009, CI=1.598-5.665) and bruxism ($p=0.046$, OR=2.221, CI=1.013-4.873) were strong risk factors for periodontitis recurrence. The molars were more prone to relapse and at higher risk than the front teeth ($p=0.015$, OR=2.663, CI=1.212-5.851).

Figure 2-b shows the results of the ROC curve analysis on the involvement of age in periodontitis recurrence. The cutoff value for the age at which the risk of recurrence increased was 62.0 years (AUC=0.603, CI=0.515-0.691, sensitivity 0.695, specificity 0.542).

6. Association between tooth loss and risk factors

Table 8 shows the association between risk factors and tooth loss events within 5 years of SPT. The results of the chi-square test showed that age, sex, smoking, tooth type, compliance, bruxism, denture use, and PD were not significantly associated with tooth loss.

Discussion

1. Clinical response to treatment based on changes in parameters at the individual level over time

Table 2 shows that all clinical parameters significantly changed after SRP in both the adult and older groups, and no difference was found between the two groups after SRP, indicating that the treatment response to SRP was similar in the adult and older groups.

When the treatment response to open flap debridement was evaluated by comparing the values after SRP with those at the start of SPT, BOP, PD 4-6 mm, and total PISA, which were significantly reduced in the adult group, did not change significantly in the older group, suggesting that the treatment response to open flap debridement in the older group may not be as marked as in the adult group. However, since these examination values were evaluated on the whole oral cavity, the progress was also influenced by other sites where the open flap debridement was not performed. Thus, if multiple sites of severe periodontitis were present, the frequency and degree of residual inflammation would differ between a treatment strategy that thoroughly removes inflammation in all sites with periodon-

Table 7 Multiple logistic analysis of periodontitis recurrence and risk factors

Factor		Odds ratio	95% CI	p-value (Prob>ChiSq)
Age (year)	≥ 65	3.009	1.598-5.665	0.001*
	<65	1		
Tooth type	Molar	2.663	1.212-5.851	0.015*
	Premolar	1.123	0.414-3.049	0.819
	Front teeth	1		
Bruxism	Yes	2.221	1.013-4.873	0.046*
	No	1		
PD (mm)	≥ 6	1.296	0.691-2.430	0.419
	<6	1		

Multiple logistic regression analysis was performed.

* : $p < 0.05$.

tal surgery and one that limits periodontal surgery, which later would be relatively chosen more in older people with no significant change.

A comparison of data from the start of SPT to 5 years at the individual level showed significant changes in the remaining and missing teeth in both groups, but no significant differences in other parameters. PCR and BOP were well below the thresholds for a good prognosis, indicating that the oral condition of both the adult and older groups was well maintained within 5 years of SPT.

In addition, a comparison at each time point between the adult and older groups showed no difference for all items at the initial visit, at the end of basic treatment, or at the start of SPT. However, the BOP positivity rate, percentage of sites with a PD of ≥ 6 mm, and total PISA were significantly increased in the older group compared with the adult group at 5 years of SPT, suggesting that the risk of periodontitis recurrence or progression within 5 years of SPT was increased in the older group.

2. Periodontitis improvement at the tooth level by open flap debridement

Although existing reports have evaluated clinical attachment level (CAL) gain, PD decrease, and bone level increase in the evaluation of treatment outcomes after periodontal surgery³⁾, since CAL and bone level data were insufficient in this study, we defined improvement of periodontitis as a decrease in PD of ≥ 2 mm at the start of SPT, i.e., after periodontal surgery,

Table 8 Association between tooth loss and prognostic risk factors at the tooth level

Variable	Disease category (N=520)		p-value	
	Tooth loss (N=7)	Remaining (N=513)		
Sex	Men	5 (71.4%)	221 (43.1%)	0.248
	Women	2 (28.6%)	292 (56.9%)	
Age (year)	≥65	1 (14.3%)	111 (21.6%)	1.000
	<65	6 (85.7%)	402 (78.4%)	
Smoking status	Yes	1 (14.3%)	84 (16.4%)	1.000
	No	6 (85.7%)	429 (83.6%)	
Tooth type	Molar	5 (71.4%)	228 (44.4%)	0.359
	Premolar	1 (14.3%)	124 (24.2%)	
	Front teeth	1 (14.3%)	161 (31.4%)	
Compliance	Regular	6 (85.7%)	495 (96.5%)	0.231
	Irregular	1 (14.3%)	18 (3.5%)	
Bruxism	Yes	1 (14.3%)	56 (10.9%)	0.559
	No	6 (85.7%)	457 (89.1%)	
Use of dentures	Yes	0 (0.0%)	22 (4.3%)	1.000
	No	7 (100.0%)	491 (95.7%)	
PD (mm)	≥6	5 (71.4%)	267 (52.0%)	0.453
	<6	2 (28.6%)	246 (48.0%)	

The chi-square test was performed. Values represent the number of samples (percentage). * : $p < 0.05$.

compared with that after SRP.

In this study, the efficacy of open flap debridement showed improvement rates of 67.4% in the adult group and 70.5% in the older group. The decrease in PD from the end of SRP to the start of SPT was 1.96 ± 1.44 mm in the adult group and 1.93 ± 1.68 mm in the older group, with no significant difference between the two groups (Table 3). Comparing these values with previous reports, Silvestri et al. reported a decrease of 1.4 ± 1.3 mm in PD 1 year after open flap debridement¹⁴, and Okuda et al. reported a decrease of 2.22 ± 0.81 mm in PD 1 year after surgery as a placebo group for enamel matrix derivatives¹⁵, which was similar to the reduction in the present study. The results of the multivariate logistic analysis also showed no association between age and periodontitis improvement (Table 5), indicating that the adult and older groups had similar treatment efficacy with open flap debridement. In this study, the PCR and compliance of the older group were similar to those of the adult group, which may have influenced the treatment effect.

The results of this study also showed that remaining PD ≥ 6 mm after SRP was significantly associated with periodontitis improvement. Pihlstrom et al. reported that 1 year after open flap debridement, the average

PD reduction in molars was 1.26 mm in areas with PD 4–6 mm, whereas 2.28 mm was observed in areas with PD ≥ 6 mm¹⁶. In addition, surgical therapy for PD ≥ 6 mm was more effective than nonsurgical therapy, resulting in PD reduction of ≥ 0.6 mm and CAL gain of ≥ 0.2 mm 1 year after treatment, but PD 4–6 mm attachment gain was greater by nonsurgical therapy in a systematic review by Heitz-Mayfield et al.¹⁷. In this study, periodontitis improvement was defined as PD reduction of ≥ 2 mm; thus, the amount of reduction was possibly small, and improvement was not considered significant when the PD was < 6 mm. In addition, the amount of adhesion gained could not be examined in this study, but it is necessary to increase the sample size and examine CAL and bone levels in the future.

3. Risk factors involved in periodontitis recurrence

The analysis of risk factors involved in periodontitis recurrence showed that age ≥ 65 years at the time of periodontal surgery, bruxism, and molars were risk factors (Tables 6 and 7). The periodontitis recurrence rates within 5 years of SPT were 7.0% in the adult group and 18.0% in the older group. The multivariate logistic regression analysis showed that the OR of recurrence in those aged ≥ 65 years was 3.009 (Table

7), indicating a high risk of periodontitis recurrence in the older group. The AUC for ROC analysis was 0.6, which does not have high predictive power, but the cut-off value for age at increased risk of recurrence was 62 years (Figure 2-b). Similar multivariate logistic regression analysis separated by age ≥ 60 years ($p=0.068$, $OR=1.761$, $CI=0.958-3.236$) or ≥ 55 years ($p=0.204$, $OR=1.495$, $CI=0.804-2.782$) showed no significant difference in either case, suggesting that age ≥ 65 years is associated with recurrence (data not shown). Therefore, the age limit for the elderly was set at 65 years in this study.

Bruxism showed an OR of 2.2 times higher and molars showed a 2.7 times higher risk of recurrence (Table 7). The prevalence of bruxism is reported to be about twice as high in patients with periodontitis^{18,19}. There are also reports that tooth loss is more common in patients with a high likelihood of bruxism¹⁹. However, a recent systematic review concluded that bruxism does not adversely affect periodontal tissues²⁰. The simultaneous presence of plaque-induced periodontitis and bruxism was found to promote connective tissue destruction²¹, and thus the control of bruxism is necessary for preventing recurrence after periodontal surgical procedures.

As has been reported for tooth types^{16,22}, open flap debridement showed a greater pocket reduction effect in nonmolar teeth than in molar teeth. However, since furcation involvement was not evaluated in this study, further investigation is needed.

Interestingly, neither bruxism nor tooth type was significantly associated with recurrence when the same chi-square test was performed only in the group aged ≥ 65 years (Supplementary Table 1), indicating that the age factor of ≥ 65 years may be independently associated with the risk of periodontitis recurrence.

The importance of compliance in maintaining periodontal status during maintenance and SPT has been reported⁴; there were no significant differences in PCR or frequency of visits between the adult and older groups. Although the results of this study did not reveal any factors specific to the older group that increase the risk of recurrence, factors such as the age-related decline in immunity and dietary changes may have an effect. According to Lang and Tonetti's periodontal disease risk assessment model, the bone-resorption age ratio and number of lost teeth also affect

the prognosis of teeth²³. In this study, the number of missing teeth tended to be slightly higher in the older group. The effects of loss patterns and presence or absence of crossbite should be examined in the future. In addition, in Table 2, the BOP positivity rate, sites with a PD of ≥ 6 mm, and increase in the total PISA are clinical indicators of the possibility of recurrence; therefore, it is necessary to pay more attention to changes in these values and conduct regular follow-up in patients aged ≥ 65 years and to consider more intensive plaque control and specialized care for sites at high risk of recurrence.

4. Risk of tooth loss in 5 years of SPT

In previous long-term maintenance studies, the frequency of tooth loss due to periodontal disease has ranged from 1.5²⁴ to 9.8%²⁵, but a review by Chambrone et al. reported a loss rate of 6.8% in a total of 10 reports⁹. In this study, the average loss rate over 5 years of SPT was 1.3%, and the average number of teeth lost per patient was 0.6, indicating a relatively good prognostic outcome. No risk factors were associated with tooth loss in this study (Table 8). Previous clinical studies on age and periodontal treatment have reported a significantly higher risk of tooth loss during the maintenance period after periodontal treatment in patients aged >60 years^{24,26,27}. However, these studies did not distinguish between periodontal surgical treatment or not. On the contrary, reports have not shown a relationship between age and tooth loss^{28,29}. The differences in the age of participants, severity of periodontitis, and compliance with treatment in these previous reports were large; further studies are needed to determine whether age is independently related to tooth loss from other factors⁹. In addition, since the rate of tooth loss due to periodontal disease is as high as 7.4% in long-term SPT cases of >10 years³⁰, further long-term follow-up is necessary.

5. Periodontal surgery in older people

The WHO and Japan define older age as age ≥ 65 years. However, the Japan Federation of Gerontological Societies and the Japan Geriatrics Society have proposed that the definition of older age be revised to ≥ 75 years based on the incidence of motor function, cognitive function, disease, and mortality³¹, indicating that most older people, especially those aged 65-74 years, maintain their physical and mental health independently.

The average life expectancy in Japan in 2021 was 81.47 years for men and 87.57 years for women³²⁾, and the healthy life expectancy is expected to be 72.68 years for men and 75.38 years for women by 2028, leaving a gap of over 10 years³³⁾. Preventing tooth loss and maintaining masticatory function are extremely important for maintaining quality of life, and periodontal surgery is one option for tooth preservation. In this study, the number of patients aged ≥ 70 years was small, with 11 people in the past 10 years. However, the number of potential periodontal surgical indications is likely to be even higher considering that the percentage with ≥ 20 teeth remaining at age 80 is over 50%²⁾.

The results of this study showed that open flap debridement had a certain therapeutic effect regardless of age, with periodontitis improvement being similar in patients aged < 65 years and ≥ 65 years, and that there was no difference in the risk of tooth loss after 5 years of SPT. The study participants were an ideal population who had no health problems and had generally good compliance, and the number of remaining teeth and PCRs at the initial visit, as well as smoking and denture use, were not different between those aged < 65 years and ≥ 65 years. Furthermore, only four patients dropped out during the SPT period, and most patients were under continuous management. Under these favorable conditions, open flap debridement may be actively considered even for patients aged ≥ 65 years. Although this study did not examine people aged ≥ 80 years, in patients aged ≥ 80 years who are sick, the decision should be made more carefully, not only because of the risk of inadequate self-care, but also because of the increased risk of interruption of hospital visits for health reasons or other reasons.

Further studies are needed to evaluate the efficacy of regenerative therapy for older people. However, evaluating the attachment level and bone level is necessary, which could not be included in this study. Collecting data on cases with long-term follow-up is recommended. Further accumulation of evidence to provide safer and more effective dental treatment for older people may contribute to extending the healthy life expectancy of the nation.

Conclusion

The results of open flap debridement in patients

aged ≥ 65 years were comparable to those in patients aged < 65 years. In older patients without underlying diseases or compliance problems, open flap debridement should be actively considered. However, age is a risk factor for recurrence and regular postoperative management should be continued with attention to changes in BOP and PD.

Conflicts of Interest

The authors declare no conflict of interest related to this paper.

Acknowledgment

For their great cooperation in conducting this research and preparing this paper, we thank Dr. Naoki Takahashi, Dr. Tetsuo Kobayashi, Dr. Noriko Sugita, Dr. Yasutaka Komatsu, Dr. Tomoki Maekawa, Dr. Haruna Miyazawa, Dr. Takehiko Kubota, Dr. Kazuhiro Okuda, Dr. Kazuhisa Yamazaki, and Dr. Hiromasa Yoshie. We also sincerely thank all doctors of the Division of Periodontology at Niigata University. This work was supported by the Japan Society for the Promotion of Science (JSPS; Tokyo, Japan) KAKENHI, grant no. JP19K19021 to T. H.

References

- 1) Office Japan cabinet. Annual report on the ageing society; 2022. www8.cao.go.jp/kourei/whitepaper/w-2022/zenbun/04pdf_index.html (cited 2022. 12. 10) (In Japanese)
- 2) Ministry of Health Labour and Welfare. Survey of dental diseases; 2016. mhlw.go.jp/toukei/list/dl/62-28-02.pdf (cited 2022. 12. 10) (In Japanese)
- 3) Nibali L, Koidou VP, Nieri M, Barbato L, Pagliaro U, Cairo F. Regenerative surgery versus access flap for the treatment of intra-bony periodontal defects: A systematic review and meta-analysis. *J Clin Periodontol* 2020; 47; Suppl 22: 320-351.
- 4) Wilson TG, Jr., Glover ME, Schoen J, Baus C, Jacobs T. Compliance with maintenance therapy in a private periodontal practice. *J Periodontol* 1984; 55: 468-473.
- 5) Kocher T, König J, Dzierzon U, Sawaf H, Plagmann HC. Disease progression in periodontally treated and untreated patients—a retrospective study. *J Clin Periodontol* 2000; 27: 866-872.
- 6) Delwel S, Binnekade TT, Perez RSGM, Hertogh CMPM, Scherder EJA, Lobbezoo F. Oral hygiene and oral health in older people with dementia: a comprehensive review with focus on oral soft tissues. *Clin Oral Investig* 2018; 22: 93-108.
- 7) Zhang Y, Niu J, Kelly-Hayes M, Chaisson CE, Aliabadi P,

- Felson DT. Prevalence of symptomatic hand osteoarthritis and its impact on functional status among the elderly: the Framingham Study. *Am J Epidemiol* 2002; 156: 1021-1027.
- 8) Schimmel M, Leemann B, Herrmann FR, Kiliaridis S, Schnider A, Müller F. Masticatory function and bite force in stroke patients. *J Dent Res* 2011; 90: 230-234.
 - 9) Chambrone L, Chambrone D, Lima LA, Chambrone LA. Predictors of tooth loss during long-term periodontal maintenance: a systematic review of observational studies. *J Clin Periodontol* 2010; 37: 675-684.
 - 10) Minabe M, Takano S, Harai K, Inagaki K. Patient-related prognostic risk factors in severe periodontitis patients after periodontal therapy. *J Jpn Soc Periodontol* 2013; 55: 170-182.
 - 11) World Health Organization. Men Ageing and Health. 2001. https://apps.who.int/iris/bitstream/handle/10665/66941/WHO_NMH_NPH_01.2.pdf (cited 2022. 12. 10)
 - 12) Checchi L, Montecvecchi M, Gatto MR, Trombelli L. Retrospective study of tooth loss in 92 treated periodontal patients. *J Clin Periodontol* 2002; 29: 651-656.
 - 13) Kanda Y. Investigation of the freely available easy-to-use software 'EZR' for medical statistics. *Bone Marrow Transplant* 2013; 48: 452-458.
 - 14) Silvestri M, Ricci G, Rasperini G, Sartori S, Cattaneo V. Comparison of treatments of infrabony defects with enamel matrix derivative, guided tissue regeneration with a nonresorbable membrane and Widman modified flap. A pilot study. *J Clin Periodontol* 2000; 27: 603-610.
 - 15) Okuda K, Momose M, Miyazaki A, Murata M, Yokoyama S, Yonezawa Y, Wolff LF, Yoshie H. Enamel matrix derivative in the treatment of human intrabony osseous defects. *J Periodontol* 2000; 71: 1821-1828.
 - 16) Pihlstrom BL, Oliphant TH, McHugh RB. Molar and non-molar teeth compared over 6 1/2 years following two methods of periodontal therapy. *J Periodontol* 1984; 55: 499-504.
 - 17) Heitz-Mayfield LJ, Trombelli L, Heitz F, Needleman I, Moles D. A systematic review of the effect of surgical debridement vs. non-surgical debridement for the treatment of chronic periodontitis. *J Clin Periodontol* 2002; 29: Suppl 3: 92-102.
 - 18) Martinez-Canut P. Predictors of tooth loss due to periodontal disease in patients following long-term periodontal maintenance. *J Clin Periodontol* 2015; 42: 1115-1125.
 - 19) Bilgin Çetin M, Sezgin Y, Maraş E, Cebeci İA. Association of probable bruxism with periodontal status: A cross-sectional study in patients seeking periodontal care. *J Periodont Res* 2021; 56: 370-378.
 - 20) Manfredini D, Ahlberg J, Mura R, Lobbezoo F. Bruxism is unlikely to cause damage to the periodontium: findings from a systematic literature assessment. *J Periodontol* 2015; 86: 546-555.
 - 21) Fan J, Caton JG. Occlusal trauma and excessive occlusal forces: narrative review, case definitions, and diagnostic considerations. *J Periodontol* 2018; 89; Suppl 1: S214-S222.
 - 22) Lindhe J, Westfelt E, Nyman S, Socransky SS, Heijl L, Bratthall G. Healing following surgical/non-surgical treatment of periodontal disease. A clinical study. *J Clin Periodontol* 1982; 9: 115-128.
 - 23) Lang NP, Tonetti MS. Periodontal risk assessment (PRA) for patients in supportive periodontal therapy (SPT). *Oral Health Prev Dent* 2003; 1: 7-16.
 - 24) Fardal Ø, Johannessen AC, Linden GJ. Tooth loss during maintenance following periodontal treatment in a periodontal practice in Norway. *J Clin Periodontol* 2004; 31: 550-555.
 - 25) McFall WT, Jr. Tooth loss in 100 treated patients with periodontal disease. A long-term study. *J Periodontol* 1982; 53: 539-549.
 - 26) Ng MC, Ong MM, Lim LP, Koh CG, Chan YH. Tooth loss in compliant and non-compliant periodontally treated patients: 7 years after active periodontal therapy. *J Clin Periodontol* 2011; 38: 499-508.
 - 27) Chambrone LA, Chambrone L. Tooth loss in well-maintained patients with chronic periodontitis during long-term supportive therapy in Brazil. *J Clin Periodontol* 2006; 33: 759-764.
 - 28) Matthews DC, Smith CG, Hanscom SL. Tooth loss in periodontal patients. *J Can Dent Assoc* 2001; 67: 207-210.
 - 29) Tsami A, Pepelassi E, Kodovazenitis G, Komboli M. Parameters affecting tooth loss during periodontal maintenance in a Greek population. *J Am Dent Assoc* 2009; 140: 1100-1107.
 - 30) Graetz C, Dörfer CE, Kahl M, Kocher T, Fawzy El-Sayed K, Wiebe JF, Gomer K, Rühling A. Retention of questionable and hopeless teeth in compliant patients treated for aggressive periodontitis. *J Clin Periodontol* 2011; 38: 707-714.
 - 31) Ouchi Y, Rakugi H, Arai H, Akishita M, Ito H, Toba K, Kai I. Japan Geriatrics Society on the definition, classification of the elderly. Redefining the elderly as aged 75 years and older: proposal from the Joint Committee of Japan Gerontological Society and the Japan Geriatrics Society. *Geriatr Gerontol Int* 2017; 17: 1045-1047.
 - 32) Ministry of Health Labour and Welfare. Life tables in 2021; 2022. <https://www.mhlw.go.jp/toukei/saikin/hw/life/life21/index.html> (cited 2022. 12. 10) (In Japanese)
 - 33) Ministry of Health Labour and Welfare. Health life expectancy in 2019; 2021. <https://www.mhlw.go.jp/content/10904750/000872952.pdf> (cited 2022. 12. 10) (In Japanese)

Shaping Ability of Controlled Memory Wire Nickel-titanium Files by Minimally Invasive Endodontics

Pil Seoung KANG, Takahito TSUKUDA, Kazuhiro ITONAGA,
Masahito YAMANE, Noriko MUTOH and Nobuyuki TANI-ISHII

Department of Endodontics, Kanagawa Dental University

Abstract

Purpose: Minimally invasive endodontics (MI Endo) has been advocated on the basis that minimal cutting of tooth substance prevents root fracture after endodontic therapy. The purpose of this study was to analyze the shaping ability of thermo-mechanically treated controlled memory (CM) wire nickel-titanium (NiTi) files using MI Endo.

Methods: Using a J-shaped root canal model, ProTaper Gold (PTG) and ProTaper Ultimate (PTU) files made of CM wire were used in the experimental group, and ProTaper Universal (PT) files made of conventional NiTi wire were used in the control group, and their cutting properties were compared. The PTU, PTG, and PT groups were further classified into two subgroups (with and without straight line (SL) access), and the root canal width displacement and median displacement were compared between the six groups in total.

Results: For the PTU and PTG groups, the root canal width displacement on the lateral side slightly increased at the 1 mm apical measurement, and there was a significant difference between the displacement on the inner and outer sides at 3-8 mm. However, in the PT control group, the displacement on the inner side increased at 3-5 mm, and the displacement on the outer side increased at 1 and 8 mm. We compared the root canal width displacement in the PTU, PTG, and PT groups between those with and without SL access, but no significant differences were observed. Comparison between the SL and no-SL PTU, PTG, and PT groups revealed no significant differences in root canal width displacement or median displacement at any of the measurement sites.

Conclusions: PTU and PTG made with CM wire resulted in accurate root canal formation with no-SL access.

Key words: minimally invasive endodontics, controlled memory wire, straight line access

Introduction

Successful endodontic therapy is based on root canal preparation that maintains the anatomical root canal morphology, and the clinical application of nickel-titanium (NiTi) files contributes to accurate root canal preparation. Root canal preparation is the basic procedure for removal of cervical dentin, in which the cervical dentin of the upper third of the root canal is formed into a flared shape¹⁻³. Straight line (SL) access facilitates accurate root canal formation by removing dentin from the root canal orifice and reducing the curvature of the root canal. However, SL access is associated with excessive cutting of cervical dentin, which has been reported to reduce tooth fracture resistance^{4,5}. Therefore, in recent years, minimally invasive endodontics (MI Endo) has been advocated, in which root canal preparation with minimal cutting of the dentin to preserve the orifice dentin is reported to prevent root fracture^{7,8}. It has been reported that cervical dentin preservation is more important than coronal occlusal dentin preservation for the prevention of root fracture^{6,7}.

MI Endo⁸ is performed mainly on the west coast of the United States with the objective of minimizing the risk of root canal fracture in comparison with standard root canal preparation. MI Endo advocates maximal preservation of healthy dentin, which influences the design of the access cavity and the choice of root canal restoration^{9,10}. Currently, based on the concept of MI Endo, TruNatomy (TN) files (Dentsply Sirona, Switzerland) have been developed to allow accurate root canal formation without the need for SL access. However, all other NiTi files require root canal preparation based on SL access.

The alloy materials of NiTi files have been improved by introducing the technology of thermo-mechanical treatment and a final surface finishing process. These materials (M wire and CM wire) possess excellent flexibility and fatigue resistance, but SL access is still recommended as the standard root canal preparation method. The crystal structure of NiTi alloys consists of three phases: the austenite phase, the martensite phase, and the R-layer (an intermediate phase between austenite and martensite), the relative proportions of which determine the metallic properties. The martensite phase has a monoclinic structure suitable for the prepa-

ration of anatomically complex curved root canals because of its lower elastic modulus and higher flexibility and fatigue resistance compared with the austenite phase¹¹⁻¹³. NiTi files for root canal preparation are treated with a final surface finishing process in addition to heat treatment and mechanical treatment to improve mechanical properties¹⁴. In 2007, the M wire NiTi alloy was developed, and the ProTaper NEXT (Dentsply Sirona), in which the austenite phase containing small amounts of martensite and the R-layer coexist at body temperature, was applied clinically¹⁵⁻¹⁷. Controlled memory (CM) wire, which was also developed in 2007, has a crystal structure mainly composed of the martensite phase as a result of thermo-mechanical treatment, and has high flexibility at the temperature setting for clinical use, but as a NiTi file, it does not exhibit super-elastic properties¹⁸⁻²⁰. The CM wire NiTi files ProTaper Ultimate (PTU: Dentsply Sirona) and ProTaper Gold (PTG: Dentsply Sirona), which are the subject of this research, have a martensite transformation start temperature (Ms) and austenite transformation end temperature (Af) of 55°C. Both files have been shown to be extremely flexible, as the martensitic state is maintained at a body temperature of 37°C²¹⁻²³. In addition, the PTU and PTG files are the successors to the ProTaper Universal (PT: Dentsply-Sirona)^{24,25} and perform root canal preparation with the same file configuration; therefore, we believe that the cutting characteristics of CM wire NiTi files can be analyzed in this study.

The purpose of this study was to analyze the effect of using CM wire NiTi files with minimally invasive root canal preparation. Conventional NiTi wire PT files and CM wire PTG and PTU files were classified according to cutting characteristics, with and without SL access. The root canal morphology was compared, and the suitability of CM wire NiTi files for minimally invasive cutting was evaluated.

Materials and Methods

1. Operator and test root canal model

The operator was a dentist with more than 10 years of experience using NiTi rotary files. For the experiment, a total of 60 J-shaped root canal models (J-type root canal model: curvature 30°, apical diameter #15, root canal taper 02, root canal length 16.5 mm: End Training block canals, Dentsply Sirona) were used.

Table 1 The files used in root canal preparation in each NiTi file system

Group	Ni-Ti File	Orifice Opener	Glide Pass	Preparation 1	Preparation 2	Preparation 3	Preparation 4
A	PTU	PTU SX	PTU Slider	PTU Shaper	PTU F1	PTU F2	
B	PTU	O. Modifier	PTU Slider	PTU Shaper	PTU F1	PTU F2	
C	PTG	PTG SX	PTU Slider	PTG S1	PTG S2	PTG F1	PTG F2
D	PTG	O. Modifier	PTU Slider	PTG S1	PTG S2	PTG F1	PTG F2
E	PT	PT SX	PTU Slider	PT S1	PT S2	PT F1	PT F2
F	PT	O. Modifier	PTU Slider	PT S1	PT S2	PT F1	PT F2

n=10

2. Root canal preparation

To analyze the effect of CM wire NiTi files on the final root canal morphology during minimally invasive cutting (no-straight line (SL) access), PTG and PTU were used in the experimental groups, and PT (conventional NiTi) was used in the control group.

Root canal preparation was evaluated by comparing the displacement of the root canal width and the median displacement of the final root canal morphology. The experimental PTU and PTG groups and the control PT group were further classified into two subgroups, SL access groups and no-SL access groups, making a total of six groups for analysis.

In each experimental group, the SL access groups used the PTU, PTG and PT files and the Orifice Opener SX, and the no-SL access groups used an orifice modifier as no straight line.

The standard of the final root canal preparation file was unified for each experimental group, and the root canal was prepared with PTU F2 (file tip diameter #25/taper 08: ISO #25/08) and PTG F2 (ISO #25/08), and the control group was similarly terminated with PT F2 (ISO #25/08). Each of the PTU, PTG, and PT file systems uses X Smart Plus (Dentsply Sirona), a drive motor dedicated to NiTi files which rotates forward (PTU: 400 rpm/4 N cm, PTG: 300 rpm/2 to 5 N cm, PT: 250 rpm/1 to 4 N cm). The working length was reached with three vertical movements as one cycle, which was repeated three times, and then the file was replaced. The root canal was irrigated with physiological saline solution after each cycle.

Table 1 shows the files used in each experimental and control group.

The PTU and PTG of the experimental groups and the PT of the control group were analyzed by comparing the NiTi file materials in a system that can com-

plete root canal preparation with the same file configuration. Before starting root canal preparation in each experimental group (A-D) and control group (E, F), apical foramen penetration was confirmed by hand with a #10 K file, and the root canal orifice was opened in groups A (PTU), C (PTG), and E (PT), in which SL access was achieved using the PTUSX, and in groups B (PTU), D (PTG), and F (PT), in which no-SL access used an O. Modifier. Then, the glide path of all groups was formed by the PTU Slider (Dentsply Sirona).

Root canals were prepared with PTU and PTG in the experimental group, and PT in the control group using the X Smart Plus drive motor (Dentsply Sirona). The files used for root canal preparation were 3 files (PTU Shapers, F1, F2 (25/08)) for PTU in groups A and B, 4 files (S1, S2, F1, F2 (25/08)) for PTG in groups C and D, and 4 files (PT S1, S2, F1 and F2 (25/08)) for PT in groups E and F.

For each NiTi system, the file was extended to the working length three times to shape the root canal, and then the file was replaced. The root canal was irrigated with physiological saline solution every time the file was replaced.

3. Evaluation of root canal morphology

The root canal morphological displacement was analyzed by comparing the amount of the root canal wall removed at the outer and inner curved parts of the root canal. An Olympus SZX16 stereoscopic microscope (Olympus, Tokyo, Japan) and a DP71 digital camera (Olympus) were used to superimpose digital images of the transparent root canal models before and after root canal preparation, and the resulting image data were imported into a PC for measurement using WinRoof software (Mitani Corp., Tokyo, Japan) (Fig. 1).

The amount of root canal wall removed was measured by setting measurement points located at 1, 2, 3,

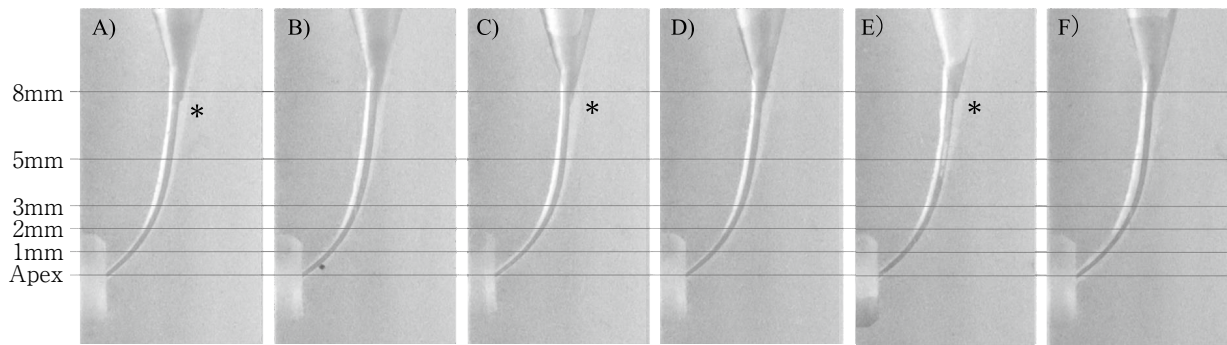


Fig. 1 Superimposition of pre- and post-preparation images
 PTU straight-line (A), PTU no straight-line (B), PTG straight-line (C), PTG no straight-line (D), PT straight-line (E), and PT no straight-line (F).
 * : Straight-line access.

5 mm and 8 mm from the root apex, and measuring the increase in the root canal width (inner and outer side: distance moved from the root canal wall before root canal preparation to the root canal wall after root canal preparation). Canal transportation (median root canal values) was measured and statistically processed.

4. Statistical processing

The measured values of root canal wall removal were statistically processed using one-way analysis of variance, the Bonferroni-Dunn multiple comparison test, and the Mann-Whitney *U* test (two-group comparison analysis) with a 5% risk rate.

Results

The morphology of the root canal after root canal formation was assessed at 1, 2, 3, 5 mm and 8 mm from the root apex, and the increase in root canal width and the median displacement on the inner and outer sides of the root canal were measured. Figure 1 shows the superimposed root canal models before and after root canal preparation in each experimental group. Flared morphology of the upper third of the root canal was observed in groups A (PTU), C (PTG), and E (PT) in the SL access groups. However, in groups B (PTU), D (PTG), and F (PT) of the no-SL access groups, the flared morphology was not observed in the upper third of the root canal at the start of root canal preparation, however, it was observed in the final root canal after the F2 file (25/08) was used (Fig. 1).

Figures 2, 3, and 4 show the increase in root canal width and the median displacement in all experimental groups.

Analysis of the increase in the root canal width by PTU and PTG in the experimental group (Fig. 2) shows that, regardless of the presence or absence of SL access, the displacement of the outer side measurement was greater than that of the inner side measurement at a site with a strong curvature of 1 mm. Furthermore, the outer side measurement of the PTG experimental group increased more significantly than the inner side measurement at the measurement site of 2 mm, and no effect of SL access or no-SL access was observed. There was no significant difference in the displacement between the medial and lateral sides at 3-8 mm in either the PTU or PTG groups.

In the PT control group, the outer side measurement increased more significantly than the inner side measurement at the 1 mm measurement site on the apical side, similar to the PTU and PTG experimental groups. The displacement on the medial side increased significantly at the 3-5 mm measurement sites on the apical side of the starting site on the inner side. There was no statistically significant difference in the increase in root canal width in the PT group, regardless of the presence or absence of SL access.

There was a median displacement (canal transportation) of 0.05-0.1 mm on the medial side at the 3-5 mm measurement site in the PT control group, and the PTU and PTG experimental groups also showed median displacements of 0.05 mm at the 3-5 mm measurement site with SL access. When comparing the PTG and PTU experimental groups with the PT control group, a significant difference was only observed in the no-SL access groups. A comparison between the PTG and PTU experimental groups showed no signifi-

cant differences at any of the measurement sites (Fig. 3).

A comparison of the median displacement between the SL access and no-SL access groups between all NiTi files (experimental groups and control group) (Fig. 4) revealed no significant difference at measurement sites from 1 to 8 mm in each group.

Discussion

NiTi files exhibit elasticity due to the coexistence of martensite and austenite phases, and the transformation from the austenite phase to the martensite phase is initiated by external stress and temperature. The martensite phase and the austenite phase exist as temperature-dependent crystal structures, and the temperature at which the NiTi alloy is heated to change to the austenite phase is defined as the Af. That is, the metallic properties of NiTi alloys are determined by changes in the crystal structure depending on the Af temperature¹¹⁻¹³.

The PT file used in the control group for this research was a conventional super-elastic NiTi wire alloy, and because its Af is lower than the body temperature of 37°C, martensite transformation does not occur and it is thought that the austenite phase exists alone. In contrast, CM wire PTG and PTU have an Af of 50–55°C, and the alloy state is mainly composed of the martensite phase at the body temperature of 37°C at the time of root canal preparation²⁶⁻²⁹. It is also

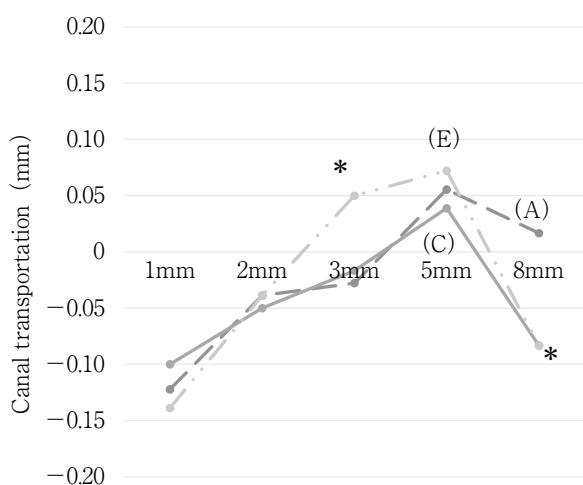


Fig. 3 Canal transportation at different levels from the apex in post-preparation by the PTU (A), PTG (C), and PT (E) straight-line group, and by the PTU (B), PTG (D), and PT (F) no straight-line group

* : Significant difference between experiment (PTU, PTG) and control (PT) (p<0.05).

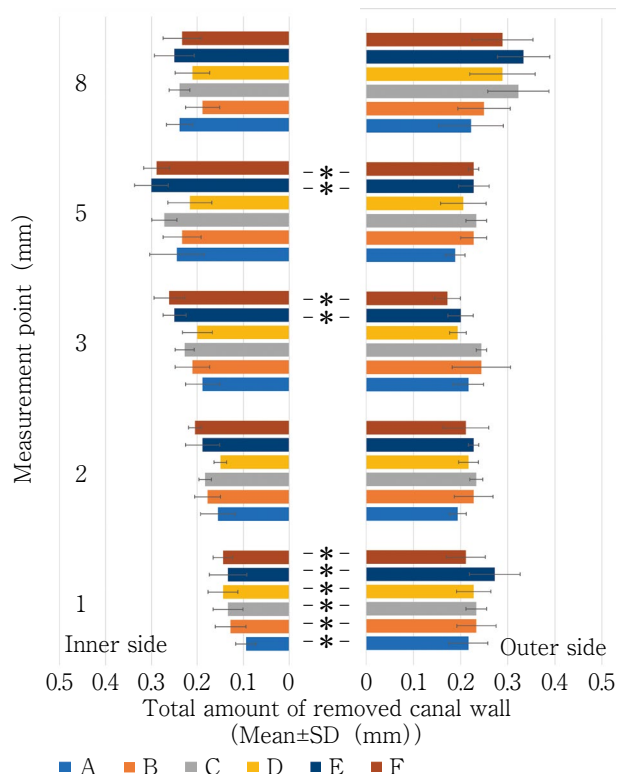
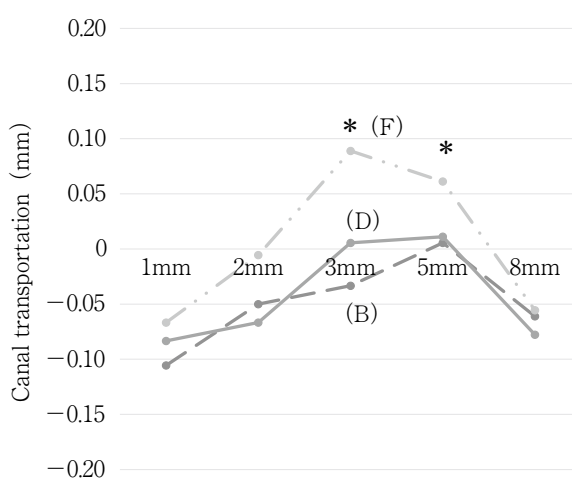


Fig. 2 Total amount of removed canal wall on the inner and outer sides

* : Significant difference between outer and inner sides (p<0.05).



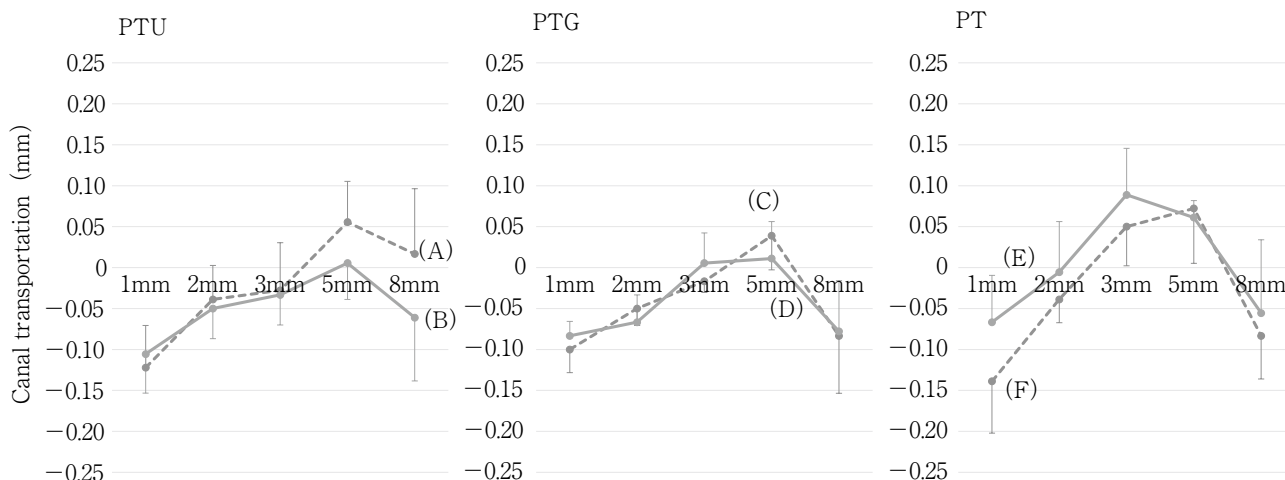


Fig. 4 Canal transportation at different levels from the apex in post-preparation between SL access (by PTU (A), PTG (C), PT (E)) and no-SL access (PTU (B), PTG (D), PT (F)) in each NiTi system

reported that the critical stress of CM wire is in the range of 128–251 MPa at 37°C, although the transformation of austenite phase is initiated in NiTi alloys by external stress. Because the critical stress of CM wire is lower than that of conventional NiTi wire, which is 490–582 MPa, CM wire maintains high flexibility due to the martensite phase even during preparation of a root canal with strong curvature²⁹. These metallic properties of CM wire are considered to be the factors that contribute to the superior elasticity and fatigue resistance of PTG and PTU.

Our analysis of the increase in root canal width using PTG and PTU made with CM wire showed that the median displacement of the root canal was within 0.12 mm of the external curve measurement, indicating that the risk of root canal displacement at the apex was reduced. In the no-SL access group, the measured displacement was 0.1 mm, which is almost negligible. Furthermore, there was no significant difference in the median displacement of the root canal between the SL access group and the no-SL access group at all measurement positions (1–8 mm) on the apical side. These results suggest that minimally invasive endodontic therapy that minimizes the cutting of cervical dentin without the need for SL access is possible as a result of the enhanced flexibility of PTG and PTU made with CM wire.

In contrast, in the PT control group, both the SL access group and the no-SL access group showed a marked increase in the medial side displacement at the

3–5 mm measurement sites on the apical side, increasing the risk of perforation of the root canal wall due to straightening of the curved root canal. A comparison of the apical displacement at 3 mm between the PT control group and the PTG and PTU experimental groups revealed no significant difference in the SL access subgroups; however, there was a significant difference between the PTG and PTU groups. These results confirm that SL access is essential for accurate root canal formation when using a conventional PT NiTi wire. In the control group, the lateral curvature displacement was greater than that in the experimental group at 1, 2, and 8 mm, suggesting that the risk of root canal perforation on the inner side also decreased, but this difference was not significant.

Currently, at the start of root canal preparation with a NiTi file, a root canal search with a manual K file is essential, yielding information about the root canal curvature, stenosis, apical foramen diameter, and root canal length. It is believed that this assists with accurate root canal preparation^{30,31}. In addition, in a curved root canal, removal of the cervical dentin ridge in the upper third of the root canal is considered to be the most important operation in root canal preparation, forming a smooth file glide path to the apical foramen^{32,33}. SL access and glide path preparation have been considered essential procedures for the safe use of NiTi files. However, root canal formation in MI Endo therapy is based on the theory of minimizing the removal of the prominent dentin in the upper third of

the root canal by SL access to prevent root fracture. This concept conflicts with conventional dental school teaching of endodontics. MI Endo therapy aims to minimize SL access by developing an accurate glide path to guide the files^{7,8)}.

In this study, we used the newly developed PTU Slider for glide path preparation. The file used was ProGlider (Dentsply Shirona), which consists of one file, and is an improvement on the Path File (Dentsply Maillefer), which required the use of three files. The PTU Slider adopts ProGlider's file taper of 2-8% to improve the multi-flare shape (0.16 mm (D0), 0.26 mm (D4), 0.44 mm (D8), 0.68 mm (D12), and 1.00 mm (D16)). To show 1.00 mm (D16), it was suggested that the glide path could be formed at the same time as forming the minimal upper root canal flare. In this study, as a result of comparing SL access and no-SL access in PTU and PTG made of CM wire, root canal width displacement and displacement in all measurement sites were not found. Furthermore, no significant difference was found in median displacement. It is considered that this result was influenced by the appropriate flaring created in the upper part of the root canal by using the PTU Slider. No-SL access in minimally invasive root canal preparation requires that the surgical field is reduced at the start of root canal preparation, which limits the operation of the instruments and makes it difficult to find a clear line of sight. Inadequate follow-up of anatomical root canal morphology was predicted, but successful outcomes were achieved for root canals prepared with CM wire NiTi files and with no-SL access for root canal preparation.

Conclusion

This study show that minimally invasive cutting of cervical dentin enables accurate root canal formation using CM wire NiTi files according to the MI Endo concept, which reduces the risk of root fracture. Root canal preparation using CM wire PTG and PTU was shown to maintain the original anatomical root canal morphology even in the no-SL access groups. PTG and PTU files were shown to be capable of preparing root canals using minimally invasive endodontic therapy due to their excellent flexibility and fatigue resistance.

Acknowledgments

We thank Helen Jeays, BDSc AE, from Edanz (<https://jp.edanz.com/ac>) for editing a draft of this manuscript.

Conflict of Interest

The authors declare that they have no conflict of interest related to this study.

Authorship Declaration

All authors contributed significantly and are in agreement with the manuscript.

References

- 1) Fransson H, Dawson VS, Frisk F, Bjørndal L, EndoReCo O, Kvist T. Survival of root-filled teeth in the Swedish adult population. *J Endod* 2016; 42: 216-220.
- 2) Aquilino SA, Caplan DJ. Relationship between crown placement and the survival of endodontically treated teeth. *J Prosthet Dent* 2002; 87: 256-263.
- 3) Pratt I, Aminoshariae A, Montagnese TA, Williams KA, Khalighinejad N, Mickel A. Eight-year retrospective study of the critical time lapse between root canal completion and crown placement: its influence on the survival of endodontically treated teeth. *J Endod* 2016; 42: 1598-1603.
- 4) Seo DG, Yi YA, Shin SJ, Park JW. Analysis of factors associated with cracked teeth. *J Endod* 2012; 38: 288-292.
- 5) Liu R, Kaiwar A, Shemesh H, Wesselink PR, Hou B, Wu MK. Incidence of apical root cracks and apical dentinal detachments after canal preparation with hand and rotary files at different instrumentation lengths. *J Endod* 2013; 39: 129-132.
- 6) Fain WD. Tooth fractures and cracks. *J Am Dent Assoc* 2021; 152: 423-424.
- 7) Krishan R, Paqué F, Ossareh A, Kishen A, Dao T, Friedman S. Impacts of conservative endodontic cavity on root canal instrumentation efficacy and resistance to fracture assessed in incisors, premolars, and molars. *J Endod* 2014; 40: 1160-1166.
- 8) Moore B, Verdellis K, Kishen A, Dao T, Friedman S. Impacts of contracted endodontic cavities on instrumentation efficacy and biomechanical responses in maxillary molars. *J Endod* 2016; 42: 1779-1783.
- 9) Goerig AC, Michelich RJ, Schultz HH. Instrumentation of root canals in molars using the step-down technique. *J Endod* 1982; 8: 550-554.
- 10) Swindle RB, Neaverth EJ, Pantera EA Jr, Ringle RD. Effect of coronal-radicular flaring on apical transporta-

- tion. *J Endod* 1991; 17: 147-149.
- 11) Torabinejad M. Passive step-back technique. *Oral Surg Oral Med Oral Pathol* 77 1994; 77: 398-401.
 - 12) Lang H, Korkmaz Y, Scheneider K, Raab WH. Impact of endodontic treatments on the rigidity of the root. *J Dent Res* 2006; 85: 364-368.
 - 13) Tang W, Wu Y, Smales RJ. Identifying and reducing risks for potential fractures in endodontically treated teeth. *J Endod* 2010; 36: 609-617.
 - 14) Pierrisnard L, Bohin F, Renault P, Barquins M. Corono-radicular reconstruction of pulpless teeth: a mechanical study using finite element analysis. *J Prosthet Dent* 2002; 88: 442-448.
 - 15) Clark D, Khademi JA. Case studies in modern molarendodontic access and directed dentin conservation. *Dent Clin North Am* 2010; 54: 275-289.
 - 16) Tang W, Wu Y, Smales RJ. Identifying and reducing risks for potential fractures in endodontically treated teeth. *J Endod* 2010; 36: 609-617.
 - 17) Reeh ES, Messer HH, Douglas WH. Reduction in tooth stiffness as a result of endodontic and restorative procedures. *J Endod* 1989; 15: 512-516.
 - 18) Pradeep P, Kumar VS, Bantwal SR, Gulati GS. Fracture-strength of endodontically treated premolars: an in vitro evaluation. *J Int Oral Health* 2013; 5: 9-17.
 - 19) Yuan K, Niu C, Xie Q, Jiang W, Gao L, Huang Z, Ma R. Comparative evaluation of the impact of minimally invasive preparation vs. conventional straight-line preparation on tooth biomechanics: a finite element analysis. *Eur J Oral Sci* 2016; 124: 591-596.
 - 20) Bürklein S, Schafer E. Minimally invasive endodontics. *Quintessence Int* 2015; 46: 119-124.
 - 21) Murdoch-Kinch CA, Mclean ME. Minimally invasive dentistry. *J Am Dent Assoc* 2003; 134: 87-95.
 - 22) Gutmann JL. Minimally invasive dentistry (Endodontics). *J Conserv Dent* 2013; 16: 282-283.
 - 23) Kenneth MH, Stephan C. Cohen's pathways of the pulp, 10th. ed. St. Louis, USA: Elsevier, 2011; 137-138.
 - 24) Peters OA, Arias A, Choi A. Mechanical properties of a novel nickel-titanium root canal instrument: Stationary and dynamic tests. *J Endod* 2020; 46: 994-1001.
 - 25) Arias A, Singh R, Peters OA. Torque and force induced by ProTaper universal and ProTaper next during shaping of large and small root canals in extracted teeth. *J Endod* 2014; 40: 973-976.
 - 26) Nguyen HH, Fong H, Paranjpe A, Flake NM, Johnson JD, Peters OA. Evaluation of the resistance to cyclic fatigue among ProTaper Next, ProTaper Universal, and Vortex Blue rotary instruments. *J Endod* 2014; 40: 1190-1193.
 - 27) Shim KS, Oh S, Kum K, Kim YC, Jee KK, Chang SW. Mechanical and metallurgical properties of various nickel-titanium rotary instruments. *Biomed Res Int* 2017; 2017: 4528601.
 - 28) Chen G, Fan W, Mishra S, El-Atem A, Schuetz MA, Xiao Y. Tooth fracture risk analysis based on a new finite element dental structure models using micro-CT data. *Comput Biol Med* 2012; 42: 957-963.
 - 29) Al-Omiri MK, Rayyan MR, Abu-Hammad O. Stress analysis of endodontically treated teeth restored with post-retained crowns: a finite element analysis study. *J Am Dent Assoc* 2011; 142: 289-300.
 - 30) Belli S, Eraslan O, Eraslan O, Eskitascioglu G. Effect of restoration technique on stress distribution in roots with flared canals: an FEA study. *J Adhes Dent* 2014; 16: 185-191.
 - 31) Sathorn C, Palamara JE, Palamara D, Messer HH. Effect of root canal size and external root surface morphology on fracture susceptibility and pattern: a finite element analysis. *J Endod* 2005; 31: 288-292.
 - 32) Sanz JL, Rodriguez-Lozano FJ, Llena C, Sauro S, Forner L. Bioactivity of bioceramic materials used in the dentin-pulp complex therapy: A systematic review. *Materials (Basel)* 2019; 27: 1015-1037.
 - 33) Yu YH, Kushnir L, Kohli M, Karabucak B. Comparing the incidence of postoperative pain after root canal filling with warm vertical obturation with resin-based sealer and sealer-based obturation with calcium silicate-based sealer: a prospective clinical trial. *Clin Oral Investig* 2021 Feb 8. doi: 10.1007/s00784-021-03814-x

Discoloration of Conventional Resin Composite Cements and Self-adhesive Resin Cements Immersed in Water for 180 Days

Ayaka HORI-ISHIKAWA, Yuka OGAWA-UZAWA, Ayako OKADA, Daichi AIZAWA, Nana SAKAEDA-NAITO,
Hiro MATSUMOTO, Kaoru OHMORI, Masao HANABUSA and Takatsugu YAMAMOTO

Department of Operative Dentistry, Tsurumi University School of Dental Medicine

Abstract

Purpose: This study aimed to evaluate the influence of 37°C water immersion for up to 180 days on the discoloration of conventional resin composite cements and self-adhesive resin cements.

Methods: Three conventional resin cements (Panavia V5, RelyX Ultimate, and Variolink Esthetic DC) and three self-adhesive resin cements (SA Luting Cement, RelyX Unicem 2, and SpeedCEM Plus) were examined in this study. Disk specimens ($\phi 15.0 \times 1.0$ mm) were fabricated using the cements and their colors were measured (CIELAB). The specimens were immersed in distilled water at 37°C for 180 days and the colors were repeatedly measured at 1, 7, 14, 21, 28, 90, and 180 days. The color differences (ΔE) were calculated for each measurement period. In addition, water sorption, water solubility, and surface free energy of the cements were measured. Data were analyzed using the Shapiro-Wilk test, Friedman's test and Bonferroni corrections, and Mann-Whitney *U*-test.

Results: All the cements except SA Luting Cement revealed clinically acceptable values of ΔE (< 3.3) at 90 days of immersion. ΔE of the cements remarkably increased after 90 days and showed values much greater than 3.3 at 180 days. All the self-adhesive resin cements demonstrated significantly greater values of water sorption than the corresponding conventional resin composite cements. As for water solubility, one of the three comparison pairs (Panavia V5 and SA Luting Cement) did not show a significant difference. The surface free energy was similar among the cements at approximately 50 mJ/m².

Conclusions: Although the water sorption of the resin cements increased due to the presence of the adhesive monomers, the discoloration did not intensify as water absorption increased. The degree of discoloration was not related to the degree of water sorption.

Key words: self-adhesive resin cement, discoloration, ΔE^*_{ab} , water sorption

Introduction

The growing demand for esthetic dentistry has pushed many manufacturers to develop tooth-colored restorative dental materials, such as dental ceramics. Resin cements have contributed to the increased use of ceramics for the following reasons: the bond strength of resin cements allows sufficient marginal sealing of dental restorations and reinforces ceramic restorations^{1,2}, and the colors of these cements closely match that of the tooth substrate.

Silica-based ceramics have sufficient translucency and allow for the passage and scattering of light³. The resulting color of the restoration is dependent on the combination of restorative materials employed, the target tooth, and the resin cement used^{4,5}. Namely, the discoloration of resin cement is essential for the long-term success of esthetic dental restoration. Several studies have examined the discoloration of resin cements⁶⁻¹¹, many of them focusing on water absorption as one of the key elements affecting color discoloration. The resin cement around a restoration's margins is exposed to the oral environment, absorbing water and other substances, such as saliva, food components, and beverages. This can influence the degradation and discoloration of dental materials. One study reported the changes in color (ΔE^*ab values) exhibited by four dual-cured resin cements and two chemically cured resin cements after one week of coffee immersion¹². The products that demonstrated greater water sorption and solubility displayed greater color changes. It was suggested that the adsorbed solution caused discoloration of the resin matrix itself, altering the resin matrix at the interface of the matrix and fillers.

In the decade since self-adhesive resin cement was introduced into dentistry, it has rapidly gained popularity due to its ease of use. Self-adhesive resin cements are based on filled polymers, which are designed to adhere to tooth structures without needing a separate adhesive or etchant¹³. Self-adhesive resin cement contains a high concentration of adhesive monomers, such as methacryloyloxydecyl dihydrogen phosphate (MDP) and glycerol phosphate dimethacrylate. As self-adhesive resin cements contain more hydrophilic monomers than conventional resin composite cements, to give them adhesive characteristics, self-adhesive resin cements

may be more susceptible to discoloration due to more water sorption; however, there is little information available about the discoloration of resin cements. This study aimed to evaluate the effects of immersion in water at a temperature of 37°C on the discoloration of self-adhesive resin cements and conventional resin composite cements. The null hypothesis was that there would be no significant differences in discoloration among the tested cements after they had been immersed in water at 37°C for 180 days.

Materials and Methods

1. Materials

Table 1 lists the six resin cements evaluated in this study and their basic formulations. They included three conventional resin composite cements (amine-free dual-activated cement): Panavia V5 (PF, Kuraray Noritake Dental, Tokyo, Japan), RelyX Ultimate (RUI, 3M ESPE, St. Paul, MN, USA), and Variolink Esthetic DC (VE, Ivoclar Vivadent, Schaan, Liechtenstein), and three self-adhesive resin cements: SA Luting Cement (SA, Kuraray Noritake Dental), RelyX Unicem 2 (RUn, 3M ESPE), and SpeedCEM Plus (SC, Ivoclar Vivadent).

2. Discoloration

Each resin cement was mixed using mixing tips and packed in a stainless-steel mold (15 mm in diameter, 1 mm in thickness) on a glass plate ($n=5$). The resin cement was covered with a transparent plastic matrix and a glass plate (thickness: 5.76 mm). The top and bottom surfaces of the resin cement were divided into nine zones, and each zone was irradiated using an LED curing light (PenCure 2000, Morita, Osaka, Japan) at 1,048 mW/cm². The light irradiation time was as instructed by the manufacturer. The tip of the light guide was placed in contact with the glass plate. Following ultrasonic cleaning for 1 min, the colors (CIELAB system) of the disks were measured at the center of the disks using a spectrophotometer (SE-2000, Nippon Denshoku Industries, Saitama, Japan) on a neutral gray background. Each disk was put together in a non-woven pouch. The specimens were immersed in distilled water (Direct Q3UV, Merck-Millipore, Darmstadt, Germany) at 37°C for up to 180 days. The distilled water was changed every week. At 1, 7, 14, 21, 28, 90, and 180 days of immersion, the disks were ultrasonically cleaned for 15 s, and their color was measured

Table 1 Compositions of the resin cements used in this study

Product name	Manufacturer	Shade	Code	Filler (vol%)	Component	Lot No	
Conventional resin composite cements	Panavia V5	Kuraray Noritake Dental	Clear	PF	38	Paste A : Bis-GMA, TEGDMA, hydrophobic aromatic dimethacrylate, hydrophilic aliphatic dimethacrylate Paste B : Bis-GMA, hydrophobic aromatic dimethacrylate, hydrophilic aliphatic dimethacrylate Fillers : dilanated barium glass filler, silanated fluoroaluminosilicate glass filler, colloidal silica, silanated aluminium oxide filler	AX0022
	RelyX Ultimate	3M ESPE	Trans-lucent	RU1	43	Base : methacrylate monomers containing phosphoric acid groups, methacrylate monomers Catalyst : methacrylate monomers Fillers : silanated fillers, alkaline (basic) fillers	4801246
	Variolink Esthetic DC	Ivoclar Vivadent	Neutral	VE	38	UDMA and further methacrylate monomers, ytterbium trifluoride mixed oxide, initiators, stabilizers and pigments	W04495
Self-adhesive resin cements	SA Luting Cement	Kuraray Noritake Dental	Trans-lucent	SA	40	Paste A : MDP, Bis-GMA, TEGDMA, HEMA, other methacrylic monomer, surface treated barium glass filler, surface treated silica filler, light initiator, dark cure initiator, pigment Paste B : surface treated barium glass filler, aluminum oxide, surface treated sodium fluoride, polymerization accelerator, silane coupling agent, pigment	2S0001
	RelyX Unicem 2	3M ESPE	Trans-lucent	RUn	43	Base paste : phosphoric acid-modified methacrylate monomers, bifunctional methacrylate Catalyst paste : methacrylate monomers Fillers : alkaline (basic) fillers, silanated fillers	4748225
	SpeedCEM Plus	Ivoclar Vivadent	Trans-lucent	SC	45	UDMA, TEGDMA, PEGDMA, methacrylated phosphoric acid ester, 1,10-decandiol dimethacrylate, copolymers, dibenzoyl peroxide, ytterbium trifluoride, barium glass, silicon dioxide	Y02748

using the same method as described above. Differences in color parameters (ΔL^* , Δa^* , and Δb^*) were determined by comparing the values seen before and after immersion, and overall changes in color (ΔE^*_{ab}) were calculated using the following equation:

$$\Delta E^*_{ab} = [(\Delta L^*)^2 + (\Delta a^*)^2 + (\Delta b^*)^2]^{1/2} \dots (1)$$

3. Water sorption and water solubility

The water sorption (W_{sp}) and water solubility (W_{sl}) of the resin cements were measured as per ISO 4049. Disk-shaped specimens were prepared using the same method as for the color measurement ($n=5$). Thickness was measured to an accuracy of 0.01 mm when calcu-

lating the volume (V) of the disks. The specimens were kept in a desiccator at 37°C for 22 hours. Then, they were placed in a second desiccator at 23°C for 2 hours, before being weighed (HR-251AZ, A & D, Tokyo, Japan). These procedures were repeated until a constant weight (m_1) was obtained. It took 18 days to reach a constant weight. The disks were then immersed in distilled water at 37°C for 1 week. Excess water was removed by blotting, and the disks were weighed (m_2). The specimens were stored again in the 37°C desiccator and weighed repeatedly, as described earlier, until a constant weight (m_3) was obtained. The following equations were used for calculating W_{sp} and W_{sl} :

$$W_{sp} = (m_2 - m_3) / V \cdots (2)$$

$$W_{sl} = (m_1 - m_3) / V \cdots (3)$$

4. Surface free energy calculation

Disk-shaped specimens (15 mm in diameter, 1 mm in thickness) were fabricated using the same stainless steel mold ($n=3$). Following light-irradiation for curing, one flat surface of the disk was serially wet-polished with up to 2000-grit SiC paper and mirror-finished with 3- μ m diamond particles. To calculate the surface free energy of the materials, contact angles (θ) were measured using a contact angle device (DMe-201, Kyowa Interface Science, Saitama, Japan). Distilled water and diiodomethane (Kanto Chemical, Tokyo, Japan) were used as liquids with known surface free energy levels for the angle measurement. Then, 0.5 μ L of each liquid was dropped onto the polished surface, and video images were recorded. The video images were automatically transferred to a connected computer, on which an image analysis program (FAMAS, Kyowa Interface Science) for angle measurement had been installed. The surface free energy (γ_S^{total}) of each material was calculated using the following equations¹⁴⁻¹⁷:

$$\gamma_L^{total} (1 + \cos\theta) = 2(\sqrt{\gamma_L^d \gamma_S^d} + \sqrt{\gamma_L^h \gamma_S^h}) \cdots (4)$$

$$\gamma_S^{total} = \gamma_S^d + \gamma_S^h \cdots (5)$$

where γ_L^{total} is the surface free energy of the liquids, γ_L^d is the dispersion force of the liquids (distilled water: 21.8 mN/m and diiodomethane: 49.5 mN/m), and γ_L^h is the hydrogen bond force of the liquids (distilled water: 51.0 mN/m and diiodomethane: 1.3 mN/m). The dispersion force (γ_S^d) and hydrogen bonding force (γ_S^h) of the solid were obtained by substituting the liquid surface free energy and the contact angle (θ) into equation (4). Surface free energy of the solids (γ_S^{total}) is the sum of γ_S^d and γ_S^h .

5. Statistical analyses

The distribution of each continuous variable was checked for normality using the Shapiro-Wilk test. The Levene test was used to assess the homogeneity of variances when normality was confirmed.

For each cement, Friedman's test was used to evaluate whether the immersion procedure affected ΔE^*_{ab} . In addition, the comparisons among the immersion periods for each cement were subjected to Bonferroni correction. The Mann-Whitney U -test was used for comparisons of W_{sp} , W_{sl} , and surface free energy between the conventional resin composite cements and the corresponding self-adhesive resin cements. The significance level was set at $\alpha=0.05$ for all statistical tests.

These analyses were carried out using IBM SPSS Statistics Ver. 23.0 (IBM SPSS, Tokyo, Japan) and EZR, which is a graphical user interface for R. More precisely, it is a modified version of R Commander designed to add statistical functions that are frequently used in biostatistics.

Results

1. Discoloration

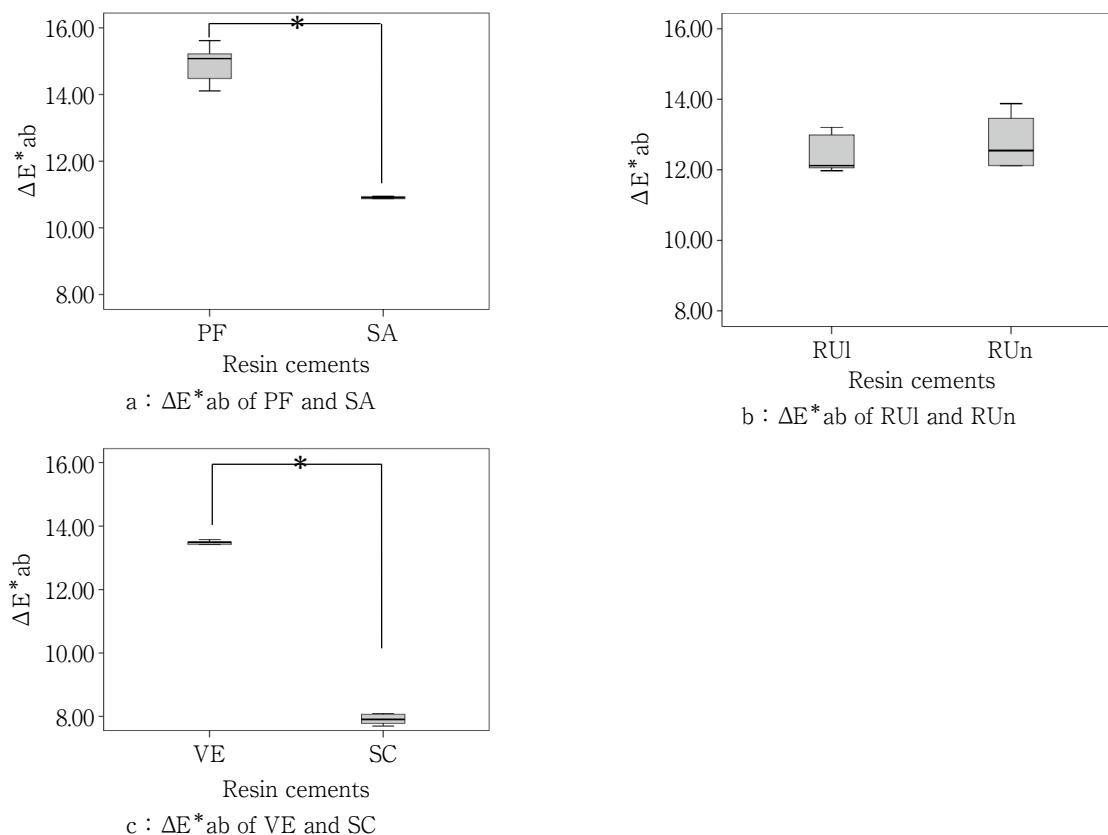
Table 2 lists the changes in ΔE^*_{ab} observed during the immersion period. During the first 90 days of the immersion period, the ΔE^*_{ab} values for all cements, except SA, remained in the clinically acceptable range, indicating that the induced color differences were indistinguishable to the human eye ($<3.3^{18}$). ΔE^*_{ab} markedly increased from 90 days to 180 days (>7.9). The ΔE^*_{ab} value of SA was 0.45 at one day and gradually increased to more than 3.3 at 28 days, reaching 10.91 at 180 days. Regarding the values seen at 180 days, two of the three conventional resin composite cements (PF and VE) exhibited slightly higher ΔE^*_{ab} values than the two self-adhesive resin cements (SA and SC). Friedman's test revealed that the immersion procedure had a significant effect on ΔE^*_{ab} ($p<0.001$). However, Bonferroni correction found no significant differences among the values for the seven immersion periods.

Figure 1 shows comparisons of the ΔE^*_{ab} values seen at 180 days between pairs of resin cements produced by the same company. RUI and RUn demonstrated similar values, while significant differences in ΔE^*_{ab} were seen between PF and SA ($p<0.001$), and between VE and SC ($p<0.001$).

Table 2 Changes of ΔE^*_{ab}

Days	1	7	14	21	28	90	180	p-value
PF, median (IQR)	0.56 (0.48-0.65)	0.75 (0.74-1.11)	1.51 (1.40-1.68)	1.56 (1.54-1.81)	1.56 (1.54-1.81)	1.59 (1.49-1.74)	15.08 (4.48-15.22)	0.000162
RUI, median (IQR)	0.83 (0.71-0.86)	0.58 (0.43-0.69)	1.68 (1.46-1.80)	1.39 (1.37-1.42)	1.01 (0.96-1.28)	1.50 (1.47-1.54)	12.12 (12.06-12.99)	0.0000715
VE, median (IQR)	0.53 (0.48-0.55)	0.76 (0.75-0.81)	1.77 (1.77-1.78)	1.55 (1.51-1.65)	1.83 (1.82-1.88)	2.16 (2.15-2.20)	13.49 (13.42-16.50)	0.0000415
SA, median (IQR)	0.45 (0.33-0.49)	2.69 (2.63-2.70)	2.63 (2.58-2.81)	2.72 (2.71-2.94)	3.44 (3.31-3.62)	5.59 (5.31-5.68)	10.91 (10.88-10.93)	0.0000474
RUn, median (IQR)	0.45 (0.44-0.47)	0.72 (0.46-0.76)	0.94 (0.82-1.00)	1.07 (0.96-1.09)	0.91 (0.86-1.29)	1.15 (1.08-1.25)	12.55 (12.12-13.46)	0.000562
SC, median (IQR)	2.82 (2.79-2.89)	1.98 (1.95-2.01)	1.04 (1.02-1.07)	0.93 (0.87-1.08)	1.19 (1.03-1.29)	1.89 (1.81-1.93)	7.91 (7.78-8.06)	0.0000457

p-values were calculated by Friedman's test. There were no significant differences by Bonferroni corrections.

**Fig. 1**

ΔE^*_{ab} values of self-adhesive resin cement and conventional resin cement made by the same company at 180 days

2. Water sorption and water solubility

Table 3 summarizes the results of comparisons of water sorption (W_{sp}) and water solubility (W_{sl}) between pairs of conventional and self-adhesive resin cements

manufactured by the same company. Significant differences in W_{sp} were observed for all combinations of conventional and self-adhesive resin cements ($p < 0.05$). In addition, two of the pairs (RUI and RUn, and VE and SC,

Table 3 Water sorption (W_{sp}) and water solubility (W_{sl}) of the resin cements ($\mu\text{g}/\text{mm}^3$)

	PF	SA	p-value
W_{sp} , median (IQR)	19.67 (19.62-19.83)	28.22 (28.10-28.73)	0.00794
W_{sl} , median (IQR)	0.50 (0.00-0.96) *	1.01 (0.50-1.02) *	0.151
	RUI	RUn	p-value
W_{sp} , median (IQR)	24.04 (24.02-25.04)	27.06 (26.90-27.59)	0.0159
W_{sl} , median (IQR)	-3.58 (-3.61--3.43)	3.04 (2.57-3.07)	0.00794
	VE	SC	p-value
W_{sp} , median (IQR)	22.12 (21.84-22.13)	30.88 (30.78-30.99)	0.00794
W_{sl} , median (IQR)	1.51 (1.11-1.84)	0.98 (0.50-0.99)	0.00794

* : Values having an asterisk were not significantly different by the Mann-Whitney U -test ($p > 0.05$).

Table 4 Surface free energy (γ_S^{total}) of the resin cements (mJ/m^2)

	Surface free energy	p-value
PF, median (IQR)	49.32 (48.97-50.90)	0.400
SA, median (IQR)	51.40 (51.27-52.17)	
RUI, median (IQR)	52.46 (51.74-53.33)	0.100
RUn, median (IQR)	48.28 (47.95-48.65)	
VE, median (IQR)	46.68 (45.35-46.96)	0.100
SC, median (IQR)	51.48 (49.95-51.84)	

p-values were calculated by the Mann-Whitney U -test.

$p=0.00794$) exhibited significant differences in W_{sl} . The difference in W_{sl} between PF and SA was not significant.

3. Surface free energy measurement

Table 4 shows comparisons of surface free energy (γ_S^{total}) values between pairs of conventional and self-adhesive resin cements manufactured by the same company. No significant differences were observed in any of the comparisons.

Discussion

Self-adhesive resin cements have been widely used for esthetic dental restoration. The procedures for applying self-adhesive resin cements can be very simple, and hence rely less on technique than those for conventional resin cements^{19,20}. However, the dentin bond strength of indirect restorations performed with self-adhesive resin cement was reported to be lower

than that of indirect restorations performed with conventional resin cement²¹. For this reason, most major research on self-adhesive resin cements has focused on their mechanical properties, while little information is available about their discoloration, despite this being an essential factor for esthetic dentistry.

Several studies have reported that self-adhesive resin cements generally exhibit more hydrophilic properties than conventional resin composite cements because their functional monomers contain acidic carboxyl or phosphate groups²²⁻²⁴. Based on these findings, there was concern about the discoloration of such cements due to water sorption. To address this, we evaluated the water sorption, water solubility, surface free energy, and discoloration of conventional resin composite cements and self-adhesive resin cements. To the best of our knowledge, the present study is the first to compare the discoloration of three self-adhesive resin cements with the discoloration of conventional resin composite cements from the same manufacturers.

The resultant data showed that the water sorption (W_{sp}) of all of the cements was below the permitted ISO standard threshold of $40 \mu\text{g}/\text{mm}^3$. In a comparison between the conventional and self-adhesive resin cements, the latter exhibited significantly greater W_{sp} than the corresponding conventional resin composite cements (Table 3). All of the self-adhesive resin cements examined in this study contained phosphoric acid monomers as functional monomers, and their hydrophilicity must have been reflected in the results. Moreover, the influence of polymerization must be considered because the degree of polymerization is a criti-

cal factor for W_{sp} . Several studies have suggested that acidic monomers in self-adhesive resin cements may chemically interfere with the amine initiator, triggering incomplete polymerization and decreasing the degree of conversion^{13,25,26}, i.e., the acidity increases the W_{sp} of self-adhesive resin cements. To solve these problems, non-amine initiation systems have been employed in some self-adhesive resin cements, including SA and RUn, which were used in this study²⁷. These cements have a more acid-compatible nature and improve the degree of conversion and polymerization rate, which are expected to lead to a reduction in W_{sp} . Thus, we may conclude that the influence of acidity on W_{sp} was relatively minor for SA and RUn.

Several studies have reported that in resin cements the compositions of the matrix and filler play a key role in W_{sp} . Bis-GMA demonstrated greater W_{sp} than UDMA due to the OH groups it possesses, which transport dye components into deeper surface layers²⁸⁻³². Such behavior of monomers could not be confirmed in this study because SC, which contained UDMA as its main monomer, exhibited the highest W_{sp} value.

The greater the percentage filler content, the less water penetrates the resin matrix, and the smaller W_{sp} and W_{sl} will be³³. Although the cements examined in this study had similar percentage filler contents (around 40 vol%), W_{sp} and W_{sl} varied among the cements. These results were consistent with several studies of other resin cements³⁴⁻³⁶.

SC demonstrated the highest ΔE^*_{ab} value after one day of immersion (2.82; Table 2). The ΔE^*_{ab} value of SA markedly increased during the first 7 days of immersion, reaching 2.69. At 28 days, all of the cements, except SA, demonstrated similar values, ranging from 0.91 (RUn) to 1.83 (VE), and only the ΔE^*_{ab} value of SA exceeded 3.3, which suggested that the color change exhibited by SA was distinguishable to the human eye¹⁸. At 90 days, the difference between the ΔE^*_{ab} value of SA and the other cements was even more prominent, with the other cements continuing to demonstrate ΔE^*_{ab} values of <3.3. Two of the three self-adhesive resin cements, but none of the conventional resin composite cements, demonstrated obvious changes in ΔE^*_{ab} , suggesting that the hydrophilicity of the adhesive monomer in SA may have affected its ΔE^*_{ab} values during short-term (<3 months) storage. In addition, the amount of functional monomers present

in SA may have affected its ΔE^*_{ab} values. However, the manufacturer did not provide the exact chemical composition of SA.

All the samples showed yellowish discoloration with the exception of PF and VE groups, and SA group exhibited the most prominent discoloration after 180 days of immersion. However, at 180 days, the ΔE^*_{ab} values of all cements exceeded 3.3 (Table 2). All of the cements showed significant discoloration after 90 days of immersion, by which time their ΔE^*_{ab} values had increased 1.8-fold (SA) to 9.5-fold (PF). These results suggested that the discoloration of the resin composite cements mainly occurred during long-term immersion (for over 3 months). Continuous exposure to water accelerated the deterioration of the mechanical properties of the cements. The adsorbed water may have caused the interface between the matrix and the filler to dissociate and discolored the resin matrix³⁷. Additionally, when water permeates into the resin cement, changes occur in its optical properties, including alterations in light transmission properties, translucency parameters, and refractive indices³⁸. These alterations could lead to the deterioration of the esthetic appearance of the resin cements. In the present study, Friedman's test revealed that the immersion period had a significant effect on ΔE^*_{ab} values; however, there were no significant differences among the ΔE^*_{ab} values of the cements. The number of specimens ($n=5$) may explain the inconsistency between these results. Interestingly, the ΔE^*_{ab} values of the self-adhesive resin cements other than the 3M ESPE products (Figure 1b) were significantly lower than those of the corresponding conventional resin composite cements at 180 days (Figure 1), while there was no significant difference in ΔE^*_{ab} between RUI and RUn since their components were similar (Table 1). Thus, the null hypothesis was rejected. The results of this study suggested that the water absorption at the matrix/filler interfaces was suspected to affect the discoloration of resin cement more than the hydrophilicity of the adhesive monomers.

The surface characteristics of the cements were investigated by comparing the cements' surface free energy levels, which were calculated from their contact angles. The cements had similar surface free energy levels of around 45 mJ/m², which disagreed with the results regarding the discoloration seen at 180 days.

This demonstrated that surface free energy and discoloration were not clearly related in this study.

The discoloration seen in this study was considered to have occurred in the body of the cements, rather than superficially. The storage medium used in this study was deionized water, which did not contain any pigments that could cause superficial stains on the cements. A previous study examined the color stability of eight self-adhesive resin cements using four kinds of media (distilled water, red wine, curry solution, and cress solution³⁶⁾). Among the media, red wine demonstrated the highest discoloration rate, followed by the curry solution. Distilled water revealed the lowest rate. The interface between fillers and the matrix serves as a path for water diffusion, along which the dye components of red wine could ooze into a deeper surface layer. The pH level varied among the four media. The varying pH levels of the storage medium could potentially have an adverse impact on the surface structure and roughness of the materials. Surface roughness induced by acidic pH levels enhances the vulnerability to external and internal discolorations of resin restorations. Further *in vitro* tests need to be performed using several media.

Conclusion

Resin cements were discolored by immersion in water, and the discoloration moderately accelerated after 90 days. Although the water sorption of the resin cements was increased by the presence of adhesive monomers, discoloration was not intensified by increased water sorption. Thus, the degree of discoloration was not related to the degree of water sorption.

Conflicts of Interests

The authors declare no conflict of interest related to this paper.

References

- 1) Burke FJ. Maximising the fracture resistance of dentine-bonded all-ceramic crowns. *J Dent* 1999; 27: 169-173.
- 2) Fleming GPJ, Cao X, Romanyk DL, Addison O. Favorable residual stress induction by resin-cementation on dental porcelain. *Dent Mater* 2017; 33: 1258-1265.
- 3) Chen XD, Hong G, Xing WZ, Wang YN. The influence of resin cements on the final color of ceramic veneers. *J Prosthodont Res* 2015; 59: 172-177.
- 4) Kelly JR, Benetti P. Ceramic materials in dentistry: historical evolution and current practice *Aust Dent J* 2011; 56: 84-96.
- 5) Rosenstiel SF, Land MF, Crispin BJ. Dental luting agents: a review of the current literature *J Prosthet Dent* 1998; 80: 280-301.
- 6) Turgut S, Bagis B. Colour stability of laminate veneers: an *in vitro* study. *J Dent* 2011; 39: e57-64.
- 7) Archegas LR, Freire A, Vieira S, Caldas DB, Souza EM. Colour stability and opacity of resin cements and flowable composites for ceramic veneer luting after accelerated ageing. *J Dent* 2011; 39: 804-810.
- 8) Schneider LFJ, Ribeiro RB, Liberato WF, Salgado VE, Moraes RR, Cavalcante LM. Curing potential and color stability of different resin-based luting materials. *Dent Mater* 2020; 36: e309-315.
- 9) Kilinc E, Antonson SA, Hardigan PC, Kesercioglu A. Resin cement color stability and its influence on the final shade of all-ceramics. *J Dent* 2011; 39: e30-36.
- 10) Pissaia JF, Guanaes BKA, Kintopp CCA, Correr GM, da Cunha LF, Gonzaga CC. Color stability of ceramic veneers as a function of resin cement curing mode and shade: 3-year follow-up. *PLoS One* 2019; 14: e0219183.
- 11) Schneider LF, Cavalcante LM, Prahl SA, Pfeifer CS, Ferracane JL. Curing efficiency of dental resin composites formulated with camphorquinone or trimethylbenzoyl-diphenyl-phosphine oxide. *Dent Mater* 2012; 28: 392-397.
- 12) Shiozawa M, Takahashi H, Asakawa Y, Iwasaki N. Color stability of adhesive resin cements after immersion in coffee. *Clin Oral Investig* 2015; 19: 309-317.
- 13) Ferracane JL, Stansbury JW, Burke FJ. Self-adhesive resin cements- chemistry, properties and clinical considerations. *J Oral Rehabil* 2011; 38: 295-314.
- 14) Owens DK, Wendt RC. Estimation of the surface free energy of polymers. *J Appl Polym Sci* 1969; 13: 1741-1747.
- 15) Żenkiewicz M. Methods for the calculation of surface free energy of solids. *J Achiev Mater Manuf Eng* 2007; 24: 137-145.
- 16) Van Oss CJ, Ju L, Chaudhury MK, Good RJ. Estimation of the polar parameters of the surface tension of liquids by contact angle measurements on gels. *J Colloid Interface Sci* 1989; 128: 313-319.
- 17) Matsumoto H, Yamamoto T, Hayakawa T. Discoloration of dental zirconia immersed in food and beverages. *Dent Mater J*. 2022; 41: 824-832.
- 18) Ruyter IE, Nilner K, Moller B. Color stability of dental composite resin materials for crown and bridge

- veneers. *Dent Mater* 1987; 3: 246-251.
- 19) De Munck J, Vargas M, Van Landuyt K, Hikita K, Lambrechts P, Van Meerbeek B. Bonding of an auto-adhesive luting material to enamel and dentin. *Dent Mater* 2004; 20: 963-971.
 - 20) Hitz T, Stawarczyk B, Fischer J, Hämmerle CH, Sailer I. Are self-adhesive resin cements a valid alternative to conventional resin cements? A laboratory study of the long-term bond strength. *Dent Mater* 2012; 28: 1183-1190.
 - 21) Peumans M, Kanumilli P, De Munck J, Van Landuyt K, Lambrechts P, Van Meerbeek B. Clinical effectiveness of contemporary adhesives: a systematic review of current clinical trials. *Dent Mater* 2005; 21: 864-881.
 - 22) Ito S, Hashimoto M, Wadgaonkar B, Svizero N, Carvalho RM, Yiu C, Rueggeberg FA, Foulger S, Saito T, Nishitani Y, Yoshiyama M, Tay FR, Pashley DH. Effects of resin hydrophilicity on water sorption and changes in modulus of elasticity. *Biomaterial* 2005; 26: 6449-6459.
 - 23) Malacarne J, Carvalho RM, de Goes MF, Svizero N, Pashley DH, Tay FR, Yiu CK, Carrilho MR. Water sorption/solubility of dental adhesive resins. *Dent Mater* 2006; 22: 973-980.
 - 24) Kimura S, Ihara K, Nohira H, Aizawa D, Sakaeda N, Hanabusa M, Ferracane JL, Yamamoto T. Changes of residual stresses on the surface of leucite-reinforced ceramic restoration luted with resin composite cements during aging in water. *J Mech Behav Biomed Mater* 2021; 123: 104711.
 - 25) Aguiar TR, Di Francescantonio M, Arrais CA, Ambrosano GM, Davanzo C, Giannini M. Influence of curing mode and time on degree of conversion of one conventional and two self-adhesive resin cements. *Oper Dent* 2010; 35: 295-299.
 - 26) Frassetto A, Navarra CO, Marchesi G, Turco G, Di Lenarda R, Breschi L, Ferracane JL, Cadenaro M. Kinetics of polymerization and contraction stress development in self-adhesive resin cements. *Dent Mater* 2012; 28: 1032-1039.
 - 27) Nima G, Makishi P, Fronza BM, Campos Ferreira PV, Braga RR, Reis AF, Giannini M. Polymerization kinetics, shrinkage stress, and bond strength to dentin of conventional and self-adhesive resin cements. *J Adhes Dent* 2022; 24: 355-366.
 - 28) Khokhar ZA, Razzoog ME, Yaman P. Color stability of restorative resins. *Quintessence Int* 1991; 22: 733-737.
 - 29) Ertaş, E, Güler AU, Yücel AC, Köprülü H, Güler E. Color stability of resin composites after immersion in different drinks. *Dent Mater J* 2006; 25: 371-376.
 - 30) Bagheri R, Burrow MF, Tyas M. Influence of food-simulating solutions and surface finish on susceptibility to staining of aesthetic restorative materials. *J Dent* 2005; 33: 389-398.
 - 31) Marghalani HY. Sorption and solubility characteristics of self-adhesive resin cements. *Dent Mater* 2012; 28: e187-198.
 - 32) Floyd CJ, Dickens SH. Network structure of Bis-GMA- and UDMA-based resin systems. *Dent Mater* 2006; 22: 1143-1149.
 - 33) Paravina RD, Roeder L, Lu H, Vogel K, Powers JM. Effect of finishing and polishing procedures on surface roughness, gloss and color of resin-based composites. *Am J Dent* 2004; 17: 262-266.
 - 34) Imamura S, Takahashi H, Hayakawa I, Loyaga-Rendon PG, Minakuchi S. Effect of filler type and polishing on the discoloration of composite resin artificial teeth. *Dent Mater J* 2008; 27: 802-808.
 - 35) Petropoulou A, Vrochari AD, Hellwig E, Stampf S, Polydorou O. Water sorption and water solubility of self-etching and self-adhesive resin cements. *J Prosthet Dent* 2015; 114: 674-679.
 - 36) Liebermann A, Roos M, Stawarczyk B. The effect of different storage media on color stability of self-adhesive composite resin cements for up to one year. *Materials (Basel)* 2017; 10: E300.
 - 37) Dietschi D, Campanile G, Holz J, Meyer JM. Comparison of the color stability of ten new-generation composites: an in vitro study. *Dent Mater* 1994; 10: 353-362.
 - 38) Almasabi W, Tichy A, Abdou A, Hosaka K, Nakajima M, Tagami J. Effect of water storage and thermocycling on light transmission properties, translucency and refractive index of nanofilled flowable composites. *Dent Mater J* 2021; 40: 599-605.

Comparison of Shaping Ability between Nickel-titanium Hand Files and Nickel-titanium Rotary Files during Glide path

Masashi YAMADA, Norio KASAHARA¹, Satoru MATSUNAGA², Tomoyuki INOSE, Hiroki IWASAWA, Ryo NAKAJIMA, Yoshiki TAMIYA and Masahiro FURUSAWA

Department of Endodontics, Tokyo Dental College

¹Department of Histology & Developmental Biology, Tokyo Dental College

²Department of Anatomy, Tokyo Dental College

Abstract

Purpose: Glide path preparation is one use of nickel-titanium (Ni-Ti) rotary files, but few studies have addressed the effectiveness of Ni-Ti hand files. In this study, we compared glide path preparation abilities between a Ni-Ti hand file and a Ni-Ti rotary file.

Methods: One board-certified endodontist conducted glide path preparation in transparent root canal models. Observations of the state of root canal preparation, centering performance, and time taken to complete glide path preparation were compared between groups prepared using a Ni-Ti hand file (HandFlex; HF group) and a Ni-Ti rotary file (WaveOne Gold Glider; GG group).

Results: Although both groups maintained the original root canal morphology during enlargement, the increase in root canal width was significantly greater in the HF group for both inner and outer sides ($p < 0.05$). Centering ratio at 1 mm from the apex differed significantly between HF and GG groups ($p < 0.01$). Glide path enlargement time was significantly shorter in the GG group ($p < 0.05$).

Conclusion: Ni-Ti hand files took longer than Ni-Ti rotary files to achieve glide path enlargement, but maintained the original anatomy of the root canal in the same way.

Key words: glide path, Ni-Ti hand files, Ni-Ti rotary files, martensitic files, centering ability

Introduction

Maintaining the anatomy of the root canal system is known to affect the success rate of root canal treatment¹⁻³. Root canal preparation with a nickel-titanium (Ni-Ti) rotary file is effective for this purpose⁴. Glide path preparation is one of the purposes of Ni-Ti rotary files. The glide path is the induction path for the Ni-Ti rotary file to progress toward the root apex. The reasons given for using a glide path include reducing the stress imposed on the file and the root canal⁵, and the enlarging effect while maintaining the anatomy of the root canal⁶. Stainless-steel hand files were formerly used for glide path preparation, but rotary files can now be used for this purpose and have been shown to be effective⁷. In actual clinical practice, however, it is often necessary to use a stainless-steel hand file, as a Ni-Ti rotary file that cannot be pre-curved may be infeasible if the root canal is inclined distally and the patient is unable to open their mouth sufficiently wide. The use of martensitic Ni-Ti rotary files has been increasing in recent years. The softness of these files means that enlargement can be carried out more safely while maintaining the anatomy of the root canal⁸, but such Ni-Ti hand files are scarce. Recently developed Ni-Ti hand files with martensitic properties are flexible and can be pre-curved. The use of a Ni-Ti hand file may permit glide path preparation in patients for whom Ni-Ti rotary files cannot be used. In this study, we investigated the effectiveness of Ni-Ti hand files in glide path preparation in terms of root canal centering ability and time required in comparison with Ni-Ti rotary files.

Materials and Methods

A HandFlex (Coltene Japan, Tokyo, Japan, HF group) was used as the Ni-Ti hand file and a WaveOne Gold Glider (Dentsply Sirona, OK, USA, GG group) as the Ni-Ti rotary file (Fig. 1). Each was used to form a glide path in a transparent root canal model. Glide path preparation was performed on a transparent root canal model by the same endodontist, who had 15 years of experience.

As transparent root canal models, ten J-shaped epoxy resin transparent curved root canal models (curvature 30°, apical foramen diameter #10, taper 2, root canal

length 16.5 mm, Endo Training block canals; Dentsply Sirona) were used in each group. These transparent root canal models were negotiated with a #10 stainless-steel hand file (K-FILES, MANI, INC., Tochigi, Japan). Working length was set as the root canal length minus 1 mm. Preparation of the root canal glide path was then conducted using each type of file. With the WaveOne Gold Glider, enlargement was conducted with an X-Smart Plus (Dentsply Sirona) using a reciprocating motion, as recommended by the manufacturer. With the HandFlex, enlargement was conducted at #15/.04 using the balanced-force technique, as recommended by the manufacturer. In the GG group the file was used three times in a pecking motion as a single action. In the HF group the file was used three times in a balance-hood-forced motion as a single action. During path preparation, both groups received positive-pressure irrigation with 1 mL of water from a syringe, which was carried out after every three actions with the file in both groups. Glide path preparation was terminated in both groups when the working length was reached (Fig. 2). We also measured the time taken to complete the glide path in each group. After glide path preparation, the transparent root canal models were photographed with a stereoscopic microscope (Stemi508, Axiocam ERc 5 s, Carl Zeiss, Baden-Württemberg, Germany). The digital images thus obtained were imported into a computer, and image analysis software (Photoshop, Adobe Inc., CA, USA) was used to superimpose and measure the root canal width pre- and post-root canal preparation. Increases in root canal width on the inner and outer sides of the curve were measured at points 1, 3, 5 mm and 7 mm from the root canal apex in the root canal models⁹, and centering ability was evaluated by calculating the centering ratio, which was defined as the smaller value of the inner or outer side increase in root canal width divided by the larger value¹⁰ (Fig. 3).

We then carried out statistical analyses; Student's *t*-test was used to compare increases in root canal width and the preparation time, with values of $p < 0.05$ considered significant. The Mann-Whitney *U* test was used to compare the centering ratio, with values of $p < 0.01$ considered significant.

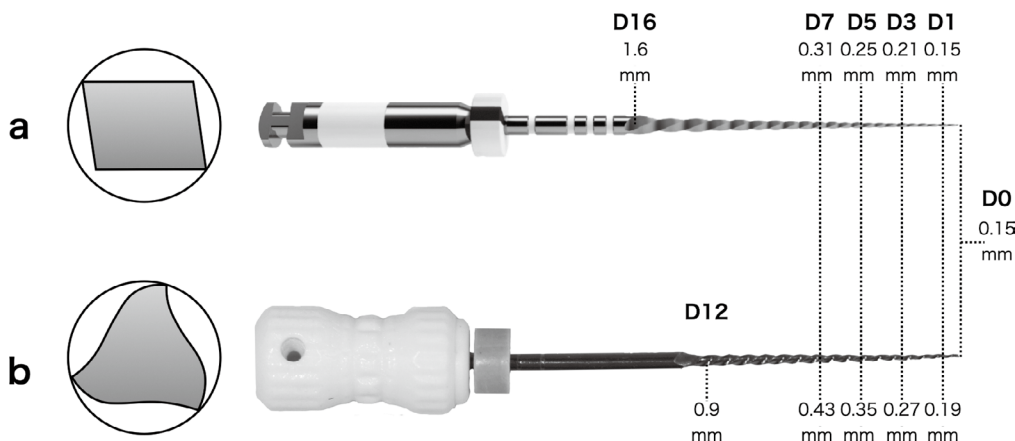


Fig. 1 Photograph of Ni-Ti files used for glide path preparation

a : WaveOne Gold Glider ; Ni-Ti rotary file. The cross-sectional form of the file is a parallel-gram with multiple tapers. b : HandFlex ; Ni-Ti hand file. The cross-sectional form of the file is a triple-helix cross with a 0.02 taper.

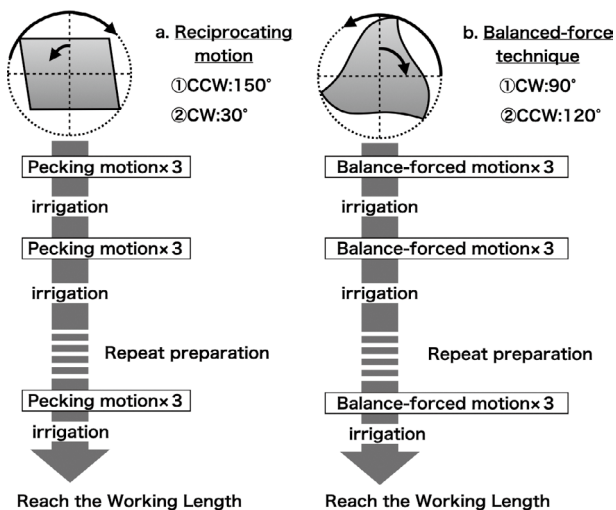


Fig. 2 Glide path protocols

a : Reciprocating motion and glide path protocols for the GG group. b : Balanced-force method and glide path protocols for the HF group.

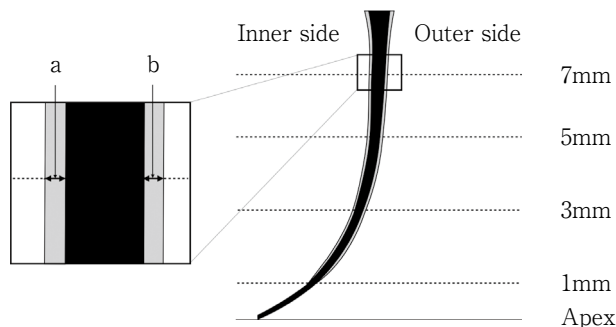


Fig. 3 Layering images before and after glide path images were superimposed and the difference between the canal configuration, in four levels of measurement plane

a : Inner side measurement width : Location of the increased width of the inner lateral wall of the root canal in the measurement plane after root canal enlargement. b : Outer side measurement width : Location of the increased width of the outer lateral wall of the root canal in the measurement plane after root canal enlargement.

Results

Observations of the state of the root canal after preparation confirmed that the original anatomy of the root canal had been maintained during enlargement in both the HF and GG groups (Fig.4). No obvious file deformation or breakage occurred in either group.

Table 1 shows the results of measurements of the increase in root canal width. In the comparison

between the HF and GG groups, increases in width on the inner side at 5 and 7 mm from the apex were significantly greater in the HF group, and the increases in width on the outer side at 3 and 5 mm from the apex were again significantly greater in the HF group ($p < 0.05$).

Figure 5 shows the centering ratio. Significant differences were also evident between the HF and GG groups at 1 mm from the apex ($p < 0.01$).

Figure 6 shows the glide path preparation time.

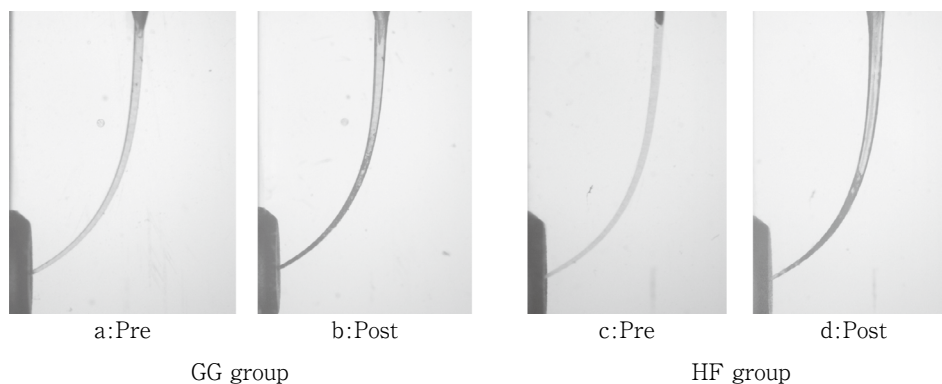


Fig. 4 Root canal model before and after glide path preparation with Ni-Ti rotary file
 a, b : Typical example of superimposed image for GG group. c, d : Typical example of superimposed image for HF group.

The original root canal anatomy was maintained during enlargement in all groups.

Table 1 Comparison of the increase in root canal width diameter in each group after glide path preparation

	Inner side				Outer side			
	1 mm	3 mm	5 mm	7 mm	1 mm	3 mm	5 mm	7 mm
HF group								
Mean	0.021	0.033	0.041 ^a	0.055 ^b	0.021	0.029 ^c	0.04 ^d	0.052
SD	0.005	0.008	0.011	0.020	0.006	0.008	0.009	0.017
GG group								
Mean	0.006	0.012	0.021 ^a	0.038 ^b	0.006	0.013 ^c	0.023 ^d	0.041
SD	0.002	0.006	0.008	0.014	0.002	0.007	0.010	0.014

The same superscripted letters indicate significant differences ($p < 0.05$).

The Ni-Ti hand file showed a significantly larger increase in root canal width diameter on the inner side.

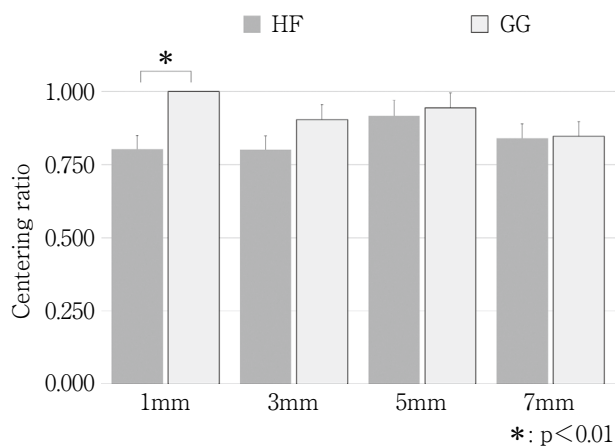


Fig. 5 Comparison of centering ratios in glide path groups

The closer the value is to 1, the higher the centering ability. * : Significant difference ($p < 0.01$)

Mean preparation time differed significantly between the HF group (147.06 ± 74.87 s) and GG group (38.33 ± 8.29 s; $p < 0.05$).

Discussion

Martensitic Ni-Ti rotary files offer better cyclic fatigue resistance and are softer than conventional austenitic files, and have been shown to permit enlargement while maintaining root canal anatomy^{9,11}. When used safely, Ni-Ti rotary files are suited to preparing the glide path while maintaining root canal morphology^{12,13}.

The Gold Glider is a file made of martensitic metal that has been treated by heating and slow cooling after cutting and processing. Although the torsional fatigue

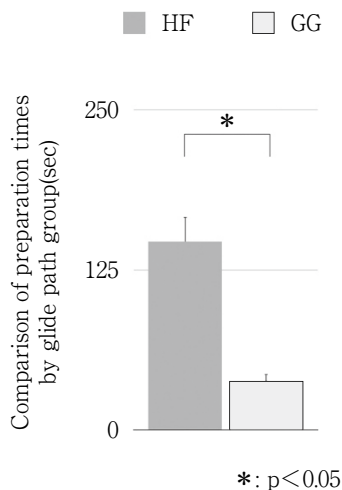


Fig. 6 Comparison of preparation times by glide path groups
* : Significant difference ($p < 0.05$)

resistance of martensitic metal is reportedly inferior to that of conventional austenitic metal¹⁴, the distinctive heat treatment given to the Gold Glider makes the file very soft, which is considered to compensate for the low torsional fracture resistance^{15,16}. Because a visible titanium oxide layer forms on martensitic metals as a result of heat treatment, they can be given a specific surface color depending on the heat treatment temperature^{13,17}. The surface of the Gold Glider has a gold coloration for this reason. The HandFlex is a Ni-Ti hand file that is also manufactured by heat treatment processing, although the details of this processing have not been made public. However, as the surface has the same gold-colored appearance as the Gold Glider, similar heat treatment processing is likely involved. In enlargement at #15/.04, the HandFlex should therefore provide similar shaping abilities in glide path preparation to those of Ni-Ti rotary files. However, this has yet to be investigated in detail.

The purpose of this study was to investigate whether Ni-Ti hand files can be used without any problems in clinical practice compared to Ni-Ti rotary files. Therefore, for the comparison we selected Ni-Ti rotary files that resemble Ni-Ti hand files in terms of clinical characteristics when used for preparing a glide path, with movements similar to the balanced-force methods, and having similar metallic properties. For these reasons, we chose the Gold Glider.

In this study, we compared the glide path prepara-

tion performance of the HandFlex and Gold Glider using standardized resin blocks including the simulated curved root canals. One disadvantage of evaluating glide path preparation performance in models is that the softened resin adheres to the file blade during preparation, potentially causing deformation or fracture of the instrument¹⁸. However, the use of resin blocks permitted the experiment to be conducted under standardized parameters, including working length, root canal diameter, and angle and radius of curvature.

In this study, observations of the models showed that both the HandFlex and Gold Glider enlarged the glide path while maintaining root canal anatomy. Both file designs are shaped as active instruments and offer high cutting efficiency¹⁹. Root canal deviation would normally be expected to be greater on the outer side¹⁴. However, the inner side exhibited significantly greater enlargement by both files, consistent with previous reports of enlargement conducted by reciprocating motions using martensitic files²⁰. This may have been because of the improved tracking performance of the Gold Glider as a result of the reciprocating motion. A similar result may have been obtained with the HandFlex because enlargement was conducted by the balanced-force technique²¹, which is the origin of reciprocating motion.

Overall, however, the increase in root canal width tended to be greater with the HandFlex. In addition, a marginally significant difference in centering ability was seen for Gold Glider at 1 mm lateral to the root apex. Root canal diameter for the model used in this study was 0.01 mm, with a taper of 0.02. The tip of the Gold Glider has a diameter of 0.15 mm with a taper of 0.02 up to 6 mm. Therefore, after loose filing with the #10 stainless-steel hand file, the file tip prepares the root canal without resistance and with no significant cutting. Preparation is then achieved at the site where the taper changes. This single glide path file produces the same effect as the crown-down technique. Therefore, we can infer that when a glide path is prepared using the Gold Glider, the root canal orifice is enlarged from near the middle of the root canal, but the apical third is less displaced by the cutting. On the other hand, the HandFlex has a taper of 0.04 and is larger than the Gold Glider. The diameter of the #15 HandFlex is markedly larger than that of the #10 stainless-steel hand file. Therefore, even with adequate loose

filing, the file tip will cut from the root canal orifice to the working length. The present results suggest that the overall amount of cutting was larger, and that slight displacement occurred at 1 mm from the root apex.

However, studies have found that differences in glide path systems have little effect on subsequent root canal preparation^{22,23}. Minor root canal deviation as a result of enlargement ≤ 0.3 mm at the apex has been shown not to pose an issue in terms of clinical outcomes²⁴. Tiny differences in the amount of cutting at the glide path stage are thus not considered clinically significant, as long as no root canal deviation is evident.

The time required for enlargement and preparation was significantly shorter with the Gold Glider than with the HandFlex. This was consistent with previous reports comparing preparation time using a stainless-steel hand file and a Ni-Ti rotary file^{16,25}. The cross-section of the Gold Glider is a parallelogram, while that of the HandFlex is a triple helix, with both representing active cross-sectional forms. The Gold Glider has two blades that are always in contact with the wall, whereas the HandFlex has three blades, and so is considered to provide a higher cutting force into the root canal wall. The HandFlex is thus considered to have a larger cutting volume than the Gold Glider, resulting in inferior centering ability on the apical side. In addition, the HandFlex has a large number of blades and the force of these blades biting into the root canal wall is strong. However, the HandFlex is used by hand, making rotation at a stable torque difficult. As a result, cutting time is increased. Although more time is needed for preparation when using the Ni-Ti hand files, we have found that it is possible to use them with little deviation. Enlargement with the HandFlex was carried out by the balanced-force technique, as recommended by the manufacturer. Based on enlargement with Ni-Ti rotary files using a pecking motion, actions were performed in sets of three. This was helpful in reducing the stress imposed on the file²³, but given that enlargement takes longer²⁶ there is scope for improvement in this method of use. However, the Ni-Ti hand files can enlarge more efficiently and accurately compared to the stainless-steel hand files.^{27,28}

Therefore, the preparation time should not be a concern in clinical use. In addition, both of these files are tapered and generate large amounts of cut fragments. Pushing out these fragments during root canal prepara-

tion disperses potential sources of infection¹², reportedly leading to increased post-procedural pain and flare-ups²⁹. Measures must be taken to deal with the large amount of cutting. Because the Gold Glider has high cutting efficiency and the HandFlex cuts an even greater amount, both generate large amounts of cut fragments. It is thus essential to pay attention to the method of enlargement³⁰ and to ensure adequate irrigation during enlargement^{12,31}.

Conclusion

Our results indicated that the HandFlex Ni-Ti hand file takes longer than the Gold Glider Ni-Ti rotary file to prepare the glide path, but adequately maintains the original anatomy of the root canal in the same way as with the Ni-Ti rotary file.

Conflict of Interest

There are no conflicts of interest to be disclosed in this study.

References

- 1) Akerblom A, Hasselgren G. The prognosis for endodontic treatment of obliterated root canals. *J Endod* 1988; 14: 565-567.
- 2) Gorni FGM, Gagliani MM. The outcome of endodontic retreatment: a 2-yr follow-up. *J Endod* 2014; 30: 1-4.
- 3) Ng YL, Mann V, Gulabivala K. A prospective study of the factors affecting outcomes of non-surgical root canal treatment: part 2: tooth survival. *Int Endod J* 2011; 44: 610-625.
- 4) Peters OA. Current challenges and concepts in the preparation of root canal systems: a review. *J Endod* 2004; 30: 559-567.
- 5) Peters OA, Peters CI, Schönenberger K, Barbakow F. ProTaper rotary root canal preparation: assessment of torque and force in relation to canal anatomy. *Int Endod J* 2003; 36: 93-99.
- 6) Kwak SW, Ha JH, Cheung GS, Kim HC, Kim SK. Effect of the glide path establishment on the torque generation to the files during instrumentation: An in vitro measurement. *J Endod* 2018; 44: 496-500.
- 7) Vorster M, van der Vyver PJ, Paleker F. Canal transportation and centering ability of WaveOne Gold in combination with and without different glide path techniques. *J Endod* 2018; 44: 1430-1435.
- 8) Elsaka SE, Elnaghy AM, Badr AE. Torsional and bend-

- ing resistance of WaveOne Gold, Reciproc and Twisted File Adaptive instruments. *Int Endod J* 2017; 50: 1077-1083.
- 9) Keskin C, Demiral M, Sarıyılmaz E. Comparison of the shaping ability of novel thermally treated reciprocating instruments. *Restor Dent Endod*. 2018; 43: e15.
 - 10) Yun HH, Kim SK. A comparison of the shaping abilities of 4 nickel-titanium rotary instruments in simulated root canals. *Oral Surg Oral Med Oral Pathol Oral Radiol Endod*. 2003; 95: 228-233.
 - 11) Kırıcı D, Kuştarıcı A. Cyclic fatigue resistance of the WaveOne Gold Glider, ProGlider, and the One G glide path instruments in double-curvature canals. *Restor Dent Endod* 2019; 44: e36.
 - 12) Low N, Zhen Jie S, Bhatia S, Davamani F, Nagendrababu V. Comparison of apical extrusion of bacteria after glide path preparation between manual K file, One G rotary, and WaveOne Gold Glider reciprocation preparations. *Eur Endod J* 2021; 6: 221-225.
 - 13) Hieawy A, Haapasalo M, Zhou H, Wang ZJ, Shen Y. Phase transformation behavior and resistance to bending and cyclic fatigue of ProTaper Gold and ProTaper Universal instruments. *J Endod* 2015; 41: 1134-1138.
 - 14) Gao Y, Gutmann JL, Wilkinson K, Maxwell R, Ammon D. Evaluation of the impact of raw materials on the fatigue and mechanical properties of ProFile Vortex rotary instruments. *J Endod* 2012; 38: 398-401.
 - 15) Prados-Privado M, Rojo R, Ivorra C, Prados-Frutos JC. Finite element analysis comparing WaveOne, WaveOne Gold, Reciproc and Reciproc Blue responses with bending and torsion tests. *J Mech Behav Biomed Mater* 2019; 90: 165-172.
 - 16) Santos CB, Simões-Carvalho M, Perez R, Vieira VTL, Antunes HS, Cavalcante DF, De-Deus G, Silva EJNL. Torsional fatigue resistance of R-Pilot and WaveOne Gold Glider NiTi glide path reciprocating systems. *Int Endod J* 2019; 52: 874-879.
 - 17) Plotino G, Grande NM, Cotti E, Testarelli L, Gambarini G. Blue treatment enhances cyclic fatigue resistance of vortex nickel-titanium rotary files. *J Endod* 2012; 40: 1451-1453.
 - 18) Roland DD, Andelin WE, Browning DF, Hsu GH, Torabinejad M. The effect of preflaring on the rates of separation for 0.04 taper nickel-titanium rotary instruments. *J Endod* 2002; 28: 543-545.
 - 19) Walsch H. The hybrid concept of nickel-titanium rotary instrumentation. *Dent Clin North Am* 2004; 48: 183-202.
 - 20) Hinata G, Shigetani Y, Yoshiba K, Okiji T. Shaping ability of reciproc nickel-titanium instruments in simulated curved canals. *Jpn J Conserv Dent* 2012; 55: 381-388. (in Japanese)
 - 21) Roane JB, Sabala CL, Duncanson MG Jr. The "balanced force" concept for instrumentation of curved canals. *J Endod* 1985; 11: 203-211.
 - 22) Alves Vde O, Bueno CE, Cunha RS, Pinheiro SL, Fontana CE, de Martin AS. Comparison among manual instruments and PathFile and Mtwo rotary instruments to create a glide path in the root canal preparation of curved canals. *J Endod* 2012; 38: 117-120.
 - 23) D'Amario M, Baldi M, Petricca R, De Angelis F, El Abed R, D'Arcangelo C. Evaluation of a new nickel-titanium system to create the glide path in root canal preparation of curved canals. *J Endod* 2013; 39: 1581-1584.
 - 24) Wu MK, Fan B, Wesselink PR. Leakage along apical root fillings in curved root canals. Part I: effects of apical transportation on seal of root fillings. *J Endod* 2000; 26: 210-216.
 - 25) Pasqualini D, Scotti N, Tamagnone L, Ellena F, Berutti E. Hand-operated and rotary ProTaper instruments: a comparison of working time and number of rotations in simulated root canals. *J Endod* 2008; 34: 314-317.
 - 26) Hata G, Uemura M, Kato AS, Imura N, Novo NF, Toda T. A comparison of shaping ability using ProFile, GT file, and Flex-R endodontic instruments in simulated canals. *J Endod* 2002; 28: 316-321.
 - 27) Carvalho LA, Bonetti I, Borges MA. A comparison of molar root canal preparation using stainless-steel and nickel-titanium instruments. *J Endod* 1999; 12: 807-810.
 - 28) Deplazes P, Peters O, Barbakow F. Comparing apical preparations of root canals shaped by nickel-titanium rotary instruments and nickel-titanium hand instruments. *J Endod* 2001; 3: 196-202.
 - 29) Pasqualini D, Mollo L, Scotti N, Cantatore G, Castellucci A, Migliaretti G, Berutti E. Postoperative pain after manual and mechanical glide path: a randomized clinical trial. *J Endod* 2012; 38: 32-36.
 - 30) De-Deus G, Brandão MC, Barino B, Di Giorgi K, Fidel RA, Luna AS. Assessment of apically extruded debris produced by the single-file ProTaper F2 technique under reciprocating movement. *Oral Surg Oral Med Oral Pathol Oral Radiol Endod* 2010; 110: 390-394.
 - 31) Bürklein S, Hinschitzka K, Dammascchke T, Schäfer E. Shaping ability and cleaning effectiveness of two single-file systems in severely curved root canals of extracted teeth: Reciproc and WaveOne versus Mtwo and ProTaper. *Int Endod J* 2012; 45: 449-461.

Influence of Additional Insertion after Reaching the Working Length on Root Canal Transportation and Extrusion of the Gutta-percha Point in Five Ni-Ti Rotary File Systems with Different Bending Properties

Fumiyasu MURAYAMA, Hirokazu SUGITA, Miki SEKIYA, Keisuke SAIGUSA,
Taro NISHIDA, Munehiro MAEDA and Masaru IGARASHI

Department of Endodontics, The Nippon Dental University School of Life Dentistry at Tokyo

Abstract

Purpose: The purpose of this study was to investigate the influence of additional insertion of the master apical file (MAF) after the file has reached its working length on root canal transportation and extrusion of the trial gutta-percha point out of the root apical foramen using five Ni-Ti rotary file systems with different bending properties.

Methods: The cantilever bending test was used to measure the bending load of the MAF. The untreated J-shaped curved root canal model blocks were obtained, and the root canals were negotiated with a #10 stainless steel K-file. Root canal preparation was performed in five groups: ProTaper Gold (PTG), TruNatomy (TN), HyFlex EDM (HEDM), WaveOne Gold (WOG), and RECIPROC Blue (RCB) to around size 25 using X-smart IQ (n=10). The post-preparation images were then obtained and superimposed on the pre-preparation images using image processing software. Additional insertions of MAF up to the working length were repeated ten, twenty, and thirty times for the post-preparation block, and the images were obtained and superimposed to measure the increase in the width diameter of the inner side and outer side. Gutta-percha points of the same size as the MAF of each group were inserted to the position of resistance of the root canal wall for each block. The length to the tip of the gutta-percha point was then measured using a digital microscope. The obtained values were statistically analyzed by the Kruskal-Wallis test with a significance level of 5%.

Results: In all files, the bending load values increased linearly and then leveled off. After unloading, the values decreased, and except for TN, the bending load became zero during unloading. At 0-1.0 mm from the apex, transportation tended to occur on the outer side of the root canal, but at 2.0 mm and above, transportation tended to occur on the inner side. In the WOG and RCB groups, transportation to the inner side of the canal was observed at 2.0 mm. No gutta-percha point extrusion was observed in the final enlarged model, but the length of extrusion increased as the number of insertions increased.

Conclusion: Additional insertion of the file caused root canal transportation inward above the root canal curvature and outward below the curvature, extending the apical reach of the gutta-percha point.

Key words: Ni-Ti rotary file, root canal transportation, extrusion of gutta-percha point

Corresponding author: Masaru IGARASHI, Department of Endodontics, The Nippon Dental University School of Life Dentistry at Tokyo, 1-9-20, Fujimi, Chiyoda-ku, Tokyo 102-0071, Japan

TEL: +81-3-3261-5698, FAX: +81-3-5216-3718, E-mail: m-igarashi@tky.ndu.ac.jp

Received for Publication: August 3, 2023/Accepted for Publication: September 14, 2023

DOI: 10.11471/odep.2023-008

Introduction

Ni-Ti rotary files are available in many file systems, which differ in the properties of the Ni-Ti alloy, file shape, usage, and preparation form¹⁻³. The differences in these properties are due to the heat treatment of alloys such as gold wire and blue wire or the associated differences in metallic phases such as R-phase and martensitic phase. These files, which are flexible due to the Ni-Ti alloy, are considered to have high root canal penetrating ability and are effective in reducing the occurrence of transportation during root canal preparation⁴⁻¹⁰. In recent years, efforts have been made to minimize the amount of root canal preparation itself using file geometry, thereby reducing root fractures that occur after root canal treatment^{11,12}. However, even Ni-Ti rotary files, which are considered to have high root canal penetrating ability, have different bending properties depending on the heat treatment, metal phase, and cross-sectional shape. For example, heat-treated files have lower bending load than those that have not been heat-treated^{13,14}, and martensitic phase files have lower bending load than austenitic phase files¹⁵. In addition, a parallelogram cross-sectional shape has lower bending load than a triangular one^{16,17}.

In general, the end of root canal preparation when using a Ni-Ti rotary file is when the tip of the file reaches the working length. However, few teeth have root canals with a circular cross-sectional morphology¹⁸. Therefore, with Ni-Ti rotary files, which are prepared by rotational manipulation, contamination remains in the root canal even after the root canal preparation is completed¹⁹. As a countermeasure, circumferential filing is repeated with the same file²⁰. In root canal preparation, file flexibility is one of the most important factors in maintaining the original root canal morphology¹⁵. When stainless steel files are used for root canal preparation, they tend to cause transportation at the root apex because of their increased stiffness and decreased flexibility as their size increases^{21,22}. Ni-Ti rotary files are considered to have high root canal penetrating ability, as well as the ability to suppress the occurrence of transportation. However, few studies have examined whether transportation occurs when root canal preparation is continued without changing the file size after the working length is

reached. It has also been reported that overfilling affects the prognosis of root canal treatment²³, since root canal filling is considered ideal to seal the root canal closely up to the working length. However, no studies have reported an association between root canal transportation and gutta-percha point extrusion with the additional insertion of the MAF.

The purpose of this study was to investigate the influence of additional insertion of the MAF after the file has reached its working length on root canal transportation and extrusion of the trial gutta-percha point out of the root apical foramen using five Ni-Ti rotary file systems with different bending properties. The parameters of interest in this study were the increase in the width diameter of the inner and outer sides, and the length of gutta-percha point extrusion outside the root apical foramen.

Materials and Methods

1. Ni-Ti rotary file systems and test materials

The file systems and gutta-percha points used in this experiment are listed in Table 1. Five different 25-mm file systems were used for root canal preparation: ProTaper Gold (PTG group, Dentsply Sirona, Ballaigues, Switzerland); TruNatomy (TN group, Dentsply Sirona); HyFlex EDM (HEDM group, Coltène-Whaledent, Altstätten, Switzerland); WaveOne Gold (WOG group, Dentsply Sirona); and RECIPROC Blue (RCB group, VDW, Munich, Germany). The following were used for glide path preparation: PTG group, ProGlider (16/.02); TN group, TruNatomy Glider (17/.02v); HEDM group, HyFlex EDM Glidepath File (15/.03); WOG group, WaveOne Gold Glider (15/.02); and RCB group, R-Pilot (12.5/.04). The files used for root canal preparation and the size and taper of each file were ProTaper Gold S1 (18/.02), S2 (20/.04), F1 (20/.07), and F2 (25/.08) in the PTG group, TruNatomy Prime (26/.04v) in the TN group, HyFlex EDM OneFile (25/.08-04) in the HEDM group, WaveOne Gold Primary (25/.07) in the WOG group, and RECIPROC Blue (25/.08) in the RCB group. Fifty J-shaped curved root canal model blocks (root canal length: 16 mm, Endo Training Bloc J-Shape ø15; Dentsply Sirona) were used as the test material for root canal preparation. Gutta-percha points used for root canal filling were ProTaper Gold Conform Fit for the PTG group, TruNatomy Conform Fit for the TN group,

Table 1 Materials used in this study

	ProTaper Gold (PTG)	TruNatomy (TN)	HyFlex EDM (HEDM)	WaveOne Gold (WOG)	RECIPROC Blue (RCB)
Glide path preparation (Size/Taper) [Lot No.]	ProGlider (16/.02) [1693705]	TruNatomy Glider (17/.02v) [1634717]	HyFlex EDM Glide- path File (15/.03) [K57846]	WaveOne Gold Glider (15/.02) [1639239]	R-Pilot (12.5/.04) [340803]
Root canal preparation (Size/Taper) [Lot No.]	ProTaper Gold S1 (18/.02) [1550304] S2 (20/.04) [1637282] F1 (20/.07) [1578319] F2 (25/.08) [1553640]	TruNatomy Prime (26/.04v) [1557969]	HyFlex EDM OneFile (25/.08-04) [K88436]	WaveOne Gold Primary (25/.07) [1638086]	RECIPROC Blue (25/.08) [340726]
Types of instrumentation	Continuous rotary motion	Continuous rotary motion	Continuous rotary motion	Reciprocating motion	Reciprocating motion
Difference in the number of pieces used for root canal preparation Single file or Multiple files	Multiple files	Single file	Single file	Single file	Single file
Gutta-percha point [Lot No.]	ProTaper Gold Conform Fit [0000338494]	TruNatomy Con- form Fit [0000267938]	HyFlex EDM gutta- percha points [L86806]	WaveOne Gold Conform Fit [0000346080]	RECIPROC Gutta-Percha [3835750]
Manufacturer	Dentsply Sirona	Dentsply Sirona	Coltène-Whaledent	Dentsply Sirona	VDW

HyFlex EDM gutta-percha points for the HEDM group, WaveOne Gold Conform Fit for the WOG group, and RECIPROC Gutta-Percha for the RCB group.

2. Experimental details

1) Cantilever bending test of Ni-Ti rotary files

To identify differences in file flexibility, a cantilever bending test was used to measure the bending load of the MAF (Fig. 1). The file was held 6.0 mm from the tip coincident with the start of the block curvature, a load was applied (load cell speed: 1.0 mm/min) until the load point set at 2.0 mm from the tip deflected 3.0 mm, and it was then unloaded until the load cell returned to the load start point, and the load values were recorded throughout the process (n=10). The load value at 2.0-mm deformation was also evaluated.

2) Measurement of root canal transportation by image superimposition

To clarify the amount of transportation of the root canal due to the additional insertion, a view of the curvature of the root canal of the untreated blocks was

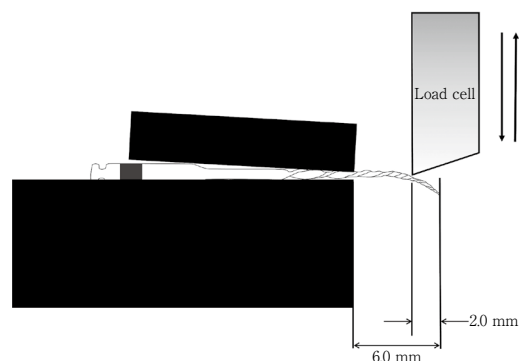


Fig. 1 Schematic diagram of the cantilever bending test (load cell speed : 1.0 mm/min)

obtained using a scanner (GT-X970; EPSON, Tokyo, Japan) to use as data before preparation of the curved surface. During image acquisition, the root canal was filled with a methylene blue solution. The working length was defined as the length of the root canal. Next, root canal preparation was performed after checking

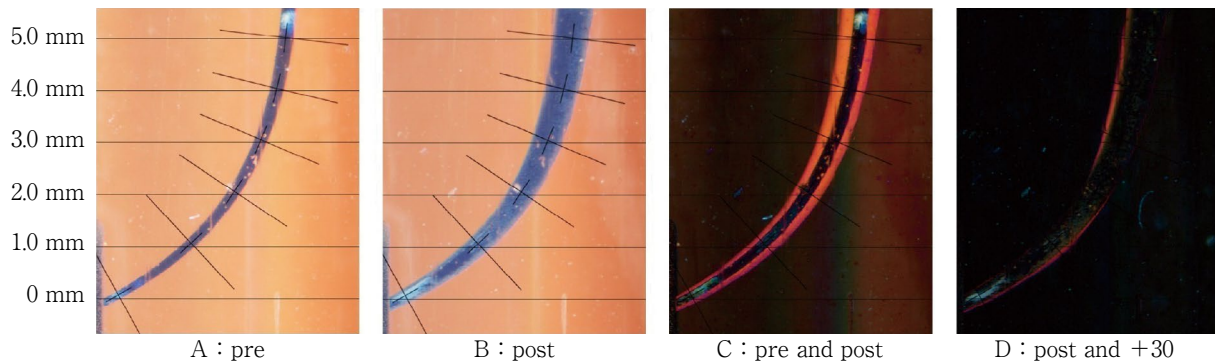


Fig. 2 Measurement points of root canal width diameter increase in this study and root canal morphology image and superimposed image

A : pre-preparation, B : post-preparation using ProTaper Gold, C : superimposed image of pre-preparation and post-preparation, D : superimposed image of post-preparation and thirty additional insertions

the negotiation of the root canal with a stainless steel hand K-file #10 (Readysteel; Dentsply Sirona). For root canal preparation, a torque control motor X-Smart IQ (Dentsply Sirona) was used. File manipulation was performed only with vertical movement along the root canal axis and with as little brushing motion as possible. The rotation speed and torque were in accordance with each manufacturer's instructions. The root canal was filled with purified water during preparation, and the root canal was rinsed with purified water every three or four insertions to ensure that there was no blockage with a #10 K file. Final enlargement was defined as the time when the MAF reached the working length once. The block was imaged with a scanner and superimposed on the image before the preparation was performed using image processing software (Adobe Photoshop 2022; Adobe Inc., San Jose, CA, USA). Next, the image after ten additional insertions of the MAF up to the working length was obtained and superimposed on the image at final enlargement. In addition, images were also obtained for the twenty and thirty insertions and superimposed in the same way. The measurement was based on the method of Yun et al.²⁴⁾, drawing a perpendicular line to the central line of the root canal and measuring the increase in canal width diameter on the outer and inner sides of the root canal wall. The measurement points in this study were 0, 1.0, 2.0, 3.0, 4.0 mm and 5.0 mm from the root apex based on the top of the root apical foramen before preparation (Fig. 2). The difference in the increase in the width diameter of the inner side from the increase in the width diameter of the outer side was calculated for each file group, and

the difference between the plus and minus was used to record in which direction the root canal transportation was occurring.

3) Measurement of gutta-percha point length extruded from the root apex

Gutta-percha points were of the same size as the MAF for each group. For the block with final enlargement and additional file insertion, a gutta-percha point was inserted without sealer to the position where the resistance of the root canal wall was obtained, and the block was trial fitted into the root canal. The length of the gutta-percha point was then measured using a digital microscope (VHX-7000; KEYENCE, Osaka, Japan) with the root surface as the reference position to determine the length of extrusion of the point from the root apex.

3. Statistical analysis

The data obtained were analyzed statistically using statistical software (SPSS Statistics version 28; IBM, Armonk, NY, USA) with the Kruskal-Wallis test and Bonferroni post hoc correction at the 5% significance level.

Results

1. Cantilever bending test of Ni-Ti rotary files

The results of the cantilever bending test are shown in Fig. 3. The average bending load at 2.0 mm is shown in Fig. 4. For all files, the load increased linearly at the beginning of loading and remained almost flat thereafter. It also decreased after unloading, and except for TN, the bending load values became zero during

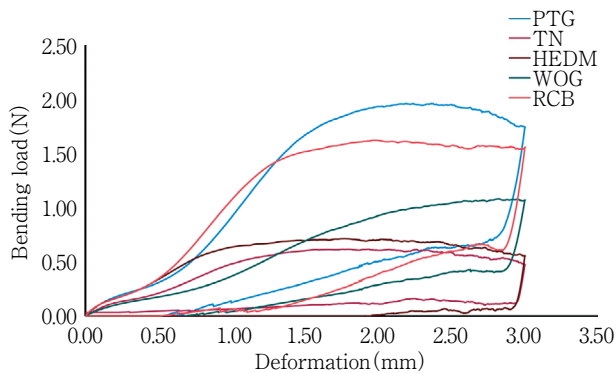


Fig. 3 Bending load-deformation curves for each group

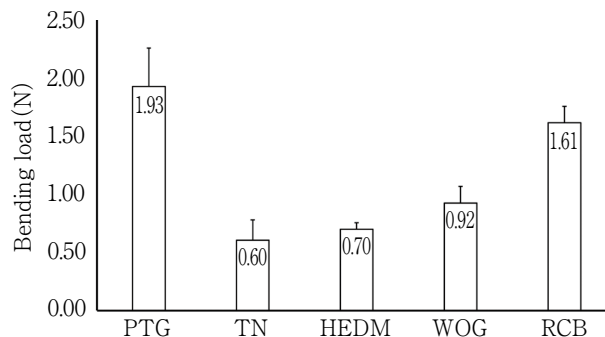


Fig. 4 Bending load value at 2.0-mm deformation for each group

unloading.

2. Root canal transportation calculated by image superimposition

File fracture due to additional insertion did not occur in any files. Figure 5 shows the increase in diameter of the outer and inner side widths when each image was superimposed. Figure 5A shows an increase of about 0.2 mm, and for the TN, the increase at 5.0 mm was about half the amount of the other files. Figures 5B-D show the amount of increase for each of the ten additional insertions after the preparation. The increase in root canal width was about 0.02 mm for both the inner and outer sides after ten additional insertions, about 0.06 mm after twenty additional insertions, and 0.06 mm for the inner side and 0.08 mm for the outer side after thirty additional insertions. Among them, the increase of 0-1.0 mm HEDM for the outer and 3.0-5.0 mm PTG for the inner were most significant. Figure 5E shows the increase before preparation and after thirty additional insertions, and compared to Fig. 5A, there was a tendency for transportation to occur on the outer side of the canal at 0-1.0 mm from the apex. On the other hand, above 2.0 mm, there was a tendency for transportation to occur toward the inner side. Figure 6 shows a comparison of the final enlargement of each group, the increase in the width of the outer and inner sides for the number of insertions, and the direction of transportation. In the comparison of each file, there was an increase in the outer side of the canal at 0-1.0 mm from the apex and the inner side of the canal at 3.0-5.0 mm from the apex, especially significantly at twenty and thirty additional insertions. In contrast, there was a slight increase at 0-1.0 mm in the inner side and 3.0-5.0 mm in the outer side. In the WOG and RCB groups,

transportation to the inner side of the canal was observed at 2.0 mm.

3. Measurement of gutta-percha length extruded from the root apex

The lengths of gutta-percha points extruded from the root apical foramen at final enlargement and at ten, twenty, and thirty additional file insertions from final enlargement are shown in Fig. 7. Compared to the mean values, there was no extrusion at final enlargement in any of the groups, with values in the order of HEDM (-0.31 mm) < WOG (-0.26 mm) < PTG (-0.22 mm) < TN (-0.19 mm) < RCB (-0.14 mm). At ten additional insertions, some files began to show extrusion, in the order of HEDM (-0.12 mm) < WOG (-0.08 mm) < PTG (-0.03 mm) < RCB (+0.01 mm) < TN (+0.07 mm). After twenty additional insertions, extrusion was seen in WOG (+0.07 mm) < HEDM (+0.10 mm) < PTG (+0.13 mm) < RCB = TN (+0.43 mm), but the mean value was within 0.5 mm. After thirty additional insertions, the results were WOG (+0.20 mm) < HEDM (+0.32 mm) < PTG (+0.57 mm) < RCB = TN (+0.94 mm), with a mean value within 1.0 mm.

Discussion

This study was conducted to compare the amount of file system preparation more clearly by using a ready-made clear curved root canal model block of uniform material and identical morphology.

In this study, bending load was first measured by a cantilever bending test. The shape of the root canal of the block used in this study was almost identical to the shape of the root canal displaced 2.0 mm when load was applied to the 2.0-mm portion from the file tip. There-

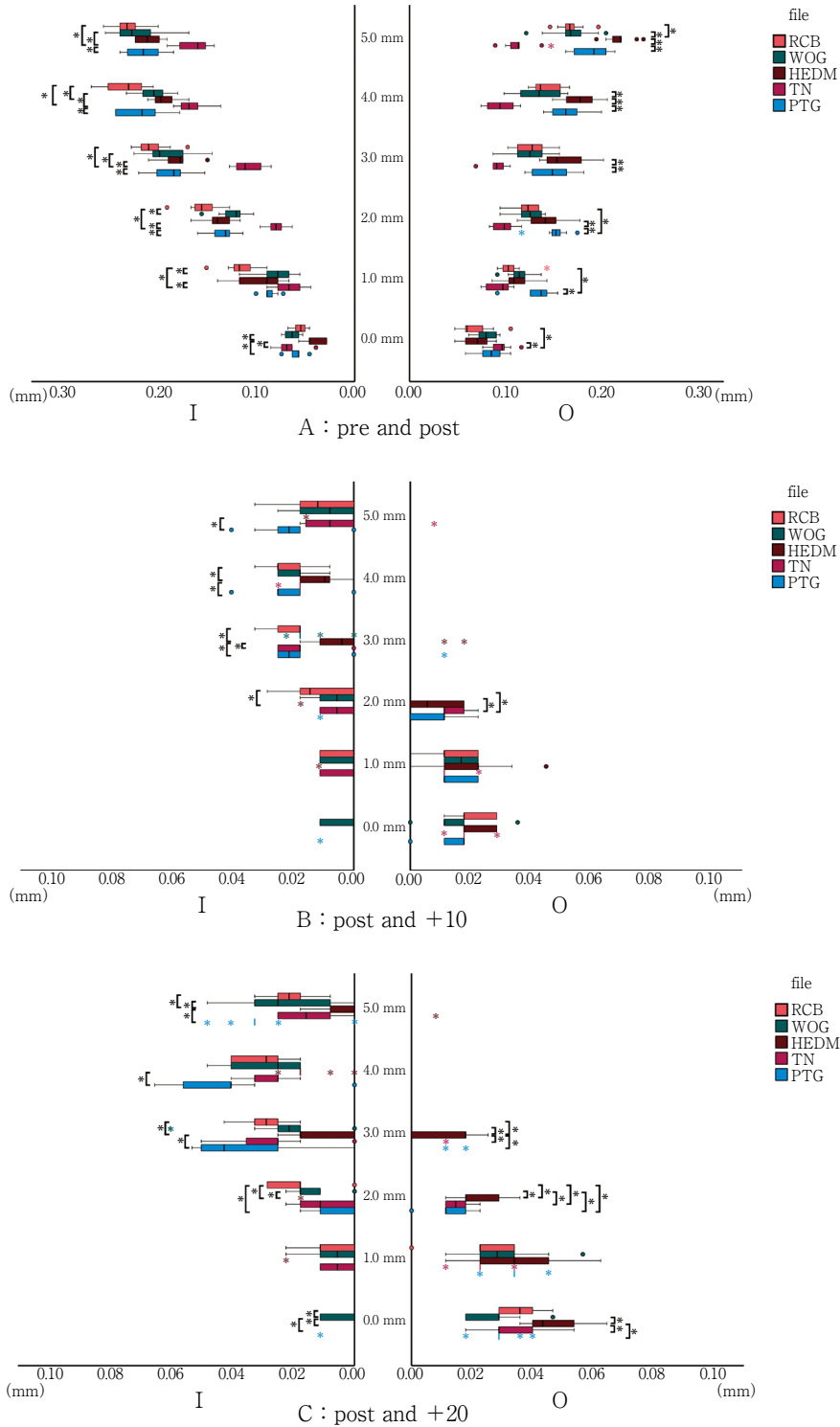


Fig. 5 Comparison between files of the increase in outer diameter and inner width diameter of the root canal and root canal transportation by the number of insertions

A : superimposition of pre- and post-preparation, B : superimposition of post-preparation and ten additional insertions, C : superimposition of post-preparation and twenty additional insertions, D : superimposition of post-preparation and thirty additional insertions, E : superimposition of pre-preparation and thirty additional insertions, I : increase in diameter of the inner canal width, O : increase in diameter of the outer canal width, ○ : outlier, ☆ : singular value

Kruskal-Wallis test. * : p < 0.05

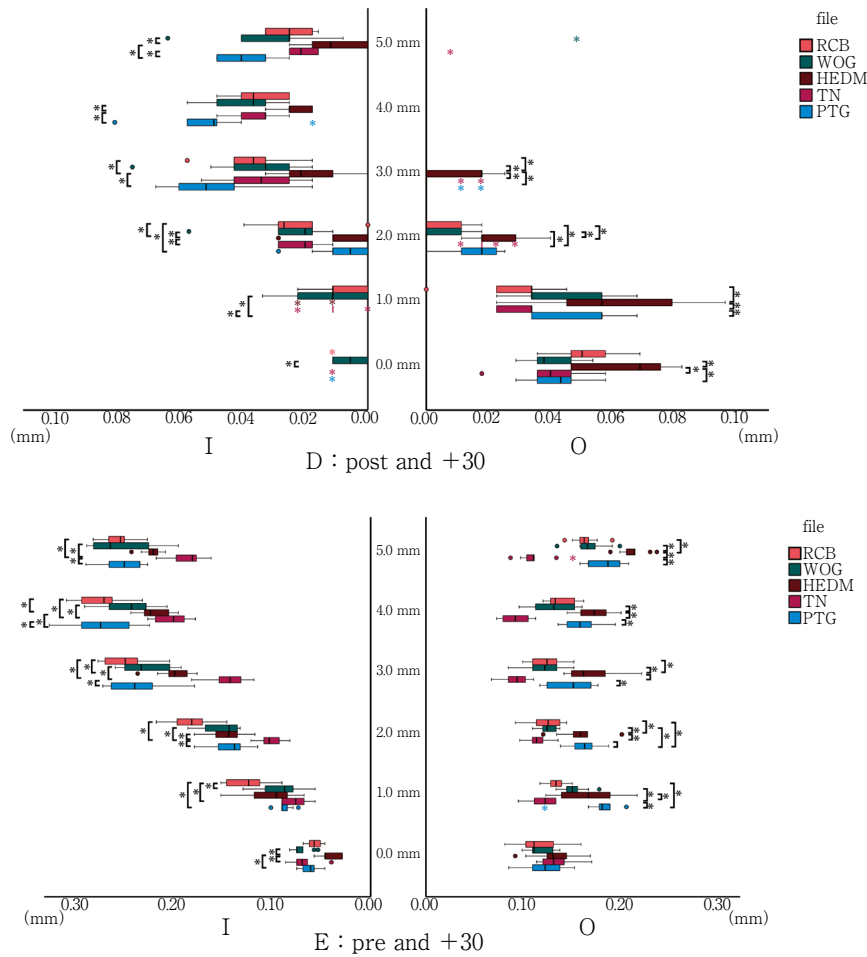


Fig. 5 Continued

fore, the bending load at 2.0 mm of the loading process was evaluated. The results showed that HEDM had the second lowest bending load when loaded and the lowest when unloaded. Therefore, HEDM exhibited high flexibility and high shape memory. PTG, RCB, and WOG had high bending load, but the bending load became zero during unloading. This was due to the R-phase or martensitic nature of the alloys. PTG and WOG used the same gold wire, but they exhibited different bending load. Hou et al.¹⁶⁾ and Schäfer et al.¹⁷⁾ reported that the file was more flexible when the cross-sectional shape was parallelogram than when triangular. The cross-section of PTG was a convex triangle, and that of WOG was a parallelogram, and the present results were like theirs. Therefore, it was suggested that the difference in the cross-sectional shape of the files affected the bending load. Unno et al.²⁵⁾ reported that TN showed flexible properties due to its thin wire diameter of 0.8 mm, unlike other files. Similarly, the

bending load of TN was low in the present study, but the bending load of TN continued to be measured during unloading. It was considered possible that this material exhibited R-phase-like dynamics with both shape memory and superelastic properties, unlike HEDM, which exhibited similarly flexible properties.

In the measurement of root canal transportation in Experiment 2, there was a tendency for transportation toward the outer side of the root canal up to 2.0 mm from the root apex. On the other hand, above 2.0 mm, there was a tendency for transportation to occur toward the inner side. This is thought to be due to an inflection point at the 2.0-mm curvature of the block used in this study, where the direction of inward and outward transportation switched. The change in transport direction near the curvature is consistent with the report of Perez et al.²⁶⁾. Although HEDM is considered to have good root canal-penetrating ability due to its high shape memory at room temperature, transporta-

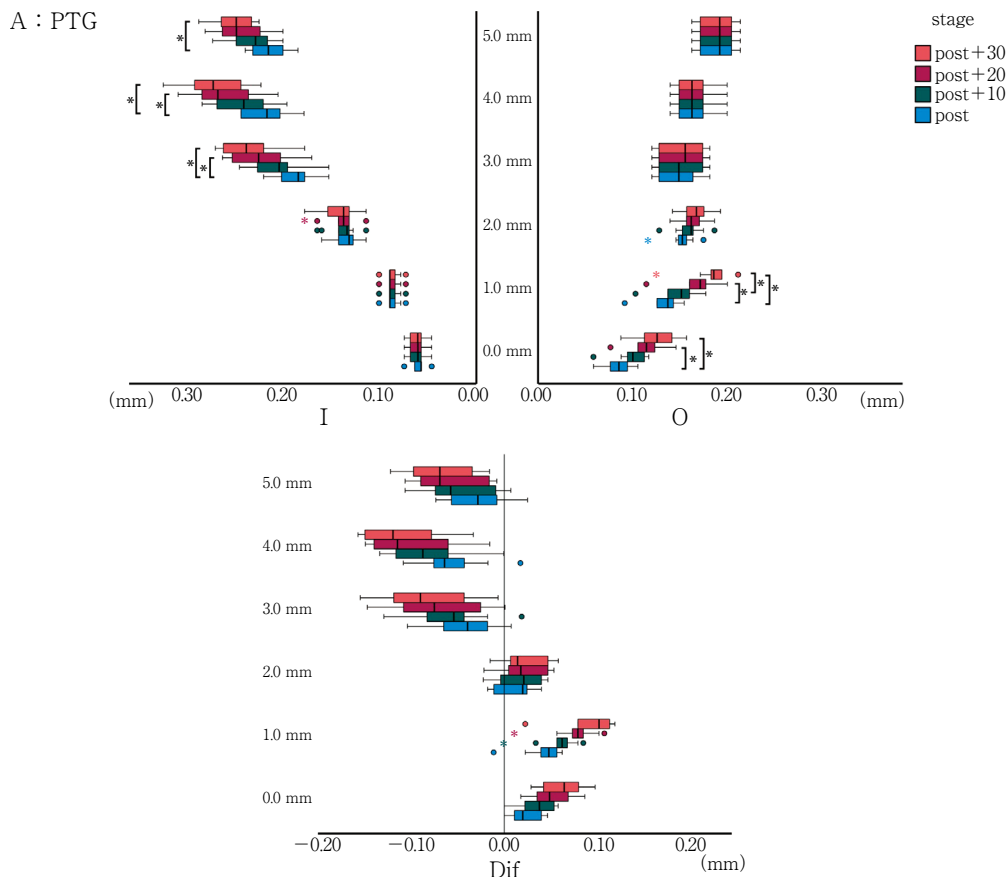


Fig. 6 Comparison of the increase in the outer diameter and inner width diameter of the root canal and root canal transportation for each file by the number of insertions

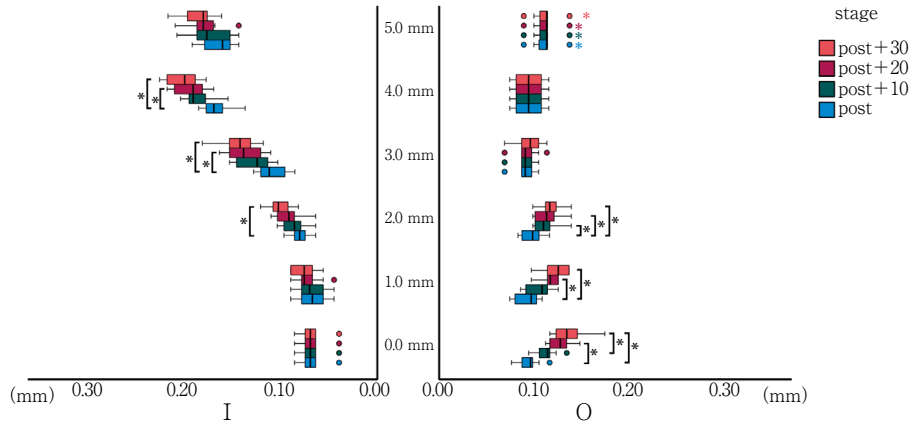
A : ProTaper Gold, B : TruNatomy, C : HyFlex EDM, D : WaveOne Gold, E : RECIPROC Blue, I : increase in diameter of the inner canal width, O : increase in diameter of the outer canal width, Dif : difference between the increase in root canal width on the outer canal side and the increase in root canal width on the inner canal side, post : superimposition of pre- and post-preparation, post+10 : superimposition of pre-preparation and ten additional insertions from post-preparation, post+20 : superimposition of pre-preparation and twenty additional insertions from post-preparation, post+30 : superimposition of pre-preparation and thirty additional insertions from post-preparation, ○ : outlier, ☆ : singular value

Kruskal-Wallis test. * : $p < 0.05$

tion to the outer wall was observed near the root apex at thirty additional insertions (Fig. 5D). The higher cutting efficiency of HEDM, which is fabricated by electrical discharge machining (EDM)¹¹⁾, may have caused more outward transportation than other files. In addition, transportation to the inner side was observed for WOG and RCB at 2.0 mm (Fig. 6D, E). This may be related to the fact that the rotation method is reciprocating motion. Files with reciprocating motion have

blades facing the opposite direction of those with continuous rotation, cutting is performed in counterclockwise rotation, and torque is released in clockwise rotation to prevent biting into the root canal wall. The continuously rotating file is not released from the torque, so outward force is applied at the curvature²⁷⁾. However, for files in reciprocating motion, the outward force generated by continuous rotation is reset by the release of torque. Therefore, it is conceivable that a relative

B : TN



C : HEDM

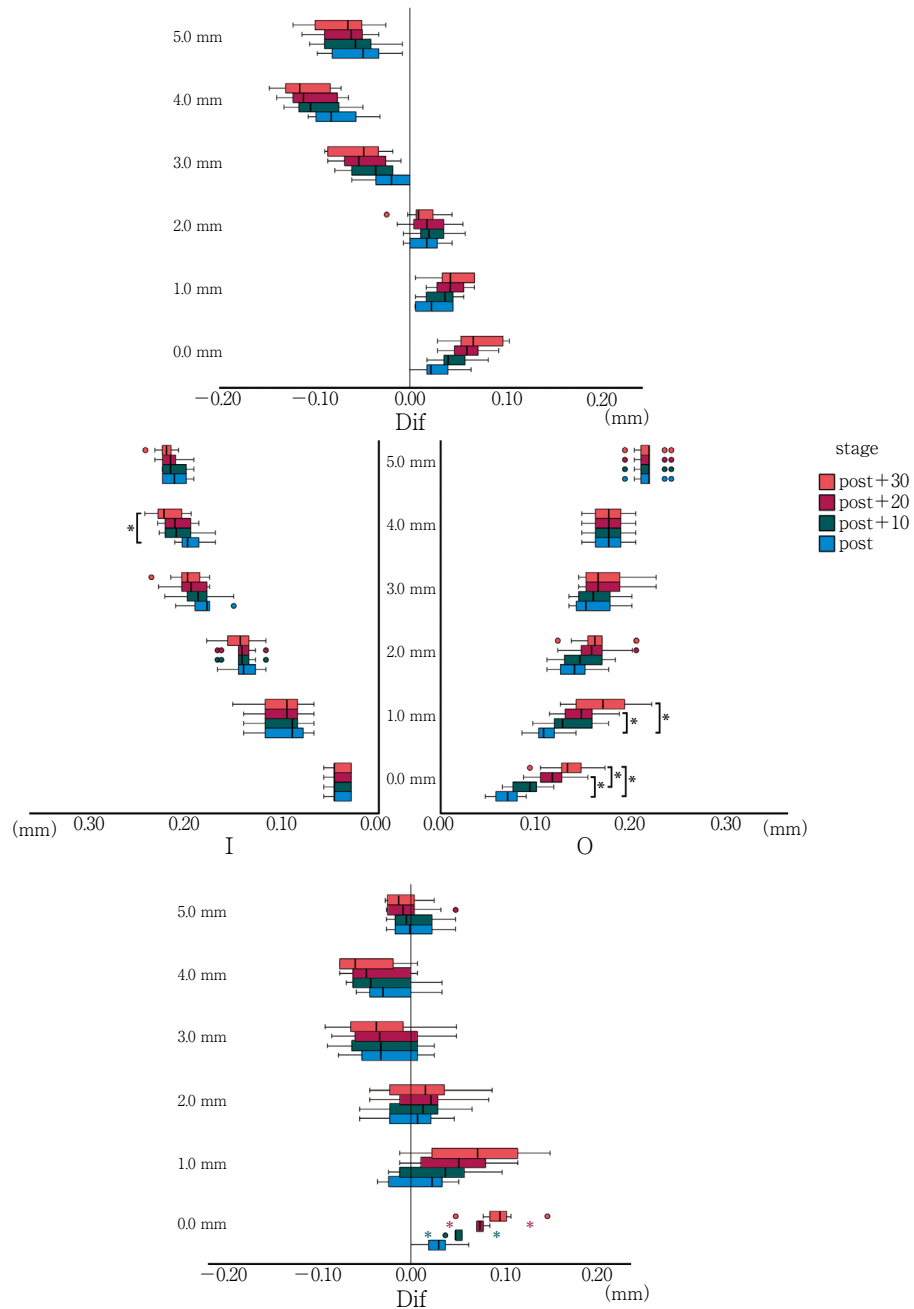
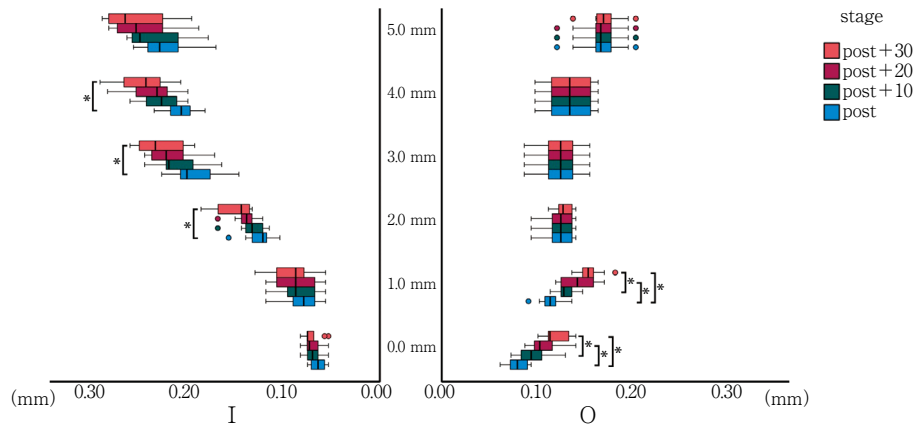


Fig. 6 Continued

D : WOG



E : RCB

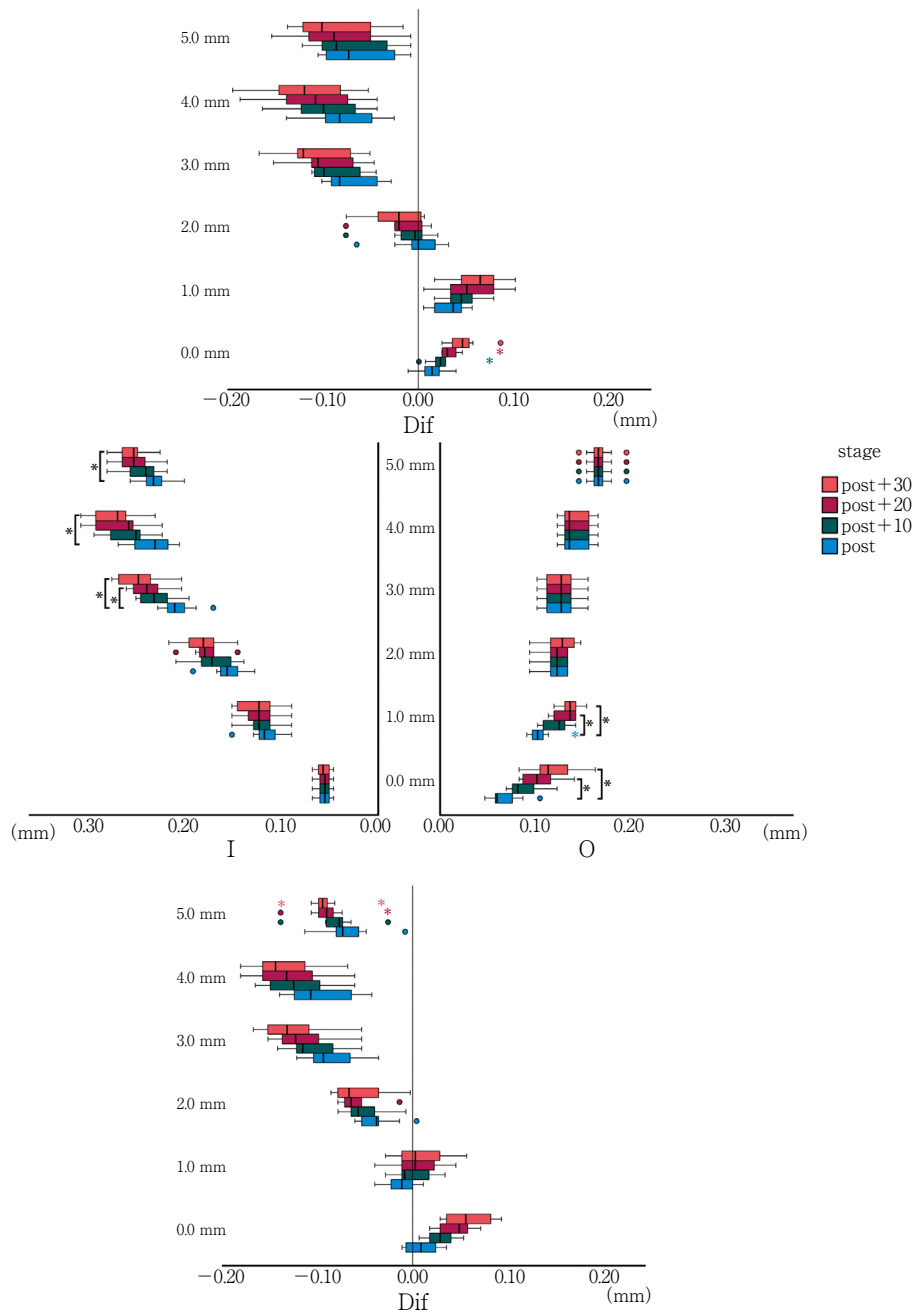


Fig. 6 Continued

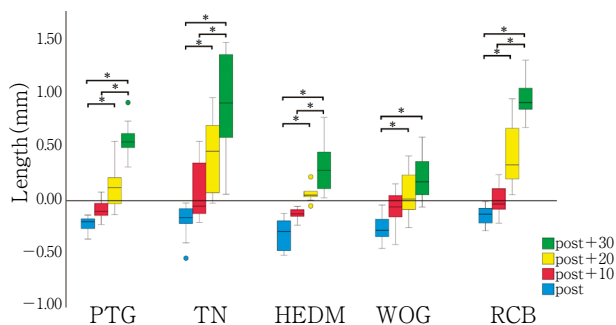


Fig. 7 Distance between the apical foramen and the tip of the gutta-percha point

post : post-preparation, post+10 : ten additional insertions from post-preparation, post+20 : twenty additional insertions from post-preparation, post+30 : thirty additional insertions from post-preparation, ○ : outlier

Kruskal-Wallis test. * : $p < 0.05$

inward force is applied. In other words, the file in reciprocating motion has stronger contact with the inner side of the canal than the file in continuous rotation due to the repetitive counterclockwise and clockwise rotational motions. Therefore, transportation to the inner side at the curvature of the canal is considered to have increased.

Furthermore, in all file systems, root canal straightening was observed, with transportation to the outer side near the root apex and transportation to the inner side in the upper part of the root canal. This was similar to that reported by al-Omari et al.²⁸⁾ who showed root canal straightening in a stainless steel file. Therefore, even when Ni-Ti files with high root canal-penetrating ability were used, additional insertion caused straightening of the root canal as with stainless steel files.

In the analysis using transparent root canal blocks, as in this study, a digital camera or flat head scanner is used to acquire images.²⁹⁻³¹⁾ Although the image acquisition methods are different, it is possible to analyze changes in root canal morphology in two dimensions by fixing the shooting position and setting the criteria for superimposition to something other than the root canal morphology. However, the comparison test of the amount of root canal preparation and transportation by superimposition of two-dimensional images is performed by superimposing images from only one direction. Therefore, only the curvature view can be com-

pared, and only the amount of two-dimensional formation and transportation can be identified. To superimpose not only one direction but the entire root canal, the images should be obtained and superimposed in a three-dimensional image using micro-computed tomography imaging or other methods. This would allow for a three-dimensional view of the transportation of the root canal and allow for a higher level of comparison. However, when X-rays are used, the object must be made of a material that does not transmit X-rays, and so consideration must be given to the composition and materials of the object.

In the present study, the file with the highest bending load was the PTG. However, transportation toward the inner side above 3.0 mm increased with each additional insertion. Compared to the PTG, the HEDM file, which has lower bending load, showed less transportation toward the inner side. In the area near the root apical foramen, transportation was greater with the HEDM file, but significantly less with the PTG. These results suggest that, in the area below the curvature near the root apical foramen, transportation is related to the cutting efficiency of the file used, whereas in the area above the curvature, it may be related to the bending load of the file.

In Experiment 3, additional insertion of the same size file up to the working length caused transportation in the area above and below the root canal curvature, excessive cutting in the root apical region, and extrusion of the gutta-percha point out of the root apical foramen. In root canal preparation using Ni-Ti rotary files, root canal filling is usually performed with a matched-taper, single-cone technique using a gutta-percha point with a matching size and taper. In addition, unlike root canal preparation with a stainless steel hand file, the gutta-percha point is not held in place by an apical sheet or apical collar, but rather by the entire root canal preparation surface. In the present study, excessive additional file insertion may have resulted in enlargement of the formation surface, thereby reducing its retention capacity and leading to extrusion of the gutta-percha point.

In the present study, the root apical foramen was defined as the narrowest part of the block used, and the root canal length was set as the working length. The most constricted area in human teeth is the physiological apical foramen, but there is a difference of approxi-

mately 1.0 mm between the physiological apical foramen and the anatomical apical foramen^{32,33}). Wu et al.³⁴) and Tsesis et al.³⁵) also stated that the position of working length should be set between the physiological and anatomical apical foramen. Transportation may have destroyed the physiological apical foramen due to the additional insertion of the file. However, the length of the gutta-percha point that was extruded in this study was approximately 1.0 mm, suggesting that extrusion of the gutta-percha point to the anatomical apical foramen may not occur. There was no significant difference between the final enlargement and the block with ten additional insertions from the final enlargement, suggesting that the tip of the gutta-percha point remained within the anatomical apical foramen. Therefore, it was suggested that up to ten additional insertions may be acceptable if the insertion method is such that no brushing motion is performed, as in the present study. However, Ricucci et al.³⁶) reported that root canal preparation and filling beyond the physiological apical foramen has a poor prognosis. As a countermeasure, it is possible that a gutta-percha point of the same size as the MAF could be used by cutting the tip of the gutta-percha point by 1.0 mm without causing extrusion even through the physiological root apical foramen. However, even if the gutta-percha point is used with a 1.0-mm cut, the conformability of the gutta-percha point decreases due to the occurrence of root canal transportation and hyperenlargement if additional file insertions are made more than ten times. As a result, a gap between the root canal wall and the gutta-percha point may occur. Eymirli et al.³⁷) reported that the use of a gutta-percha point of the same size and taper as the MAF promoted the penetration of the bioceramic sealer into the dentin tubules, leading to improved point conformance. Therefore, if further root canal preparation is desired after considering the compatibility of the gutta-percha point with the root canal wall, the same size file should continue to be used, and no additional insertions should be made. Instead, root canal preparation should be performed with the minimum number of insertions up to the working length using a larger size file, followed by root canal filling using a gutta-percha point of the same size. It is also important to promote the reduction of bacteria in the root canal by sonication with sodium hypochlorite solution or by chemical cleaning using ultrasonic cleaning, rather than by mechanical

root canal preparation alone.

Conclusion

This study investigated the influence of additional insertion of the MAF after the file has reached its working length on root canal transportation and extrusion of the trial gutta-percha point out of the root apical foramen using five Ni-Ti rotary file systems with different bending properties. The following conclusions were reached.

1. In the bending load measurement, the averages of the load values when loading a 2.0-mm position were compared, and the relationship was $PTG > RCB > WOG > HEDM > TN$.
2. Additional insertion of the file up to its working length caused transportation to the inner side above the root canal curvature and to the outer side below the curvature, with an increasing degree of transportation and a tendency to straighten the root canal.
3. In the reciprocating motion file, transportation to the inner side occurred at the root canal curvature, and the increase in root canal width diameter was significantly greater with RCB compared to TN and HEDM at the final enlargement and at the superposition of thirty additional insertions.
4. Additional insertion of the file up to the working length extended the apical reach of the gutta-percha point, and an average of 0.94 mm of extrusion from the root apical foramen was observed for RCB and TN after thirty additional insertions.
5. Up to ten additional insertions to the working length of the file after the working length is reached in root canal preparation may be acceptable.

Conflict of Interest

The authors declare no conflict of interest related to this paper.

References

- 1) Liang Y, Yue L. Evolution and development: engine-driven endodontic rotary nickel-titanium instruments. *Int J Oral Sci* 2022; 14: 12.
- 2) Ruddle CJ, Machtou P, West JD. The shaping movement: fifth-generation technology. *Dent Today* 2013; 32: 94, 96-99.

- 3) Igarashi M, Kitajima K, Arai K. Current of NiTi rotary files reached to single file system. *JJEA* 2014; 35: 3-15.(in Japanese)
- 4) Silva EJ, Muniz BL, Pires F, Belladonna FG, Neves AA, Souza EM, De-Deus G. Comparison of canal transportation in simulated curved canals prepared with ProTaper Universal and ProTaper Gold systems. *Restor Dent Endod* 2016; 41: 1-5.
- 5) van der Vyver PJ, Paleker F, Vorster M, de Wet FA. Root canal shaping using nickel titanium, M-Wire, and Gold Wire: A micro-computed tomographic comparative study of One Shape, ProTaper Next, and WaveOne Gold instruments in maxillary first molars. *J Endod* 2019; 45: 62-67.
- 6) Gagliardi J, Versiani MA, de Sousa-Neto MD, Plazas-Garzon A, Basrani B. Evaluation of the shaping characteristics of ProTaper Gold, ProTaper NEXT, and ProTaper Universal in curved canals. *J Endod* 2015; 41: 1718-1724.
- 7) Pinheiro SR, Alcalde MP, Vivacqua-Gomes N, Bramante CM, Vivan RR, Duarte MAH, Vasconcelos BC. Evaluation of apical transportation and centring ability of five thermally treated NiTi rotary systems. *Int Endod J* 2018; 51: 705-713.
- 8) Venino PM, Citterio CL, Pellegatta A, Ciccarelli M, Maddalone M. A micro-computed tomography evaluation of the shaping ability of two nickel-titanium instruments, HyFlex EDM and ProTaper Next. *J Endod* 2017; 43: 628-632.
- 9) Belladonna FG, Carvalho MS, Cavalcante DM, Fernandes JT, de Carvalho Maciel AC, Oliveira HE, Lopes RT, Silva EJNL, De-Deus G. Micro-computed tomography shaping ability assessment of the new blue thermal treated Reciproc instrument. *J Endod* 2018; 44: 1146-1150.
- 10) Drukteinis S, Peciuliene V, Bendinskaite R, Brukiene V, Maneliene R, Rutkunas V. Shaping and centering ability, cyclic fatigue resistance and fractographic analysis of three thermally treated NiTi endodontic instrument systems. *Materials* 2020; 13.
- 11) Kumar M, Paliwal A, Manish K, Ganapathy SK, Kumari N, Singh AR. Comparison of canal transportation in TruNatomy, ProTaper Gold, and Hyflex electric discharge machining file using cone-beam computed tomography. *J Contemp Dent Pract* 2021; 22: 117-121.
- 12) Pérez Morales MLN, Gonzalez Sanchez JA, Olivieri JG, Elmsmari F, Salmon P, Jaramillo DE, Terol FD. Micro-computed tomographic assessment and comparative study of the shaping ability of 6 nickel-titanium files: An in vitro study. *J Endod* 2021; 47: 812-819.
- 13) Miyara K, Yahata Y, Hayashi Y, Tsutsumi Y, Ebihara A, Hanawa T, Suda H. The influence of heat treatment on the mechanical properties of Ni-Ti file materials. *Dent Mater J* 2014; 33: 27-31.
- 14) Ebihara A, Yahata Y, Miyara K, Nakano K, Hayashi Y, Suda H. Heat treatment of nickel-titanium rotary endodontic instruments: effects on bending properties and shaping abilities. *Int Endod J* 2011; 44: 843-849.
- 15) Silva EJNL, Ajuz NC, Martins JNR, Antunes BR, Lima CO, Vieira VTL, Braz-Fernandes FM, Versiani MA. Multimethod analysis of three rotary instruments produced by electric discharge machining technology. *Int Endod J* 2023; 56: 775-785.
- 16) Hou XM, Yang YJ, Qian J. Phase transformation behaviors and mechanical properties of NiTi endodontic files after gold heat treatment and blue heat treatment. *J Oral Sci* 2020; 63: 8-13.
- 17) Schäfer E, Bürklein S, Donnermeyer D. A critical analysis of research methods and experimental models to study the physical properties of NiTi instruments and their fracture characteristics. *Int Endod J* 2022; 55 Suppl 1: 72-94.
- 18) Bueno MR, Estrela C, Azevedo BC, Cintra Junqueira JL. Root canal shape of human permanent teeth determined by new cone-beam computed tomographic software. *J Endod* 2020; 46: 1662-1674.
- 19) Crozeta BM, Silva-Sousa YTC, Leoni GB, Mazzi-Chaves JF, Fantinato T, Baratto-Filho F, Sousa-Neto MD. Micro-computed tomography study of filling material removal from oval-shaped canals by using rotary, reciprocating, and adaptive motion systems. *J Endod* 2016; 42: 793-797.
- 20) Paqué F, Balmer M, Attin T, Peters OA. Preparation of oval-shaped root canals in mandibular molars using nickel-titanium rotary instruments: A micro-computed tomography study. *J Endod* 2010; 36: 703-707.
- 21) Esposito PT, Cunningham CJ. A comparison of canal preparation with nickel-titanium and stainless steel instruments. *J Endod* 1995; 21: 173-176.
- 22) Lam TV, Lewis DJ, Atkins DR, Macfarlane RH, Clarkson RM, Whitehead MG, Brockhurst PJ, Moule AJ. Changes in root canal morphology in simulated curved canals over-instrumented with a variety of stainless steel and nickel titanium files. *Aust Dent J* 1999; 44: 12-19.
- 23) Lin LM, Rosenberg PA, Lin J. Do procedural errors cause endodontic treatment failure? *J Am Dent Assoc* 2005; 136: 187-193.
- 24) Yun HH, Kim SK. A comparison of the shaping abilities of 4 nickel-titanium rotary instruments in simulated root canals. *Oral Surg Oral Med Oral Pathol Oral Radiol Endod* 2003; 95: 228-233.
- 25) Unno H, Ebihara A, Hirano K, Kasuga Y, Omori S, Nakatsukasa T, Kimura S, Maki K, Okiji T. Mechanical properties and root canal shaping ability of a nickel-titanium rotary system for minimally invasive endodontic

- treatment: A comparative in vitro study. *Materials* 2022; 15: 7929.
- 26) Perez F, Schoumacher M, Peli JF. Shaping ability of two rotary instruments in simulated canals: stainless steel ENDOflash and nickel-titanium HERO Shaper. *Int Endod J* 2005; 38: 637-644.
 - 27) Franco V, Fabiani C, Taschieri S, Malentacca A, Bortolin M, Del Fabbro M. Investigation on the shaping ability of nickel-titanium files when used with a reciprocating motion. *J Endod* 2011; 37: 1398-1401.
 - 28) al-Omari MA, Dummer PM, Newcombe RG, Doller R. Comparison of six files to prepare simulated root canals. 2. *Int Endod J* 1992; 25: 67-81.
 - 29) Berutti E, Paolino DS, Chiandussi G, Alovise M, Cantatore G, Castellucci A, Pasqualini D. Root canal anatomy preservation of WaveOne reciprocating files with or without glide path. *J Endod* 2012; 38: 101-104.
 - 30) Plotino G, Grande NM, Falanga A, Di Giuseppe IL, Lamorgese V, Somma F. Dentine removal in the coronal portion of root canals following two preparation techniques. *Int Endod J* 2007; 40: 852-858.
 - 31) Sekiya M, Maeda M, Nishida T, Igarashi M. Evaluation of root canal wall displacement and working time in simulated curved root canals using various reciprocating files. *Jpn J Conserv Dent* 2020; 63: 405-413.
 - 32) Hoer D, Attin T. The accuracy of electronic working length determination. *Int Endod J* 2004; 37: 125-131.
 - 33) Mousavi SA, Farhad A, Shahnasari S, Basiri A, Koleh-douzan E. Comparative evaluation of apical constriction position in incisor and molar teeth: An in vitro study. *Eur J Dent* 2018; 12: 237-241.
 - 34) Wu M-K, Wesselink PR, Walton RE. Apical terminus location of root canal treatment procedures. *Oral Surg Oral Med Oral Pathol Oral Radiol Endod* 2000; 89: 99-103.
 - 35) Tsesis I, Blazer T, Ben-Izhack G, Taschieri S, Del Fabbro M, Corbella S, Rosen E. The precision of electronic apex locators in working length determination: A systematic review and meta-analysis of the literature. *J Endod* 2015; 41: 1818-1823.
 - 36) Ricucci D, Langeland K. Apical limit of root canal instrumentation and obturation, part 2. A histological study. *Int Endod J* 1998; 31: 394-409.
 - 37) Eymirli A, Sungur DD, Uyanik O, Purali N, Nagas E, Cehreli ZC. Dentinal tubule penetration and retreatability of a calcium silicate-based sealer tested in bulk or with different main core material. *J Endod* 2019; 45: 1036-1040.

Clinical Assessment of Root Caries Treatment Based on the Discoloration of Silver Diamine Fluoride as a Caries Indicator

Yuki MURASE¹, Hanemi TSURUTA¹, Tomohiro TAKAGAKI¹, Shusuke KUSAKABE¹,
Masaomi IKEDA², Michael F BURROW³ and Toru NIKAIIDO¹

¹Department of Operative Dentistry, Division of Oral Functional Science and Rehabilitation,
Asahi University School of Dentistry

²Oral Prosthetic Engineering, Medical, and Dental Science and Technology, Graduate School of Medical and Dental Sciences,
Tokyo Medical and Dental University (TMDU)

³Restorative Dental Sciences, Faculty of Dentistry, University of Hong Kong

Abstract

Purpose: This clinical study aimed to evaluate whether changes were observed in saliva test outcomes before and after application of 38% silver diamine fluoride (SDF) in elderly patients with root caries lesions. Following this, the root caries discolored by SDF was restored to verify SDF as a potential caries indicator for the removal of carious tissue on root surfaces.

Methods: This study was approved by the Research Ethics Committee of Asahi University, School of Dentistry (Approval Number: 32031). Twenty elderly patients with root caries visiting the Operative Dentistry Clinic of Asahi University Medical and Dental Center between March 2021 to March 2022 were recruited. The caries risk of these patients was evaluated using a saliva test kit (Salivary Multi Tests; SMT) before and after SDF application (at the first and the second visits). The values of SMT measurement before and after SDF application were analyzed for six items: cariogenic bacterial count, saliva acidity, buffering capacity, leukocytes, protein, and ammonia. Caries removal was guided by the staining from SDF as a caries indicator using an excavator, then a resin composite restoration was placed. Each clinical procedure was photographed.

Results: There were 20 participants: 15 males and 5 females (mean age 76.5 years). The total number of teeth with root caries lesions was 90 (51 incisors, 23 premolars, and 16 molars). There were no significant differences in the SMT results before and after the SDF application ($p > 0.05$). However, the coefficient of variation values before and after SDF application tended to be different among the evaluated items. The coefficient of variation was 1.97 for caries-causing bacteria, while it ranged from 0.26 to 0.69 for the other items. From the photographs of the clinical cases, application of SDF discolored and arrested the root caries lesions. This led to a reduction in bacterial adherence as well as gingival inflammation. The resin composite restorations for the teeth with root caries lesions were deemed successful during the observation period (max. 10 months).

Conclusion: No significant difference was found in each item of SMT measurement before and after the application of SDF. However, the bacterial count exhibited a significant variation, suggesting suppression of the bacterial adherence on the root caries lesion by the application of SDF. SDF application could be used as a favorable indicator for diagnosis and excavation of carious root tissue when a restoration is required.

Key words: silver diamine fluoride, root caries, saliva test

Corresponding author: Hanemi TSURUTA, Department of Operative Dentistry, Division of Oral Functional Science and Rehabilitation, Asahi University School of Dentistry, 1851, Hozumi, Mizuho, Gifu 501-0296, Japan

TEL & FAX: +81-58-329-1442, E-mail: hanemi@dent.asahi-u.ac.jp

Received for Publication: May 31, 2023/Accepted for Publication: October 6, 2023

J-STAGE advance published date: November 8, 2023

DOI: 10.11471/odep.2023-007

Introduction

The 8020 movement has been promoted by the Japanese Ministry of Health, Labour and Welfare and the Japan Dental Association since 1989; this is a campaign to preserve more than 20 natural teeth in people by the age of 80 years so as to enjoy a high quality of oral health, which influences overall quality of life. Today, more than half of the elderly population have achieved this goal¹⁾. However, there is a new concern about the increased risk of root caries in the elderly population because of root surface exposure due to recession of periodontal tissue, decrease of saliva secretion, and also a decline of patients' manual dexterity which affects oral hygiene²⁾. A decrease of saliva leads to a decrease in buffering capacity and also a reduced supply of Ca/PO₄ ions which are necessary for remineralization³⁾. In addition, an increasing number of elderly people with physical/mental disabilities are unable to receive sufficient oral care⁴⁾. Thus, attention should be paid to the prevention and management of the initial stages of root caries.

Root caries progresses circumferentially around the exposed root surface⁵⁾; this makes the restoration of root caries challenging because of the difficulty of controlling moisture as well as manipulating instruments during preparation and restoration due to the curvature of the surface. The clinical treatment of root caries includes caries risk management and the arresting of active root caries in its early stages. Recently, several studies⁶⁻⁸⁾ have reported that 38% silver diamine fluoride (SDF) is highly effective in inhibiting the progression of active root caries lesions, and its excellent inhibitory effect was stated in the caries treatment guidelines of the Japanese Society of Conservative Dentistry⁹⁾. Thirty-eight percent SDF contains high concentrations of fluoride and silver ions. Both ions play important roles in inhibiting the initiation and progression of root caries; fluoride ions are mainly effective for the mineral component of dentin (hydroxyapatite) to inhibit dentin demineralization and promote remineralization¹⁰⁾, while silver ions are known to adsorb onto the dentin collagen to inhibit collagen degradation¹¹⁾ and are also known to have an antibacterial effect inhibiting bacterial adhesion onto the dentin surface¹²⁾. However, discoloration of SDF-treated dentin has been

noted to be an esthetic drawback^{13,14)}. It was demonstrated that the discoloration sites after the application of SDF to carious dentin almost coincided with the caries-infected stained dentin (non-remineralizable tissue) when a caries detector dye solution was applied¹⁵⁾. This means that root dentin caries could be removed by using SDF discoloration as a caries indicator. It was reported that the site of root caries dentin stained red by a caries-detecting dye solution (Caries Check, CC, Nishika, Shimonoseki, Japan) almost coincided with that of SDF, however, the site discolored with SDF was harder than the CC-stained site, suggesting that SDF application could also precipitate reminerals into the caries-infected dentin¹⁵⁾.

The present clinical study aimed to evaluate whether the values obtained from a saliva test before and after application of 38% SDF to root caries in elderly patients differed. Following this, the root caries was removed according to the zone of discoloration (SDF-stained zone) to verify whether SDF has the potential to be used as a caries indicator for the removal of carious root tissue.

Materials and Methods

1. Research participants

This study was approved by the Research Ethics Committee of Asahi University, School of Dentistry (Approval Number: 32031). The participants were elderly patients requiring treatment of root caries lesions who attended the Operative Dentistry Clinic, Asahi University Medical and Dental Center between March 2021 and March 2022. Informed consent was obtained from 20 patients, which included the purpose of this study and detailed information about the treatment of root caries including the use of SDF.

2. Saliva test

Saliva tests for each participant were performed twice: before and after SDF application (at the first and the second visits) using a proprietary saliva test kit (Salivary Multi Tests, SMT, Lion, Tokyo, Japan). Data were obtained from the SMT and compared before and after the application of SDF for each participant. The following six items were tested, namely cariogenic bacterial count, saliva acidity, buffering capacity, leukocytes, protein, and ammonia.

The mean values of the test data obtained before and

Table 1 Age, sex, and number of root carious teeth for each participant

Subject	Age	Sex (Male/Female)	Number of root caries			
			Anterior tooth	Premolar	Molar	Total
1	68	M	0	1	0	1
2	70	M	3	0	3	6
3	70	F	1	2	1	4
4	71	M	2	0	1	3
5	72	M	1	0	1	2
6	72	M	3	3	2	8
7	72	M	2	0	0	2
8	73	F	0	1	1	2
9	75	M	1	0	0	1
10	75	M	12	0	0	12
11	75	M	4	0	0	4
12	77	M	5	1	0	6
13	79	M	1	1	0	2
14	81	F	3	4	1	8
15	81	F	3	0	0	3
16	81	M	2	1	2	5
17	83	M	1	2	0	3
18	84	F	3	2	1	6
19	85	M	1	2	1	4
20	86	M	3	3	2	8
Total	—	M15/F5	51	23	16	90
Mean±SD	76.5±5.5	—	—	—	—	—

after SDF application were compared and statistically analyzed using a paired-sample *t*-test and Wilcoxon signed-rank test at the 5% level of confidence. In addition, the change rate (the ratio of the test values before and after SDF application) was calculated for each item to obtain a coefficient of variation (the ratio of the standard deviation to the mean).

3. Photographing of the root caries

Each patient's root caries lesions were photographed before and after the application of SDF to confirm the presence of discoloration of the root caries due to the SDF treatment. From the photographs, the presence of biofilm formation on the carious lesions and the degree of gingival inflammation associated with the teeth having root caries lesions were also evaluated.

4. Root caries treatment

For treatment of the root caries lesions at the second visit, the carious lesions were removed based on black discoloration from the SDF as the indicator. A spoon excavator (Round #2, YDM, Tokyo, Japan) was used to remove caries until the discoloration was no longer

present. In addition, a caries-detecting solution (Caries Check) was applied to the lesion to confirm the complete removal of the caries-infected dentin. If the lesion was stained red by the caries detector, those parts of the lesion stained red were also removed. Thereafter, a two-step self-etch adhesive (Clearfil SE Bond 2, Kuraray Noritake Dental, Tokyo, Japan) was applied to the cavity and a resin composite (Clearfil Majesty ES Flow, Kuraray Noritake Dental) was placed according to the manufacturer's instructions. Photographs were taken for each restorative step to investigate the applicability of 38% SDF for root caries treatment.

Results

1. Participants and root carious teeth

Data on the age, sex, and number of teeth with root caries lesions of each participant are summarized in Table 1. Twenty patients (15 males and five females) with a mean age of 76.5 years old were recruited. The total number of root caries lesions included in this

Table 2 Values of SMT measurement, change rate, and coefficient of variation for each item

Inspection item	Before*	After*	Change rate	Coefficient of variation
Cariogenic bacterial count	22.9±16.6	34.7±25.1	10.89±21.43	1.97
Saliva acidity	54.2±21.7	54.6±21.1	1.22±0.84	0.69
Buffering capacity	40.1±23.1	42.1±24.1	1.25±0.74	0.59
Leucocyte	75.7±21.8	73.0±25.2	1.01±0.27	0.26
Protein	66.3±22.7	66.7±22.6	1.16±0.59	0.51
Ammonia	47.2±22.5	43.4±27.7	1.09±0.58	0.53

* : There were no significant differences in each item between before and after the SDF application period ($p>0.05$).

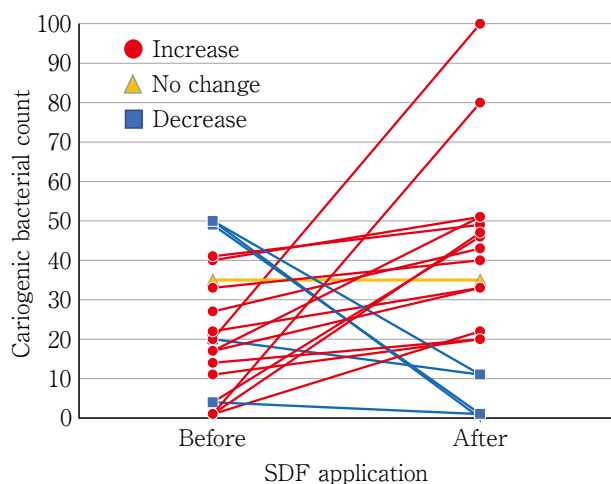


Fig. 1 Change of cariogenic bacterial count before and after SDF application for each patient, showing an increase in 14 cases ($p<0.05$), no change in 1 case ($p>0.05$) and a decrease in 5 cases ($p<0.05$), statistically

study was 90 (51 anterior teeth, 23 premolars, and 16 molars).

2. SMT measurement

Table 2 shows the values of SMT measurement, the change rate and the coefficient of variation for each item. There were no significant differences in each item between the before and after SDF application periods ($p>0.05$). The coefficient of variation was 1.97 for the cariogenic bacterial count, while that of the other items ranged from 0.26 to 0.69. Figure 1 shows the change of cariogenic bacterial count before and after SDF application for each patient. The bacterial counts varied for each patient, including an increase in 14 cases ($p<0.05$), no change in 1 case ($p>0.05$) and a decrease in 5 cases ($p<0.05$).

3. Representative case of root caries treatment using SDF

Figure 2 shows a representative case of the root caries treatment using SDF. Root caries lesions were located on the lower incisors (#32 and #33), as shown in Fig. 2-a. The teeth were cleaned using a brush and prophylaxis paste (Message Plus, Fine, Shofu, Kyoto, Japan). SDF was then applied on the root lesions for 3 minutes with a micro brush (Fig. 2-b). The SDF-treated lesion showed discoloration at the second visit after one week (Fig. 2-c). After the tooth surface was cleaned, the SDF-stained area could be clearly observed with the lesion showing a surface that was much harder and arrested, while the surrounding intact enamel and dentin of the teeth were not discolored. The gingival inflammation appeared to be reduced around the SDF-treated root surfaces (Fig. 2-d). The black-discolored lesions were carefully removed using a spoon excavator (Round #2, YDM) (Fig. 2-e). The lesion was stained red by a caries detector dye solution (Caries Check), which revealed that many lesions had only been partly excavated (Fig. 2-f). After completion of cavity preparation (Fig. 2-g), a resin composite was placed in the usual manner (Fig. 2-h). No discomfort was observed in any case during the follow-up period (maximum period: 10 months).

Discussion

Root surface exposure due to recession of the periodontal tissue and biofilm accumulation on the root surface can easily lead to the formation of root caries in the elderly if all cariogenic factors exist⁵. In addition, the risk of caries increases in the elderly due to a decrease in saliva secretion, and difficulty in self-care of

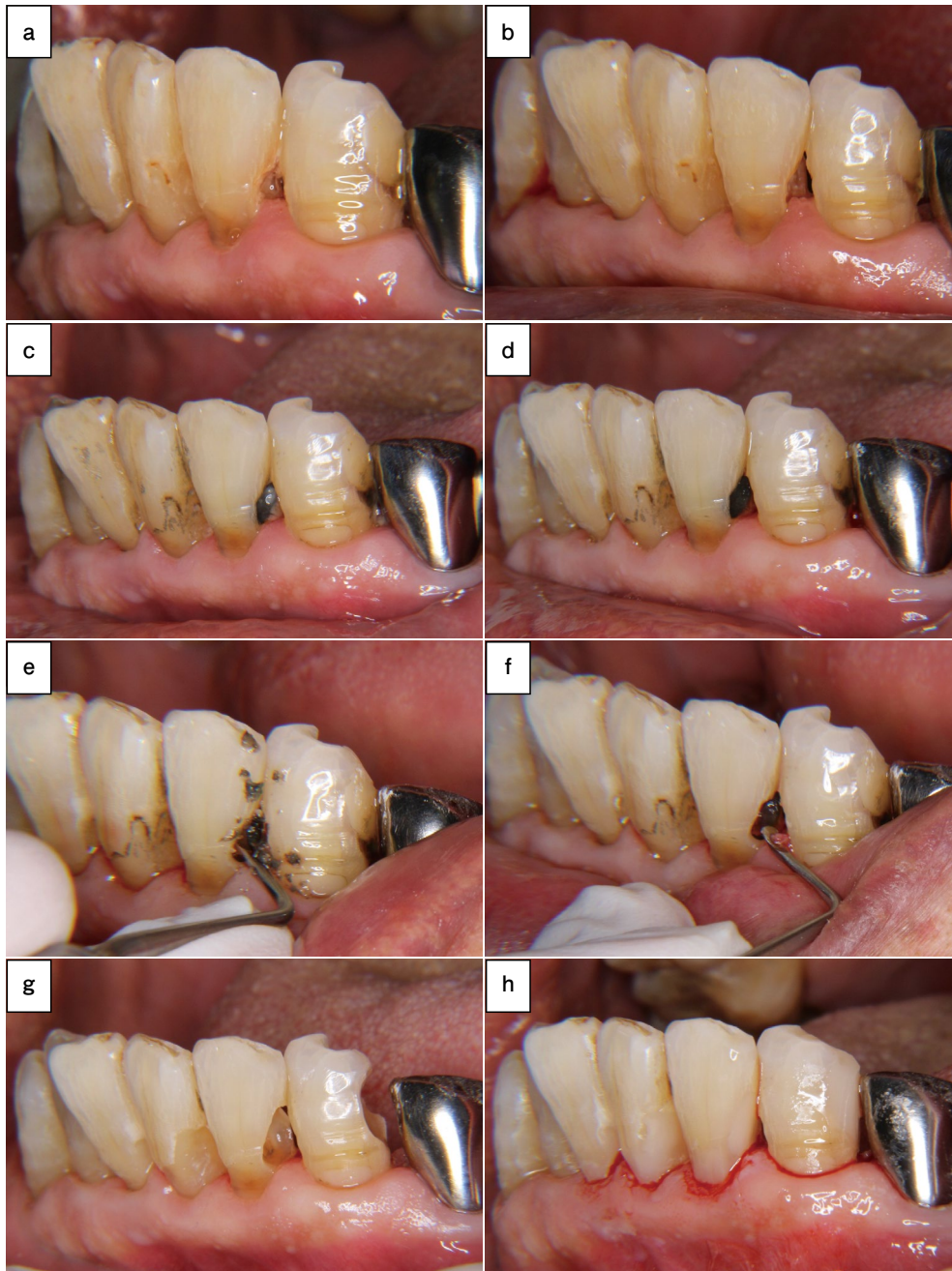


Fig. 2 Representative case of root caries treatment using SDF

a : Root caries lesions (#32 and #33). b : SDF was applied for 3 minutes after cleaning. c : Discoloration of the SDF-treated lesion after one week. d : The SDF-stained area could be clearly observed, while the surrounding intact enamel and dentin of the teeth were not discolored. The gingival inflammation was reduced around the SDF-treated root surfaces. e : The black-discolored lesions were carefully removed using a spoon excavator. f : The lesion that was stained red with Caries Check was observed to only have been partly excavated. g : Completion of cavity preparation. h : Final restorations.

their remaining teeth²⁻⁴). Therefore, general oral hygiene instruction is often not sufficient for managing the risk of root caries in the elderly¹⁶). A more definitive and effective approach is necessary for root caries management and treatment for this group of patients.

This study aimed to evaluate the effect of SDF application on root caries lesions as well as SMT measurement. The study also investigated the clinical efficacy of SDF application for the management and treatment of root caries. Since this study was performed during the COVID-19 pandemic, 20 patients with 90 root carious teeth could be recruited.

Saliva tests were performed using SMT to obtain the following six items¹⁷). The cariogenic bacterial count was obtained from measurements of the reductive activity of resazurin with gram-positive bacteria. Values for saliva acidity were obtained from hydrogen ion content detected by color change of a pH indicator, while buffering capacity was determined by color change of complex pH indicators in the presence of defined amounts of acid. It is important to know the above three items since they are key indicators to determine the caries risk level of patients. The values for leukocytes were obtained by the measurement of enzymatic activity of leukocyte esterase using a dye-binding technology used in urinary examination. The protein values were obtained by measuring total protein content also using a dye-binding technology used for urinary examination. The items for leukocyte and proteins are related to determining periodontal disease. The values for ammonia were detected from an enzyme cycling method used in blood examination, which was related to halitosis.

Interestingly, the value obtained by SMT measurement did not change for each parameter before and after SDF application (Table 2). However, the coefficient of variation of the cariogenic bacteria count was 1.97, while the coefficients of the other five items were around 0.7 or less. This fact suggested that SDF application impacts only the results for the bacterial count. Takahashi et al.¹²) evaluated the effect of SDF application on root dentin with regard to biofilm formation using an oral biofilm reactor. They concluded that biofilm formation and insoluble glucan adhesion were prevented by the application of 38% SDF. They also reported that almost all *Streptococcus. mutans* cells were dead on the root dentin surface treated with 38%

SDF based on fluorescence photomicrographic observations¹²). This means that the biofilm formed on the root dentin surface was easily removed from the SDF-treated dentin surface, even if the bacteria that were left on the surface were probably inactive. In the current study, the results of the bacterial counts were also variable (Fig. 1). The caries risk factors of the elderly patients were variable, including saliva secretion and quality of oral hygiene⁴). From the examination of the photographs before and after SDF application²), the SDF-treated lesions were discolored and seemed arrested and also gingival inflammation seemed improved. These facts suggested that SDF application could prevent the attachment of bacteria on the treated root surfaces even if the oral hygiene of patients remained poor. Further studies should be carried out to evaluate the effect of SDF application on the periodontal status by using periodontal evaluation measurements, such as probing depth and bleeding on probing.

The amount of saliva secreted by the elderly patients who participated in this study was greatly reduced, making saliva collection challenging. Sufficient control of the intraoral environment before saliva collection was also challenging. SMT measurement was performed in this study, however, caries risk assessment using SMT measurement may be challenging for elderly patients.

Conclusions

1. No significant difference was found in the seven items of SMT measurement before and after the application of SDF. However, the bacterial count exhibited a significant variation, suggesting that SDF application may influence bacterial adhesion on dentin surfaces affected by root caries.
2. From the clinical cases, the application of SDF demonstrated discoloration of the root caries lesions, and an anti-inflammatory effect of the gingiva around the root carious teeth.
3. SMT measurement might be challenging for caries risk assessment for elderly patients.

Acknowledgment

This study was supported by an 8020 Research Grant for fiscal 2021 from the 8020 Promotion Foundation (21-5-10) and a Grant-in-Aid from the Japan Society for the Promotion of Science (21K09924).

Conflict of Interest

There are no conflicts of interest to disclose regarding this study.

References

- 1) Shinsho F. New strategy for better geriatric oral health in Japan: 80/20 movement and Healthy Japan 21. *Int Dent J* 2001; 51: 200-206.
- 2) Chan AKY, Tamrakar M, Jiang CM, Lo ECM, Leung KCM, Chu CH. Common medical and dental problems of older adults: A narrative review. *Geriatrics (Basel)* 2021; 6: 76.
- 3) Dibello V, Lobbezoo F, Lozupone M, Sardone R, Ballini A, Berardino G, Mollica A, Coelho-Júnior HJ, De Pergola G, Stallone R, Dibello A, Daniele A, Petruzzi M, Santarcangelo F, Solfrizzi V, Manfredini D, Panza F. Oral frailty indicators to target major adverse health-related outcomes in older age: a systematic review. *Geroscience* 2023; 45: 663-706.
- 4) Ji M, Fu D, Liao G, Zou L. A bibliometric analysis of studies on root caries. *Caries Res* 2023; 57: 32-42.
- 5) Kreher D, Korn V, Meißner T, Haak R, Schmalz G, Ziebolz D. How do carious root lesions develop after the end of professional preventive measures?—Preliminary findings of a randomized clinical trial. *Odontology* 2022; 110: 805-813.
- 6) Zhang W, McGrath C, Lo EC, Li JY. Silver diamine fluoride and education to prevent and arrest root caries among community-dwelling elders. *Caries Res* 2013; 47: 284-290.
- 7) Oliveira BH, Cunha-Cruz J, Rajendra A, Niederman R. Controlling caries in exposed root surfaces with silver diamine fluoride: A systematic review with meta-analysis. *J Am Dent Assoc* 2018; 149: 671-679.
- 8) Zhang OL, Niu JY, Yin IX, Yu OY, Mei ML, Chu CH. Bioactive materials for caries management: A literature review. *Dent J (Basel)* 2023; 11: 59.
- 9) Hayashi M, Momoi Y, Fujitani M, Fukushima M, Imazato S, Kitasako Y, Kubo S, Nakashima S, Nikaido T, Shimizu A, Sugai K, Takahashi R, Unemori M, Yamaki C. Evidence-based consensus for treating incipient enamel caries in adults by non-invasive methods: recommendations by GRADE guideline. *Jpn Dent Sci Rev* 2020; 56: 155-163.
- 10) Shimizu M, Matsui N, Hamba H, Obayashi S, Sayed M, Takahashi M, Tsuda Y, Nikaido T, Tagami J. Micro-CT assessment of the effect of silver diammine fluoride on inhibition of root dentin demineralization. *Dent Mater J* 2021; 40: 1041-1048.
- 11) Thanatvarakorn O, Islam MS, Nakashima S, Sadr A, Nikaido T, Tagami J. Effects of zinc fluoride on inhibiting dentin demineralization and collagen degradation in vitro: A comparison of various topical fluoride agents. *Dent Mater J* 2016; 35: 769-775.
- 12) Takahashi M, Matin K, Matsui N, Shimizu M, Tsuda Y, Uchinuma S, Hiraishi N, Nikaido T, Tagami J. Effects of silver diamine fluoride preparations on biofilm formation of *Streptococcus mutans*. *Dent Mater J* 2021; 40: 911-917.
- 13) Sayed M, Matsui N, Hiraishi N, Nikaido T, Burrow MF, Tagami J. Effect of glutathione bio-molecule on tooth discoloration associated with silver diamine fluoride. *Int J Mol Sci* 2018; 19: 1322.
- 14) Sayed M, Matsui N, Hiraishi N, Inoue G, Nikaido T, Burrow MF, Tagami J. Evaluation of discoloration of sound/demineralized root dentin with silver diamine fluoride: In-vitro study. *Dent Mater J* 2019; 38: 143-149.
- 15) Sayed MM, Nikaido T, Abdou A, Burrow MF, Tagami J. Potential use of silver diamine fluoride in detection of carious dentin. *Dent Mater J* 2021; 40: 820-826.
- 16) Hiraishi N, Sayed M, Takahashi M, Nikaido T, Tagami J. Clinical and basic evidence of silver diamine fluoride on root caries management. *Jpn Dent Sci Rev* 2022; 58: 1-8.
- 17) Lion Pro. Oral Healthcare Online. Salivary Multi Test. <https://lionpro.lionshop.jp/check/> (cited 2023.04.22) (in Japanese).

The Effects of Dietary pH Changes on Tooth Staining of the Enamel Surface

Hiroki SUGITO^{1,2}, Takako EGUCHI¹, Rika TANAKA³, Akiko HARUYAMA² and Takashi MURAMATSU²

¹Department of Dental Hygiene, Tokyo Dental Junior College

²Department of Operative Dentistry, Cariology and Pulp Biology, Tokyo Dental College

³Misono Garden Dental Clinic

Abstract

Purpose: Patients' demand for dental esthetics has increased in recent years. Additionally, teeth bleaching can improve self-care and oral cavity awareness. However, bleaching is not permanent as the consumption of foods and drinks can cause re-discoloration of teeth. Tooth staining may be caused by drinks such as coffee, wine, and tea, and foods such as curry. However, the mechanism by which these substances cause staining has yet to be clarified. Therefore, in this study we examined the effects of colored food on the enamel surface by dietary pH changes.

Methods: Extracted mandibular anterior bovine teeth were used as samples. The enamel samples were divided into four groups: turmeric (TM group), red pepper (RP group), tomato (TO group), and Milli-Q water (MQ group) as a control. The samples were immersed in 30 mL of solution for 3 hours in a 37°C incubator while being shaken. Color changes were measured before and after immersion. For colorimetry, L^* , a^* and b^* in the CIE1976 $L^*a^*b^*$ color system were measured using a micro-area spectrophotometer, and ΔL^* , Δa^* , and Δb^* were obtained. Furthermore, the immersion solution was evaluated before and after immersion using a pH meter. A 3D laser microscope was used to measure the surface roughness of enamel.

Results: The results revealed that the Δa^* value, which indicated redness, and the Δb^* value, which indicated yellowness, increased due to the influence of natural ingredients in the TM and RP groups. The various natural pigments in food, such as curcumin in the TM group and carotenoids in the RP group, are thought to be involved in the coloration. The enamel surface roughness of the TO group changed significantly before and after immersion. The pH of the TO group was 4.0, which was below the enamel critical pH of 5.5.

Conclusion: The results of this study suggest that tooth staining of the enamel surface is affected by dietary pH changes.

Key words: tooth staining, colorimetry, surface roughness of enamel

Introduction

In recent years, people have become increasingly interested in esthetics and request teeth bleaching. Teeth bleaching can improve teeth color, making people more aware of maintaining their teeth color¹⁾. It is considered that raising people's awareness of oral disease prevention through esthetics may improve their quality of life. However, teeth bleaching is not permanent, and the teeth color may gradually return to the state prior to treatment²⁾. Pigmentation on the tooth surface due to the consumption of colored food and drinks may cause color reversal of whitened teeth²⁾. Therefore, it is recommended to refrain from consuming colored foods and drinks to prolong the bleaching effect²⁾.

Nowadays, many foods and drinks come in various colors. Studies on color preference for foods have revealed that people tend to gravitate towards warm colors, such as yellow and orange^{3,4)}. Therefore, color directly affects interest and motivation in consuming foods and drinks^{3,4)}. These studies emphasized the high importance of food and drink color, and so seasonings, spices, coloring agents, etc. are used to add color. Depending on the condition of the oral cavity, consuming them in large amounts can cause a change in color of the teeth.

Factors that affect a change in tooth color can be divided into extrinsic and intrinsic factors^{1,5)}. The effects of drinks on tooth staining have already been discussed^{1,5,6)}. Exogenous coloring can be caused by pigments in fluids, such as coffee, wine, black or green tea, and tobacco tar⁶⁾. In addition, curry is a well-known cause of exogenous coloring. However, the mechanism by which foods cause tooth staining has not been elucidated. Dental care professionals must instruct patients on how to prevent exogenous staining and color reversion after teeth bleaching and list the foods that are likely to cause staining.

Thus, in this study, we used bovine teeth to determine the effects of colored foods on the enamel surface. The null hypothesis was that tooth staining of the enamel surface is not affected by dietary changes.

Materials and Methods

1. Sample preparation

Forty-eight extracted mandibular anterior bovine teeth that had been cryopreserved were used as samples. After thawing, a diamond cut saw (MC-130D, Maruto Instrument Co., Ltd., Tokyo, Japan) was used to cut the cervical area and incisal portion under water injection. The central enamel part of the cervical area was excised. After cutting, the enamel surface on the labial side of the crown was polished with water-resistant abrasive paper (#1,000) such that the polished surface was parallel to the measurement table. This was used as the standard polished surface for the analysis of enamel surface roughness.

2. Preparation of immersion solution

Turmeric (TM) (S&B turmeric [powder], S&B Foods Inc., Tokyo, Japan), red pepper (RP) (S&B red pepper [powder], S&B Foods Inc.), and tomato (TO) (La Preziosa [peeled tomatoes in tomato juice], Camel Coffee Co., Ltd., Tokyo, Japan), which are ingredients of curry and reportedly affect teeth, were used to immerse the enamel samples. Milli-Q water (MQ) was used as a control. A 2% aqueous solution dissolved in MQ was used for turmeric and red pepper. Each sample was immersed in 30 mL of the solution⁷⁾. The samples in each group were randomly assigned to color change analysis (n=5) or enamel surface roughness analysis (n=7).

3. pH measurement

The pH of the immersion solution was evaluated by measuring the solution before and after immersion using a pH measuring instrument (Desktop pH meter LAQUA F-71, Horiba, Ltd., Kyoto, Japan). Measurements were performed after calibrating using standard solutions. The temperature of the immersion solution during measurement was kept at 37°C using a thermometer, which was the same temperature as when the sample was colored. Three measurements were obtained for each immersion solution, and the average value was calculated as the pH value.

4. Staining method

One enamel sample was immersed in 30 mL of each immersion solution in an incubator at 37°C for 3 hours while being shaken. After immersion, the samples were taken out, immediately washed thoroughly with dis-

tilled water, dried naturally, and then measured for color changes and surface roughness.

5. Observation method

1) Color changes

Colorimetry was performed using a micro-area spectrophotometer (MSP-300H, Nippon Denshoku Industries Co., Ltd., Tokyo, Japan) before and after immersion in the immersion solution. Colorimetry was performed at five points in the center of each sample, and the average value was used as the measured value. Using the CIE1976L^{*}a^{*}b^{*} color system, the measurement results were obtained for L^{*}, which represents lightness, a^{*}, which represents the saturation of reds and greens, and b^{*}, which represents the saturation of yellows and blues. Furthermore, the differences between the values before and after immersion were defined as ΔL^* , Δa^* and Δb^* , and the standard error was calculated. Moreover, ΔE^*ab , which expresses color difference, was obtained using the following formula:

$$\Delta E^*ab = [(\Delta L^*)^2 + (\Delta a^*)^2 + (\Delta b^*)^2]^{1/2}$$

The change in color was measured.

2) Enamel surface roughness by 3D laser microscope

Surface roughness was measured using a 3D laser microscope (LEXT OLS4000, Olympus Co., Tokyo, Japan). Arithmetic mean roughness (Sa) denotes the surface roughness, and the reference polished surface was measured at five points per sample. The average value \pm standard error was calculated. The measurement area was set to $645 \times 645 \mu\text{m}$, and the cutoff value was set to $80 \mu\text{m}^7$. Sa₀ denotes the reference value before treatment, and Sa₁ the value after treatment.

6. Statistical processing

Regarding the color change, normality was confirmed between the four groups of color difference values by Dunnett's multiple comparison test ($p < 0.05$ or $p < 0.01$). In cases where normality could not be confirmed, Steel's multiple comparison test was performed.

In the test of surface roughness value, the paired *t*-test was performed for those with a normal distribution. The Wilcoxon signed-rank sum test was performed when normality could not be confirmed ($p < 0.05$).

Table 1 Results of the pH measurements (mean \pm SE)

	before treatment	after treatment
MQ	6.903 \pm 0.077	6.965 \pm 0.031
TM	6.603 \pm 0.001	6.920 \pm 0.027
RP	5.616 \pm 0.004	6.009 \pm 0.008
TO	4.446 \pm 0.000	4.464 \pm 0.012

MQ : Milli-Q water, TM : turmeric, RP : red pepper, TO : tomato

Results

1. pH

Table 1 shows the pH before and after immersion. MQ and TM showed near neutral pH, while RP and TO both showed acidic pH. Particularly, the pH of TO was lowest among the four, well below the critical pH. No significant change in pH was observed before and after immersion in each solution at 37°C.

2. Color changes

Figures 1 to 3 show the results of comparison between groups by considering the difference between the values before and after immersion.

There was no significant difference in ΔL^* between the MQ group and all other groups (Figure 1). A significant difference in Δa^* was observed between the MQ group and all other groups (Figure 2). There was a significant difference in Δb^* between the MQ and TM groups, and between the MQ and RP groups. However, there was no significant difference between the MQ and TO groups (Figure 3).

Figure 4 shows the measurement results of the color difference value (ΔE^*ab). ΔE^*ab , which expresses the color difference (i.e., change in color), was highest in the TM group. No significant difference was observed between the MQ group and all other groups.

3. Enamel surface roughness by 3D laser microscope

Figure 5 shows the surface roughness measurements. Changes in Sa values before and after immersion in each group were different in all groups ($p < 0.05$). Moreover, the Sa values after immersion significantly increased in the TO group.

Discussion

Nowadays, many foods and drinks come in various

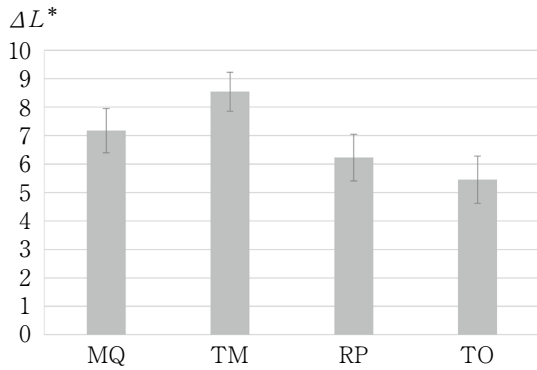


Fig. 1 Results of the color changes for ΔL^* values

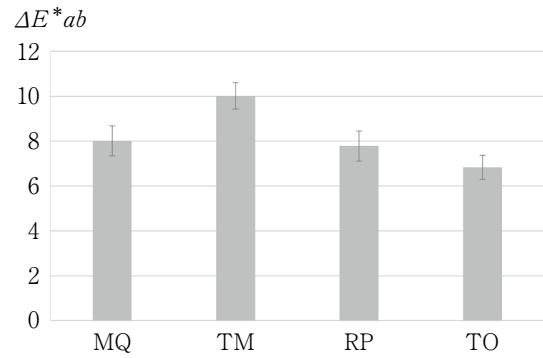


Fig. 4 Results of the color difference value for ΔE^*_{ab}

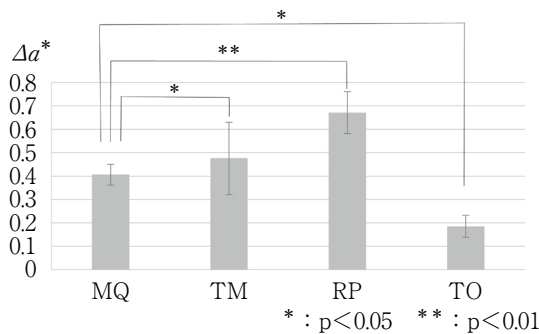


Fig. 2 Results of the color changes for Δa^* values

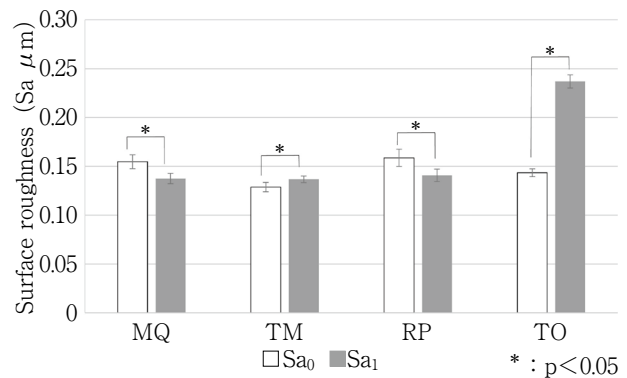


Fig. 5 Results of the surface roughness measurements
Sa₀ : before treatment, Sa₁ : after treatment.

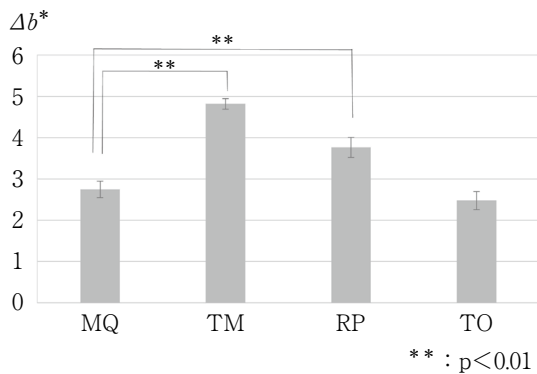


Fig. 3 Results of the color changes for Δb^* values

colors. In particular, coffee, wine, and tea are likely to cause teeth staining⁸⁾. Tea products, which are consumed by all ages from children to adults, include caffeine, polyphenols, and tea stains, which are well-known causes of coloration⁹⁾. Furthermore, frequent intake of water with low pH demineralizes teeth¹⁰⁾. On the other hand, some foods use a lot of coloring. Therefore, we

conjectured that the pH of each food is related to the pH of drink, and that the intake of a large amount of colored foods may have some effect on the color changes of teeth and enamel surface. Consequently, in this study, we investigated the effects of colored foods on the enamel surface by dietary pH changes.

1. Literature on foods that cause tooth staining

Curry and vegetables reportedly cause tooth staining^{11,12)}. Ghai et al.¹¹⁾ examined the possibility that Indian food contains ingredients that cause tooth erosion (acid erosion), and thereby cause tooth staining. They reported that ingredients in Indian cuisine have erosive effects, and that some ingredients, such as tomatoes and red pepper powder, may erode enamel. Moreover, some ingredients showed decreased pH with increased cooking temperature. These findings suggest that these spices used in cooking affect tooth staining, and that pH also affects the surface roughness of

enamel.

2. Color change based on food characteristics (pigment component)

The Δb^* value showed a tendency to increase in all groups, and a significant difference was observed between the MQ group and these groups, suggesting an increase in the yellow color. Leu et al. reported that the yellow component of turmeric in curry is curcumin, which is a diketone natural pigment¹³). In this study, the curcumin in turmeric acted to increase the Δb^* value, which indicates yellow color.

Red peppers, or hot peppers, contain a carotenoid that gives them a red color called capsanthin. However, capsanthin is also contained in paprika and is a natural pigment that gives an orange-to-red color¹⁴). This suggests that the reason why the Δb^* values changed in the RP group was that these values were also affected by the action of capsanthin, a natural pigment, which changed the color to orange.

The TO group is similar to the RP group. Tomatoes contain a natural carotenoid pigment called lycopene, which changes the color from orange to red¹⁵). This may be the same reason for the change in Δb^* value in the RP group, since this value may have been affected by lycopene, based on the color change to orange. In addition to tomatoes, beets are considered to be involved in tooth staining. de Araújo et al.¹²) reported that people with discolored teeth consume large quantities of beets. Moreover, beets contain a betacyanidin-based natural pigment called betanin¹⁶). In this study, we focused on turmeric, red pepper, and tomato and observed the color change. Spices and vegetables contain various pigments, and also have various characteristics, such as oil solubility, color change depending on pH, and resistance to heat and acid. This suggests that the characteristics of natural pigments contained in food must be considered when assessing color change.

3. Color change based on the relationship between tooth surface and pH

Regarding enamel surface roughness, there was a difference before and after immersion in the MQ, TM, and RP groups. In particular, in the TO group, the values tended to increase after immersion, suggesting that the enamel surface had become rough. The critical pH at which enamel demineralizes is 5.5^{17,18}). Tahmassebi et al.¹⁰) reported that low pH drinks may cause erosion

of the enamel surface. In this study, the TO group had a rougher enamel surface than the MQ, TM, and RP groups. This was due to the fact that the pH of the TO group was 4.0, which was well below the enamel critical pH of 5.5, suggesting that demineralization of the enamel surface increased the roughness.

In addition, a significant difference was observed in the MQ group before and after immersion. This may have been due to the surface roughness of the sample used in the experiment; further verification is required in the future.

4. Interaction between tooth surface and pigment components

In addition to pigments, interaction between the tooth surface and pigment component causes color change. Nathoo¹⁹) reported that the coloring in foods, drinks, and tobacco is associated with ionic bonds, hydrogen bonds, and hydrophobic interactions, and coloration occurs when the calcium in the oral cavity and saliva-derived proteins are oxidized and calcified. In this study, although the immersion time was as short as 3 hours, it was speculated that calcium, which is a component of teeth, bonded with curcumin and capsanthin, causing a color change. Thus, changes in teeth color are caused by the pH of the foods and drinks that are normally consumed in daily life, demineralization of teeth due to pH, outflow of calcium that occurs due to the demineralization, action of saliva in the oral cavity, and so forth. Therefore, it is necessary to consider the frequency of intake of turmeric and red pepper and other oral conditions when addressing changes in tooth color.

In addition, whitened teeth are more susceptible to staining than normal teeth since the surface layer of the enamel becomes rougher after bleaching^{6,20}). However, this study did not consider the surface roughness of teeth after bleaching; it is necessary to investigate the roughness of the enamel surface after bleaching and how this affects the change in teeth color.

Curry and vegetables reportedly cause tooth staining. Curry is often cooked using turmeric, red pepper, tomato, and various other spices. Mixing various foods may cause color changes and enamel surface roughness. During immersion, color changes and enamel surface roughness may occur depending on changes in the pH of food due to temperature and immersion time. In this study, the temperature was set to 37°C, and immersion was performed for 3 hours. Therefore, it is

necessary to investigate the change in pH with temperature rise and immersion time in the future.

In this study, we conducted an experiment to clarify the effects of spices and vegetables on teeth; however, these have several positive effects on the body. For example, turmeric is well-known to improve liver function. It is important to understand the characteristics of each food and provide instructions to patients regarding their esthetic and health demands, rather than refraining from eating and drinking because of tooth staining.

Conclusion

This study was conducted to clarify the effects of food on the enamel surface of teeth. The results suggest that the Δa^* value, which represent redness, and the Δb^* value, which represents yellowness, increased due to the influence of the natural components in turmeric and red pepper. Tomato had a pH lower than the enamel critical pH of 5.5, suggesting that it may be involved in the roughening of the enamel surface.

Conflicts of Interest

The authors declare no conflict of interest related to this paper.

Acknowledgements

This work was supported in part by the FUTOKU foundation (2022) for T.E.

References

- Goldstein RE, Garber DA. A new role for restorative dentistry. Complete Dental Bleaching. Quintessence Publishing: Chicago; 1995. 1-23.
- Rosenstiel SF, Gegauff AG, Johnston WM. Duration of tooth color change after bleaching. J Am Dent Assoc 1991; 122: 54-59.
- Zellner DA, Kautz MA. Color affects perceived odor intensity. J Exp Psychol Hum Percept Perform 1990; 16: 391-397.
- Zellner DA, Whitten LA. The effect of color intensity and appropriateness on color-induced odor enhancement. Am J Psychol 1999; 112: 585-604.
- Visio D, Gaffar A, Fakhry-Smith S, Xu T. Present and future technologies of tooth whitening. Compend Contin Educ Dent 2000; 21 (Suppl 28): S36-S43.
- Efeoglu N, Wood D, Efeoglu C. Microcomputerised tomography evaluation of 10% carbamide peroxide applied to enamel. J Dent 2005; 33: 561-567.
- Eguchi T, Satou R, Miake Y, Sugihara N. Comparison of resistance of dentin to erosive acid after application of fluoride to teeth. J Hard Tissue Biol 2020; 29: 193-202.
- Omata Y, Uno S, Nakaoki Y, Tanaka T, Sano H, Yoshida S, Sidhu SK. Staining of hybrid composites with coffee, oolong tea, or red wine. Dent Mater J 2006; 25: 125-131.
- Joiner A, Muller D, Eloffsson UM, Malmsten M, Arnebrant T. Adsorption from black tea and red wine onto in vitro salivary pellicles studied by ellipsometry. Eur J Oral Sci 2003; 111: 417-422.
- Tahmassebi JF, Duggal MS, Malik-Kotru G, Curzon MEJ. Soft drinks and dental health: a review of the current literature. J Dent 2006; 34: 2-11.
- Ghai N, Burke FJT. Mouthwatering but erosive? A preliminary assessment of the acidity of a basic sauce used in many Indian dishes. Dent Update 2012; 39: 721-726.
- de Araújo LSN, dos Santos PH, Anchieta RB, Catelan A, Fraga Briso AL, Fraga Zaze ACS, Sundfeld RH. Mineral loss and color change of enamel after bleaching and staining solutions combination. J Biomed Opt 2013; 18 (10): 108004.
- Leu T-H, Maa M-C. The molecular mechanisms for the antitumorigenic effect of curcumin. Curr Med Chem Anticancer Agents 2002; 2: 357-370.
- Kennedy LE, Abraham A, Kulkarni G, Shettigar N, Dave T, Kulkarni M. Capsanthin, a plant-derived xanthophyll: a review of pharmacology and delivery strategies. AAPS PharmSciTech 2021; 22: 203.
- Story EN, Kopec RE, Schwartz SJ, Harris GK. An update on the health effects of tomato lycopene. Annu Rev Food Sci Technol 2010; 1: 189-210.
- Gliszczynska-Swiglo A, Szymusiak H, Malinowska P. Betanin, the main pigment of red beet: molecular origin of its exceptionally high free radical-scavenging activity. Food Addit Contam 2006; 23: 1079-1087.
- Stephan RM, Miller BF. A quantitative method for evaluating physical and chemical agents which modify production of acids in bacterial plaques on human teeth. J Dent Res 1943; 22: 45-51.
- Stephan RM. Intra-oral hydrogen-ion concentrations associated with dental caries activity. J Dent Res 1944; 23: 257-266.
- Nathoo SA. The chemistry and mechanisms of extrinsic and intrinsic discoloration. J Am Dent Assoc 1997; 128 (Suppl): 6S-10S.
- Rodrigues JA, Marchi GM, Ambrosano GMB, Heymann HO, Pimenta LA. Microhardness evaluation of in situ vital bleaching on human dental enamel using a novel study design. Dent Mater 2005; 21: 1059-1067.

Evaluation of the Hardness of Infected Root Canal Dentin with Fluorescence Excitation

Shuya SHIBANO, Mie MAYERS, Tokuji HASEGAWA¹, Takashi TAKAKI² and Katsuhiko ISATSU

Department of Perioperative Medicine, Division of Medical and Dental Cooperative Dentistry,
Showa University School of Dentistry

¹Department of Conservative Dentistry, Division of Comprehensive Dentistry, Showa University School of Dentistry

²Center of Electron Microscopy, Showa University

Abstract

Purpose: This study aimed to evaluate the association between infection and hardness in root canal dentin by irradiating infected root canal dentin with blue light at a wavelength of approximately 405 nm.

Methods: A total of 10 healthy human extracted teeth and 10 human extracted teeth with infected dentin were used as samples and semi-cut sections were prepared as longitudinal sections of the root canal. The root canal walls were observed using a stereo microscope under blue light at a wavelength of approximately 405 nm to measure the fluorescence spectrum and Vickers hardness. Subsequently, the area was observed using a scanning electron microscope.

Results: In teeth with infected root canals, blue-light irradiation at a wavelength of approximately 405 nm induced fluorescence excitation at wavelengths of approximately 620 and 680 nm. In the healthy teeth, no significant difference was observed in Vickers hardness in the region with fluorescence excitation of up to 500 μm from the root canal wall; however, in the infected teeth, a significant decrease in Vickers hardness was observed in the region with fluorescence excitation of up to 500 μm from the root canal wall. Furthermore, in the infected teeth, a bacterium-like structure was observed via electron microscopy on the root canal wall surface, and in the dentin tubules in areas with fluorescence excitation, whereas in areas without fluorescence excitation, there were few bacterium-like structures.

Conclusion: This study suggests that blue light of approximately 405-nm wavelength is useful in detecting infected areas in the root canal wall.

Key words: blue light, infected root canal dentin, Vickers hardness

Introduction

Apical periodontitis is a lesion in which bacterial infection in the root canal causes periodontal tissue inflammation and destruction. It is generally known that many bacteria inhabit the oral cavity. In healthy teeth, on the other hand, the pulp is sealed within the dentin, and thus cannot be infected by bacteria. Basically, the pulp of a healthy tooth cannot be infected, but if for some reason a pathway between the pulp and the oral cavity is established, infection can occur. Pathway development is thought to be mainly caused by either pulp exposure due to caries, fissures, or trauma, or by dentin tubules in the dentin exposed by enamel destruction^{1,2)}. Pulp infection caused by a pathway for oral bacteria results in pulpitis, and as the infection progresses, the pulp vasculature is compromised, resulting in pulp necrosis. If left untreated, this condition can lead to apical periodontitis, in which pulp cavity infection spreads beyond the root apex and destroys the surrounding periodontal tissue¹⁾.

However, it is difficult to observe the inside of the root canal with the naked eye, and infected dentin may remain in the root canal, causing recurrence of apical periodontitis. Although microscopes enable precise observation of the inside of root canals, they are expensive, huge, not easily portable, and also require skill and training to operate. Even if a root canal can be observed using a microscope, there is currently no indicator to show which part of the canal wall is infected. Thus, the current practice is to mechanically enlarge the root canal using hand cutting instruments, or nickel-titanium rotary files, chemically clean the canal with endodontic irrigants such as sodium hypochlorite^{3,4)}, and apply calcium hydroxide preparations to sterilize the root canal³⁻⁵⁾.

Our previous studies focused on the fact that red fluorescence excitation was observed when infected dentin was irradiated with blue light of approximately 405-nm wavelength. We observed that bacteria were present in infected areas where red fluorescence excitation was seen. Furthermore, when red fluorescence excitation was observed by irradiating a paper point with a root canal wiped with blue light of approximately 405-nm wavelength, the tooth in question was found to be infected in a bacterial culture test^{6,7)}.

As an extension of these studies, the present study aimed to evaluate the usefulness of blue light in the treatment of infected root canals by visualizing infected areas of root canal dentin using blue light and showing bacterial erosion of infected areas using Vickers hardness testing and electron microscopy.

Materials and Methods

1. Specimen preparation

In this study, human extracted teeth were used for sample preparation. The study protocol was approved by the ethics committee of Showa University (21-004-A). Tooth extractions were performed at Showa University Dental Hospital, or Showa University Fujigaoka Hospital.

Due to the limited number of healthy teeth available as a control group, no restrictions were placed on the types of teeth used in this study. When collecting the extracted teeth, we collected teeth with apical periodontitis, in which infection of the root canal was expected, and vital teeth with periodontitis or pericoronitis of wisdom tooth, in which the tooth structure was not infected.

The extracted teeth were immersed in 10% neutral buffered formalin and stored at room temperature for disinfection so as not to affect hardness⁸⁾. Subsequently, the teeth were rinsed with sterile purified water, and a semi-cut section was prepared by cutting the root canal longitudinally under water injection using a diamond disk. To prepare the specimens, the cut surface was polished with water-resistant abrasive paper to a roughness of #2000 under water injection.

2. Observation of fluorescence using a stereo microscope under blue light

The polished surface was placed on a glass slide with a flat pressure machine so that it was horizontal, and the surrounding area was fixed with self-polymerizing resin. Then, the samples were observed using a stereo microscope under blue light of approximately 405-nm wavelength in a dark room. A total of 10 teeth were allocated to each group: the infected group of samples in which red fluorescence was observed in the root canal wall, and the healthy group of samples in which no red fluorescence was observed.

3. Fluorescence measurement

After observation under the stereo microscope, the

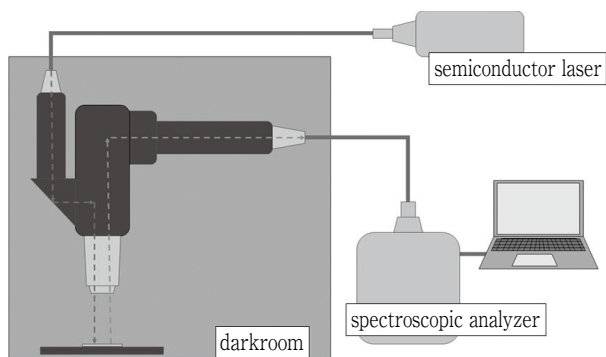


Fig. 1 Microscopic fluorescence measurement system

The sample was irradiated with blue laser light, the induced fluorescence was analyzed using a spectrometer (MCPD7700, Otsuka Electronics Co., Ltd., Tokyo, Japan), and the fluorescence spectrum was recorded.

healthy group was first examined using a microscopic fluorescence measurement system (Fig. 1) to measure the red fluorescence spectrum produced by blue light of approximately 405-nm wavelength when irradiated at distances of 100, 300, 500, and 700 μm from the root canal wall. To confirm the absence of red fluorescence, the fluorescence spectrum was measured at 10 points along the root canal wall. In the infected group, the fluorescence spectrum at 100 μm before and after the boundary between the infected and healthy areas was measured at 10 points along the root canal wall.

4. Evaluation of Vickers hardness of the root canal wall in the healthy group

Because dentin tubules generally run radially from the pulp side to the enamel-dentin boundary and root surface, the closer they are to the outside, the lower their density per unit area, and the greater their hardness and the closer they are to the pulp side, the higher their density and the lower their hardness^{9,10}. Therefore, to elucidate the hardness decrease of the root canal wall due to infection and the hardness change of the root canal wall due to the difference in dentin tubule density, we measured the Vickers hardness of the fluorescence spectrum measurement sites near the root canal wall of healthy teeth using a microhardness tester (FM-300, Future-Tech Corp., Kanagawa, Japan). The Vickers hardness test was performed with a load of 300 gf and a loading time of 10 seconds. Furthermore, we determined whether the difference was negligible. Using healthy teeth, hardness by distance from

the root canal for each of the 10 teeth was used to determine the extent to which differences in hardness by distance from the root canal caused by differences in dentin tubule density in the measurement range, should be considered in this study.

5. Evaluation of Vickers hardness of the root canal wall in infected root canals

Vickers hardness was then determined at the fluorescence spectrum measurement sites and the change in Vickers hardness before and after the boundary where fluorescence excitation occurred was evaluated.

Hardness measurement of root canal dentin has been previously used to investigate the effects of endodontic irrigants and lubricants on the dentin. The Vickers hardness test, which is commonly used for this purpose, was also employed in the present study^{11,12}.

The receiver operating characteristic curve was created using the hardness of root canal wall dentin in healthy and infected teeth to determine the extent to which infection weakens the hardness of the root canal wall dentin.

6. Observation of samples using a scanning electron microscope

Half of the infected teeth were observed using an electron microscope (FlexSEM 1000, Hitachi High-Tech Corp., Tokyo, Japan). Formalin adhering to the sample was washed by agitation with phosphate-buffered saline for 10 min. The samples were then dehydrated with ethanol at concentrations of 50%, 60%, 70%, 80%, 90%, 99%, 100%, and again 100%, in that order, for 10 min each. Next, critical point drying using a critical point dryer (931.GL, Tousimis, Maryland, USA) was performed on the samples. The sample was then fixed to the sample table with carbon tape so that the observation surface was as horizontal as possible, and degassed in a vacuum until the next day. Finally, the sample surface was coated with osmium using an osmium coater (HPC-1SW, Shinkuu Device Co., Ibaraki, Japan), and observed using an electron microscope.

7. Statistical analysis

Vickers hardness of the root canal wall in healthy teeth was evaluated by Scheffé's method. Statistical analysis was conducted using EZR software (Saitama Medical Center, Jichi Medical University, Saitama, Japan)¹³. The differences between the results obtained from the two methods were assessed using Fischer's exact probability test and analysis of variance. Vickers

Table 1 Vickers hardness of the root canal dentin by distance from the canal wall in healthy teeth

Distance from root canal wall	Number	Minimum	Maximum	Mean	SD
100 μm	10	38.06	55.32	45.6	5.7
300 μm	10	42.57	53.8	49.3	3.74
500 μm	10	45.03	59.46	52.8	4.33
700 μm	10	51.41	74.51	63.7	6.57

Vickers hardness of the root canal wall was measured using sound teeth to determine if there was a significant increase or decrease in the range of root canal wall hardness measurements.

Vickers hardness was measured at distances of 100, 300, 500, and 700 μm from the root canal wall in healthy teeth, and the mean value of each distance was calculated. As a result, Vickers hardness increased with increasing distance from the root canal wall, particularly at a distance of 700 μm from the canal wall, and the increase in hardness was significantly greater than those in other areas.

hardness of the root canal wall with and without fluorescent excitation in infected root canals was evaluated by the *t*-test.

Results

1. Healthy teeth

Red fluorescence was not observed when the healthy group was irradiated with blue light. When blue light of approximately 405-nm wavelength was irradiated at distances of 100, 300, 500, and 700 μm from the root canal wall and the fluorescence spectrum was measured, a waveform with a peak wavelength of approximately 500 nm was observed; however, the specific waveform seen in infected tooth structure was not observed. Vickers hardness was measured at the fluorescence spectrum measurement site and the average value of each sample was calculated according to the distance from the root canal wall. The results indicated that Vickers hardness increased with increasing distance from the root canal wall except for one of the 10 samples (Table 1). In that outlier sample, Vickers hardness at 100 μm from the root canal wall was slightly higher than those at 300 and 500 μm . The results indicated no significant differences between the distances of 100–300, 300–500, and 100–500 μm , but a significant difference was observed between the distance of 700 μm and all other distances ($p < 0.05$; Scheffé's method).

2. Teeth with infected root canals

When the infected group was irradiated with blue light, red fluorescence excitation was observed (Fig. 2).

Fluorescence spectrum measurements showed a specific fluorescence spectrum with two peaks at approximately 620- and 680-nm wavelengths in the vicinity of the infected root canal wall (Fig. 3). A peak was observed at approximately 500 nm, similar to that of the healthy teeth. Away from the root canal wall, a waveform similar to that of the healthy teeth was observed. Fluorescence spectra were recorded at 100 μm before and after the boundary where the specific fluorescence spectrum disappeared at a distance of 500 μm from the root canal wall. Furthermore, Vickers hardness was measured at the fluorescence spectrum measurement site, and the average hardness before and after the boundary was calculated. The results indicated that in all 10 specimens, the hardness was lower in the area with the specific fluorescence spectrum than in the area without (Table 2).

In the infected teeth, Vickers hardness was used to evaluate the degree of attenuation in the area with fluorescence excitation compared with the area without fluorescence excitation as a percentage. Vickers hardness at distances of 100, 300, and 500 μm from the root canal wall measured on a healthy tooth was used to calculate the percentage difference in hardness for every 200 μm . The proportion of both groups was included in the receiver operating characteristic curve, and the optimal cutoff value that maximized the sum of specificity and sensitivity was determined to be 91.9% (Fig. 4).

3. SEM

After measuring the fluorescence spectrum and

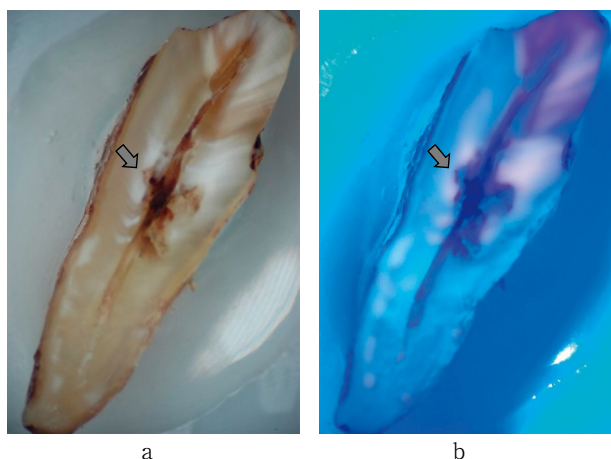


Fig. 2 Findings with incident light and blue light
 a) The boundary between the infected and healthy dentin could not be distinguished when the samples were observed under a stereo microscope. b) When blue light was irradiated, red fluorescence was observed from the infected dentin (arrow), and the boundary between the infected and healthy dentin was clearly defined.

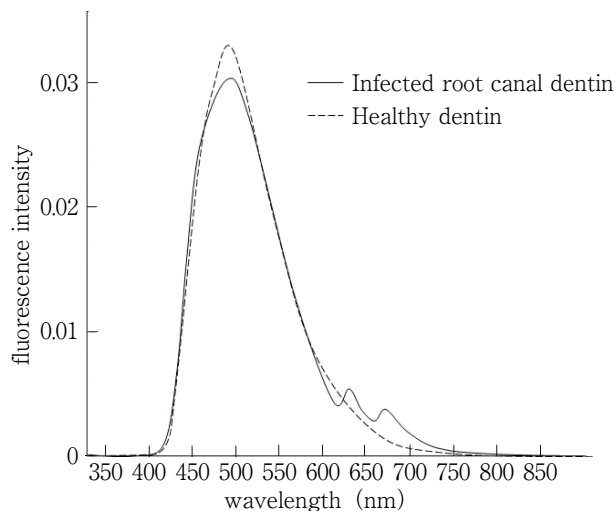


Fig. 3 Fluorescence spectrum of infected and healthy dentin in the root canal dentin

The fluorescence intensity on the vertical axis and the wavelength on the horizontal axis were plotted on a graph of the fluorescence excitation generated by blue-light irradiation of the samples. Specific wave-forms were observed at approximately 620 and 680 nm in the infected root canal dentin. No specific wave-forms were observed in the healthy dentin.

Table 2 Vickers hardness before and after the boundary between the areas with and without fluorescence excitation in healthy teeth

Fluorescence excitation	Number	Minimum	Maximum	Mean	SD
Presence	10	20.22	52.3	37.6	9.77
Absence	10	27.12	58.33	43.4	10.02

To examine whether the presence or absence of infection causes significant hardness attenuation in the root canal wall, using a tooth with an infected root canal, Vickers hardness was measured at a distance of 100 μm before and after the boundary where a specific fluorescence spectrum disappeared at a distance of 500 μm from the root canal wall, and the respective average values before and after the boundary were calculated. The hardness of the area with a specific fluorescence spectrum was significantly lower than that of the area without ($p < 0.05$).

Vickers hardness of the infected group, half of them were observed under an electron microscope. Bacterium-like structures were seen on the surface of the root canal wall and in the dentin tubules of the indentations in areas with fluorescence excitation. On the other hand, few bacterium-like structures were observed in the dentin tubules of the indentations in areas without fluorescence excitation (Fig. 5).

Discussion

In recent years, based on the philosophy of minimal intervention dentistry proposed by the FDI World Dental Federation, it has been recommended that dental caries treatment should focus on the protection of healthy tooth structure¹⁴. In the treatment of infected root canals, the protection of healthy dentin can reduce the risk of root fracture and help extend the life of the

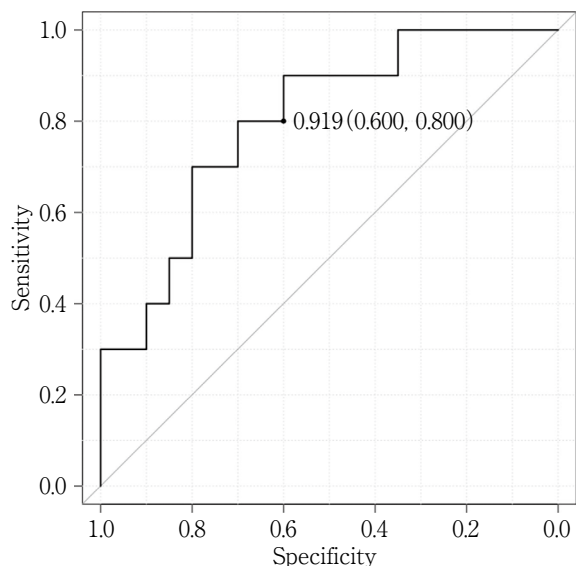


Fig. 4 ROC curve based on the rate of change of Vickers hardness

A receiver operating characteristic (ROC) curve was created by combining the rate of hardness change for every $200\ \mu\text{m}$ of the healthy tooth and the rate of hardness change between $200\ \mu\text{m}$ across the boundary between the infected and healthy areas of the infected root canal tooth. The cutoff value was derived from the ROC curve to maximize the sum of sensitivity and specificity.

tooth. For this purpose, it is effective to visualize the infected root canal wall using some methods and selectively remove the infected area instead of blindly grinding and mechanically expanding the root canal wall as in the current method for treating infected root canals.

In this study, the presence or absence of bacterial infection in root canal dentin, which emits red fluorescence excitation when irradiated by blue light of approximately 405-nm wavelength, was examined via fluorescence spectrum and Vickers hardness measurement as well as microstructural observation using an electron microscope. Our previous studies have demonstrated that bacterial infection occurs in crown dentin with red fluorescence excitation in response to blue light; however, the effect of blue light on root canal dentin has not been investigated. The present study aimed to evaluate the effectiveness of blue light on infected root canals in relation to hardness.

In the infected root canal dentin and crown dentin caries, red fluorescence excitation was produced by blue light of approximately 405-nm wavelength, and a

specific fluorescence spectrum with two peaks at approximately 620 and 680 nm was observed. No specific fluorescence spectrum was observed in the root canal walls of the healthy teeth, or at sites away from the root canals of the infected teeth. These results suggest that blue light of approximately 405-nm wavelength is useful for detecting infected root canal dentin and dentin caries in the crown.

The hardness of the root canal wall of healthy teeth was measured and the results were evaluated. The results showed that only the area $700\ \mu\text{m}$ from the root canal wall had significantly higher hardness than the other measured areas ($p < 0.05$). Therefore, it was suggested that a hardness comparison between 100 and $500\ \mu\text{m}$ is worth considering, although the hardnesses of 100, 300, and $500\ \mu\text{m}$ are not exactly equal in healthy teeth.

Based on these results, fluorescence spectra at $100\ \mu\text{m}$ before and after the boundary where the specific fluorescence spectrum disappears up to $500\ \mu\text{m}$ from the root canal wall were recorded at 10 points each along the root canal wall using an infected tooth, and Vickers hardness at that site was measured. For each sample, the average of Vickers hardness before and after the boundary was calculated and a *t*-test was conducted. The hardness of the area with a specific fluorescence spectrum was significantly lower than that of the area without ($p < 0.05$). Therefore, in the areas where fluorescence was observed, the dentin was considered to be weakened by the root canal infection.

The optimal cutoff value for hardness reduction due to root canal infection obtained from the receiver operating characteristic curve generated was 91.9%. This suggests that if there is a boundary between the presence and absence of fluorescence within a distance of $500\ \mu\text{m}$ from the canal wall in an infected tooth, the hardness is approximately reduced to 91.9% or less before and after the boundary. Thus, if the percentage of hardness change is above 91.9% after removal of $200\ \mu\text{m}$ of the root canal wall, it can be inferred that the healthy dentin has been approximately reached.

Electron microscopy of infected root canals showed the presence of bacterium-like structures on the root canal wall surface and in the dentin tubules at the indentations in areas with fluorescence excitation, but few bacterium-like structures were observed in areas without fluorescence excitation, suggesting that the

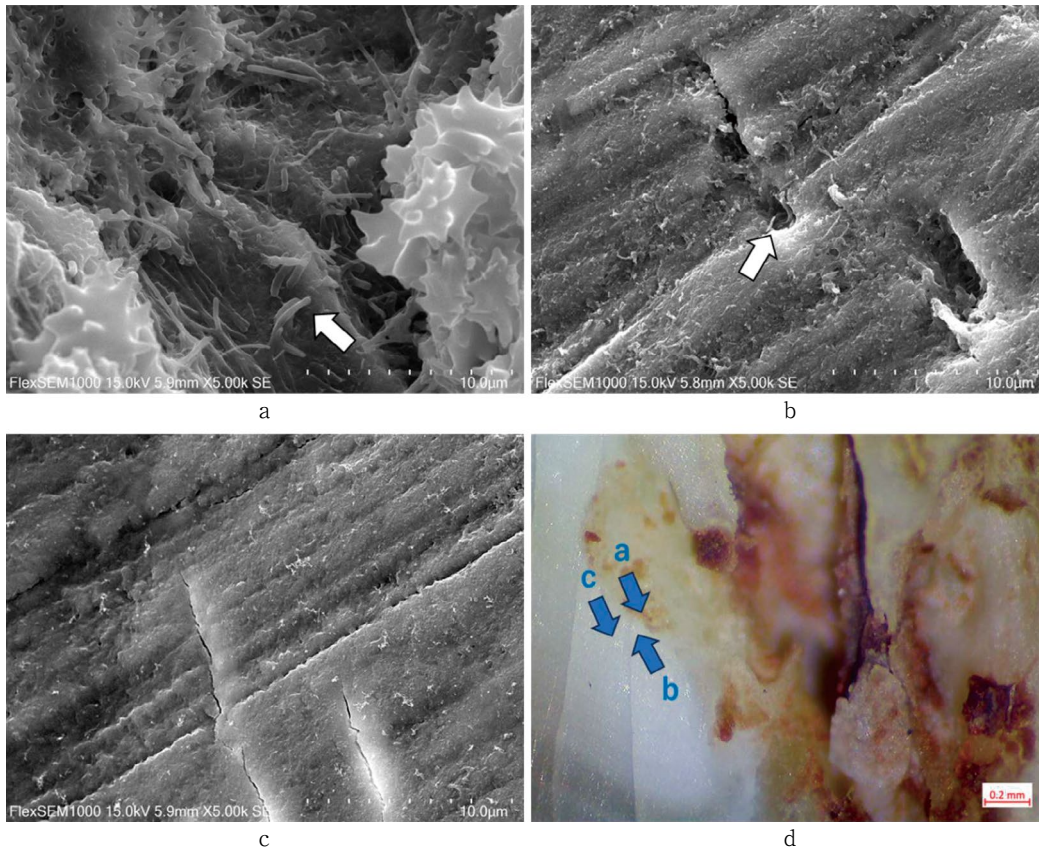


Fig. 5 Scanning electron microscope (SEM) image of a tooth with infected root canal

The root canal wall surface layer of an infected tooth and the site where the Vickers hardness test was conducted were observed using an electron microscope.

- a) Root canal wall surface : the presence of bacterium-like structures was observed (arrow).
- b) Dentin tubules in the area with specific fluorescence spectrum : the presence of bacterium-like structures was observed (arrow).
- c) Dentin tubules in the area without specific fluorescence spectrum : bacterium-like structures were rarely observed.
- d) Stereo microscopic image of the areas observed with SEM.

presence of bacteria contributes to the occurrence of fluorescence excitation and weakening of the root canal dentin. However, there appeared to be a difference in size between the bacterium-like structures present on the root canal wall surface and those present in the dentin tubules. Since the bacteria present may differ depending on the location of the root canal wall dentin, future studies should use PCR techniques to identify the bacterial species present.

The Vickers indenter may sometimes fail to measure the hardness of the unlined area near the surface of the root canal wall due to cracking or sinking of the surrounding area. Thus, it is necessary to improve the measurement direction, for example, by seeking the lining of the tooth structure.

Future studies should also determine whether removal of root canal dentin with fluorescence excitation has a superior therapeutic effect.

In this study, Vickers hardness was used as an indicator of weakening of root canal dentin caused by bacteria, but nanoindentation is an indicator of microstructural weakening due to caries¹⁵). Future studies should consider using nanoindentation.

This experiment was conducted extraorally using extracted teeth; it would be difficult to apply this test method directly to actual clinical practice. Therefore, instruments to observe the inside of root canals and new instruments for cutting the root canal wall should be developed and the clinical application of blue light to root canals should be considered.

Conclusion

In this study, we measured the fluorescence of infected dentin in the root canal wall using a microscopic fluorescence measurement system, measured the Vickers hardness at the site, and observed the microstructure of the indentation via electron microscopy. The results suggest that blue light produces red fluorescence excitation in root canal wall infected dentin as well as dentin caries. This study demonstrated that blue light at a 405-nm wavelength may be useful for detecting infected sites in root canals. In actual clinical practice, it is difficult to observe the inside of a root canal using techniques such as those in this study. Therefore, incorporation of blue light into a dental endoscope that can be inserted into the root canal, which we studied, can be applied to clinical practice¹⁶⁾. However, for curved root canals, it is difficult to use a dental endoscope or selectively remove the infected areas even if they can be observed using a dental endoscope. Therefore, further study of the hardness relationship between infected and healthy dentin as well as the development of an instrument that can blindly and selectively polish hardness below the threshold between infected and healthy dentin in the root canal wall will facilitate the establishment of more treatments for infected root canals based on minimal intervention dentistry. Thus, future research should focus on two areas: identification of the infected area in the root canal wall via fluorescence excitation, and removal of the infected dentin using the hardness threshold as a guide.

Acknowledgments

We would like to thank the dentists of our department for their cooperation in collecting the teeth and the staff of the Center of Electron Microscopy for their help in observing the specimens.

Conflicts of Interest

The authors declare no conflict of interest related to this paper.

References

1) Gomes BPFA, Herrera DR. Etiologic role of root canal

- infection in apical periodontitis and its relationship with clinical symptomatology. *Braz Oral Res* 2018; 32: e69.
- 2) Nair PR. Apical periodontitis: A dynamic encounter between root canal infection and host response. *Periodontol* 2000 1997; 13: 121-148.
- 3) Karamifar K, Tondari A, Saghiri MA. Endodontic periapical lesion: An overview on the etiology, diagnosis and current treatment modalities. *Eur Endod J* 2020; 5: 54-67.
- 4) Valera MC, Silva KC, Maekawa LE, Carvalho CA, Koga-Itô CY, Camargo CH, Lima RS. Antimicrobial activity of sodium hypochlorite associated with intracanal medication for *Candida albicans* and *Enterococcus faecalis* inoculated in root canals. *J Appl Oral Sci* 2009; 17: 555-559.
- 5) Siqueira JF Jr, Lopes HP. Mechanisms of antimicrobial activity of calcium hydroxide: A critical review. *Int Endod J* 1999; 32: 361-369.
- 6) Yamada M, Arimoto T, Morisaki H, Kuwata H, Isatu K, Hasegawa T. Qualitative and quantitative investigation of pathological structures in caries infected with *Streptococcus mutans* using fluorescence, molecular, and histological methods. *Jpn J Conserv Dent* 2017; 60: 245-254.
- 7) Takino H, Isatsu K, Hasegawa T. Analysis of an immediate diagnostic technique for detecting root canal bacteria using light-induced fluorescence. *Jpn J Conserv Dent* 2018; 61: 171-177.
- 8) Salem-Milani A, Zand V, Asghari-Jafarabadi M, Zakari-Milani P, Banifateme A. The effect of protocol for disinfection of extracted teeth recommended by center for disease control (CDC) on microhardness of enamel and dentin. *J Clin Exp Dent* 2015; 7: e552-e556.
- 9) Pashley D, Okabe A, Parham P. The relationship between dentin microhardness and tubule density. *Endod Dent Traumatol* 1985; 1: 176-179.
- 10) Soukup JW, Hetzel SJ, Stone DS, Eriten M, Ploeg HL, Henak CR. Structure-function relationships in dog dentin. *J Biomech* 2022; 141: 111218.
- 11) Naseri M, Eftekhari L, Gholami F, Atai M, Dianat O. The effect of calcium hydroxide and nano-calcium hydroxide on microhardness and superficial chemical structure of root canal dentin: An ex vivo study. *J Endod* 2019; 45: 1148-1154.
- 12) Saha SG, Sharma V, Bharadwaj A, Shrivastava P, Saha MK, Dubey S, Kala S, Gupta S. Effectiveness of various endodontic irrigants on the micro-hardness of the root canal dentin: An in vitro study. *J Clin Diagn Res* 2017; 11: ZC01-ZC04.
- 13) Kanda Y. Investigation of the freely available easy-to-use software 'EZR' for medical statistics. *Bone Marrow Transplant* 2013; 48: 452-458.

- 14) FDI World Dental Federation. FDI policy statement on minimal intervention dentistry (MID) for managing dental caries: Adopted by the general assembly: September 2016, Poznan, Poland. *Int Dent J* 2017; 67: 6-7.
- 15) Joves GJ, Inoue G, Sadr A, Nikaïdo T, Tagami J. Nanoindentation hardness of intertubular dentin in sound, demineralized and natural caries-affected dentin. *J Mech Behav Biomed Mater* 2014; 32: 39-45.
- 16) Hasegawa T, Ikeda S, Isatsu K. Application to endodontic treatment of experimental oral endoscope system—Securing of stable operative field—. *JSCD* 2016; 144: 141, Abst. No. P83. (in Japanese)

Effect of an MDP-based Cleaner on Adhesion to Dentin Contaminated with a Temporary Luting Cement

Taiho IDONO, Shojiro SHIMIZU, Tomohiro TAKAGAKI,
Michael F. BURROW* and Toru NIKAIIDO

Department of Operative Dentistry, Division of Oral Functional Science and Rehabilitation, Asahi University School of Dentistry

*Restorative Dental Sciences, Faculty of Dentistry, University of Hong Kong

Abstract

Purpose: The aim of this study was to investigate the effect of temporary luting cement removal using a new 10-methacryloyloxydecyl dihydrogen phosphate (MDP)-based cleaner (KATANA Cleaner) on the dentin adhesion of a resin cement.

Methods: Intact human dentin was ground with 600-grit SiC paper and divided into three groups. The first group was left untreated with the temporary cement (Con). For the other groups, dentin surfaces were covered with a temporary luting cement (Temporary Hard) and stored in water for one week. The temporary luting cement was removed using an ultrasonic scaler (US), and then treated with KATANA Cleaner for 10 s (KC). A resin composite block (KATANA Avencia Block) was bonded to the dentin using a resin cement (Panavia V5). The specimens were immersed in water for 24 h then cut into beams. These were subjected to thermal cycling stress for 0 cycles (TC0) or 5,000 cycles (TC5000). A microtensile bond strength test was performed at a crosshead speed of 1 mm/min. Data were statistically analyzed with two-way ANOVA and *t*-test with Bonferroni correction at a significance of 5%. The fractured specimens after debonding were examined using scanning electron microscopy and electron diffraction spectroscopy.

Results: No significant differences were noted in microtensile bond strengths between Con-TC0 and KC-TC0, between KC-TC0 and KC-TC5000 and between Con-TC5000 and US-TC0. The temporary luting cement covered the dentin surface in the US group, and partially remained in the KC group. Energy-dispersive X-ray spectrometric analysis revealed a distinct Zn peak in the US group, while the peak was significantly decreased in the KC group.

Conclusion: The combined method with an ultrasonic scaler and the MDP-based cleaner effectively removed temporary luting cement contaminants on dentin surfaces, thus securing durable bonding of a resin cement to dentin used for indirect restorations.

Key words: MDP-based cleaner, dentin bond strength, resin cement

Introduction

Recently, increasing demand among patients for esthetic restorative treatments has boosted the need for metal-free crown restorations¹. Computer-aided design/computer-aided manufacturing (CAD/CAM)-based restorations have become more popular^{2,3}, mainly with ceramic and resin-based composite materials^{4,5}. Since CAD/CAM resin composites and ceramics are more brittle than metal alloys^{6,7}, the clinical success of these restorations is greatly enhanced by integration of the restorative materials with the underlying tooth structure. Otherwise, there is a risk of fracture or detachment of the restorations⁸.

In clinical practice, there are several factors that may inhibit adhesion during clinical procedures, especially for indirect restorations^{9,10}. Saliva contamination has been reported to be a major factor reducing the long-term durability of the adhesion of resin cement to the fitting surface of CAD/CAM resin blocks¹¹. A temporary crown is generally placed with a temporary luting cement until the next patient visit to protect the prepared dentin and pulp from bacterial infection, suppress hypersensitivity, and prevent tooth movement¹². However, the temporary cement is not easily removed before the final cementation, contaminating the adherend and reducing the adhesion of the resin cement to dentin^{12,13}. Therefore, contamination by the temporary luting cement must be prevented to ensure clinical success of metal-free restorations.

A previous study investigated the mechanical removal of temporary cement with an ultrasonic scaler, but no significant effect was noted compared to the control (no mechanical cleaning)¹⁴. In contrast, another paper reported that cleaning off a temporary cement with a rotating cone-shaped brush under water-spray effectively removed the contaminants, recovering the adhesion to dentin¹⁴. Such variable results indicate that the overall outcome might also depend on the type of resin cement used. Cleaning the temporary cement with a cone-shaped brush alone was insufficient¹⁵. As no practical method for removing a temporary cement has yet been established¹⁶, there is an urgent need to establish clinical procedures for effectively removing temporary luting cements to achieve reliable adhesion.

Recently, a phosphate-based functional monomer,

10-methacryloyloxydecyl dihydrogen phosphate (MDP)-containing cleaner, was developed to remove contaminants such as saliva, blood and temporary luting cements/filling materials. This study investigated the effect of the MDP-based cleaner on the bonding of a resin cement to dentin contaminated with a temporary luting cement.

Materials and Methods

1. Materials used in this study

The materials used in this study are listed in Table 1. A resin cement, Panavia V5 (Kuraray Noritake Dental, Tokyo, Japan) was used with the associated self-etching primer (Tooth Primer, Kuraray Noritake Dental) according to the manufacturer's instructions. A phosphoric acid etchant (K-Etchant Syringe, Kuraray Noritake Dental) and a silane coupling agent (Clearfil Ceramic Primer Plus, Kuraray Noritake Dental) were used for the pretreatment of a CAD/CAM resin block (KATANA Avencia Block, Kuraray Noritake Dental). A polycarboxylate-based temporary luting cement (HY-Bond Temporary Cement, Hard, Shofu, Kyoto, Japan) was used, which is commonly used by Japanese clinicians. A MDP-containing cleaner (KATANA Cleaner, Kuraray Noritake Dental) was used for removing the contaminants from the temporary luting cement on the dentin surface.

2. Microtensile bond strength test

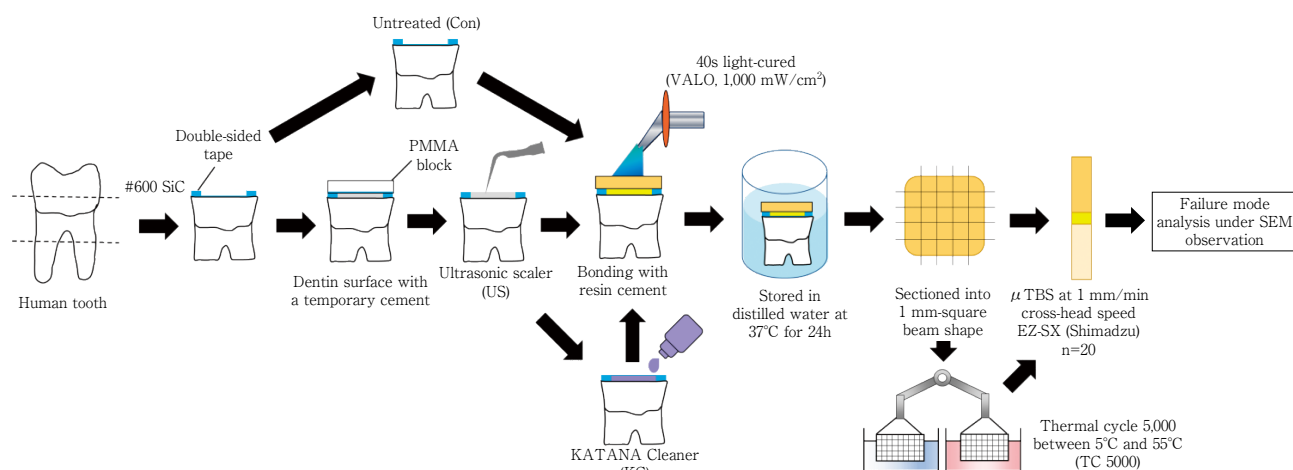
Specimen preparation procedures for the microtensile bond strength (μ TBS) test are illustrated in Fig. 1. This study was approved by the ethics committee of Asahi University School of Dentistry (No. 25148). Intact human molars were cut perpendicular to the long axis of the teeth to expose the superficial dentin, which was ground with 600-grit SiC paper to standardize the smear layer. Vinyl tape (100 μ m thick) was placed on the dentin surface to ensure a uniform thickness of the cement space.

The specimens were divided into the following three groups. The dentin surface was left without temporary cement in the control group (Con). For the experimental groups, a polymethyl methacrylate (PMMA) block was placed on the dentin surface with a temporary cement (HY-Bond Temporary Cement, Hard) and stored at room temperature for 30 min for complete setting of the cement. The specimens were then stored

Table 1 Materials used in this study

Material	Manufacturer	Composition	Lot. No
KATANA Avencia Block	Kuraray Noritake Dental, Tokyo, Japan	Alumina filler (20 nm), Silica filler (40 nm), Resin monomer	769
Panavia V5		MDP, HEMA, Hydrophilic aliphatic dimethacrylate, Accelerators, Water	34007
		Paste A : Bis-GMA, TEGDMA, Hydrophobic aromatic dimethacrylate, Hydrophilic aliphatic dimethacrylate, Initiators, Accelerators, Silanated barium glass filler, Silanated fluoroaluminosilicate glass filler, Colloidal silica	390130
		Paste B : Bis-GMA, Hydrophobic aromatic dimethacrylate, Hydrophilic aliphatic dimethacrylate, Silanated barium glass filler, Silanated aluminium oxide filler, Accelerators, dl-Camphorquinone, Pigments	390130
Clearfil Ceramic Primer Plus		3-Methacryloxypropyl trimethoxysilane, MDP, Ethanol	1P0051
KATANA Cleaner		Water, MDP, Triethanolamine, Polyethyleneglycol, Accelerator, Dyes	CGO004
HY-Bond Temporary Cement (Hard)	Shofu, Kyoto, Japan	Powder : Zinc oxide, Silica, Magnesium oxide, Tannin fluoride compound, Colorant etc.	91916
		Liquid : Acrylic acid-tricarboxylic acid copolymer, Sodium salt, Purified water	42016
K-Etchant Sylinge	Kuraray Noritake Dental, Tokyo, Japan	Phosphoric acid (35%), Polyethyleneglycol, Colloidal silica, Water, Pigment	570141

Bis-GMA ; Bisphenol A di (2-hydroxy propoxy) dimethacrylate, HEMA ; 2-Hydroxyethyl methacrylate, MDP ; Methacryloyloxydecyl, dihydrogen phosphate, TEGDMA : Triethylene glycol methacrylate.

**Fig. 1** Specimen preparations for μ TBS testing and SEM/EDS analysis

in water at 37°C for one week. Then, the PMMA block was manually removed with a dental explorer. An ultrasonic scaler (ENAC OE-3, Osada, Tokyo, Japan) was used in the output mode 2 for 10 s to remove any visible contaminants on the dentin surface using careful visual examination (US). The dentin surface was addi-

tionally scrubbed with KATANA Cleaner for 10 s (KC). All specimens were rinsed with distilled water and dried just before the bonding procedure.

The CAD/CAM resin block was cut into sections of 2-mm thickness with a low-speed cutting machine (Isomet1000, Buehler, Lake Bluff, IL, USA) and ground

with #600-grit SiC paper under a stream of water. The surface of the resin block was abraded with 50- μm alumina (DANVILLE, San Ramon, CA, USA) at a distance of 10 mm with an air pressure of 0.2 MPa immediately before the bonding procedure^{17,18}. Subsequently, the resin blocks were sonicated in 99.9% ethanol for 2 min and air-dried. Next, phosphoric acid etch (K-Etchant Syringe) was applied on the surface for 5 s, followed by rinsing with distilled water and air-drying. A silane coupling agent (Clearfil Ceramic Primer Plus) was finally applied to the specimen surface for 10 s and gently air-dried.

For the dentin side, a self-etching primer (Tooth Primer) was applied to the dentin surface for 20 s and air-dried. A resin cement (Panavia V5) was then applied to the dentin surface and the CAD/CAM block was placed and pressed onto the dentin surface. A LED light curing unit (VALO Curing Light, ULTRADENT PRODUCTS, South Jordan, UT, USA) was used in the standard mode (1,000 mW/cm²) on the top of the CAD/CAM block to directly cure the resin cement for 40 s through the CAD/CAM block. Afterwards, the bonded specimens were kept at room temperature for 30 min, and stored in water at 37°C for 24 h. The specimens were cut perpendicular to the dentin-resin cement interface to make beam-shaped specimens (1 mm \times 1 mm) using a low-speed diamond cutting machine (Isomet 1000). The specimens were then subjected to thermal stress at 5–55°C for 30 s dwell time using a thermal cycling machine (K178, Tokyo Giken, Tokyo, Japan) for 0 cycles (TC0) or 5,000 cycles (TC5000), respectively. A μTBS test was performed using a universal testing machine (EZ-SX, Shimadzu, Kyoto, Japan) at a crosshead speed of 1 mm/min.

3. Fracture mode analysis

The fracture modes of the debonded specimens after μTBS testing were examined using a scanning electron microscope (SEM, S-4500, Hitachi, Ibaraki, Japan) after the fractured specimens were osmium-coated (HP-IS, Vacuum Devices, Horiba, Mito, Japan). The fracture modes were categorized as follows: adhesive failure at the interface between dentin and resin cement (AD), cohesive failure in the resin cement (CR), adhesive failure at the interface between the resin cement and CAD/CAM resin block (AR), cohesive failure in dentin (CD) and mixed failure including the combinations of AD+CR and AD+CD as illustrated in Fig. 2.

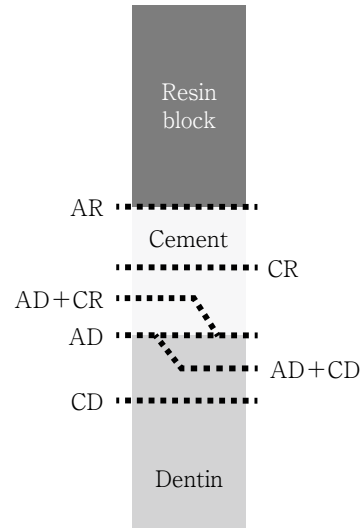


Fig. 2 Illustration of categorization of the fracture modes after debonding

AD : Adhesive failure at the interface between the dentin and resin cement

CR : Cohesive failure in the resin cement

AR : Adhesive failure at the interface between the resin cement and CAD/CAM resin block

CD : Cohesive failure in the dentin

4. SEM and EDS analysis of the dentin surface

The dentin surface of each group was prepared in the same manner as the specimens prepared for the μTBS test. The dentin surfaces were osmium-coated, and observed using an SEM. In addition, elemental analyses of Ca, P, and Zn were performed using an energy-dispersive X-ray spectrometer (EDS, EMAX-7000, Horiba, Tokyo, Japan) attached to the SEM at an acceleration voltage of 1.5 kV.

5. Statistical analysis

The number of specimens was 20 for each group. The data obtained from the μTBS test were analyzed using the Shapiro–Wilk test for normality and Levene’s test for homogeneity of variance. Statistical analysis was then performed using two-way analysis of variance (ANOVA) and the Bonferroni-corrected *t*-test at a significance level of 5%.

Results

1. Microtensile bond strength

Table 2 shows the results of the μTBS test. Two-way ANOVA analysis revealed the interaction between “material” and “thermal cycling.” There were no sig-

Table 2 Microtensile bond strengths of dentin with/without thermal cycles (TC)

Group	TC0	TC5000
Control	51.2±12.8 ^A	36.1±8.5 ^B
US	35.0±9.8 ^B	24.7±7.8 ^C
KC	51.8±10.1 ^A	52.6±14.5 ^A

N=20, Mean (MPa) ±SD

Same superscript letters indicate no significant difference ($p > 0.05$). Thermal stress for 0 (TC0) and 5,000 cycles (TC5000).

nificant differences in μ TBS between Con-TC0 and KC-TC0, between KC-TC0 and KC-TC5000, and between Con-TC5000 and US-TC0, respectively.

2. Observation of fractured surface morphology

Figure 3 shows representative SEM images of the fractured surfaces after the μ TBS test. Figure 4 shows the different fracture mode percentages for the specimens for each group. The fracture mode was mainly cohesive failure in the resin cement (CR) in all groups, except for KC-TC5000. Compared to Con-TC0, adhesive failure (AD) was more commonly observed in US-TC0 and KC-TC0. Mixed failure including cohesive fracture in dentin (AD+CD) was observed only in the control groups. For the KC groups, both adhesive failure between the resin cement and dentin (AD) and mixed failure (AD+CR) tended to increase from TC0 to TC5000.

3. SEM observation of dentin-bonded surface

Figure 5 shows the secondary electron images of the dentin surface of each group. For the control group, the smear layer and the scratch marks created by the 600-grit SiC paper were observed on the dentin surface. For the US group, residual temporary cement covered the entire dentin surface. For the KC group, scratch marks were observed the same as the control group, however, small amounts of temporary cement residue were noted. In addition, dentinal tubule openings were not observed with the partial removal of the smear layer.

4. EDS analysis of the dentin surface for each group

Figure 6 shows the SEM images (Upper) and the EDS line analysis (Lower) of the Con, US, and KC groups, respectively. From the EDS analysis, the two peaks of P and Ca belonging to dentin were confirmed in all groups, which decreased in the US group compared to

the control group and a peak for Zn was clearly identified. The Zn peak was also identified in the KC group, but the amount of Zn in KC was much smaller than that in US, while the amounts of P and Ca in KC were relatively higher than those in US.

Figure 7 shows the elemental mapping images for each group. In the control group, P and Ca belonging to dentin apatite were detected on the entire surface. In the US group, P and Ca were also detected, and Zn was strongly detected, matching the area of the temporary cement residues on the dentin surface observed in the SEM images. Small amounts of Zn were also detected in various sites of the SEM images in the KC group.

Discussion

In this study, we investigated the effect of removing temporary cement contaminants from the dentin surface using an ultrasonic scaler and MDP-based cleaner. We also evaluated the dentin bonding performance when a CAD/CAM resin block was bonded to dentin with a resin cement. The temporary cement, HY-bond Temporary Cement (Hard), is a polycarboxylate-based cement which is widely used for temporization for indirect restorations. The output modes of the ultrasonic scaler range from mode 1 to mode 4, which is a variation in intensity, mode 4 being the strongest. The optimal output mode was determined in a pilot study. The results were as follows: mode 1- the sonication was too weak to remove the temporary material sufficiently, and residual cement was visually confirmed; mode 2- contaminants from the temporary cement were entirely removed by visual inspection; modes 3 and 4- sonication was too strong and was found to damage the dentin surface, with scratches from the scaler tip chipping the dentin surface. Therefore, output mode 2 was selected for this experiment.

The MDP-containing cleaner, KATANA Cleaner, was tested in this study. MDP is a functional monomer used in many adhesive systems. MDP is known to play a role in self-etching dentin in the presence of water, resulting in stable chemical bonding with the calcium in hydroxyapatite of human teeth¹⁹⁻²¹. On the other hand, MDP has a hydrophilic group and a hydrophobic group in one molecule, and so has the possibility to exert a surfactant effect. In this study, the action of MDP in KC was believed to be due to the surfactant effect. The

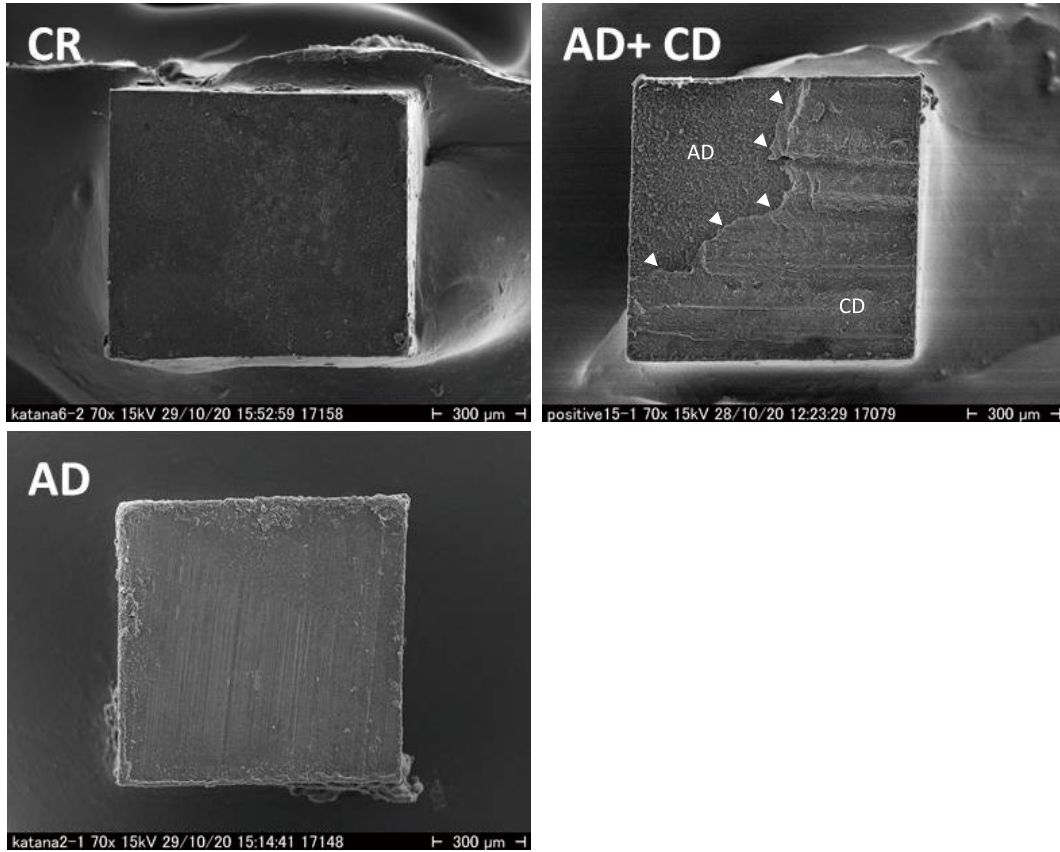


Fig. 3 Representative SEM images of the fractured specimens after the μ TBS testing
 CR : Cohesive failure in the resin cement
 AD : Adhesive failure at the interface between the dentin and resin cement
 AD+CD : Mixed failure of AD and cohesive failure in the dentin (CD).($\times 70$)
 The white arrows in the SEM images indicate the boundary between AD and CD.

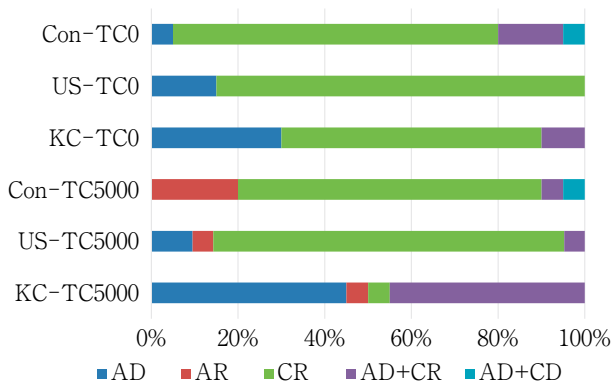


Fig. 4 Results of the failure mode analysis after debonding of specimens
 AD : Adhesive failure at the interface between the dentin and resin cement
 CR : Cohesive failure in the resin cement
 AR : Adhesive failure at the interface between the resin cement and CAD/CAM resin block
 CD : Cohesive failure in the dentin

temporary cement used in this study has hydrophobic characteristics. When KC is applied on the contaminated dentin surface, MDP probably forms a micelle structure by surrounding and dispersing the hydrophobic temporary cement. The micelle structures can be easily removed and washed out.

The control group without contamination revealed the highest bond strength of 50 MPa at TC0, however, the bond strength decreased in US, whereas the bond strength was recovered in KC to the same value as that of the control group. This strongly suggested that removing the temporary cement with the combination of ultrasonic scaler and the MDP-based cleaner would be very effective before bonding of a resin cement to dentin.

After the thermal cycling, the bond strengths decreased in the Con and US groups. In contrast, no decrease was found in the KC group, suggesting

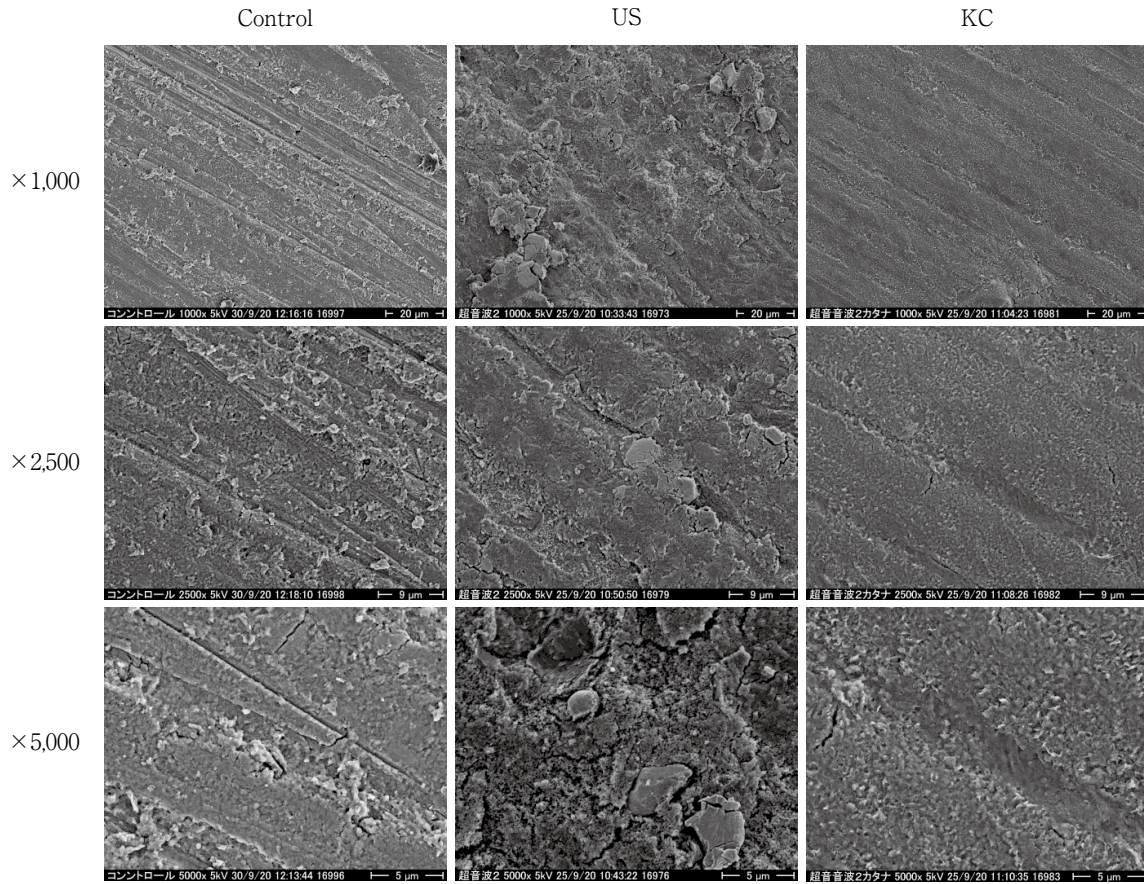


Fig. 5 Representative SEM photographs of the dentin surface after removal of the temporary filling material

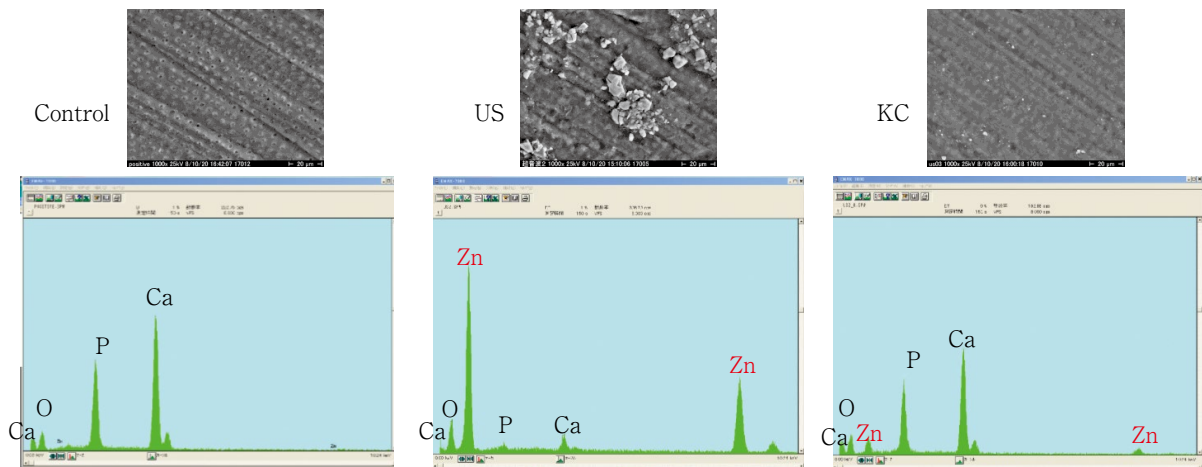


Fig. 6 SEM (Upper) and EDS line analysis (Lower) of the dentin surface for each group

improvement of dentin bond durability with the KC treatment, which may be due to the surfactant effect and also the formation of MDP-Ca salt by application of KC. The results of the fracture mode analysis (Fig. 4) showed that the main fracture mode was cohesive fail-

ure in resin cement (CR) in all the groups, except for KC-TC5000. The rate of adhesive failure at the resin cement-dentin interface (AD) increases at TC5000. In KC-TC5000, AD and AD+CR were mainly observed, which is believed to be due to the effect of the

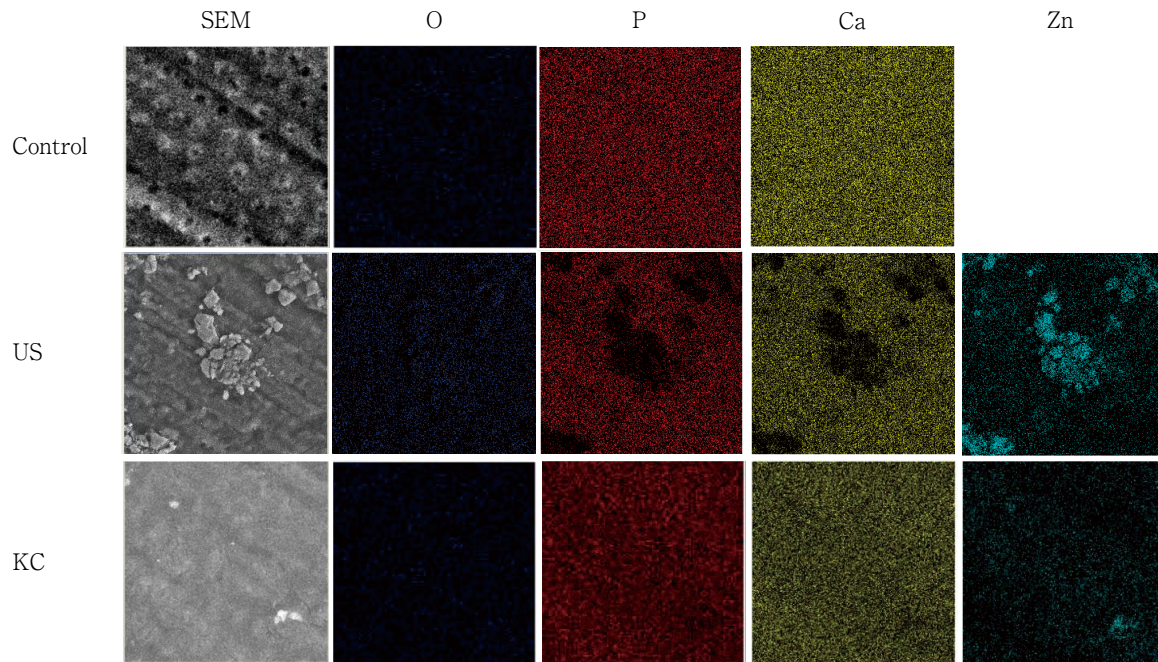


Fig. 7 EDS mapping analysis of the dentin surface for each group

KATANA Cleaner on the dentin surface, but the main reason remains unclear. Further morphological investigations of the bonded interface should be performed.

The SEM image of the dentin surface in the control group (Fig. 5) showed that the dentin surface was entirely covered with a smear layer, while the residues of the temporary cement remained in the US group, despite complete removal of the contaminants confirmed by visual inspection. From the EDS analysis (Figs. 6 and 7), Zn was detected, which must have been derived from zinc oxide (ZnO) in the temporary cement in the US group. The remarkable reduction of the Zn peak in the KC group (Fig. 6) suggested that the residual temporary cement on the dentin surface of KC is much less than that of US, however, KC could not completely remove all of the contamination caused by the temporary cement. Therefore, it is concluded that the combination of an ultrasonic scaler and KC could remove the temporary cement efficiently, resulting in improvement of bonding between the resin cement and dentin.

Only one type of temporary cement material was used in this study. Further studies should be undertaken to investigate the effect of different types of temporary cements to establish a reliable method for removing contaminants from temporary luting cements.

Conclusion

The combined method with an ultrasonic scaler and the MDP-based cleaner effectively removed contaminants from a temporary luting cement on dentin surfaces, thus securing durable bonding of a resin cement to dentin used for indirect restorations.

Conflict of Interest

The authors declare no conflicts of interest associated with this manuscript.

References

- 1) Mine A, Kabetani T, Kawaguchi-Uemura A, Higashi M, Tajiri Y, Hagino R, Imai D, Yumitate M, Ban S, Matsumoto M, Yatani H. Effectiveness of current adhesive systems when bonding to CAD/CAM indirect resin materials. *Jpn Dent Sci Rev* 2019; 55: 41-50.
- 2) Duret F, Blouin JL, Duret B. CAD-CAM in dentistry. *J Am Dent Assoc* 1988; 117: 715-720.
- 3) Raigrodski AJ. All-ceramic full-coverage restorations: Concepts and guidelines for material selection. *Pract Proced Aesthet Dent* 2005; 17: 249-256.
- 4) Coldea A, Swain MV, Thiel N. Mechanical properties of polymer-infiltrated-ceramic-network materials. *Dent Mater* 2013; 29: 419-426.

- 5) Ruse ND, Sadoun MJ. Resin-composite blocks for dental CAD/CAM applications. *J Dent Res* 2014; 93: 1232-1234.
- 6) Spitznagel FA, Boldt J, Gierthmuehlen PC. CAD/CAM ceramic restorative materials for natural teeth. *J Dent Res* 2018; 97: 1082-1091.
- 7) Hampe R, Theelke B, Lümekemann N, Eichberger M, Stawarczyk B. Fracture toughness analysis of ceramic and resin composite CAD/CAM material. *Oper Dent* 2019; 44: 190-201.
- 8) Inomata M, Harada A, Kasahara S, Kusama T, Ozaki A, Katsuda Y, Egusa H. Potential complications of CAD/CAM-produced resin composite crowns on molars: A retrospective cohort study over four years. *PLoS One* 2022; 17: e0266358.
- 9) Gilbert S, Keul C, Roos M, Edelhoff D, Stawarczyk B. Bonding between CAD/CAM resin and resin composite cements dependent on bonding agents: Three different in vitro test methods. *Clin Oral Investig* 2016; 20: 227-236.
- 10) Higashi M, Matsumoto M, Kawaguchi A, Miura J, Minamino T, Kabetani T, Takeshige F, Mine A, Yatani H. Bonding effectiveness of self-adhesive and conventional-type adhesive resin cements to CAD/CAM resin blocks. Part I: Effects of sandblasting and silanization. *Dent Mater J* 2016; 35: 21-28.
- 11) Kawaguchi-Uemura A, Mine A, Matsumoto M, Tajiri Y, Higashi M, Kabetani T, Hagino R, Imai D, Minamino T, Miura J, Yatani H. Adhesion procedure for CAD/CAM resin crown bonding: Reduction of bond strengths due to artificial saliva contamination. *J Prosthodont Res* 2018; 62: 177-183.
- 12) Takimoto M, Ishii R, Iino M, Shimizu Y, Tsujimoto A, Takamizawa T, Ando S, Miyazaki M. Influence of temporary cement contamination on the surface free energy and dentine bond strength of self-adhesive cements. *J Dent* 2012; 40: 131-138.
- 13) Watanabe EK, Yamashita A, Imai M, Yatani H, Suzuki K. Temporary cement remnants as an adhesion inhibiting factor in the interface between resin cements and bovine dentin. *J Prosthodont* 1997; 10: 440-452.
- 14) Kanakuri K, Kawamoto Y, Matsumura H. Influence of temporary cement remnant and surface cleaning method on bond strength to dentin of a composite luting system. *J Oral Sci* 2005; 47: 9-13.
- 15) Tajiri-Yamada Y, Mine A, Nakatani H, Kawaguchi-Uemura A, Matsumoto M, Hagino R, Yumitate M, Ban S, Yamanaka A, Miura J, Van Meerbeek B, Yatani H. MDP is effective for removing residual polycarboxylate temporary cement as an adhesion inhibitor. *Dent Mater J* 2020; 39: 1087-1095.
- 16) Carvalho EM, Carvalho CN, Loguercio AD, Lima DM, Bauer J. Effect of temporary cements on the micro tensile bond strength of self-etching and self-adhesive resin cement. *Acta Odontol Scand* 2014; 72: 762-769.
- 17) Ali A, Takagaki T, Naruse Y, Abdou A, Nikaido T, Ikeda M, Tagami J. The effect of elapsed time following alumina blasting on adhesion of CAD/CAM resin block to dentin. *Dent Mater J* 2019; 38: 354-360.
- 18) Naruse Y, Takagaki T, Matsui N, Sato T, Ali A, Ikeda M, Nikaido T, Tagami J. Effect of alumina-blasting pressure on adhesion of CAD/CAM resin block to dentin. *Dent Mater J* 2018; 37: 805-811.
- 19) Yoshihara K, Nagaoka N, Okihara T, Kuroboshi M, Hayakawa S, Maruo Y, Nishigawa G, De Munck J, Yoshida Y, Van Meerbeek B. Functional monomer impurity affects adhesive performance. *Dent Mater* 2015; 31: 1493-1501.
- 20) Yoshida Y, Nagakane K, Fukuda R, Nakayama Y, Okazaki M, Shintani H, Inoue S, Tagawa Y, Suzuki K, De Munck J, Van Meerbeek B. Comparative study on adhesive performance of functional monomers. *J Dent Res* 2004; 83: 454-458.
- 21) Li N, Nikaido T, Takagaki T, Sadr A, Makishi P, Chen J, Tagami J. The role of functional monomers in bonding to enamel: Acid-base resistant zone and bonding performance. *J Dent* 2010; 38: 722-730.

Color Evaluation of Porcelain Laminate Veneer Restorations Bonded with a Single-shade Resin Composite

Toshinari TOYAMA, Mikihiro KOBAYASHI, Rintaro SUGAI, Yuiko NIIZUMA and Atsufumi MANABE

Department of Conservative Dentistry, Division of Aesthetic Dentistry and Clinical Cariology,
Showa University School of Dentistry

Abstract

Purpose: To evaluate the effect of single-shade resin composites on the color of porcelain laminate veneer (PLV) restorations comprising lithium disilicate (LDS) cemented to an underlying tooth of two different shades. The evaluation was carried out using the CIEDE2000 color-difference formula and a translucency parameter.

Methods: Ceramic blocks (A2, HT, IPS e.max CAD, Ivoclar) of 1 mm thickness were fired and assumed to be PLV. Their adhered surfaces were polished with grit-silicon carbide paper (#1200), and their measurement surfaces were mirror-polished. Four resin composites were used as luting materials to fill the 50- μ m space between the PLV and the 2-mm-thick standardized underlying tooth, which was then photo-polymerized to serve as the specimen. The following luting materials were used in the present study: single-shade GRACEFIL Universal LoFlo (GC), Clearfil Majesty ES Flow (Kuraray Noritake Dental), Omnicroma Flow (Tokuyama Dental), and A2 shade GRACEFIL LoFlo (GC). A2 and A4 resin composites (Filtek Supreme Ultra, 3M ESPE) polished with water-resistant polishing paper (#600) were assumed as the underlying tooth (underlying structure). Forty specimens were produced and immersed in distilled water at 37°C for 30 days. There were two conditions for the color of the underlying structure and four conditions for the luting material (n=5). A Vitae Easy Shade V (VITA) digital spectrophotometer was used to determine the color of each specimen. The PLVs were investigated before and after cementation, and after immersion in water (Day 1, 3, 7, and 30) on the underlying structure. The data were analyzed using the 1976 CIEL*a*b* color system and CIEDE2000 (ΔE_{00}). ΔE_{00} was calculated for the underlying structure spacing and compared to a threshold considered acceptable in clinical practice ($\Delta E_{00} > 1.8$). The translucency parameter (TP), determined by the color difference between the black and white backgrounds, was also evaluated. The statistical significance of each of the ΔE_{00} and TP values at Day 30 was determined by the Shapiro-Wilk and Levene tests and one-way analysis of variance (ANOVA).

Results: The one-way ANOVA results showed no significant differences in the ΔE_{00} (p=0.32) or TP (p=0.23) values between the luting materials at Day 30. However, the ΔE value between the underlying structure of A2 and A4 exceeded the threshold value ($\Delta E_{00} > 1.8$).

Conclusion: The present study suggests that the color of the underlying tooth has more influence on the final color of the PLV restoration than the single-shade resin composite.

Key words: porcelain laminate veneer, single-shade resin composite, color

Introduction

Porcelain laminate veneer (PLV) restorations are one of the most commonly used esthetic treatments for tooth discoloration and morphological abnormalities, and are relatively minimally invasive. In addition, PLV is clinically highly popular among patients because of its superior esthetics, optical properties, and biocompatibility¹⁻⁸. Studies examining 21- to 25-year survival rates of feldspathic porcelain laminate veneers reported high survival rates and long-term stability¹. In recent years, lithium disilicate ceramics (LDS) have been widely used in PLV restorations because of their excellent esthetic properties². The color of the final PLV restoration might be influenced by the thickness and translucency of the veneer restoration, depending on the amount of light scattering and reflection⁸. It has also been reported that the color of the resin cement has a significant influence on the color of the restoration after cementation because of the high translucency of the LDS. Furthermore, it has been reported that the color of the underlying tooth also greatly affects the overall color of the PLV restoration³. Because such restorations are generally fabricated with a PLV thickness of 0.5-1.0 mm⁴, the color of the resin cement interposed between the translucent LDS and the underlying tooth can have an important influence on the clinical success of the restoration⁵.

Dual-cure resin cements are widely used for cementation of ceramic restorations⁹. However, these cements have a short working time and can cause color changes over time, especially yellowing of the cement because of oxidation of reactive groups of tertiary amines and polymerization inhibitors, which might affect the color after PLV restoration^{10,11}. Therefore, light-cured resin composites are sometimes used to bond PLV to enamel¹². Such composites are available in a variety of shades and restore human teeth, which express many shades of color. However, clinician skill and experience are necessary to select the appropriate shade for each individual tooth and achieve an esthetic restoration. Therefore, single-shade resin composites with a simple shade system have been developed and clinically used in resin composites in recent years. The characteristic feature of color reproduction with monochromatic resin composites is that unlike resin compos-

ites that use pigments to express color, the filler content, shape, and size have a photochemical effect and blend with the color of the surrounding tooth structure¹³. Therefore, the present authors hypothesized that using a single-shade resin composite as a luting material in PLV restorations would suppress the influence of luting material on the final PLV color, rendering the procedure simple and esthetic.

In this study, PLVs were placed on the underlying tooth by using a single-shade light-cured resin composite, and color changes were measured with a spectrophotometer. Spectrophotometers are often used to evaluate the color of PLVs after restoration *in vitro* because they can standardize and quantify color; the color difference (ΔE_{00}) by using CIEDE2000 indicates a change in color, and clinically, ΔE_{00} of >1.8 indicates a dominant color discrepancy¹⁴. In several studies, a post-cementation ΔE_{00} of >1.8 was considered a clinically unacceptable color discrepancy. It is also important to provide natural tooth-like transparency in treatment with LDS¹⁵. Appropriate transparency enables PLVs to appear natural¹⁶. The translucency parameter (TP) is frequently used to measure the translucency of ceramics¹⁷. Therefore, in this study, the influence of the luting material on the translucency of PLVs was also evaluated by using the TP. Although there have been studies on post-cementation coloration of PLV restorations using LDS, there are few studies on the effect of single-shade resin composites as a bonding material between the underlying tooth and PLV on the coloration of PLV restorations. The purpose of this *in vitro* study was to evaluate the effect of resin composites with a wide range of color compatibility on the color of PLV restorations by using the color difference and transparency.

Materials and Methods

Table 1 shows the materials used in this study. IPS e.max CAD (Ivoclar Vivadent, Schaan, Liechtenstein), an LDS-based ceramic block, was used as the PLV. The shade of the ceramic block was selected to be A2, a highly translucent type. The underlying teeth were prepared by using Filtek Supreme Ultra (3M ESPE, St. Paul, MN, USA) in A2 or A4, and the PLV was bonded to the underlying tooth by using a single-shade flowable resin composite. GRACEFIL Universal LoFlo (GUF: GC,

Table 1 Materials used in this study

	Code	Manufac- turer	Main composition		Filler con- tents (wt%)	Lot Number
			Matrix	Filler		
Resin composite (Luting material)						
GRACEFIL LoFlo	CNT	GC	Bis-MEPP	Barium glass	69	2212151
GRACEFIL Univeral LoFlo	GUF	GC	Bis-MEPP, TEGDMA, UDMA	Silicon dioxide, Strontium glass	69	2304281
Clearfil Majesty ES Flow	ESF	Kuraray Noritake Dental	TEGDMA	Barium glass filler, Silanated silica, Nano-cluster filler	75	CC0052
Omnichroma Flow	OCF	Tokuyama Dental	UDMA, TEGDMA	SiO ₂ -ZrO ₂ filler	71	042B3
Resin composite (Underlying structure)						
Filtek Supreme Ultra		3M ESPE	Bis-GMA, UDMA, Bis-EMA, TEGDMA	SiO ₂ -ZrO ₂ non-agglomerated filler	78.5	A2: 9906824 A4: 9849212
Ceramic block (PLV)						
IPS e-max CAD		Ivoclar Vivadent	Lithium disilicate glass-ceramic (SiO ₂ , Li ₂ O, K ₂ O, P ₂ O ₅ , ZrO ₂ , Al ₂ O ₃ , MgO)			Z00VL9

Tokyo, Japan), Clearfil Majesty ES Flow (ESF: Kuraray Noritake Dental, Tokyo, Japan), Omnichroma Flow (OCF: Tokuyama Dental, Tokyo, Japan), and GRACEFIL LoFlo (CNT: GC) in the A2 shade were used. These four types of light-curing flowable resin composites were used as luting materials.

1. Specimen preparation

To prepare the specimens, IPS e.max CAD was prepared to a thickness of 1 mm by using an automatic precision cutting machine (Isomet, Buehler, Lake Bluff, IL, USA) and fired in a fast sintering furnace (CEREC SpeedFire, Dentsply Sirona, Bensheim, Germany).

After firing, the surface polished with grit-silicon carbide paper (#1200) was assumed to be the adherend and the surface was mirror-polished with aluminum oxide powder (0.05 μm : MICROPOLISH II, Buehler was assumed as the color measurement surface. The tooth was fabricated with A2 and A4 resin composites, adjusted to a 2-mm-thick rectangle using a silicone guide, and photo-polymerized and assumed as the underlying tooth (underlying structure). Light irradiation was performed by using the normal mode of a light irradiator (G-Light Prima II Plus, GC) with an 8.0-mm-diameter irradiation port at a light intensity of 1,200 mW/cm² for 90 s each side. The underlying struc-

ture surfaces were polished with water-resistant abrasive paper (#600). After polishing, the PLVs and underlying tooth were ultrasonically cleaned for 10 min and dried. As a pretreatment for adhesion, the surfaces of the underlying structure and the PLV were sand-blasted for 5 s using sand with an average grain size of 50 μm at a pressure of 0.3 MPa. They were then coated with a silane coupling agent (Clearfil Ceramic Primer Plus, Kuraray Noritake Dental). Aluminum spacers (50 μm thick) were fixed between the PLVs and underlying structure, and luting material was loaded and photo-polymerized. Light irradiation was performed on one side of the specimen in two sections for 30 s each, for a total of 120 s from both sides, and the polymerized specimens were used as the test specimens. A total of 40 specimens were prepared and then immersed in distilled water at 37°C for 30 d.

2. Color analysis

Specimens were colorimetrically measured with a digital spectrophotometer (Easy Shade V, VITA Zahnfabrik, Bad Säckingen, Germany) before bonding the PLVs to the underlying structure [before cementation (BC)]; immediately after cementation with luting material (Day 0), and at 1, 3, 7, and 30 days after immersion in water. Colorimetry was performed on a black back-

ground under room light at the same time and location. The specimens were guided to define the color measurement site and angle to enable reproducible color measurement. Before each color measurement, the specimens were calibrated as specified by the manufacturer; the same area was measured three times and the average value was used as the measured value. The color was analyzed by using the 1976 CIE $L^*a^*b^*$ color system to obtain lightness L^* (white to black), a^* (red to green), and b^* (yellow to blue). The overall color was calculated by using CIEDE2000 (ΔE_{00}). The difference in color between the underlying structure of A2 and A4 was also calculated by using ΔE_{00} . Each ΔE_{00} was compared with the threshold considered acceptable in clinical practice ($\Delta E_{00} > 1.8$). The parameters and formulas for calculating ΔE_{00} are shown in a subsequent paragraph. The difference ($\Delta L'$), saturation difference ($\Delta C'$), and hue difference ($\Delta H'$) were calculated to compute ΔE_{00} ^{18,19} (0 is the value immediately after cementation, and n is the value measured on each measurement day).

$$\begin{aligned}\Delta L' &= L_n - L_0 \\ \Delta C' &= [(a_n)^2 + (b_n)^2]^{1/2} - [(a_0)^2 + (b_0)^2]^{1/2} \\ \Delta H' &= [(\Delta a)^2 + (\Delta b)^2 - (\Delta C)^2]^{1/2} \\ \Delta E_{00} &= \left[\left(\frac{\Delta L'}{K_L S_L} \right)^2 + \left(\frac{\Delta C'}{K_C S_C} \right)^2 + \left(\frac{\Delta H'}{K_H S_H} \right)^2 \right. \\ &\quad \left. + R_T \left(\frac{\Delta C'}{K_C S_C} \right) \left(\frac{\Delta H'}{K_H S_H} \right) \right]^{1/2},\end{aligned}$$

where S_L , S_C , and S_H denote the heavy value coefficients; the Patrick factors for K_L , K_C , and K_H were set to 1.

The colorimetric conditions were two conditions for different colors of the underlying structure and four conditions for different luting materials ($n=5$).

3. Transparency analysis

Translucency is a visual assessment of a material's masking ability, or the extent to which the material can reveal the appearance of the underlying background. The TP is determined by calculating the color difference between a black and white background for specimens of the same thickness.

In this study, low foam vinyl chloride boards (AcrySunday, Tokyo, Japan) with black and white backgrounds were used. The following formula was used for calculating TP¹⁷.

$TP = [(L_B^* - L_W^*)^2 + (a_B^* - a_W^*)^2 + (b_B^* - b_W^*)^2]^{1/2}$, where subscripts B and W refer to color coordinates

over black and white backgrounds, respectively.

4. Statistical analysis

ΔE_{00} and TP values for each specimen at Day 0-30 were calculated as mean \pm standard deviation (SD). The normality and homoscedasticity of the ΔE_{00} and TP values at Day 30 were verified using the Shapiro-Wilk and Levene tests, and analyzed by one-way analysis of variance (ANOVA) only between luting materials in each specimen. ΔE_{00} between A2 and A4 underlying structure and ΔE_{00} because of cementation were compared with an acceptable threshold ($\Delta E_{00} > 1.8$). The data were analyzed at a significance level of 0.05 using the JMP Pro 17 software package (SAS Institute, Cary, NC, USA).

Results

1. Color analysis

The Shapiro-Wilk and Levene tests were used to assess the normality of ΔE_{00} at Day 30 in each specimen, indicating that the data were normally distributed and homoscedastic. One-way ANOVA indicated no significant difference in ΔE_{00} between the different luting materials ($p=0.32$). Figures 1 and 2 show changes over time in specimens for each condition, Table 2 shows each parameter from 0-30 days, and Table 3 shows ΔE_{00} . Figures 3 and 4 show graphs of E_{00} for 0-30 days.

The ΔE_{00} values for each condition at Day 30 were: 4.5 ± 0.5 for CNT, 4.7 ± 0.6 for GUF, 4.8 ± 0.2 for ESF, and 4.7 ± 0.6 for OMC for the A2 underlying structure; and 4.3 ± 1.1 for CNT, 4.5 ± 0.8 for GUF, 4.5 ± 0.3 for ESF, and 4.3 ± 0.6 for OMC for the A4 underlying structure. The ΔE_{00} values before and after cementation were: 4.7 ± 0.5 for CNT, 5.7 ± 1.2 for GUF, 4.5 ± 0.8 for ESF, and 4.5 ± 0.4 for OMC for the A2 underlying structure; and 6.4 ± 1.9 for CNT, 6.9 ± 1.4 for GUF, 6.2 ± 1.3 for ESF, and 6.8 ± 1.2 for OMC for the A4 underlying structure. All of these values were greater than the acceptable threshold ($\Delta E_{00} > 1.8$). Table 4 shows the ΔE_{00} values of the color difference between the underlying structure of A2 and A4: CNT was 5.5 ± 0.5 , GUF was 4.4 ± 0.8 , ESF was 5.3 ± 1.2 , and OCF was 5.2 ± 0.5 at Day 30; which are all > 1.8 in all conditions.

2. Transparency analysis

The Shapiro-Wilk and Levene tests were used to evaluate the normality of TP from Day 30 in each specimen, indicating that the data were normally distrib-

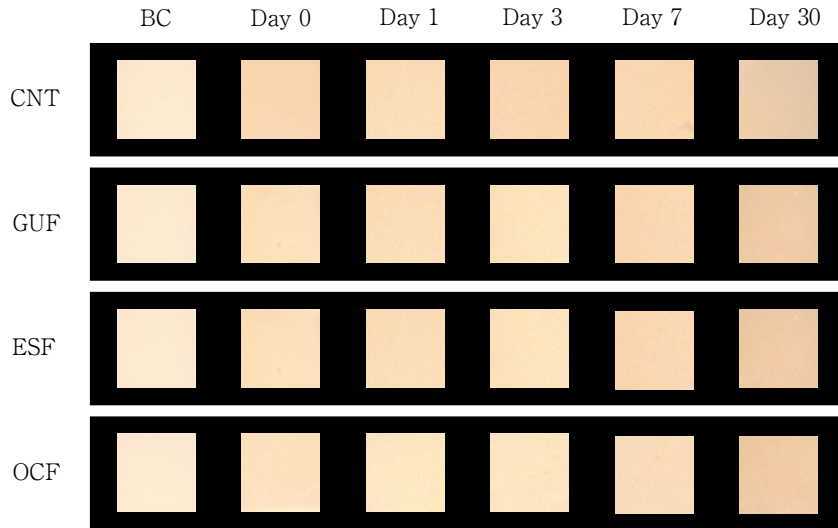


Fig. 1 Representative image obtained before cementation (BC), and 30-day color change of the specimen with the A2 underlying tooth
 CNT : GRACEFIL Low Flow, GUF : GRACEFIL Universal Low Flow,
 ESF : Clearfil Majesty ES Flow, OCF : Omnichroma Flow

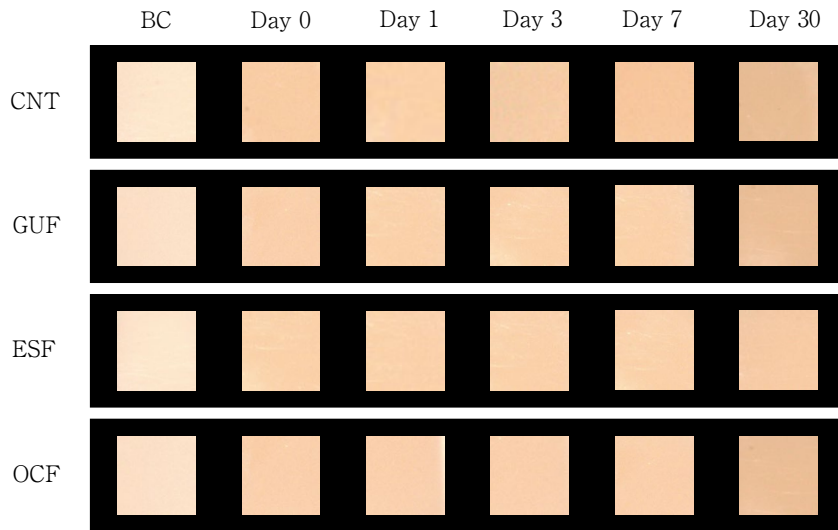


Fig. 2 Representative image obtained before cementation (BC), and 30-day color change of the specimen with the A4 underlying tooth
 CNT : GRACEFIL Low Flow, GUF : GRACEFIL Universal Low Flow,
 ESF : Clearfil Majesty ES Flow, OCF : Omnichroma Flow

uted and homoscedastic. A one-way ANOVA indicated no significant difference in the TP between the luting material for any of the days ($p=0.23$). Table 5 shows the TP for each condition. The TP values at Day 30 for each condition were 8.7 ± 2.9 for CNT, 12.4 ± 2.8 for GUF, 11.0 ± 0.8 for ESF, and 10.4 ± 1.0 for OCF for the A2 underlying structure; and 10.6 ± 0.8 for CNT, 9.5 ± 2.5 for GUF, 8.1 ± 0.6 for ESF, and 10.4 ± 2.6 for GUF for the A4 underlying structure.

Discussion

Clinically, PLV restorations are affected by the color of the resin cement and that of the underlying tooth^{20,21}. Therefore, it is important to investigate the influence of the color of the resin cement and underlying tooth used in the final PLV restoration.

The CIELAB color space system quantifies color by

Table 2 Results evaluated as mean of color parameters (L*, a*, b*) before cementation (BC) and over 30 days (n=5)

	CNT			GUF			ESF			OCF			
	L*	a*	b*	L*	a*	b*	L*	a*	b*	L*	a*	b*	
A2	BC	81.9	-1.8	11.3	82.5	-1.8	11.7	82.4	-1.8	11.4	82.2	-1.8	11.8
	Day 0	75.8	-0.8	13.4	75.7	-0.7	14.1	76.4	-0.9	13.0	76.6	-1.2	12.4
	Day 1	77.9	-0.9	14.3	77.1	-0.8	15.2	78.5	-0.9	14.5	78.7	-1.2	13.7
	Day 3	76.0	-0.7	14.5	74.1	-1.4	13.7	74.8	-1.8	12.3	75.2	-1.9	11.8
	Day 7	74.9	-1.0	13.2	73.8	-1.1	13.2	74.0	-1.0	13.3	74.9	-1.2	12.5
	Day 30	75.7	0.7	19.8	74.7	2.6	20.4	74.7	1.6	20.0	75.0	1.3	19.6
A4	BC	77.5	-1.1	11.5	78.5	-1.3	10.7	78.1	-1.2	11.7	78.1	-1.1	11.7
	Day 0	69.5	0.6	15.2	69.8	0.4	15.1	70.2	0.2	14.3	69.7	0.3	15.0
	Day 1	71.2	0.8	16.7	71.4	0.6	16.2	71.1	0.6	16.3	71.4	0.3	15.7
	Day 3	67.7	-0.3	14.6	68.2	-0.4	14.5	68.7	-0.1	14.8	68.8	-0.1	14.6
	Day 7	67.8	-0.3	14.9	68.1	0.1	14.1	68.0	0.0	13.9	68.4	0.0	14.2
	Day 30	68.3	2.5	21.0	68.9	2.1	22.1	69.2	2.4	22.2	69.5	2.6	21.5

Table 3 Results of color change evaluated as mean $\Delta E_{00} \pm SD$ of specimens at Day 30 of immersion in water and before and after cementation (n=5)

	Color parameters (ΔE_{00})							
	CNT		GUF		ESF		OCF	
	A2	A4	A2	A4	A2	A4	A2	A4
Day 30	4.5±0.5	4.3±1.1	4.7±0.6	4.5±0.8	4.8±0.2	4.5±0.3	4.7±0.6	4.3±0.6
Cementation (Day 0)	4.7±0.5	6.4±1.9	5.7±1.2	6.9±1.4	4.5±0.8	6.2±1.3	4.5±0.4	6.8±1.2

One-way ANOVA indicates no significant (p=0.32) difference in ΔE_{00} between the various luting materials (Line).

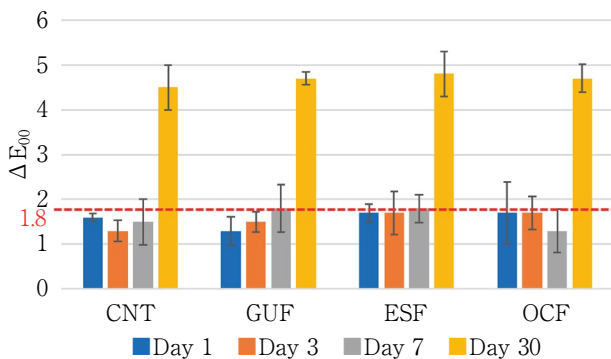


Fig. 3 Mean and standard deviation values for ΔE_{00} at Day 1, 3, 7, and 30 in the A2 underlying tooth

Color evaluation after submersion in water for 30 days with various luting materials (CNT, GUF, ESF, OCF) (n=5). The red dotted line indicates the acceptability threshold ($\Delta E_{00} > 1.8$).

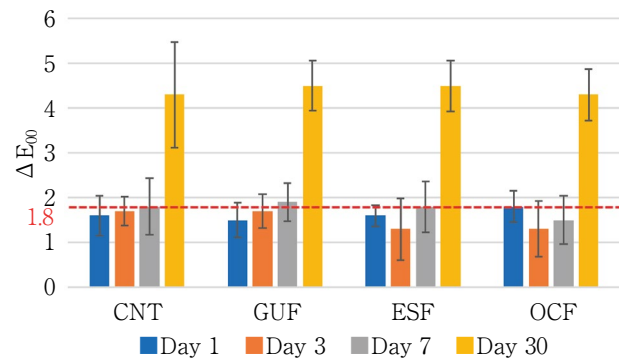


Fig. 4 Mean and standard deviation values for ΔE_{00} at Day 1, 3, 7, and 30 in the A4 underlying tooth

Color evaluation after submersion in water for 30 days with various luting materials (CNT, GUF, ESF, OCF) (n=5). The red dotted line indicates the acceptability threshold ($\Delta E_{00} > 1.8$).

using mathematical formulas to objectively determine color variation¹⁸). Recently, CIEDE2000 (ΔE_{00})—which uses saturation and hue to correct the color range perceived by humans—has been recommended for color analysis¹⁹.

The amount of change in each color was analyzed using ΔE_{00} . However, ΔE_{00} can only calculate the amount of color change and cannot analyze up to the color direction. Therefore, parameters L, a, and b (which indicate the direction of each color change) were analyzed. This study compared the effect of resin composites (termed single-shade, which can reproduce many shades of color) on the color of PLV restorations when cemented to an underlying structure of two different shades. In this study, ANOVA indicated that there was no statistically significant difference in ΔE_{00} from Day 30 by resin composite type, $p=0.32$. There was also no significant difference in the TP values between cements for any of the days and underlying structure conditions. In areas where the PLV thickness is thin, the transparency is high and the saturation might decrease when a luting material with low saturation is used²²). The resin composites used in this study

were single-shade, with the exception of CNT. OCF uses structural color to match the color of the tooth²³). The structural color of OCF is based on the results of photochemical processes of diffraction, interference, and scattering^{23,24}). Therefore, they are not supposed to fade, in contrast to resin composites that use pigments as color²⁴). However, ESF and GUF—unlike OCF—match the color with the surrounding dentin by adjusting light diffusion and light transmission^{25,26}). However, in the present study, no significant difference in ΔE_{00} was found between the luting materials, including CNT in the A2 shade. Differences in commercially available luting materials do not affect the color of PLV restorations²⁷). In this study, a single-shade resin composite was used as the luting material, and the results were similar. In this study, the color decreased after PLV cementation and a ΔE_{00} well above 1.8 was observed; in PLV restorations, the color difference decreases before and after cementation as the ceramic thickness increases²¹). In this study, all PLV specimen thicknesses were adjusted to 1.0 mm to standardize the conditions. Clinically, PLV thicknesses range from 0.5–1.0 mm, and although the results of this study might differ for the minimum thickness, the color change because of cementation was consistent with previous reports³). The effect of the difference in the color of the underlying structure, A2 and A4, on the overall color was investigated; the ΔE_{00} value between the underlying structure exceeded the acceptable threshold in all conditions and was visually recognizable. This suggests that the difference in the color of the underlying structure, A2 and A4, affected the color of the PLV restorations. As the ceramic thickness decreases in PLV restorations, the masking ability decreases and the color of the underly-

Table 4 Results of color change assessed by mean $\Delta E_{00} \pm SD$ between underlying teeth of different color over 30 days (n=5)

	Color parameters (ΔE_{00})			
	CNT	GUF	ESF	OCF
Day 0	5.3±0.8	4.9±0.8	5.0±1.4	5.7±0.8
Day 1	5.5±1.0	5.2±0.7	5.6±1.7	5.6±0.7
Day 3	6.3±1.3	4.6±1.1	5.8±1.7	5.8±0.7
Day 7	4.5±0.5	4.7±1.1	4.8±0.2	4.7±0.6
Day 30	5.5±0.5	4.4±0.8	5.3±1.2	5.2±0.5

Table 5 Results evaluated by mean TP±SD over 30 days (n=5)

	Translucency parameter (TP)							
	CNT		GUF		ESF		OCF	
	A2	A4	A2	A4	A2	A4	A2	A4
Day 0	6.2±1.0	6.0±1.9	6.8±2.0	6.4±2.9	7.0±0.3	5.4±2.6	6.2±2.0	5.2±1.9
Day 1	6.0±0.7	6.5±1.7	7.5±1.3	7.1±3.1	5.9±0.7	5.4±2.1	5.9±0.5	5.4±1.3
Day 3	6.8±2.1	8.4±2.7	7.8±2.4	8.7±2.8	8.8±1.0	6.3±3.4	8.2±2.7	6.5±1.4
Day 7	8.6±0.6	7.0±0.8	10.0±1.7	7.1±1.2	9.0±1.2	6.5±3.2	9.4±0.8	8.6±1.2
Day 30	8.7±2.9	10.6±0.8	12.4±2.8	9.5±2.5	11.0±0.8	8.1±0.6	10.4±1.0	10.4±2.6

One-way ANOVA indicates no significant ($p=0.23$) difference in TP between the various luting materials (Line).

ing structure as well as the color of the cement are evident²⁸⁾. In the present study, the color of the underlying structure affected the final color when the PLV was as thick as 1 mm.

No significant differences were found between luting materials in terms of the TP values; a higher TP value corresponded to a lower masking effect and opacity²⁹⁾. The color of PLV restorations might be affected by slight changes in the opacity and translucency³⁰⁾. The degree of translucency is directly related to the reflection of light^{30,31)}, and if the transparency decreases and the surface reflects more light, the color of the PLV tends to be whiter^{7,30)}. Although compositional differences affect the transparency of resin composites^{30,32)}, using luting materials with different shade-matching mechanisms does not affect TP values in PLV restorations within the limitations of this study.

In this study, the cement space was set at a thickness of 50 μm versus a 2-mm underlying structure and 1-mm PLV. The lack of difference in ΔE_{00} between the different luting materials might have been because of the narrow cement space relative to the overall thickness of the specimens, which might have had little effect on the color. However, the ΔE_{00} value at Day 30 under all conditions exceeded the acceptable threshold, indicating a change in color. Tertiary amines are responsible for the discoloration of dual-cure resin cements over time^{10,11)}, but in the present study a light-cured resin composite was used as the resin cement. In addition, a light-cured resin composite was used as a standardized underlying structure instead of human teeth to examine the effect of color. Therefore, there is a possibility that the underlying structure itself was discolored by water. The effect of discoloration of the underlying structure on the overall color tone cannot be denied, which is a limitation of the present study. Different base resins of resin composites have different quantities of unreacted monomers and water absorbency, and thus the effect of immersion in water on the color has been reported, especially a^* and b^* ³²⁾. The present study also indicated that the values of a^* and b^* changed significantly over time. Therefore, it is possible that the color change indicates a change in photo-polymerization resin composite although not as much as in the chemical polymerization resin composite.

Conclusion

In PLV restorations with LDS, differences in the single-shade resin composite used for cementation did not affect the final color and transparency. In contrast, the color of the underlying structure influenced the final color of the PLV restoration.

Conflict of Interest

The authors declare no conflicts of interest associated with this manuscript.

References

- 1) Shetty A, Kaiwar A, Shubhashini N, Ashwini P, Naveen Dn, Adarsha Ms, Shetty M, Meena N. Survival rates of porcelain laminate restoration based on different incisal preparation designs: An analysis. *J Conserv Dent* 2011; 14: 10-15.
- 2) Sasse M, Krummel A, Klosa K, Kern M. Influence of restoration thickness and dental bonding surface on the fracture resistance of full-coverage occlusal veneers made from lithium disilicate ceramic. *Dent Mater* 2015; 31: 907-915.
- 3) Turgut S, Bagis B. Colour stability of laminate veneers: An in vitro study. *J Dent* 2011; 39 (Suppl 3): e57-e64.
- 4) Magne P, Kwon KR, Besler C, Hodges JS, Douglas WH. Crack propensity of porcelain laminate veneers—A simulated operator evaluation. *J Prosthet Dent* 1999; 81: 327-334.
- 5) Heffernan MJ, Aquilino SA, Diaz Arnold AM, Haselton DR, Stanford CM, Vargas MA. Relative translucency of six all-ceramic systems. Part II. Core and veneer materials. *J Prosthet Dent* 2002; 88: 10-15.
- 6) Calamia JR, Calamia CS. Porcelain laminate veneers: Reasons for 25 years of success. *Dent Clin North Am* 2007; 51: 399-417.
- 7) Kurklu D, Azer SS, Yilmaz B, Johnston WM. Porcelain thickness and cement shade effects on the colour and translucency of porcelain veneering materials. *J Dent* 2013; 41: 1043-1050.
- 8) Azer SS, Rosenstiel SF, Seghi RR, Johnston WM. Effect of substrate shades on the color of ceramic laminate veneers. *J Prosthet Dent* 2011; 106: 179-183.
- 9) Rosenstiel SF, Land MF, Crispin BJ. Dental luting agents: A review of the current literature. *J Prosthet Dent* 1998; 80: 280-301.
- 10) Koishi Y, Tanoue N, Atsuta M, Matsumura H. Influence of visible-light exposure on colour stability of current

- dual-curable luting composites. *J Oral Rehabil* 2002; 29: 387-393.
- 11) Hekimoglu C, Anil N, Etikan I. Effect of accelerated aging on the color stability of cemented laminate veneers. *Int J Prosthodont* 2000; 13: 29-33.
 - 12) Nathanson D, Banasr F. Color stability of resin cements—An in vitro study. *Pract Proced Aesthet Dent* 2002; 14: 449-455.
 - 13) Suh YR, Ahn JS, Ju SW, Kim KM. Influences of filler content and size on the color adjustment potential of nonlayered resin composites. *Dent Mater J* 2017; 36: 35-40.
 - 14) Paravina RD, Ghinea R, Herrera LJ, Bona AD, Igiel C, Linninger M, Sakai M, Takahashi H, Tashkandi E, Mar Perez MD. Color difference thresholds in dentistry. *J Esthet Restor Dent* 2015; 27 (Suppl 1): S1-S9.
 - 15) Kelly JR, Benetti P. Ceramic materials in dentistry: Historical evolution and current practice. *Aust Dent J* 2011; 56: 84-96.
 - 16) Yu B, Ahn J-S, Lee YK. Measurement of translucency of tooth enamel and dentin. *Acta Odontol Scand* 2009; 67: 57-64.
 - 17) Johnston WM, Ma T, Kienle BH. Translucency parameter of colorants for maxillofacial prostheses. *Int J Prosthodont* 1995; 8: 79-86.
 - 18) CIE (Commission Internationale de l'Eclairage). Colorimetry technical report, 2nd ed. CIE Pub. No 15. Bureau Central da La CIE: Vienna, Austria; 1986.
 - 19) CIE (Commission Internationale de l'Eclairage). Colorimetry technical report, 3rd ed. CIE Pub. No 15. Bureau Central da La CIE: Vienna, Austria; 2004.
 - 20) Pires LA, Novais PM, Araújo VD, Pegoraro LF. Effects of the type and thickness of ceramic, substrate, and cement on the optical color of a lithium disilicate ceramic. *J Prosthet Dent* 2017; 117: 144-149.
 - 21) Turgut S, Bagis B. Effect of resin cement and ceramic thickness on final color of laminate veneers: An in vitro study. *J Prosthet Dent* 2013; 109: 179-186.
 - 22) Silami FD, Tonani R, Alandia-Román CC, Pires-de-Souza Fde C. Influence of different types of resin luting agents on color stability of ceramic laminate veneers subjected to accelerated artificial aging. *Braz Dent J* 2016; 27: 95-100.
 - 23) Kobayashi S, Nakajima M, Furusawa K, Tichy A, Hosaka K, Tagami J. Color adjustment potential of single-shade resin composite to various-shade human teeth: Effect of structural color phenomenon. *Dent Mater J* 2021; 40: 1033-1040.
 - 24) Dumanli AG, Savin T. Recent advances in the biomimicry of structural colours. *Chem Soc Rev* 2016; 45: 6698-6724.
 - 25) Forabosco E, Consolo U, Mazzitelli C, Kaleci S, Generali L, Checchi V. Effect of bleaching on the color match of single-shade resin composites. *J Oral Sci* 2023; 65: 232-236.
 - 26) Karadas M. The effect of different beverages on the color and translucency of flowable composites. *Scanning* 2016; 38: 701-709.
 - 27) Kandil BSM, Hamdy AM, Aboelfadl AK, El-Anwar MI. Effect of ceramic translucency and luting cement shade on the color masking ability of laminate veneers. *Dent Res J* 2019; 16: 193-199.
 - 28) Blumentritt FB, Cancian G, Saporiti JM, de Holanda TA, Barbon FJ, Boscato N. Influence of feldspar ceramic thickness on the properties of resin cements and restorative set. *Eur J Oral Sci* 2021; 129: e12765.
 - 29) Johnston WM, Reisbick MH. Color and translucency changes during and after curing of esthetic restorative materials. *Dent Mater* 1997; 13: 89-97.
 - 30) Fujita K, Nishiyama N, Nemoto K, Okada T, Ikemi T. Effect of base monomer's refractive index on curing depth and polymerization conversion of photo-cured resin composites. *Dent Mater J* 2005; 24: 403-408.
 - 31) Duarte Jr S, Perdigão J, Lopes M. Composite resin restorations—Natural aesthetic and dynamics of light. *Pract Proced Aesthet Dent* 2003; 15: 657-664.
 - 32) Camargo FM, Della Bona Á, Moraes RR, De Souza CC, Schneider LF. Influence of viscosity and amine content on C=C conversion and color stability of experimental composites. *Dent Mater* 2015; 31: e109-e115.

Comparison of Root Canal Preparation Ability of Three Gold Wire-based NiTi Rotary File Systems in Simulated Curved Root Canals

Miki SEKIYA, Shuntaro NAKAYAMA*, Fumiyasu MURAYAMA, Kentaro FURUTA,
Yoshiyuki INUYAMA, Munehiro MAEDA, Kazuo KITAMURA* and Masaru IGARASHI

Department of Endodontics, The Nippon Dental University School of Life Dentistry at Tokyo

*Division of General Dentistry 1 (Endodontics), The Nippon Dental University Hospital

Abstract

Purpose: The purpose of this study was to evaluate the effects of the ProTaper Ultimate (PTU), which has a new design based on integrated technology, on preparation ability in simulated curved root canals compared with previous gold wire-based nickel titanium rotary file systems.

Methods: The surfaces of J-shaped simulated root canals in clear resin blocks were scanned as image files. The working length was defined as the root canal length minus 1 mm. The negotiation of all root canals was confirmed with a stainless steel #10 K-file. The blocks were divided into three groups of 10 each (PTU, ProTaper Gold [PTG], and WaveOne Gold [WOG]) and randomly prepared through size #25. The inner and outer displacements of the root canal wall were measured from superimposed images before and after preparation. In addition, the working times of each group and process were measured. The Kruskal-Wallis test followed by the Steel-Dwass test were used for all comparisons and statistical analyses.

Results: Regarding root canal wall displacement, no significant difference was observed in all groups at 1 mm and 2 mm from the root canal apex, except for 1 mm on the inner side of the curvature ($p < 0.05$). At 3 mm and 4 mm from the root canal apex, the root canal wall displacement of PTU was significantly smaller than those of PTG and WOG in the inner side of the curvature, while it was significantly larger in the outer side of the curvature ($p < 0.05$). PTU prepared the inner and outer sides most evenly among the three groups. The total working time and the root canal wall shaping time in each group were longer in the order of $WOG < PTU < PTG$. Both times were significantly different among the three groups ($p < 0.01$). In addition, PTU had the smallest variance and preparation took almost the same amount of time even when the experiment was performed multiple times. On the other hand, there was no significant difference between groups in the time required for glide path preparation.

Conclusion: The curved root canals at the measurement points were prepared most evenly by PTU in this study. Also, the total working time and the root canal wall shaping time were significantly reduced with PTU compared to PTG, and both times of PTU were close to the measurement time of WOG.

Key words: ProTaper Ultimate, ProTaper Gold, WaveOne Gold, nickel titanium instruments

Introduction

The instruments and procedures used for root canal treatment have changed substantially over time. In particular, the development and improvement of nickel titanium (NiTi) rotary files has been remarkable¹⁾. It is now well-known that NiTi rotary files are more flexible than conventional stainless steel files and have a higher ability to follow curved root canals. The current NiTi rotary files have enabled root canal preparation that maintains the anatomical shape with a minimal amount of cutting, resulting in the establishment of a simple file system.

NiTi rotary files are becoming the gold standard of root canal preparation instruments, replacing hand files²⁻⁵⁾. One of the factors that has greatly improved the characteristics of NiTi rotary files in particular is the strengthening of NiTi alloy by various heat treatment methods, which have enhanced the material properties of many types of NiTi alloys⁶⁾. Heat treatment technology has greatly increased the resistance to repeated fatigue, improved the flexibility of the file, and made it possible to design the file shape to optimize shaping performance. NiTi rotary files continue to be developed with this technology^{3-5,7)}.

Since its introduction in 2001, the ProTaper system (Dentsply Sirona, Ballaigues, Switzerland) has undergone constant evolution and improvements owing to advances in technology and accompanying unique file designs⁸⁾. In particular, ProTaper NEXT using M-wire and ProTaper Gold (PTG) using gold wire appeared after the heat treatment of NiTi alloys began, followed by the latest file system, ProTaper Ultimate (PTU), which inherited the characteristics of the previous ProTaper file system⁹⁾. Each PTU file was subjected to individual heat treatment and design to maximize the performance of each of its roles, and all heat treatment technology and file designs were integrated within the system.

The method for evaluating the displacement of the root canal wall when preparing a curved root canal is often used as a means to clarify the cutting efficiency of NiTi rotary files. However, to the best of our knowledge, no studies have compared PTU and previous gold wire-based NiTi rotary file systems in terms of the amount of root canal wall displacement and working

time during root canal preparation of curved root canals.

Given this background, the purpose of the present study was to evaluate the effects of PTU on preparation ability in simulated curved root canals compared with previous gold wire-based NiTi rotary file systems by comparing the displacement of the inner and outer curvatures of the root canal wall and the working time of the file used for each group and process.

Materials and Methods

1. Preparation materials

Thirty J-shaped simulated root canals in clear resin blocks (root canal length: 16 mm, 0.02 taper, Endo Training Bloc J-Shape ϕ 15, Dentsply Sirona) were used in this study. The working length was unified to 15 mm, which was 1 mm inside the apical foramen.

The preparation groups were defined as PTU, PTG, and WaveOne Gold (WOG) (Dentsply Sirona), which are the three types of file systems based mainly on gold wire.

2. Preparation of J-shaped simulated root canals in clear resin blocks

All blocks were divided into three groups of 10 each, and negotiation was confirmed with a #10 K stainless steel file (SSK) (READYSTEEL FlexoFile; Dentsply Sirona). Next, the model blocks were prepared through size #25 according to the operation method specified by the manufacturer in each system-specific mode programmed in the X-Smart IQ motor handpiece (Dentsply Sirona). All root canal preparations were performed by a single operator with 6 years of clinical experience in a state in which the root canal morphology of the block was not visible. In addition, the order of root canal preparation was randomly selected in each group. To achieve the same conditions as the effect of root canal irrigants on files in clinical practice, frequent root canal irrigation with 3% sodium hypochlorite solution (NaOCl) (amplitude, 2-3 mm) was commonly performed using a syringe (2.5 mL; Terumo, Tokyo, Japan) and irrigation needle (30 G; Dentsply Sirona) during root canal preparation. In addition, the files were cleaned of debris and the root canals recapitulated with a #10 SSK after each time.

PTU was used with all files (400 rpm and 4.0 Ncm torque). After securing straight-line access with an SX

(20/.03), glide path preparation was performed using the Slider (16/.02). In the presence of viscous chelating agents (15% EDTA; Glyde, Dentsply Sirona), the Slider instrument reached the apical side once with gentle up-and-down movements. Next, under 3% NaOCl infiltration, a Shaper (20/.04) shaping file was used in a gentle brushing motion until the working length was reached. After that, the finishing files were used up to the working length by moving up and down in the order of F1 (20/.07) and F2 (25/.08). The files inserted to the working length were not left for more than one second and immediately removed from the root canal to complete the preparation.

The number of PTG revolutions was unified at 300 rpm. SX and S1 were used with a torque value of 4.0 Ncm, ProGlider with 2.0 Ncm, S2 and F1 with 1.5 Ncm, and F2 with 3.0 Ncm. After straight-line access to the root canal orifice had been created with an SX (19/.04) in the presence of 15% EDTA, the glide path was prepared with ProGlider (16/.02). The S1 (18/.02) and S2 (20/.04) shaping files were prepared in order along the glide path under 3% NaOCl irrigation until the working length was reached. At that time, a brushing motion was performed on the root canal wall until light resistance was felt. The F1 (20/.07) and F2 (25/.08) finishing files were inserted deep into the root canal by vertical movement until reaching the working length. All files inserted to the working length were then immediately withdrawn from the root canal to complete the root canal preparation.

Regarding WOG, straight-line access was prepared using the PTG SX, and then a WOG Glider (15/.02) was used to prepare the glide path up to the working length with a gentle up-and-down reciprocating motion. Next, primary (25/.07) weak pecking motions were repeated two or three times to shape to the coronal 1/3. Using the same procedure, root canal preparation was performed to the crown side 2/3 and then to the working length. As soon as the working length was reached, the file was removed from the root canal to complete the root canal preparation.

3. Evaluation of simulated root canal preparations

Before the root canal preparations, the curved surface of each block was scanned as an image file using a flatbed color image scanner (1200 dpi, GT-X970; EPSON, Tokyo, Japan). The positional conditions were unified so

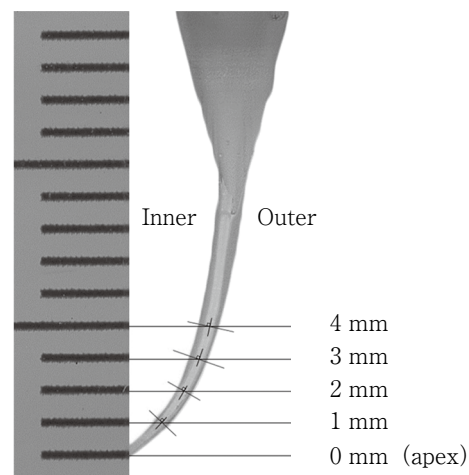


Fig. 1 Measurement method for root canal wall displacement

that the blocks could always be scanned at the same position. After root canal preparation, the blocks were scanned again and superimposed with the images scanned beforehand using Photoshop CS6 (Adobe, San Jose, CA, USA). The measurement points of the root canal wall displacement were set to 1 mm, 2 mm, 3 mm, and 4 mm from the root canal apex. The measurement method followed that of Yun et al.¹⁰⁾. A line perpendicular to the long axis of the root canal was drawn at each measurement point, and the amount of root canal wall displacement (the distance of the root canal wall before and after preparation) was measured in the inner and outer sides of the curvature (Fig. 1).

Measurement of the root canal preparation time was started after confirmation of the negotiation by the SSK and completion of straight-line access to the root canal orifice with the SX file in each file system. The total time needed to complete the preparation for each group was calculated by subtracting the time required for root canal irrigation, instrument exchange, cleaning of debris, and recapitulation from the measured time until the end of root canal preparation. Using the same method, the time required for glide path preparation and subsequent root canal shaping in each group was also calculated.

4. Statistical analysis

All values were expressed as mean \pm standard deviation. SPSS Statistics (version 28; IBM Japan, Tokyo, Japan) and Kyplot 6.0 (KyensLab, Tokyo, Japan) were used for the statistical analysis, with the significance level set at 5%.

Table 1 Root canal wall displacement at each measurement point in the inner and outer sides of the curvature in each group (mm) (mean±standard deviation)

The measurement points from apex	ProTaper Ultimate		ProTaper Gold		WaveOne Gold	
	Inner	Outer	Inner	Outer	Inner	Outer
4 mm	0.17±0.01	0.13±0.01**	0.23±0.02	0.12±0.02**	0.21±0.03	0.12±0.01**
3 mm	0.15±0.02	0.12±0.01**	0.19±0.02	0.10±0.01**	0.17±0.02	0.11±0.01**
2 mm	0.11±0.02	0.10±0.01**	0.12±0.02	0.10±0.01**	0.11±0.02	0.10±0.01**
1 mm	0.07±0.01	0.08±0.01**	0.09±0.01	0.08±0.01**	0.08±0.01	0.08±0.01*

Statistically significant differences were observed between the inner and outer sides of the curvature in each group (Wilcoxon signed-rank test, * $p < 0.05$, ** $p < 0.01$)

Normality was confirmed by the Shapiro-Wilk test, followed by one-way analysis of variance (ANOVA) if normality was observed, and the Kruskal-Wallis test if not. The post-hoc test after one-way ANOVA was performed by Tukey's test or the Games-Howell test depending on the results of Levene's test for equality of variances. In addition, the Steel-Dwass test was used for the post-hoc test after the Kruskal-Wallis test.

Results

In this study, no file fractures, perforations, apical blockages, or loss of working length were observed in any group.

1. Simulated root canal wall displacement

The root canal wall displacement at each measurement point on the inner and outer sides of the curvature in each group is shown in Table 1. At 1 mm and 2 mm from the root canal apex, the displacement of the inner and outer sides of the curvature were almost equal in each group. At 3 mm and 4 mm from the root canal apex, PTG and WOG were displaced to the inner side of the curvature. PTU had the most equal displacement of the inner and outer sides of the curvature at 2 mm, 3 mm, and 4 mm from the root canal apex.

The comparison of root canal wall displacement in each group is shown in Fig. 2. At 1 mm and 2 mm from the root canal apex, significant differences were observed between PTU and PTG and between PTG and WOG only on the 1 mm inner side of the curvature ($p < 0.01$). At 3 mm and 4 mm from the root canal apex, the root canal wall displacement of PTU was significantly smaller than PTG and WOG in the inner side of the curvature, while it was significantly larger in the outer side of the curvature ($p < 0.05$).

2. Measurement of simulated root canal preparation time

The measurement times in each group and for each process are shown in Fig. 3, and the times needed to complete each file system's procedure and each file are shown in Fig. 4.

The total time needed to complete preparation in each group was longer in the order of WOG (27.05 ± 4.87 s) < PTU (32.20 ± 1.66 s) < PTG (50.01 ± 5.24 s), and significant differences were observed between all groups ($p < 0.01$). On the other hand, the time required for glide path preparation was 6.55 ± 1.27 s, 6.55 ± 1.27 s, and 6.26 ± 1.39 s in PTU, PTG, and WOG, respectively, with no significant differences observed between any groups. The root canal shaping time of each group was longer in the order of WOG (20.79 ± 0.69 s) < PTU (25.99 ± 0.26 s) < PTG (43.46 ± 0.89 s), with significant differences observed between all groups ($p < 0.01$).

Discussion

Ideal root canal preparation involves minimizing the transposition of the root canal after preparation and providing a continuous taper from the root canal orifice to the apex while preserving the original root canal morphology¹¹⁻¹³. Especially in the case of curved root canals, it has been reported that the success rate of root canal treatment is 78.9% if the curvature can be followed, and 42.9% if it cannot¹⁴. Furthermore, in recent years, emphasis has been placed on minimizing the amount of root canal dentin removed, based on the concept of minimal intervention (MI)¹⁵⁻¹⁷.

In this study, we compared the amount of root canal wall displacement and working time during root canal preparation of simulated curved root canals using the

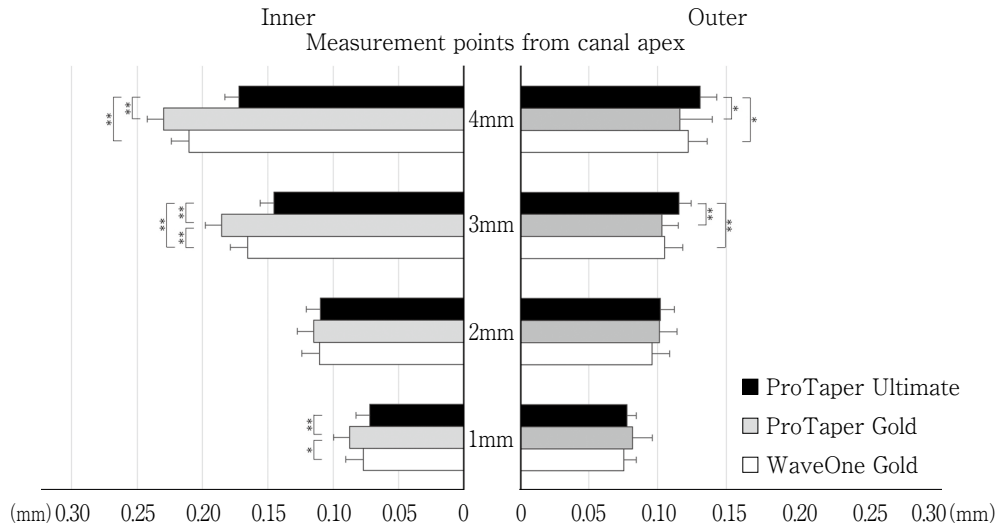


Fig. 2 Root canal wall displacement at each measurement point in the inner and outer sides of the curvature in each group
Kruskal-Wallis test followed by Steel-Dwass test, *p<0.05 ; **p<0.01.

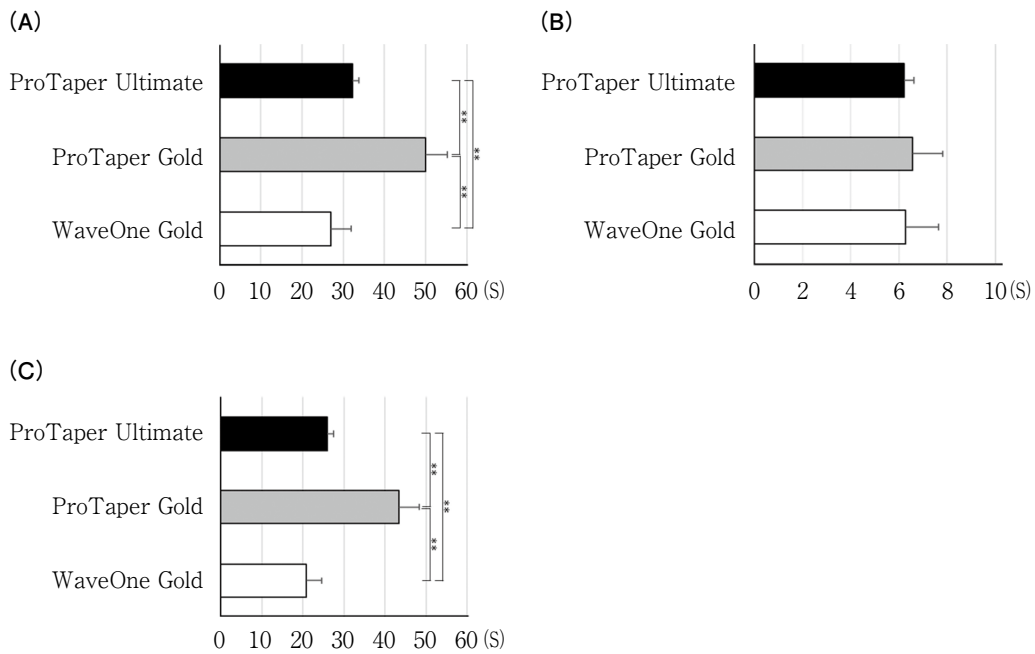


Fig. 3 Measurement time in each group and for each process
Kruskal-Wallis test followed by Steel-Dwass test, *p<0.05 ; **p<0.01
(A) Total time needed to complete preparation, (B) Glide path preparation time, (C) Root canal shaping time

ProTaper system and the WaveOne system, based on gold wire. The ProTaper system performs root canal preparation using the full-length method in which multiple files have different roles. In addition, multiple tapers are added to one file. As a result, a simpler system with fewer files than the conventional NiTi rotary file system has been realized⁸. The WaveOne system pre-

vents the file from over-engagement and releases excessive torque through a reciprocating motion based on Roane’s balanced force technique to avoid straightening of the root canal curvature¹⁸. Therefore, a single-file system was established and simple root canal preparation was realized in a short time.

Regarding root canal preparation in curved root

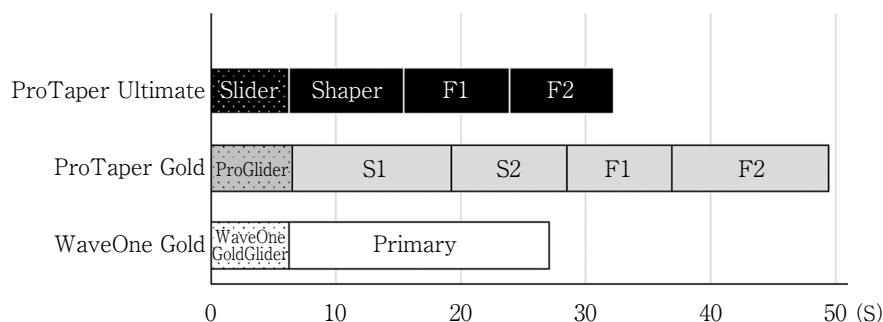


Fig. 4 Measurement time needed to complete each file system's procedure

canals, ideally the displacement of the root canal wall should be in the ratio of inner side to outer side=1 : 1 (inner side/outer side=1)¹¹. In this study, PTU had the most equal displacement of the inner and outer sides of the curvature at 2 mm, 3 mm, and 4 mm from the root canal apex, which was the closest to the ideal root canal preparation morphology. This result indicated that the central axis of PTU was close to the central axis of the root canal. Many studies have shown that more flexible instruments produce more centered root canal preparations^{19,20}. Therefore, PTU was considered to have higher flexibility and ability to follow the root canal up to the apex than other file systems due to its unique file diameter and cross-sectional design. However, at 1 mm and 2 mm on the apical side, a significant difference was observed between PTG and other systems only on the inner side of the curvature at 1 mm. This result was consistent with the report by Shi et al. who studied the centering ability of PTG and WOG²¹. In addition, this result was thought to be affected not only by the file cross-sectional design and the file taper, but also by the number of times the file reached the working length. PTG is a full-length method and multi-file system. In addition, in the present study, the PTG system had the largest number of files used in the root canal preparation protocol. Therefore, in PTG, it seems that the displacement occurred because of the file reaching the working length multiple times. In particular, the NiTi rotary file systems used in this study were mainly made of highly flexible gold wire. Thus, when inserted into a curved root canal, all files follow the inner curved wall without causing springback, which explains why there was a significant difference only on the inner side of the curvature in this study. However, the displacement of the inner and outer sides of the curvature were almost equal in each

group at 1 mm and 2 mm from the root canal apex. Therefore, it was suggested that all file systems had good followability near the root canal apex.

The total working time and root canal wall shaping time in each group were longer in the order of WOG < PTU < PTG. This result was consistent with that reported by Bürklein et al.²² and Bane et al.²³, who compared the time required for root canal preparation using multi- and single-file systems. Accordingly, it was shown that the time needed to complete each file system's procedure was affected by the number of files used to shape the root canal. In addition, PTU had the smallest variance, which indicates that the PTU system has little variation in technique and can be prepared in the same amount of time, even if it is used multiple times. Comparing the time needed to complete each file system's procedure, PTU and PTG, which are multi-file systems, had a shorter operating time per file than WOG, the single-file system. Therefore, it was thought that PTU and PTG can be reused after sterilization because fatigue is less likely to accumulate in files compared with WOG, which is for single use.

On the other hand, no significant difference in the time required for glide path preparation was seen between any groups. As one of the precautions when using NiTi rotary file systems, almost all manufacturers currently recommend glide path preparation, which is an essential step for the safe and effective use of NiTi rotary systems²⁴⁻²⁷. Cassim et al.²⁸ reported that glide path preparation reduced the risk of torsional stress and instrument fracture and maintained the original root canal anatomy with less modification of the root canal curvature and fewer root canal aberrations. In addition, Keskin et al.²⁹ reported that glide path preparation improved the shaping ability of NiTi files. It has been stated that glide path preparation using hand files

should be used from #10 to #15^{24,25)} or from #10 to #20³⁰⁻³²⁾. However, glide path preparation using hand files takes a long time and involves the risk of transportation from the root canal morphology at the apex. The NiTi rotary files for glide path preparation can establish the glide path in a shorter time than hand files³³⁾. Regarding glide path preparation files, Slider and Pro-Glider used in a continuous rotational motion are made of M-wire, and the WOG Glider used in a reciprocating motion is made of gold wire. Gold wire has lower cutting force than M-wire due to the higher proportion of martensitic phase. However, it is thought that the reciprocating motion freed the narrow root canal from the torsional fractures that tend to occur with small files, and enabled efficient glide path preparation to the root canal apex. Therefore, in addition to improving machinability and root canal followability through heat treatment technology, by combining a file rotation method according to the properties of the NiTi alloy, it is thought that glide path preparation in a short time is possible using any file system.

These results suggest that root canal preparation by PTU was closest to the ideal curved root canal preparation that avoids excessive enlargement based on the MI concept and provides excellent root canal followability, with working time closer to WOG than PTG. In addition, we considered that all file systems based on gold wire had good followability near the root canal apex and reduced the risk of inappropriate root canal preparation.

Conclusion

As a result of this study, the following conclusions were reached:

1. The curved root canals at the measurement points were prepared most evenly by PTU.
2. All gold wire-based NiTi rotary file systems used in this study had good followability near the root canal apex.
3. The total working time and the root canal wall shaping time were significantly reduced with PTU compared to the previous PTG system, and both times of PTU were close to the measurement time of the WOG single-file system.
4. All NiTi rotary files used for glide path preparation in this study achieved smooth performance in a short time.

Conflict of Interest

The authors declare no conflict of interest related to this paper.

References

- 1) Thompson SA. An overview of nickel-titanium alloys used in dentistry. *Int Endod J* 2000; 33: 297-310.
- 2) Civjan S, Hugeti EF, DeSimoni LB. Potential applications of certain nickel-titanium (Nitinols) alloys. *J Dent Res* 1975; 54: 89-96.
- 3) Hülsmann M, Peters OA, Dummer PMH. Mechanical preparation of root canals: shaping goals, techniques and means. *Endod Topics* 2005; 10: 30-76.
- 4) Haapasalo M, Shen Y. Evolution of nickel-titanium instruments from past to future. *Endod Topics* 2013; 29: 3-17.
- 5) Ruddle CJ, Machtou P, West JD. The shaping movement: fifth-generation technology. *Dent Today* 2013; 32: 96-99.
- 6) Liang Y, Yue L. Evolution and development: engine-driven endodontic rotary nickel-titanium instruments. *Int J Oral Sci* 2022; 14: 12.
- 7) Gavini G, Santos MD, Caldeira CL, Machado MEL, Freire LG, Iglecias EF, Peters OA, Candeiro GTM. Nickel-titanium instruments in endodontics: a concise review of the state of the art. *Braz Oral Res* 2018; 32: e67.
- 8) Gagliardi J, Versiani MA, Sousa-Neto MD, Plazas-Garzon A, Basrani B. Evaluation of the shaping characteristics of ProTaper Gold, ProTaper NEXT, and ProTaper Universal in curved canals. *J Endod* 2015; 41: 1718-1724.
- 9) Advanced Endodontics. PROTAPER ULTIMATE FILE SYSTEM. <https://www.endoruddle.com/PTUltimate> (cited 2023.8.13)
- 10) Yun H, Kim SK. A comparison of the shaping abilities of 4 nickel-titanium rotary instruments in simulated root canals. *Oral Surg Oral Med Oral Pathol Oral Radiol Endod* 2003; 95: 228-233.
- 11) Schilder H. Cleaning and shaping the root canal. *Dent Clin North Am* 1974; 18: 269-296.
- 12) Ruddle CJ. Endodontic canal preparation: breakthrough cleaning and shaping strategies *Dent Today* 1994; 13: 44-49.
- 13) Yu DC, Schilder H. Cleaning and shaping the apical third of a root canal system. *Gen Dent* 2001; 49: 266-270.
- 14) Pettiette MT, Delano EO, Trope M. Evaluation of success rate of endodontic treatment performed by students with stainless-steel K-files and nickel-titanium hand files. *J Endod* 2001; 27: 124-127.
- 15) Gluskin AH, Peters CI, Peters OA. Minimally invasive endodontics: challenging prevailing paradigms. *Br Dent J* 2014; 216: 347-353.

- 16) Ericson D. What is minimally invasive dentistry? *Oral Health Prev Dent* 2004; 2: 287-292.
- 17) Gutmann JL. Minimally invasive dentistry (Endodontics). *J Conserv Dent* 2013; 16: 282-283.
- 18) Roane JB, Sabala CL, Duncanson MG. The “balanced force” concept for instrumentation of curved canals. *J Endod* 1985; 11: 203-211.
- 19) Al-Omari MA, Dummer PM, Newcombe RG. Comparison of six files to prepare simulated root canals. Part 1. *Int Endod J* 1992; 25: 57-66.
- 20) Silva EJ, Tameirão MD, Belladonna FG, Neves AA, Souza EM, De-Deus G. Quantitative transportation assessment in simulated curved canals prepared with an adaptive movement system. *J Endod* 2015; 41: 1125-1129.
- 21) Shi L, Zhou J, Wan J, Yang Y. Shaping ability of ProTaper Gold and WaveOne Gold nickel-titanium rotary instruments in simulated S-shaped root canals. *J Dent Sci* 2022; 17: 430-437.
- 22) Bürklein S, Schäfer E. Apically extruded debris with reciprocating single-file and full-sequence rotary instrumentation systems. *J Endod* 2012; 38: 850-852.
- 23) Bane K, Faye B, Sarr M, Niang SO, Ndiaye D, Machtou P. Root canal shaping by single-file systems and rotary instruments: a laboratory study. *Iran Endod J.* 2015; 10: 135-139.
- 24) Patiño PV, Biedma BM, Liébana CR, Cantatore G, Bahillo JG. The influence of a manual glide path on the separation rate of NiTi rotary instruments. *J Endod* 2005; 31: 114-116.
- 25) Dhingra A, Neetika. Glide path in endodontics. *Endodontology* 2014; 26: 217-222.
- 26) Kwak SW, Ha JH, Cheung GS, Kim HC, Kim SK. Effect of the glide path establishment on the torque generation to the files during instrumentation: an in vitro measurement. *J Endod* 2018; 44: 496-500.
- 27) Ha JH, Park SS. Influence of glide path on the screw-in effect and torque of nickel-titanium rotary files in simulated resin root canals. *Restor Dent Endod* 2012; 37: 215-219.
- 28) Cassim I, Van der Vyver PJ. The importance of glide path preparation in endodontics: a consideration of instruments and literature. *South African Dent J* 2013; 68: 324-327.
- 29) Keskin C, Sarıylmaz E, Demiral M. Shaping ability of Reciproc Blue reciprocating instruments with or without glide path in simulated S-shaped root canals. *J Dent Res Dent Clin Dent Prospects* 2018; 12: 63-67.
- 30) D’Amario M, Baldi M, Petricca R, De Angelis F, El Abed R, D’Arcangelo C. Evaluation of a new nickel-titanium system to create the glide path in root canal preparation of curved canals. *J Endod* 2013; 39: 1581-1584.
- 31) Ajuz NC, Armada L, Gonçalves LS, Debelian G, Siqueira JF Jr. Glide path preparation in S-shaped canals with rotary pathfinding nickel-titanium instruments. *J Endod* 2013; 39: 534-537.
- 32) Lim YJ, Park SJ, Kim HC, Min KS. Comparison of the centering ability of Wave-one and Reciproc nickel-titanium instrument in stimulated curved canals. *Restor Dent Endod* 2013; 38: 21-25.
- 33) Berutti E, Cantatore G, Castellucci A, Chiandussi G, Pera F, Migliaretti G, Pasqualini D. Use of nickel-titanium rotary PathFile to create the glide path: comparison with manual preflaring in simulate root canals. *J Endod* 2009; 35: 408-412.

2-deoxy-D-glucose Inhibits Cell Activity by Inhibiting Intracellular Glucose Metabolism in Human Gingival Fibroblasts

Yoichiro TAGUCHI, Hirohito KATO, Runbo LI, Tsurayuki TAKAHASHI, Daisuke KIMURA,
Kosho KASHITANI, Niina MASU, Hitoshi AZUMA, Chizuko OGATA and Makoto UMEDA

Department of Periodontology, Osaka Dental University

Abstract

Purpose: Cellular energy metabolism by glucose plays an essential role in tissue wound healing. The use of 2-deoxy-D-glucose (2-DG) to suppress energy metabolism through the glycolytic system is similar to a low glucose environment. Therefore, the purpose of this study was to investigate the effect of 2-DG-induced reduction in glucose metabolism on cell viability.

Methods: We examined the proliferation, migration, cytotoxicity, H₂O₂ production, glucose transporter type 1 expression, lactic acid production, and ATP synthesis after the intracellular uptake of three different concentrations of 2-DG into HGnFs.

Results: 2-DG suppressed intracellular glucose metabolism, which led to a reduction in the cellular activity of human gingival fibroblasts (HGnFs). However, there were no changes in cytotoxicity or H₂O₂ production, and the effects on glucose metabolism were different from those in a low glucose environment.

Conclusion: This study showed that the suppression of intracellular glucose metabolism in HGnFs by 2-DG may delay wound healing in periodontal tissues.

Key words: glucose, 2-DG, gingival fibroblasts

Introduction

Human gingival fibroblasts (HGnFs) are the most abundant cellular component of periodontal tissue and play an important role in the wound healing of gingival and oral mucosal tissues¹. During wound healing, HGnFs produce various growth factors and are actively involved in the formation of granulation tissues, especially the synthesis of collagen. Collagen is a complex extracellular matrix that is important for the regeneration of functional periodontal tissue². Wound healing depends on collagen synthesis, which is directly dependent on the proliferative and migratory capacity of HGnFs³. Thus, the proliferation and migration of HGnFs are considered the most important factors of wound healing.

HGnFs utilize the glycolytic pathway to promote their proliferation and migration⁴. The role of glucose in cell proliferation is highly dependent on glucose metabolism, which provides a source of energy as well as metabolites for the biosynthesis of nucleic acids and membrane lipids⁵. However, when the existing blood vascular system is disrupted by surgery or other treatments or trauma, cells are exposed to a stressful micro-environment characterized by low glucose concentrations. Furthermore, the blood supply in periodontal tissues after trauma or periodontal surgery is significantly lower than that in healthy periodontal tissues, and periodontal tissues are exposed to a low glucose concentration environment. Previous studies have been conducted under various glucose conditions to mimic the high glucose concentration model of the diabetic state.

We have also conducted several previous studies that mimicked various clinical environments by increasing or decreasing glucose concentrations⁶. However, few studies have investigated cell behavior under low glucose concentrations that mimic the environment of an inadequate nutrient supply. A low glucose environment can be obtained using 2-deoxy-D-glucose (2-DG) or by intentional glucose reduction. 2-DG, a glucose molecule in which the 2-hydroxyl group is replaced by a hydrogen atom, is not metabolized by the glycolytic system. How 2-DG inhibits cell growth is not entirely clear, but it is taken up by cellular glucose transporters, similar to glucose⁷, but it is not metabolized by the glycolytic system, analogous to an environment where energy

cannot be generated because of the lack of glucose⁸).

In our previous study, we reported the impact of low glucose levels on the proliferation and migration of HGnFs, primarily attributable to their inability to generate energy⁹. Building upon this premise, our current investigation delves into the behavior of HGnFs, encompassing their proliferation and migration, through the lens of wound healing. This is achieved by employing 2-DG to artificially create a low glucose environment, mirroring situations where HGnFs face energy production challenges.

The results of this study unveil how 2-DG influences cellular energy metabolism, effectively mirroring conditions characterized by low glucose concentrations. Insights drawn from this study have important implications for both future research and clinical applications. By shedding light on how cells respond to low glucose environments, this research paves the way for a deeper understanding of cellular dynamics in settings marked by nutrient insufficiency. These insights could be leveraged in future studies to explore novel therapeutic approaches or interventions targeting cells struggling with energy deficits, thereby enhancing their prospects for clinical application in conditions related to glucose metabolism irregularities.

Materials and Methods

1. Cell culture and culture conditions with 2-DG solution

HGnFs were obtained from ScienCell Research Laboratories (San Diego, CA, USA). HGnFs were incubated in Dulbecco's modified eagle medium (DMEM) (Nacalai Tesque, Kyoto, Japan) with a normal glucose concentration (100 mg/dL), and one of three 2-DG concentrations (100, 500, 1,000 μ M).

2. Cell proliferation assay

HGnFs were plated in 96-well microplates at 1×10^4 cells/mL in a 100 μ L culture medium. The cells were cultured to adhere for 24 h, and then the medium was exchanged to a medium with different 2-DG concentrations (100, 500, 1,000 μ M). Proliferation data were determined using Cell Count Reagent SF (Nacalai Tesque) and analyzed using SoftMax Pro Microplate Data Acquisition and Analysis software (Version 7.0, Molecular Devices, Sunnyvale, CA, USA).

For live and dead staining, HGnFs were stained with

calcein-acetoxymethylester (calcein-AM) and propidium iodide (PI) solutions, respectively (Dojindo, Kumamoto, Japan). Images of the stained cells were obtained using a BZ-II all-in-one fluorescence microscope (Keyence Corporation, Osaka, Japan).

3. Wound-healing assay

Wound-healing assays were performed using a wound-repair assay kit (Ibidi GmbH, Martinsried, Germany) following the manufacturer's instructions. Briefly, HGnFs were plated at 3.5×10^4 cells/70 μ L in a cell culture insert. When the cells reached complete confluence, the culture insert was lifted and the medium was replaced with a serum-free medium with different 2-DG concentrations (100, 500, 1,000 μ M). Then, images of each wound at 0 and 24 h were photographed and analyzed.

4. Cytotoxicity assay and Reactive Oxygen Species (ROS) detection

Lactate dehydrogenase (LDH) activity was measured using the Cell Cytotoxicity LDH Assay Kit-WST kit (Dojindo), following the manufacturer's instructions. HGnFs were plated in 96-well microplates at 2×10^4 cells/mL in 100 μ L culture medium. The cells were cultured to adhere for 24 h, and then the medium was exchanged to a medium with different 2-DG concentrations (100, 500, 1,000 μ M) and incubated for 24 h. The absorbance of each well was measured at 490 nm. ROS levels were measured using a hydrogen peroxide fluorometric detection kit. Briefly, the culture supernatants of HGnFs were collected and pipetted into a black 96-well microplate (Nunclon Delta Surface 96-well microplate, Thermo Scientific, Waltham, MA, USA) and incubated for 10 min at room temperature in the dark, and the fluorescence was measured at 570 nm excitation and 600 nm emission.

5. Immunofluorescence staining

Following 2-DG stimulation, cells were incubated with primary antibodies against human type I collagen (Abcam, Cambridge, UK), glucose transporter type 1 (GLUT1) (Abcam), and ATP5B (Santa Cruz Biotechnology, Inc., Dallas, TX, USA). Fluorescent immunostaining was performed using Alexa Fluor 488R-conjugated secondary antibodies (Thermo Fisher Scientific) and nuclei were stained with 4',6-diamidino-2-phenylindole (DAPI) (Dojindo). Images of stained cells were obtained by fluorescence microscopy. These images were then analyzed.

6. Gene expression in HGnFs

Total RNA was isolated using an RNeasy Mini Kit (Qiagen, Venlo, Netherlands). RNA from each sample was reverse-transcribed to cDNA using a PrimeScript Reagent Kit (Takara Bio Inc., Shiga, Japan). The gene expression of GLUT1 (TaqMan Gene Expression Assay; Applied Biosystems, Thermo Fisher Scientific) was quantified using the StepOnePlus Real-Time PCR System (Thermo Fisher Scientific).

7. Measurement of lactic acid production and ATP levels

Lactic acid production was measured using a Lactate Assay Kit-WST (Dojindo) according to the manufacturer's instructions. HGnFs were stimulated with different concentration of 2-DG (100, 500, 1,000 μ M), the supernatants collected for analysis, and the data normalized to DNA. ATP levels were determined using the CellTiter-Glo 2.0 luminescent cell viability assay (Promega, Madison, WI, USA). Briefly, 1×10^4 cells/100 μ L were loaded into each well in a 96-well plate. The cells were cultured to adhere for 24 h, and then the medium was exchanged to a medium with different 2-DG concentrations. Then, the cells were incubated for 24, 48, 72, or 120 h. After the addition of 100 μ L volume of CellTiter-Glo reagents, relative luminescence units were measured following the manufacturer's instructions.

Results

1. Cell proliferation

Figure 1 shows the effects of various 2-DG concentrations on HGnF proliferation after culturing for 24, 48, 72, and 120 h. The number of live cells stained with calcein-AM solution decreased proportionally at 72 and 120 h. However, no detectable dead cells were found after staining with PI solution, regardless of the concentration of 2-DG used. HGnF proliferation was significantly increased by 100 μ M 2-DG for the first 72 h. Subsequently, 2-DG significantly suppressed the proliferation of HGnFs and decreased the number of live cells stained with calcein-AM.

2. Wound healing capability

The wound healing capability of HGnFs was examined using a scratch assay. Figure 2 shows that 100 μ M 2-DG significantly promoted wound healing. By contrast, incubation with 1,000 μ M 2-DG significantly inhib-

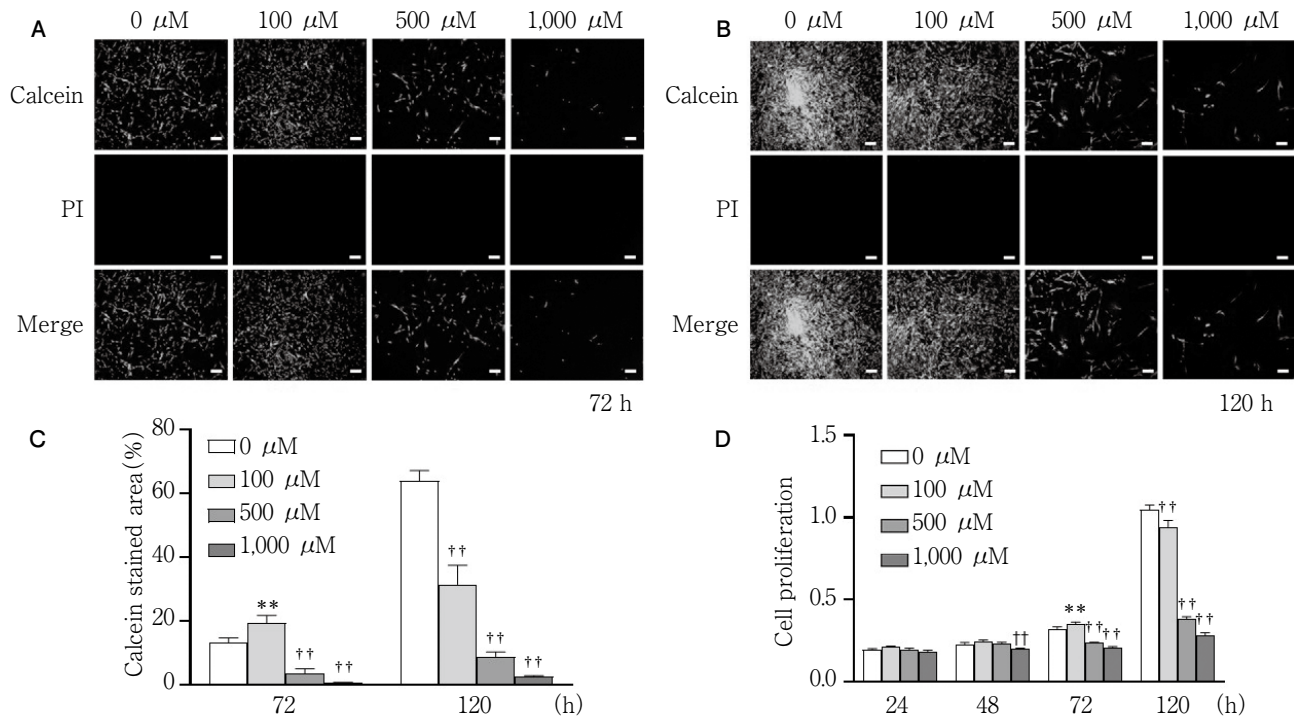


Fig. 1 Different 2-deoxy-D-glucose (2-DG) concentrations affect the proliferation of human gingival fibroblasts (HGnFs) (A and B) HGnFs stained by calcein-AM and PI were photographed under a fluorescence microscope after incubation with 2-DG for 72 and 120 h. (C) Viable and dead cell staining is presented as the percentage of the calcein-stained area. (D) Cell proliferation was measured after incubation with 2-DG for 24, 48, 72, and 120 h. Scale bars : 500 μm. ** : $p < 0.01$, significant increase compared with the control group ; † † : $p < 0.01$, significant decrease compared with the control group.

ited cell migration.

3. Cytotoxicity and cellular stress

Figure 3A shows that cytotoxicity was generally low in the 2-DG-stimulated groups. In addition, cytotoxicity was reduced in the 1,000 μM 2-DG group.

Hydrogen peroxide (H_2O_2), a marker of ROS, was measured after culturing for 24, 72, and 120 h. Figure 3B shows no significant change in H_2O_2 production in the 2-DG-stimulated groups, indicating a general absence of cellular stress related to 2-DG stimulation.

4. Glucose uptake capability

Figure 4 shows that GLUT1 expression in HGnFs increased as the concentration of 2-DG was increased as analyzed by immunofluorescence staining and real-time PCR. The expression of GLUT1 mRNA was significantly increased in the 500 and 1,000 μM 2-DG groups after 72 h.

5. Glycolysis levels

Lactate production and intracellular ATP levels under low glucose conditions were measured after culturing HGnFs with 2-DG for 24, 72, and 120 h. Figure 5

shows that lactate production was significantly decreased by 500 and 1,000 μM at 72 h; however, at 120 h, lactate production was partially decreased in all 2-DG-stimulated groups. By contrast, lactate production was significantly decreased in the 1,000 μM group at 24, 72, and 120 h.

The intracellular ATP levels were significantly increased by 100 μM 2-DG at 72 h, and at 120 h, were significantly decreased in all 2-DG-stimulated groups. The activity of ATP5B was improved by 100 and 500 μM 2-DG at 72 h, with the highest increase detected for 100 μM 2-DG. After 120 h, ATP5B activity in the 2-DG-stimulated groups was significantly reduced compared with that in the 0 μM 2-DG group.

Discussion

This study investigated the effect of an environment in which energy metabolism cannot be performed, on HGnFs using 2-DG as an *in vitro* gingival wound healing model. Our results showed that different concentra-

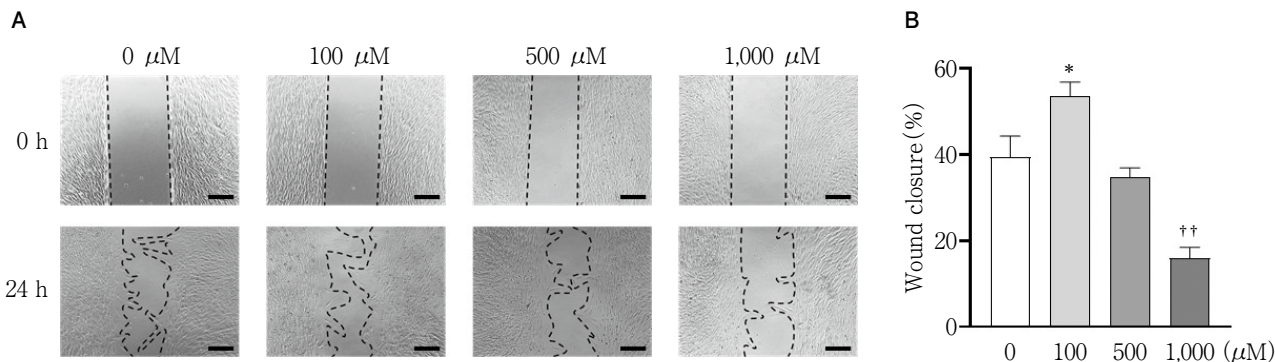


Fig. 2 Different 2-DG concentrations affect the wound-healing capability of HGnFs

(A) The process of wound healing assay was photographed at 0 and 24 h. Scale bars : 500 μm. (B) The data of the wound-healing assay are presented as the ratio of the final scratch size to initial scratch size. * : p<0.05, significant increase compared with the control group ; † † : p<0.01, significant decrease compared with the control group.

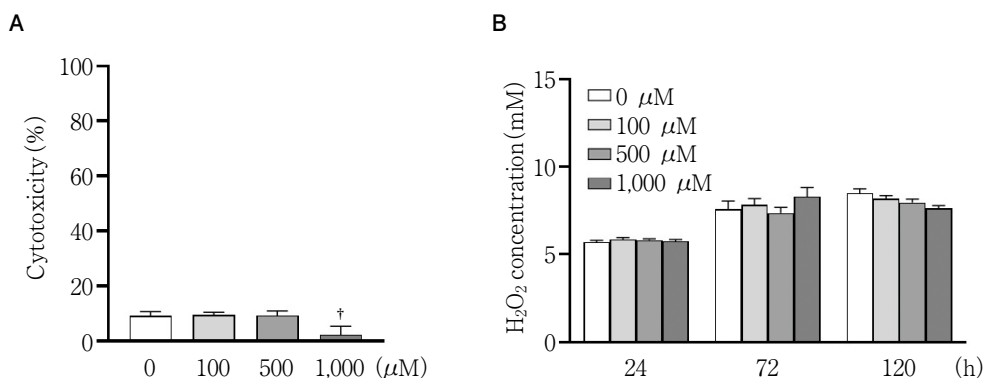


Fig. 3 The addition of 2-DG did not affect the cellular stress levels of HGnFs

(A) Cytotoxicity (LDH level) was determined after 24 h of incubation with 2-DG. (B) The level of ROS was examined using a hydrogen peroxide (H₂O₂) detection kit. After 24, 72, and 120 h of incubation with 2-DG, the supernatant was collected and the level of H₂O₂ was measured by a microplate reader. † : p<0.05, significant decrease compared with the control group.

tions of 2-DG induced different cellular functions, such as cell proliferation and migration. These results are similar to our previous study on the effect of low glucose environments on HGnFs⁹⁾. The optimal concentration of 2-DG was not determined in this study. In the present study, different concentrations of 2-DG were added to inhibit cellular glucose metabolism to different degrees, and experiments were carried out at three concentrations, as the aim was to investigate the biological changes in the cells.

In Fig. 1, the data show that 2-DG did not alter HGnFs' cell proliferation at 48 h. However, a significant inhibition of cell proliferation by 2-DG was observed at 72 and 120 h. This early increase in proliferation likely corresponds to the phase in which cells are adapting to

the low glucose environment induced by 2-DG, and they initiate energy production. In contrast, at later time points, it is conjectured that the inhibition of glucose metabolism caused by 2-DG suppressed the cell proliferation. Many studies have reported that 2-DG suppressed the proliferation and migration of cancer cells¹⁰⁻¹²⁾. Our previous results showed that a low glucose environment suppressed the proliferation and migration of HGnFs and affected their cellular activities. The present results suggest that 2-DG suppresses the proliferation and migration of HGnFs by reducing their energy metabolism.

In the present study, no cytotoxicity or production of H₂O₂, a reactive oxygen species, was observed when the energy metabolism of HGnFs was inhibited by

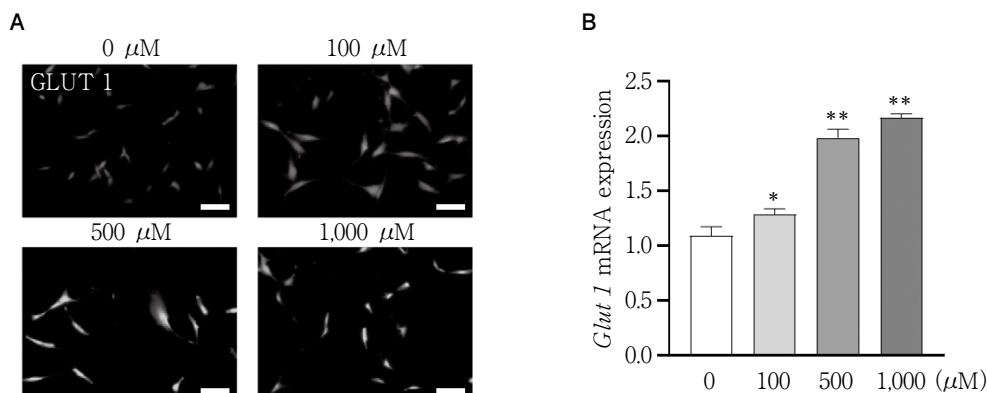


Fig. 4 2-DG increases Glut 1 expression in HGnFs

(A) HGnFs were photographed by a fluorescence microscope after incubation with a fluorescently labeled secondary antibody. Nuclei were stained with DAPI. (B) The gene expression of GLUT1 mRNA was determined by qPCR of stimulated HGnFs incubated for 72 h. Scale bars : 100 μ m. * : $p < 0.05$, ** : $p < 0.01$, significant increase compared with the control group.

2-DG. Our previous studies showed that cytotoxicity and the production of H_2O_2 and ROS increased with decreasing glucose concentrations under a low glucose environment. Cytotoxicity and H_2O_2 production differ between low glucose environments and the *in vitro* environment induced by 2-DG in this study. Vibhuti et al. reported that the cytotoxicity of HGnFs and production of ROS increased with increasing concentrations of 2-DG¹³. In Fig. 3, no ROS formation was observed following 2-DG treatment. This observation suggests that 2-DG may diminish cellular glucose metabolism and, consequently, decrease the oxidative phosphorylation process. Under conditions of low glucose, there is typically a reduction in oxidative phosphorylation within the mitochondria, leading to a decrease in ROS production. Therefore, the decrease in glucose metabolism induced by 2-DG is likely to contribute to the suppression of ROS production. This aligns with the absence of cellular stress, indicating that 2-DG may exert relatively safe effects on cells. We previously reported that a low glucose environment was detrimental to HGnFs, by inducing inflammatory cytokine expression and cellular stress¹⁴. These results are similar to the low glucose environment and the *in vitro* environment using 2-DG in the present study, whereby energy production is reduced because of decreased cellular metabolism via the glycolytic system. However, in terms of the cytotoxicity of HGnFs, it may be different.

Glucose metabolism consists of two processes: glu-

cose uptake and glycolysis. During glucose uptake, transportation across the cellular membrane is the main rate-limiting step, which is determined by the facilitated diffusion of GLUTs¹³. GLUT1 is responsible for the low level of basal glucose uptake required to maintain respiration in all cells¹⁴. In the present study, a concentration-dependent increase in the expression of GLUT1 was observed when HGnFs were cultured with 2-DG. We reported that low glucose enhanced the expression of GLUT1 in HGnFs, which suggests that low glucose might enhance glucose uptake proportionally as HGnFs sense glucose deprivation⁸. Furthermore, the elevated expression of GLUT1 occurs in environments where there is reduced cellular metabolism via the glycolytic pathway.

Glycolysis is a complex biochemical process mediated by multiple glycolytic genes and pathways. Lactate is an intermediate cellular metabolite of the glycolytic pathway and is produced in the cytoplasm through the reduction of pyruvate¹⁵, and ATP is the end metabolite of glycolysis¹⁶. Thus, their levels may reflect the level of glycolytic activity of a cell¹⁷⁻¹⁹. Our results¹⁴ showed that lactate and ATP production were relatively increased in the 100 μ M 2-DG group at 72 h, which might indicate enhanced glycolytic activity. However, there was a decrease in lactate and ATP production compared with that in the control group at 120 h as the 2-DG concentration was upregulated, similar to our previous studies using low glucose environments. This

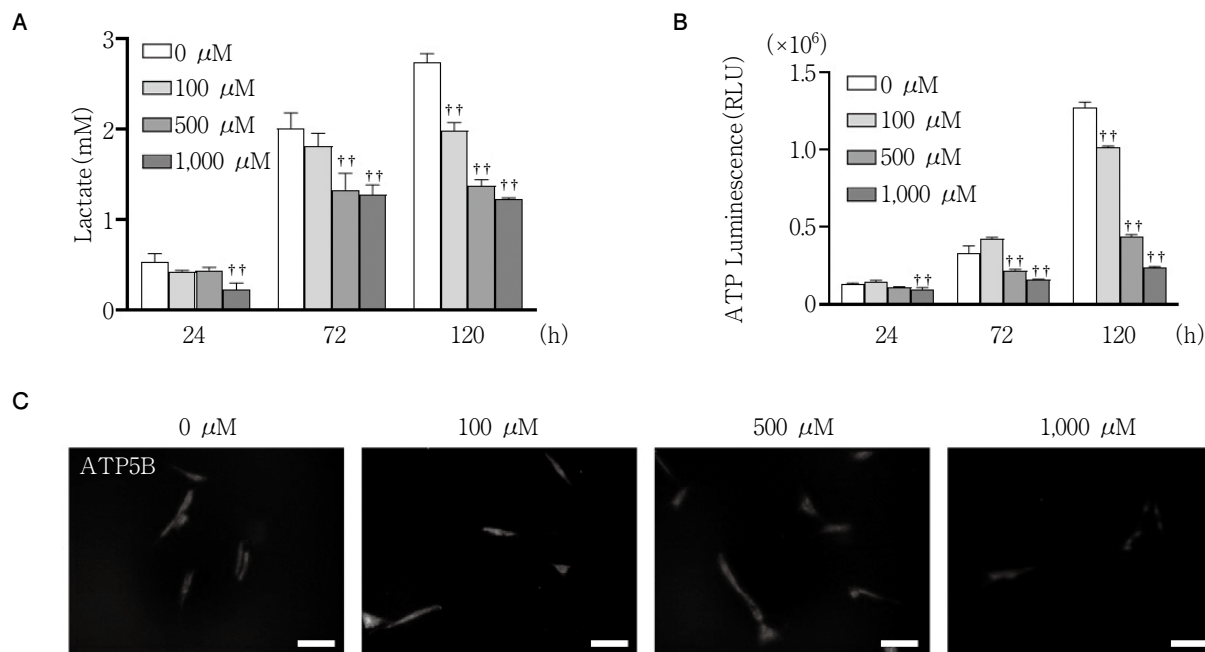


Fig. 5 The addition of 2-DG affects the glycolysis levels in HGnFs

(A) Lactate production by HGnFs exposed to 2-DG was measured after incubation for 24, 72, and 120 h. (B) The level of intracellular ATP was determined by luminescence using a microplate reader after incubation for 24, 72, and 120 h. (C) The activity of ATP5B was photographed by a fluorescence microscope after incubation for 120 h. Scale bars : 100 μm . † † : $p < 0.01$, significant decrease compared with the control group.

result indicated that glucose metabolism in the 100 μM 2-DG group was higher than that in the control group in the first 72 h, which might explain the enhanced wound healing capacity of the 100 μM 2-DG group at 72 h. At 120 h, glucose metabolism was reduced in all 2-DG groups, which might indicate that glucose uptake was not sufficient to support glucose consumption levels compared with that in the control group, ultimately leading to the suppression of wound healing. Of note, a small amount of ATP was produced in the group without glucose.

Energy metabolism via glycolysis in HGnFs is important for the wound healing of periodontal tissues. Hard tissue regeneration of alveolar bone cannot occur without the connective tissue wound healing process induced by HGnFs. In this respect, the intracellular and extracellular glucose metabolic environments of HGnFs are essential.

It is important to examine the cellular energy metabolism status of HGnFs by incorporating 2-DG into their cells, as in this study, to examine wound healing in connective tissues. In future research, we would like to use animal experiments to examine any differences

between *in vivo* low glucose environments and a low glucose environment induced by 2-DG incorporation.

Conclusion

The results of this study suggest that the intracellular uptake of 2-DG by HGnFs suppresses energy metabolism by the glycolytic system and is similar to a low glucose environment.

Conflicts of Interest

The authors declare no conflicts of interest associated with this manuscript.

Acknowledgments

This study was partially supported by Grants-in-Aids for Scientific Research from the Japan Society for the Promotion of Science (21K09946, 22K17084, 22K09993 and 23K19761).

References

- 1) Hakkinen L, Uitto VJ, Larjava H. Cell biology of gingival

- wound healing. *Periodontol* 2000; 24: 127-152.
- 2) Kirsner RS, Eaglstein WH. The wound healing process. *Dermatol Clin* 1993; 11: 629-640.
 - 3) Akiyama SK, Yamada SS, Chen W, Yamada KM. Analysis of fibronectin receptor function with monoclonal antibodies: roles in cell adhesion, migration, matrix assembly, and cytoskeletal organization *in vivo*. *J Cell Biol* 1989; 109: 863-875.
 - 4) Cam H, Balciunaite E, Blais A, Spektor A, Scarpulla RC, Young R, Kluger Y, Dynlacht BD. A common set of gene regulatory networks links metabolism and growth inhibition. *Mol Cell* 2004; 16: 399-411.
 - 5) Herzig S, Shaw RJ. AMPK: guardian of metabolism and mitochondrial homeostasis. *Nat Rev Mol Cell Biol* 2018; 19: 121-135.
 - 6) Kato H, Taguchi Y, Tominaga K, Kimura D, Yamawaki I, Noguchi M, Yamauchi N, Tamura I, Tanaka A, Umeda M. High glucose concentrations suppress the proliferation of human periodontal ligament stem cells and their differentiation into osteoblasts. *J Periodontol* 2016; 87: e44-51.
 - 7) Ralser M, Wamelink MM, Struys EA, Joppich C, Krobitsch S, Jakobs C, Lehrach H. A catabolic block does not sufficiently explain how 2-deoxy-D-glucose inhibits cell growth. *Proc Natl Acad Sci USA* 2008; 105: 17807-17811.
 - 8) Pelicano H, Martin DS, Xu RH, Huang P. Glycolysis inhibition for anticancer treatment. *Oncogene* 2006; 25: 4633-4646.
 - 9) Li R, Kato H, Taguchi Y, Umeda M. Intracellular glucose starvation affects gingival homeostasis and autophagy. *Sci Rep* 2022; 12: 1230.
 - 10) Zhang D, Li J, Wang F, Hu J, Wang S, Sun Y. 2-Deoxy-D-glucose targeting of glucose metabolism in cancer cells as a potential therapy. *Cancer Lett* 2014; 355: 176-183.
 - 11) Sottnik JL, Lori JC, Rose BJ, Thamm DH. Glycolysis inhibition by 2-deoxy-D-glucose reverts the metastatic phenotype *in vitro* and *in vivo*. *Clin Exp Metastasis* 2011; 28: 865-875.
 - 12) Christofi M, Le Sommer S, Mólzer C, Klaska IP, Kuffova L, Forrester JV. Low-dose 2-deoxy glucose stabilises tolerogenic dendritic cells and generates potent *in vivo* immunosuppressive effects. *Cell Mol Life Sci* 2021; 78: 2857-2876.
 - 13) Vibhuti A, Muralidhar K, Dwarakanath BS. Differential cytotoxicity of the glycolytic inhibitor 2-deoxy-D-glucose in isogenic cell lines varying in their p53 status. *J Cancer Res Ther* 2013; 9: 686-692.
 - 14) Li R, Kato H, Taguchi Y, Deng X, Minagawa E, Nakata T, Umeda M. Glucose starvation-caused oxidative stress induces inflammation and autophagy in human gingival fibroblasts. *Antioxidants* 2022; 11: 1907.
 - 15) Yang S, Guo L, Su Y, Wen J, Du J, Li X, Liu Y, Feng J, Xie Y, Bai Y, Wang H, Liu Y. Nitric oxide balances osteoblast and adipocyte lineage differentiation via the JNK/MAPK signaling pathway in periodontalligament stem cells. *Stem Cell Res Ther* 2018; 9: 2489-2495.
 - 16) Mueckler M, Caruso C, Baldwin SA, Panico M, Blench I, Morris HR, Allard WJ, Lienhard GE, Lodish HF. Sequence and structure of a human glucose transporter. *Science* 1985; 229: 941-945.
 - 17) Rabinowitz JD, Enerbäck S. Lactate: the ugly duckling of energy metabolism. *Nat Metab* 2020; 2: 566-571.
 - 18) Neely JR, Grotyohann LW. Role of glycolytic products in damage to ischemic myocardium. Dissociation of adenosine triphosphate levels and recovery of function of reperfused ischemic hearts. *Circ Res* 1984; 55: 816-824.
 - 19) Wu Y, Dong Y, Atefi M, Liu Y, Elshimali Y, Vadgama JV. Lactate, a neglected factor for diabetes and cancer interaction. *Mediators Inflamm* 2016; 2016: 6456018.

Development and Clinical Evaluation of Anti-aspiration Gauze Roll

Assessment of Water Absorbency and Usability of Gauze Roll—An Exploratory Study

Chiharu KAWAMOTO, Ryotaro YAGO, Mai FUKUYAMA, Toru TANAKA*,
Hidehiko SANO* and Atsushi TOMOKIYO*

Department of Restorative Dentistry, Division of Oral Health Science, Hokkaido University Graduate School of Dental Medicine

*Department of Restorative Dentistry, Division of Oral Health Science, Hokkaido University Faculty of Dental Medicine

Abstract

Purpose: Cotton roll is widely used in dentistry for moisture control and isolation. However, cases of air-way obstruction due to aspiration of the cotton roll have been reported, and some cases have even resulted in death. In this study, we developed an anti-aspiration gauze roll (AAGR) by attaching a thread to the gauze roll as an alternative to conventional cotton roll to prevent aspiration and forgetting to remove the cotton roll.

Methods: A water absorption test was conducted to evaluate the anti-moisture ability. Three types of prototypes, large (300×30 mm), medium (250×30 mm), and small (150×30 mm), were prepared according to the size of gauze used. The length of the cotton yarn was 300 mm. An *in vitro* water absorption test was conducted in accordance with the test method stipulated in the standards for medical gauze and medical cotton established by the Japanese Ministry of Health, Labour, and Welfare to evaluate the moisture control ability of AAGR. Each specimen (n=10) was immersed in 25°C distilled water for 3 minutes, left on a net for 1 minute, and weighed. For statistical analysis, one-way ANOVA was performed using statistical analysis software, followed by multiple comparison tests using the Tukey HSD test. The significance level was set at 5%. A clinical evaluation was conducted by surveying dentists about the usability of AAGR in clinical use. In the clinical evaluation, dentists were asked to use AAGR instead of cotton roll in clinical situations and complete a questionnaire. AAGR (large) was used for adult patients, and AAGR (small) was used for pediatric patients. The survey items included treatment details, water absorption capacity and speed, gauze portion size, gauze thread length and thickness, ease of use, and expectations for preventing aspiration.

Results: In the water absorption test, there was a statistically significant difference in the amount of water absorbed among each group: the amount in descending order was AAGR (large), control group, AAGR (medium), and AAGR (small). In the questionnaire survey, the results for adults showed that all items were rated as equal to or better than the conventional cotton roll, but the results for children showed that there were areas for improvement regarding water absorption volume, water absorption speed, thickness, and ease of use.

Conclusion: The results of the water absorption test showed that AAGR (large) absorbs more water than cotton roll and has superior moisture control ability. The use of AAGR is expected to prevent both forgetting to remove moisture control tools, and their accidental ingestion or aspiration.

Key words: cotton roll, prevention of aspiration, water absorption test, questionnaire survey

Corresponding author: Chiharu KAWAMOTO, Department of Restorative Dentistry, Division of Oral Health Science, Hokkaido University Graduate School of Dental Medicine, Kita 13, Nishi 7, Kita-ku, Sapporo 060-8586, Japan

TEL: +81-11-706-4261, FAX: +81-11-706-4878, E-mail: chipa@den.hokudai.ac.jp

Received for Publication: September 14, 2023/Accepted for Publication: November 21, 2023

DOI: 10.11471/odep.2023-015

Introduction

Accidental ingestion and aspiration are potential complications that can occur during dental procedures¹⁾. Incident reports from FY 2012 to FY 2017 in the Hokkaido University Hospital Dental Department showed that accidental ingestion and aspiration were the second-most reported incidents after soft tissue injuries (7 in FY 2012, 2 in FY 2013, 5 in FY 2014, 4 in FY 2015, 3 in FY 2016, and 4 in FY 2017).

The risk of accidental ingestion or aspiration is reported²⁻⁴⁾ to be particularly high in pediatric dental treatment. Cases of airway obstruction due to aspiration of cotton rolls are often reported^{5,6)}. Moisture control and isolation are essential for treatment in dentistry, and rubber dam is known to be the first choice as a procedure for this purpose^{7,8)}. However, this is not always possible in all cases, and cotton rolls are used in such cases⁹⁻¹¹⁾. While such accidents rarely occur, when they do happen, the risk is very high. In fact, a case was reported¹²⁾ in which a 2-year-old girl died at a dental clinic in Saitama due to airway obstruction caused by the aspiration of a cotton roll used during dental treatment. Therefore, when dentists use cotton rolls it is necessary to take precautions to prevent accidental ingestion and aspiration.

Another occasional problem in clinical practice is forgetting to remove the cotton roll from the oral cavity. Similar cases have been reported not only in dentistry but also in medical surgery; the Japan Council for Quality Health Care reported¹³⁾ 70 cases of gauze left in the body between 2015 and 2018. However, both cotton roll and gauze are indispensable for treatment in any field of medical surgery.

In the context of these circumstances, we considered the development of a new tool to replace the conventional cotton roll for the purpose of preventing aspiration and forgetting to remove the cotton roll. Initially, a prototype was made with a thread attached to the cotton roll so that the cotton roll could be instantly removed from the oral cavity by pulling the thread to prevent aspiration, but there was a concern that the attached thread was vulnerable to detachment. Therefore, the Anti-Aspiration Gauze Roll (AAGR), in which a thread is sewn onto a rolled gauze, was devised and patented¹⁴⁾ after prototype production.

In this study, to investigate whether AAGR can be used in clinical practice as an alternative to conventional cotton roll, a water absorption test was conducted to evaluate its moisture control ability, and a clinical evaluation was made through a questionnaire survey of operators regarding its usability and feel in dental practice.

The null hypothesis was that AAGR does not absorb as much or more water as existing cotton rolls.

Materials and Methods

1. Preparation of prototypes of AAGR

Fabrication of prototypes of AAGR was outsourced to Japan Medical Products Co., Ltd. The prototype was made by rolling medical gauze (Japanese Pharmacopoeia) into a roll and sewing it with cotton thread. A 30×300 mm rolled gauze was used as the large size, 30×250 mm as the medium size, and 30×150 mm as the small size. The length of the cotton yarn was 300 mm (Fig. 1). Three prototypes were prepared for various patients, including infants, children, adults, the elderly, and those requiring nursing care. The actual prototype (Fig. 2) and a schematic diagram are shown in Fig. 3. As a control group, conventional cotton rolls (Dentalmen II, Hakujuji Co., Ltd., Japan) with cotton threads tied to them were prepared in the same manner as the prototypes. The size and dimensions of each specimen are shown in Table 1.

2. Water absorption test

In vitro water absorption tests were conducted to confirm the moisture control ability of the prototypes. This experiment was conducted in accordance with the test method stipulated in the standards for medical gauze and medical cotton established by the Japanese Ministry of Health, Labour and Welfare¹⁵⁾. First, the prototypes and cotton rolls (n=10) were weighed using a scale (AUX220, Shimadzu, Japan). After immersing the sample in distilled water for 3 minutes, the sample was left on the wire mesh of a No. 10 sieve for 1 minute, allowed to drip water, and then weighed (Fig. 4).

One-way ANOVA was performed on the water absorption test using statistical analysis software (SPSS28, IBM, Armonk, New York, USA), and multiple comparison tests were conducted using the Tukey HSD test. The significance level was set at 5%.

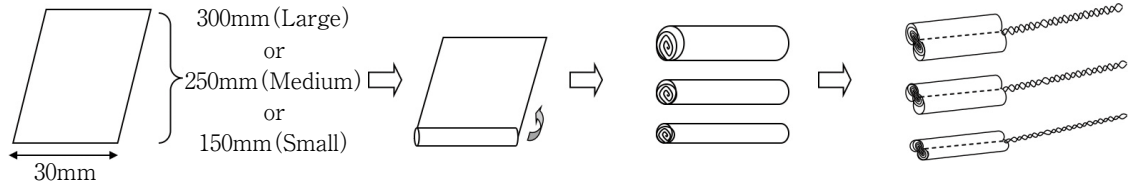


Fig. 1 Method of preparing the Anti-aspiration Gauze Roll

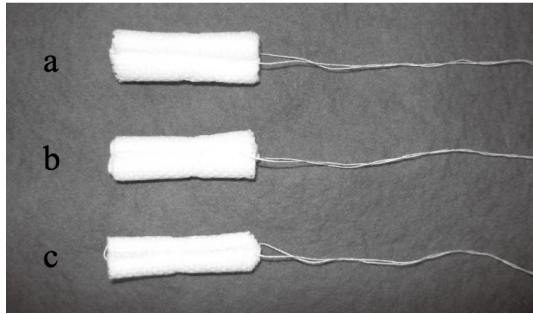


Fig. 2 Prototype of the Anti-aspiration Gauze Roll
a : AAGR (large), b : AAGR (medium), c : AAGR (small)

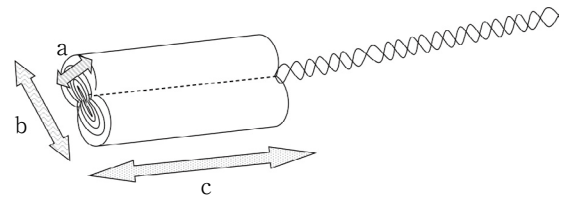


Fig. 3 Schematic diagram of the Anti-aspiration Gauze Roll
(a) Short diameter, (b) Long diameter, (c) Length

Table 1 Dimensions of each material

Sample	Length	Long diameter	Short diameter
Large	30 mm	12 mm	8 mm
Medium	30 mm	10 mm	7 mm
Small	30 mm	10 mm	5 mm
Cotton Roll	30 mm	Diameter 10 mm	

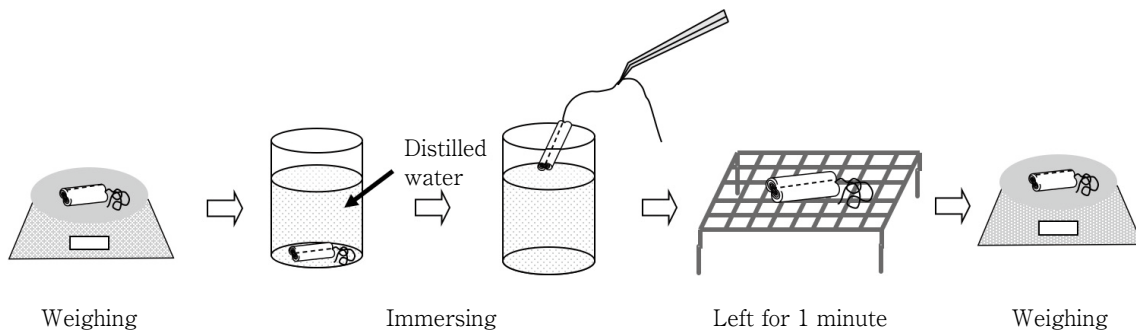


Fig. 4 Water absorption test method

Samples were weighed, immersed in distilled water for 3 minutes, left on a sieve wire mesh for 1 minute, and weighed again.

3. Questionnaire survey

Compared to conventional cotton roll, AAGR has a different shape and material, so its ease of use and moisture control ability were expected to be different

from those of conventional cotton roll. Therefore, we conducted a questionnaire survey of dentists regarding the ease of use and moisture control ability of the AAGR instead of placement of cotton roll during dental

treatment. This study was conducted after obtaining approval (021-0180) from the Ethical Review Board for Life Science and Medical Research, Hokkaido University Hospital.

A total of 38 dentists affiliated with Hokkaido University Hospital, who agreed to participate in the questionnaire survey after receiving an explanation of the study, were enrolled in the study.

The patients were those who went to or were hospitalized at Hokkaido University Hospital for dental treatment and did not refuse to participate after receiving

an oral explanation of the main points of the study.

The age-sex distribution of the patients is shown in Table 2.

AAGR (large) was used for adult patients, and AAGR (small) was used for pediatric patients.

Since cotton rolls are used in a variety of dental procedures, the procedures were not limited. Examples of the clinical use of AAGR are shown in Fig. 5. Consent was obtained from the patient in the case of adults and from the parent or guardian in the case of children. The questionnaire survey included the following items: treatment details, water absorbency, water absorption speed, gauze portion size, thread length and thickness, ease of use, and expectations for preventing aspiration (Fig. 6).

The questionnaire survey was not statistically analyzed as it was an exploratory study.

Table 2 Age-sex distribution of the patients

Male (Number of participants)	11
Female (Number of participants)	27
Minimum age	3
Maximum age	77
Average age	43.55

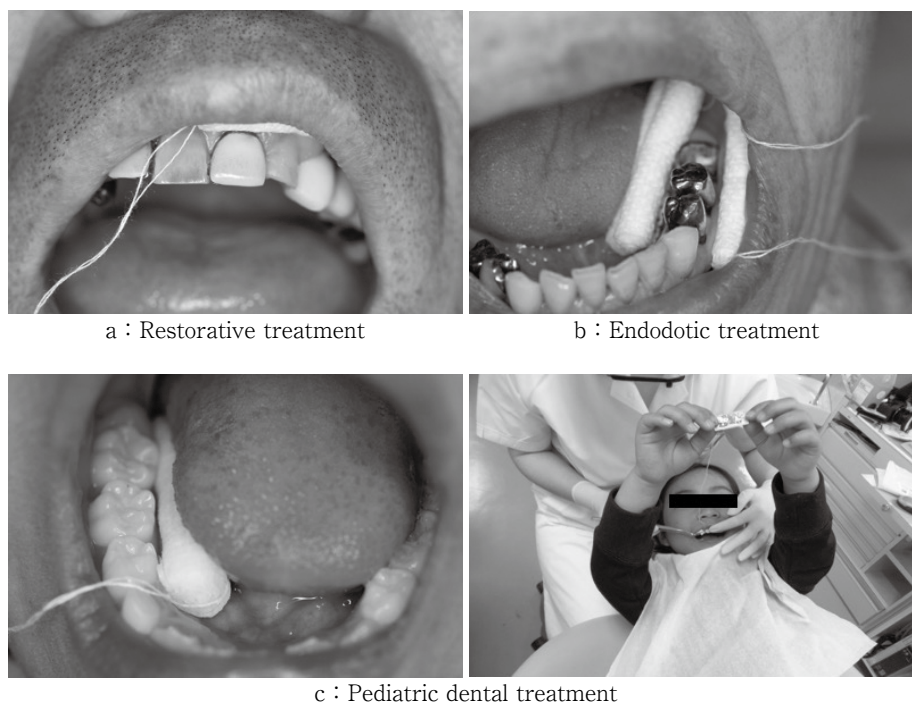


Fig. 5 Examples of the Anti-Aspiration Gauze Roll used in clinical treatments

- a : Composite resin filling for anterior teeth.
- b : Example of use for moisture control and isolation in a case in which a rubber dam could not be used.
- c : The left photo shows a case in which the gauze was used during fluoride application. On the right is a case in which the gauze was applied with a seal attached to the tip of the string and shown to the child as an applied method of treatment.

Questionnaire on clinical evaluation of Anti-Aspiration Gauze Roll
 I agree. I disagree.
 [Operator] Clinical department _____ Name _____
 [Patient] Age ____ Sex ____ Treatment details _____

- How is the amount of water absorption compared to conventional cotton roll?
 (1) Good (2) Same level (3) Poor (4) Other
- How is the water absorption speed compared to conventional cotton roll?
 (1) Faster (2) Same level (3) Slower (4) Other
- How is the length of the Gauze Roll?
 (1) Adequate (2) Long (3) Short (4) Very long (5) Very short
- How is the thickness the Gauze Roll?
 (1) Adequate (2) Thick (3) Thin (4) Very thick (5) Very thin
- How is the length of the thread?
 (1) Adequate (2) Long (3) Short (4) Very long (5) Very short
- How is the thickness of the thread?
 (1) Adequate (2) Thick (3) Thin (4) Very thick (5) Very thin
- How about ease of use?
 (1) Excellent (2) Good (3) Fair (4) Poor (5) Very poor
- Can the use of anti-aspiration gauze roll be expected to prevent aspiration compared to conventional cotton roll?
 (1) Yes (2) Neither (3) No (4) Other
- Would you like to use it again?
 (1) Yes (2) Depends on the case (3) No (4) Other
- Please feel free to include any other comments you may have.

Fig. 6 Questionnaire survey

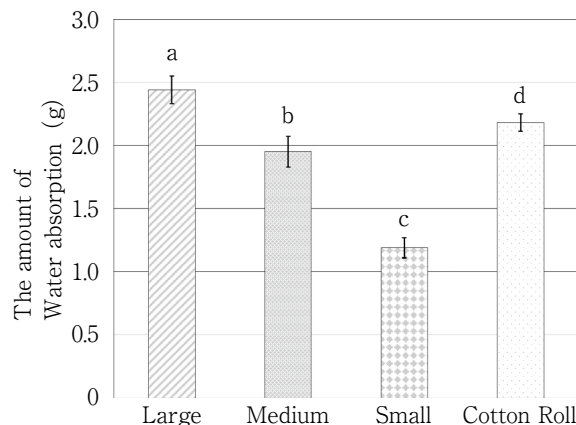


Fig. 7 Results of absorption test
 Different letters indicate a significant difference ($p < 0.05$).

Table 3 Descriptive statistics

Specimens	Mean	Std. Deviation	N
Large	2.4435	0.10938	10
Medium	1.9472	0.11841	10
Small	1.1942	0.07694	10
Cotton Roll	2.1809	0.06690	10
Total	1.9414	0.48053	40

Dependent variable : Amount of water absorption

Results

The results of the water absorption test are shown in Fig. 7 and the details of the statistical analysis in Table 3-5. In the water absorption test, the results of one-way ANOVA and Tukey HSD test showed significant differences in water absorption among the groups. Based on these results, it is concluded that AAGR (large) can absorb as much or more water as existing cotton rolls. Therefore, the null hypothesis is rejected.

The results of the survey are shown in Fig. 8. The treatment details of the 38 cases included endodontic treatment in 15 cases, prosthetic treatment in 10 cases, restorative treatment in 5 cases, fissure sealant in 5 cases, hypersensitivity treatment in 2 cases, and infiltration anesthesia in 1 case. The results for adults showed that all items received a positive rating, but the results for children showed that there were areas for improvement regarding water absorption volume, water absorption speed, thickness, and ease of use. Regarding thickness, AAGR was found to fit more easily into the oral cavity than conventional cotton roll.

Other comments included: (i) There are situations when moisture control is desired, such as when attaching a restoration or prosthesis to a mandibular molar, but the risk of ingestion or aspiration makes it unavoidable to perform the procedure without moisture control. In such cases, this product can provide high-quality treatment while minimizing the risk. (ii) I would like to use this product in situations where the risk of accidental ingestion or aspiration is high, such as house call dentistry or when the patient is uncooperative. (iii) It can prevent forgetting to remove gauze during surgery.

Discussion

In this case, the cotton roll used at Hokkaido University Hospital was defined as the control. Cotton rolls vary in size depending on the product. In this study, from the viewpoint of whether AAGR can be used as a substitute for cotton rolls, we considered that the water absorbing capacity must be equal to or greater than

Table 4 Multiple comparisons

Specimens	The amount of Water absorption	Mean Difference	Std. Error	Sig.	95% Confidence Interval	
					Lower Bound	Upper Bound
Large	Medium	0.4963*	0.4265	<0.001	0.3815	0.6112
	Small	1.2493*	0.4265	<0.001	1.1344	1.3642
	Cotton Roll	0.2626*	0.4265	<0.001	0.1477	0.3774
Medium	Large	-0.4963*	0.4265	<0.001	-0.6112	-0.3815
	Small	0.7530*	0.4265	<0.001	0.6381	0.8678
	Cotton Roll	-0.2338*	0.4265	<0.001	-0.3486	-0.1189
Small	Large	-1.2493*	0.4265	<0.001	-1.3642	-1.1344
	Medium	-0.7530*	0.4265	<0.001	-0.8678	-0.6381
	Cotton Roll	-0.9867*	0.4265	<0.001	-1.1016	-0.8719
Cotton Roll	Large	-0.2626*	0.4265	<0.001	-0.3774	-0.1477
	Medium	0.2338*	0.4265	<0.001	0.1189	0.3486
	Small	0.9867*	0.4265	<0.001	0.8719	1.1016

Dependent variable : Amount of water absorption

Based on observed means.

The error term is Mean Square (Error) =0.009.

*The mean difference is significant at the 0.05 level.

Table 5 Homogeneous subsets

Tukey HSD ^{a,b}	N	Subset			
		1	2	3	4
Spesimens					
Small	10	1.1942			
Medium	10		1.9472		
Cotton Roll	10			2.1809	
Large	10				2.4435
Sig.		1.000	1.000	1.000	1.000

Means for groups in homogeneous subsets are displayed.

Based on observed means.

The error term is Mean Square (Error) =0.009.

a : Uses Harmonic Mean Sample Size =10.000.

b : Alpha=0.05.

that of cotton rolls. Therefore, three different sizes were established to examine the sizes that would be acceptable for clinical use. AAGR(large) absorbed more water than the conventional cotton roll of similar size, suggesting that it has a high moisture control effect and sufficient potential for clinical application.

Most of the survey results, where the target patients were adults, gave positive ratings to all items in the questionnaire. However, when comparing children and adults, negative opinions of cases involving children were noted regarding water absorption volume, water

absorption speed, thickness, and ease of use. This may be attributed to the size of AAGR (small) used for pediatric patients. Initially, the AAGR (small) was assumed to be appropriate for children because of their small mouths. However, children produce a large amount of saliva and the AAGR (small) was insufficient in terms of water absorption and speed, which likely affected its ease of use. In addition, the results of water absorption tests showed that AAGR (small) absorbed significantly less water than conventional cotton roll. Based on these findings, it is considered that a gauze with greater water absorption would be suitable for children. Regarding the opinion that the AAGR fits easily into the adult oral cavity, the reason may be that conventional cotton roll is somewhat difficult to insert between the tongue and teeth and might not be stable when the space is small. However, the AAGR can be freely adjusted due to its flexible form to fit the place where it is to be installed.

The majority of dentists who participated in the survey answered that the length of the thread was “appropriate,” but there were also a few comments such as the current length is too short to wrap around the finger, and concern that if the thread is too long, it may get tangled during the procedure. Most of the dentists answered that the thread thickness was “appropriate”

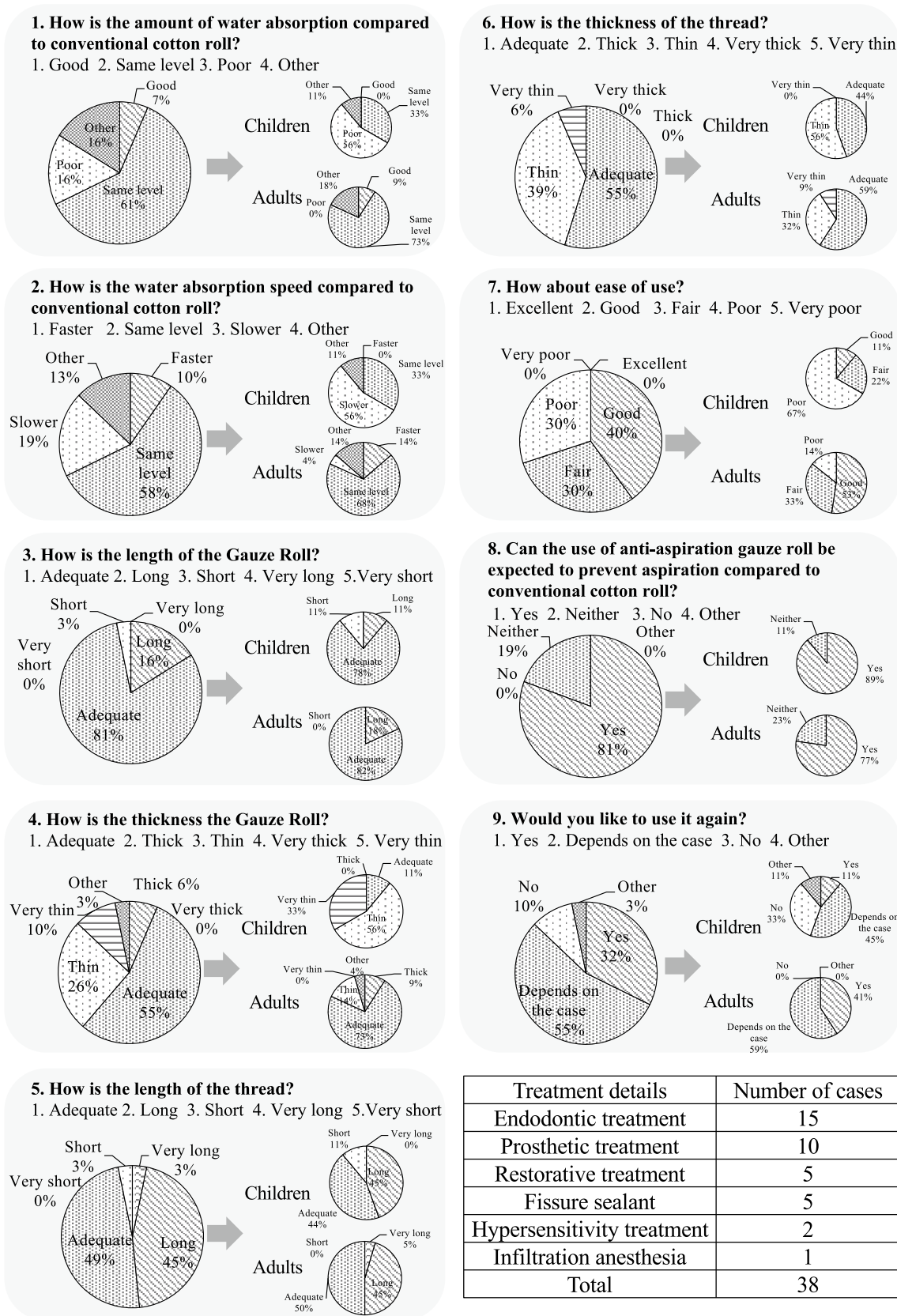


Fig. 8 Results of questionnaire survey

We conducted a questionnaire survey of 38 dentists regarding the ease of use and moisture control ability of the AAGR instead of placement of cotton roll during dental treatment.

Treatment details	Number of cases
Endodontic treatment	15
Prosthetic treatment	10
Restorative treatment	5
Fissure sealant	5
Hypersensitivity treatment	2
Infiltration anesthesia	1
Total	38

or “thin,” and there was no response indicating it was “thick”. We expect the ease of use of the thread can be improved by making it a little thicker. The question “Can the use of anti-aspiration gauze roll be expected to prevent aspiration compared to conventional cotton roll?” was answered in the affirmative by approximately 80% of the dentists. Another commented, “I feel safe because it has a string, so I don’t forget to pick it up.”

The survey results indicate that the use of AAGR may help prevent accidental ingestion and aspiration. However, the ease of use of the AAGR needs to be improved in the future to make it even easier for dentists to use in clinical practice.

Thus, the AAGR may have the potential to be used as an alternative to conventional cotton rolls without placing a special burden on the dentist.

Conclusion

AAGR (large) absorbs more water than conventional cotton rolls.

To the question “Can the use of anti-aspiration gauze roll be expected to prevent aspiration compared to conventional cotton roll?” 81% of respondents answered in the affirmative.

Conflict of Interest

The authors declare no conflict of interest related to this paper.

References

- 1) Hou R, Zhou H, Hu K, Ding Y, Yang X, Xu G, Xue P, Shan C, Jia S, Ma Y. Thorough documentation of the accidental aspiration and ingestion of foreign objects during dental procedure is necessary: review and analysis of 617 cases. *Head Face Med* 2016; 12: 23.
- 2) Fuangtharnthip P, Pujarern P, Pachimsawat P, Loeksomphot P, Janjarussakul P, Manopatanakul S. Accidental swallowing of dental objects during pediatric dental care in Thailand. *J Int Soc Prev Community Dent* 2021; 11: 671-677.
- 3) Zitzmann NU, Elsasser S, Fried R, Marinello CP. Foreign body ingestion and aspiration. *Oral Surg Oral Med Oral Pathol Oral Radiol Endod* 1999; 88: 657-660.
- 4) Cossellu G, Farronato G, Carrassi A, Angiero F. Accidental aspiration of foreign bodies in dental practice: clinical management and prevention. *Gerodontology* 2015; 32: 229-233.
- 5) Hisanaga R, Hagita K, Nojima K, Katakura A, Morinaga K, Ichinohe T, Konomi R, Takahashi T, Takano N, Inoue T. Survey of accidental ingestion and aspiration at Tokyo Dental College Chiba Hospital. *Bull Tokyo Dent Coll* 2010; 51: 95-101.
- 6) Sato C, Watanabe A, Ueda S, Ichiki T, Abe S. A case of bronchial obstruction caused by a dental instrument (cotton roll). *J Jpn Soc Respir Endoscopy* 2014; 36: 207. (in Japanese)
- 7) Buttke TM. More on rubber dam use. *J Am Dent Assoc* 2016; 147: 316-317.
- 8) Abreu-Placeres N, Yunes Fragoso P, Cruz Aponte P, Garrido LE. Rubber Dam Isolation Survey (RDIS) for adhesive restorative treatments. *Eur J Dent Educ* 2020; 24: 724-733.
- 9) Hatirli H, Yasa B, Çelik EU. Clinical performance of high-viscosity glass ionomer and resin composite on minimally invasive occlusal restorations performed without rubber-dam isolation: a two-year randomised split-mouth study. *Clin Oral Investig* 2021; 25: 5493-5503.
- 10) Olegário IC, Moro BLP, Tedesco TK, Freitas RD, Pássaro AL, Garbim JR, Oliveira R, Mendes FM; CARDEC 03 collaborative group; Raggio DP. Use of rubber dam versus cotton roll isolation on composite resin restorations’ survival in primary molars: 2-year results from a non-inferiority clinical trial. *BMC Oral Health* 2022; 22 (1): 440.
- 11) Carvalho TS, Sampaio FC, Diniz A, Bönecker M, Van Amerongen WE. Two years survival rate of Class II ART restorations in primary molars using two ways to avoid saliva contamination. *Int J Paediatr Dent* 2010; 20: 419-425.
- 12) Nikkei Inc. A 2-year-old child died after choking on cotton roll in his throat during treatment at a dental clinic in Saitama, Japan. <https://www.nikkei.com/article/DGXNZO09232810V10C10A6CC1000> (cited 2023.9.11)
- 13) Japan Council for Quality Health Care. Cases of gauze left in the body (14th Report). https://www.med-safe.jp/pdf/report_2018_2_R002.pdf (cited 2023.9.11)
- 14) Chiharu Watanabe, Japan Patent Kokai 2012-139322 (2012.7.26)
- 15) Ministry of Health, Labour and Welfare, Japan. Standards for medical gauze and medical cotton. https://www.mhlw.go.jp/web/t_doc?dataId=00tb2853&data Type=1&pageNo=1 (cited 2023.9.11)

Three-dimensional Analysis of the Shaping Characteristics and Ability of a Novel Ni-Ti Rotary File

Kazuma MATSUMOTO¹, Haruna HIROSE¹, Kota ISSHI², Seishiro FUJIMASA¹,
Shingo KANEMARU¹, Tsukasa YANAGI³ and Etsuko MATSUZAKI^{1,4}

¹Section of Operative Dentistry and Endodontology, Department of Odontology, Fukuoka Dental College

²Central Dental Laboratory, Fukuoka Dental College Medical and Dental General Hospital

³Section of Oral Implantology, Department of Oral Rehabilitation, Fukuoka Dental College

⁴Oral Medicine Research Center, Fukuoka Dental College

Abstract

Purpose: To compare the shaping characteristics and ability of the JIZAI (JZ) Ni-Ti rotary file to two other Ni-Ti files that have a similar operating environment to JZ, HyFlex CM (HCM) and ProTaper Next (PTN).

Methods: Root canal preparation was performed in a J-shaped canal model using the three file systems (n=4), and dental cone-beam computed tomography (CBCT) was performed. The three-dimensional images were superimposed before and after instrumentation at the same position. The X-, Y-, and Z-axes were set 1 mm coronal to the root apex, and the cross-sectional morphology, the extent of transportation, and the volume of the shaped root canal wall were evaluated.

Results: The cross-sectional morphology of the root canal was round, similar to the original root canal morphology with JZ and PTN. The HCM showed an elliptical tendency toward the sagittal direction. The transportation was relatively larger with JZ and smaller with HCM, with no significant difference between the files. The shaped root canal wall volume was greatest with HCM and least with JZ, with no significant difference between the files.

Conclusion: JIZAI had equivalent shaping ability to HyFlex CM and ProTaper Next in terms of transportation and shaped root canal wall volume, and therefore might be useful for safe preparation of root canals.

Key words: Ni-Ti rotary files, root canal preparation, three-dimensional imaging

Introduction

Ni-Ti alloy files (Ni-Ti files) are commonly used to prepare curved root canals¹⁾. Compared to conventional stainless-steel files, Ni-Ti files have greater flexibility and closely follow the path of the root canal due to a lower modulus of elasticity. The root canal is often curved in the apical third of the root. A stainless-steel file of size #35 or more does not have sufficient flexibility, and therefore tends to deviate from the original canal pathway, resulting in transportation of the canal center and the formation of a ledge or zip. Conventionally, transportation towards the outer side and inner side of the curvature has been used to evaluate the shaping ability of Ni-Ti files²⁻⁵⁾.

The low elastic modulus and breaking torque of Ni-Ti files lead to instrument separation. Therefore, endodontic files should have flexibility and high fracture resistance. This has been achieved through heat treatment of the austenite phase of conventional Ni-Ti alloys^{6,7)}. One such file is HyFlex CM (HCM; Coltene, Langenau, Germany). This file comprises the R and martensite phases resulting from heat treatment. When inserted into a curved root canal, the file does not return to its original shape due to its super elasticity, and no load is applied to the file^{8,9)}. In 2012, the ProTaper Next (PTN; Dentsply Maillefer, Ballaigues, Switzerland) file was introduced; the offset design of the file prevents it from biting into the dentin, thereby preventing separation¹⁰⁾. The file is fabricated using M-wire, which is martensitic at room or body temperature, austenitic at 43-50°C, and returns to the martensitic phase when cooled, resulting in flexibility¹¹⁻¹³⁾. Recently, a file with even greater flexibility has been manufactured through electrical discharge machining^{5,14)}. A new Ni-Ti file, JIZAI (JZ; Mani, Tochigi, Japan), which was recently launched in Japan, comprises the R and/or martensite phase at room or body temperature and is used in a unidirectional rotation mode¹⁵⁾. Single-length preparation was performed using two files: #25/0.04 and #25/0.06. This file alleviates one of the drawbacks of Ni-Ti files, namely the screw-in-effect due to the cross-sectional shape with a land like an irregular rectangle with a circular arc on one side^{16,17)}.

To date, a wide range of Ni-Ti files have been introduced, and research has chiefly focused on their flexibil-

ity and ability to follow the root canal path. Shaping ability is two-dimensionally (2D) evaluated by superimposing radiographs obtained before and after root canal preparation²⁻⁵⁾. On the other hand, Peters et al.¹⁸⁾ evaluated the surface area of the root canal by three-dimensional (3D) analysis, and observed that the Ni-Ti file did not contact $\geq 35\%$ of the root canal surface area. Therefore, 2D evaluation is not sufficient to explore the true shaping abilities before and after root canal preparation. In this study, we investigated the shaping characteristics and ability of JZ through a 3D analysis, and compared the findings with those of HCM and PTN, which are similar to JZ in terms of the mode of rotary motion, number of files used, point size, and taper.

Materials and Methods

1. Ni-Ti files and models

We used the following three types of Ni-Ti files (21 mm): JZ, #25/0.04 and #25/0.06; PTN, #17/0.04-0.075 and #25/0.06-0.07; and HCM, #15/0.04 and #25/0.06. J-shaped epoxy resin transparent root canal models (Dentsply Sirona, York, PA, USA; curvature, 30°; apical foramen diameter, #10; root canal taper, 0.02; root canal length, 17.0 mm; n=4) were used for root canal preparation. A root canal model which did not undergo any instrumentation was used as the control.

2. Root canal preparation

The operator was a dentist with 5 years of experience using Ni-Ti files. The working length of the root canal was determined using a #10 stainless steel K (SSK; Mani) file. After setting the working length to 17 mm and preparing a glide path with #15 and #20 SSK, the root canal was prepared using two types of files in each group. An endodontic motor, Tri Auto ZX 2 (J. Morita Corp., Tokyo, Japan), was used with the auto-reverse setting. Root canal preparation was performed by inserting the file in the root canal three times with light pressure with continuous rotation of the file such that the root length shaped per insertion did not exceed 3 mm. The rotation speed and torque used were 300 rpm and 3 N (JZ), 300 rpm and 2 N (PTN), and 500 rpm and 2.4 N (HCM), respectively, according to the manufacturer's recommendations. The root canal was irrigated with distilled water using a syringe. Recapitulation with a #10 SSK was performed to avoid clogging of the root apex with debris. This cycle was repeated until the sec-

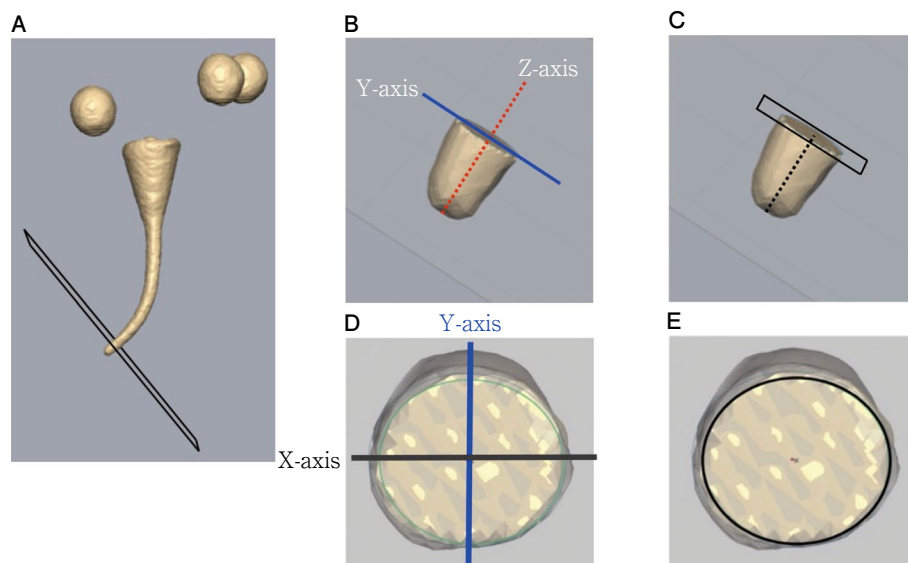


Fig. 1 Three-dimensional analysis of the models after root canal preparation

Covers with three spherical reference points were placed on the models, and dental CBCT was performed (A). The Z-axis (axial) was set to pass through the center of the root canal and apex 1 mm coronal to the apex and the corresponding root cross-section was considered the reference plane (B, C). The Y-axis (sagittal) was set along the direction of internal and external curvature perpendicular to the Z-axis (B, D), and the X-axis (coronal) was set perpendicular to the Y-axis (D). The intersection of the X-, Y-, and Z-axes was considered the shaping center (after instrumentation), and the canal center (before instrumentation) (E).

ond file reached the working length.

3. Dental cone-beam computer tomography (CBCT) and 3D analysis

Dental CBCT (3D Accuitomo F17, J. Morita Corp.) was performed to obtain 3D data before and after root canal preparation. A radiopaque material, Calcipex II (Nippon Shika Yakuhin Co., Ltd., Yamaguchi, Japan), was placed in the root canal using a syringe and accessory tip provided by the manufacturers. To prevent dead space in the model, the extrusion of Calcipex II from the apex was confirmed, and the syringe with the accessory tip was tightly inserted into the root canal orifice. The imaging conditions for dental CBCT were as follows: voxel size, 125 μm ; 50 kW; 1.0 mA. A cover with three spherical reference points (Fig. 1A) was attached to each model prior to dental CBCT imaging. These covers were made from a room-temperature polymerizing resin (Fixpeed, GC Corp., Tokyo, Japan) and Scanning Resin (Yamahachi Dental Mfg. Co., Aichi, Japan), a radiopaque instant polymerizing resin. The 3D data were reconstructed using ZedView Ver. 9.0 3D planning software (ZedView, LEXI Co. Ltd., Tokyo,

Japan) and displayed as images using Geomagic Freeform (3D Systems Inc., Rock Hill, SC, USA) (Fig. 1). The reference plane for evaluation was set 1 mm coronal to the apex, and the Z-axis (axial) was set as that passing through the center of the root canal and apex (Fig. 1B, C). In addition, the Y-axis (sagittal) was set as the direction of internal and external curvature perpendicular to the Z-axis, and the X-axis (coronal) was set perpendicular to the Y-axis (Fig. 1B, D). The intersection of the X-, Y-, and Z-axes was set as the shaping center, and the cross-section was considered the reference plane (Fig. 1E). The top part of Fig. 1E represents the inner curvature, while its bottom part represents the outer curvature. The distance of canal center transportation and the volume of the shaped root canal wall were calculated after superimposing the 3D data before and after root canal preparation using Geomagic Freeform (3D Systems Inc.). In addition, the angle of canal center transportation was measured by setting the internal curvature direction from the X-axis to 0–180° and the external curvature direction to 180–360°.

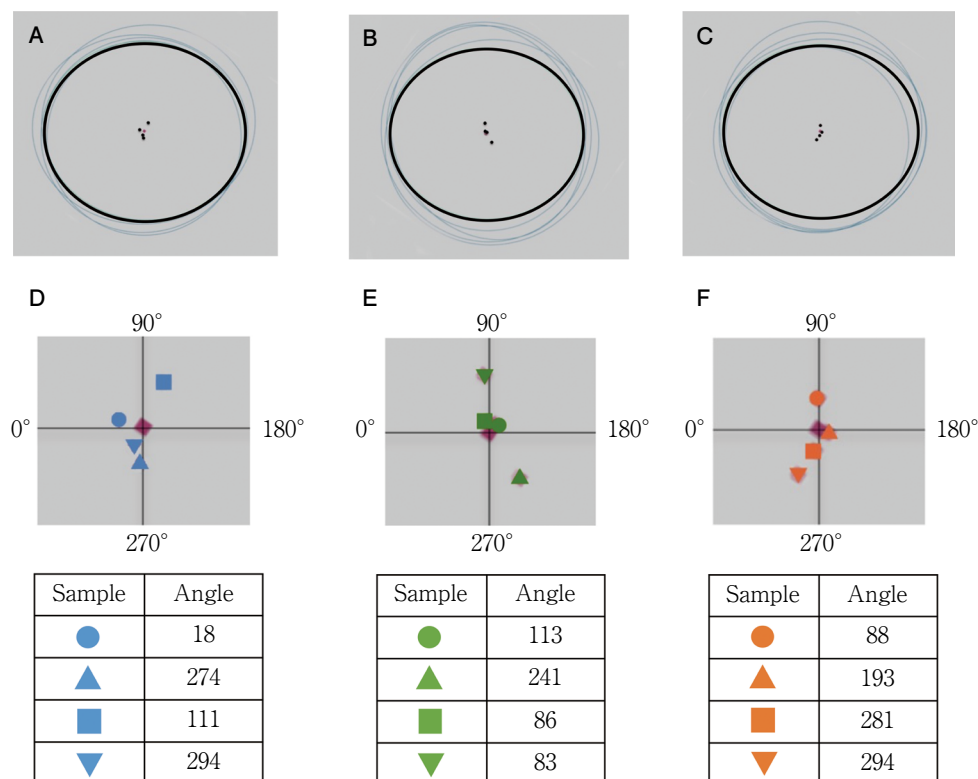


Fig. 2 Three-dimensional analysis of root canal formation with three types of files (n=4)

Shaping cross-section with JZ (A), HCM (B), and PTN (C). The black line indicates the original root canal before instrumentation, and the blue line indicates the shaped root canal wall after instrumentation (A-C). The canal center transportation with JZ (D), HCM (E), and PTN (F). The angle of canal center transportation was measured by setting the internal curvature direction from the X-axis to 0-180° and the external curvature direction to 180-360°, as shown at the bottom of each figure.

JZ, JIZAI Ni-Ti rotary file ; HCM, HyFlex CM Ni-Ti rotary file ; PTN, ProTaper Next Ni-Ti rotary file

4. Statistics

Median values of transportation of the canal center and volume of the shaped root canal wall for each group were analyzed by the Kruskal-Wallis test (Bell-Curve for Excel, Social Survey Research Information Co., Ltd., Tokyo, Japan) to identify significant differences. A p-value of <0.05 was considered to be statistically significant.

Results

We examined the cross-sectional morphology of the root canal following preparation with JZ, HCM, and PTN as an evaluation of the 3D shaping characteristics. The cross-section of the root canal tended to be circular following preparation with JZ and PTN (Fig. 2A, C),

similar to that in the control model. It tended to be elliptical after preparation with HCM, with the major axis along the Y-axis (Fig. 2B).

Next, we investigated the 3D characteristics and ability of the canal center transportation based on the file used. Although none of the files showed a tendency for deviation in a specific direction as shown in Fig. 2D, E, and F, the canal center transportation along the X-axis was the least with PTN (Fig. 2F). There was no characteristic transportation of the canal center along the Y-axis. As shown in Fig. 3A, the median value of transportation of the canal center was the largest with JZ and the least with HCM; however, no significant differences were observed between the files.

Further, we examined the volume of the shaped root canal wall as an evaluation of the shaping ability. As

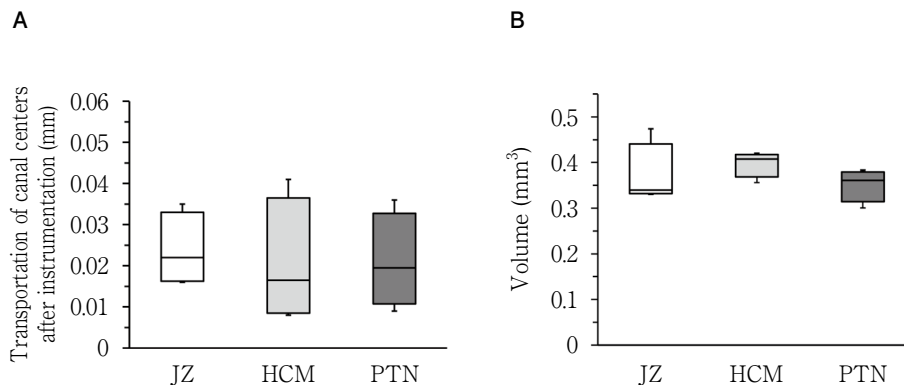


Fig. 3 Three-dimensional analysis of the canal center transportation and the volume of the shaped root canal wall at 1 mm coronal to the apex (n=4)

The distance of canal center transportation (A) and the volume of the shaped root canal wall (B).

JZ, JIZAI Ni-Ti rotary file ; HCM, HyFlex CM Ni-Ti rotary file ; PTN, ProTaper Next Ni-Ti rotary file

shown in Fig. 3B, the median value of volume was the largest with HCM and the least with JZ, with no significant difference between the files.

Discussion

In this study, we analyzed the shaping characteristics and ability of three types of Ni-Ti files, including a new file. It has been observed that approximately $\geq 35\%$ of the root canal surface area does not contact the Ni-Ti file during preparation¹⁸. This fact prompted us to think of using 3D analysis to evaluate the shaping characteristics and ability. Therefore, we performed 3D analysis using highly accurate CBCT images.

A previous 3D analysis¹⁹ showed that the extent of sagittal deviation was greatest at 1 mm coronal to the apex. Therefore, in this study, we analyzed the canal center transportation, the cross-sectional morphology, and the volume of the shaped root canal wall 1 mm coronal to the root apex. There was no significant difference in the median value of transportation of the canal center between the files, but JZ was the largest among all files. However, a 2D evaluation by Nakatsukasa et al.¹⁵ at 1 mm coronal to the root apex showed that the extent of deviation with JZ was slightly smaller but not significantly different from that with PTN. This discrepancy might be explained by the fact that the evaluation equivalent to the Y-axis (sagittal) transportation in this study was carried out by 2D analysis. In our 3D analysis, we evaluated both the X-axis (coronal) trans-

portation and the Y-axis transportation. We found that the Y-axis transportation was similar between the two files, whereas the X-axis transportation tended to be larger with JZ than with PTN.

On the other hand, HCM showed the least average transportation of the canal center but the largest amount of root canal wall removal. Compared to the other two files, the cross-section of HCM is slightly elliptical, with the long axis in the Y-axis direction of the inner and outer curvature. A previous micro-computed tomography study on the extent of transportation in the direction of the internal and external curvature found smaller deviation with HCM than with PTN¹⁹, which is consistent with the present results. The cross-section of the blade of HCM is triangular, that of PTN is rectangular, and that of JZ is irregularly rectangular. PTN and JZ have an offset design in which the rotation axis is away from the center of their cross-section^{10,16,17}. On rotation, this creates a wave-like motion that enables shaping of the root canal wall in three dimensions. HCM is not a land type, and the rake angle of the file is large^{8,9}. The present results do not clarify whether there is a relationship between the movement of the file during shaping and the morphology of the shaping surface. However, in clinical settings, the canals should be carefully shaped when there is a risk of perforating the side of the inner curvature, which is considered a danger zone. Therefore, clarifying the shaping characteristics of the file through a 3D analysis can help prevent endodontic procedural acci-

dents. Regarding the morphology of the shaping cross-section, we believe that the ideal shape is that of the control model, which resembles the original root canal morphology. JZ and PTN showed similar X- and Y-axis deviations and shaping cross-sections as those of the original root canal. However, relatively less shaping along the X-axis was observed with HCM, which showed a large deviation along the Y-axis. In the case of such a shape, for example, in cases requiring endodontic retreatment, residual infected dentin may be present due to inadequate canal preparation during the initial treatment. Therefore, selecting the Ni-Ti file based on each case may be necessary. Specifically, in buccolingually compressed root canals, selecting JZ or PTN may be helpful for adequate canal preparation.

The manufacturer recommends using a brushing motion for PTN and a light pecking motion for JZ and HCM. In this study, all three groups were operated with a light pecking motion, and the shaping characteristics were analyzed under conditions that excluded the possibility of the difference in motion affecting the results. Therefore, if the PTN is operated using the motion recommended by the manufacturer, it is possible that the results of this experiment may not match.

The shaping characteristics of Ni-Ti files have been evaluated with dental CBCT and micro-computed tomography with high resolution^{20,21}. Placement of reference points is necessary for 3D superposition; however, no well-defined method has been reported yet. In this study, we fabricated a cover to standardize the spheres made of radiopaque Scanning Resin that serve as three reference points, and used it during CBCT imaging.

Conclusions

In this study, we examined the 3D extent of canal center transportation and the morphology of the shaping cross-section, and the volume of shaped root canal wall following preparation with JZ, a Ni-Ti file recently introduced in Japan. The results of 3D analysis revealed that JZ had equivalent shaping ability to HCM and PTN. Therefore, JZ might be useful for safe preparation of root canals.

Acknowledgments

This research was partially supported by JSPS Grants-in-Aid for Scientific Research (JP20K9969, 23K09193). The authors thank Dr. Michito Maruta (Section of Bioengineering, Department of Dental Engineering, Fukuoka Dental College) for his assistance with the preliminary experiment. We also thank Editage (www.editage.jp) for their English language editing services.

Conflict of Interest

The authors declare no conflict of interest related to this manuscript.

References

- 1) Zupanc J, Vahdat-Pajouh N, Schäfer E. New thermomechanically treated NiTi alloys—a review. *Int Endod J* 2018; 51: 1088-1103.
- 2) Lu Shi, Wagle S. Comparing the centering ability of different pathfinding systems and their effect on final instrumentation by Hyflex CM. *J Endod* 2017; 43: 1868-1871.
- 3) Silva EJ, Tameirão MD, Belladonna FG, Neves AA, Souza EM, De-Deus G. Quantitative transportation assessment in simulated curved canals prepared with an adaptive movement system. *J Endod* 2015; 41: 1125-1129.
- 4) Saleh AM, Vakili Gilani P, Tavanafar S, Schäfer E. Shaping ability of 4 different single-file systems in simulated S-shaped canals. *J Endod* 2015; 41: 548-552.
- 5) Özyürek T, Yılmaz K, Uslu G. Shaping ability of Reciproc, WaveOne GOLD, and HyFlex EDM single-file systems in simulated S-shaped canals. *J Endod* 2017; 43: 805-809.
- 6) Kim HC, Yum J, Hur B, Cheung GS. Cyclic fatigue and fracture characteristics of ground and twisted nickel-titanium rotary files. *J Endod* 2010; 36: 147-152.
- 7) Zhou HM, Shen Y, Zheng W, Li L, Zheng YF, Haapasalo M. Mechanical properties of controlled memory and superelastic nickel-titanium wires used in the manufacture of rotary endodontic instruments. *J Endod* 2012; 38: 1535-1540.
- 8) Santos Lde A, Bahia MG, de Las Casas EB, Buono VT. Comparison of the mechanical behavior between controlled memory and superelastic nickel-titanium files via finite element analysis. *J Endod* 2013; 39: 1444-1447.
- 9) Gündoğar M, Özyürek T. Cyclic fatigue resistance of Oneshape, Hyflex EDM, Wave One Gold, and Resipro Blue nickel-titanium instruments. *J Endod* 2017; 43: 1192-1196.

- 10) Mittal R, Singla MG, Garg A, Dhawan A. A comparison of apical bacterial extrusion in manual, ProTaper rotary, and One Shape rotary instrumentation techniques. *J Endod* 2015; 41: 2040-2044.
- 11) Alapati SB, Brantley WA, Iijima M, Clark WA, Kovarik L, Buie C, Johnson WB. Metallurgical characterization of a new nickel titanium wire for rotary endodontic instruments. *J Endod* 2009; 35: 1589-1593.
- 12) Ye J, Gao Y. Metallurgical characterization of M-Wire nickel titanium shape memory alloy used for endodontic rotary instruments during low-cycle fatigue. *J Endod* 2012; 38: 105-107.
- 13) Peteira ES, Gomes RO, Leroy AM, Singh R, Peters OA, Bahia MG, Bahia MG. Mechanical behavior of M-Wire and conventional NiTi wire used to manufacture rotary endodontic instruments. *Dent Mater* 2013; 29: e318-324.
- 14) Gomaa MA, Osama M, Badr AE. Shaping ability of three thermally treated nickel-titanium systems in S-shaped canals. *Aust Endod J* 2021; 47: 435-441.
- 15) Nakatsukasa T, Ebihara A, Kimura S, Maki K, Nishijo M, Tokita D, Okiji T. Comparative evaluation of mechanical properties and shaping performance of heat-treated nickel titanium rotary instruments used in the single-length technique. *Dent Mater J* 2021; 40: 743-749.
- 16) Diemer F, Calas P. Effect of pitch length on the behavior of rotary triple helix root canal instruments. *J Endod* 2004; 30: 716-718.
- 17) Ha JH, Park SS. Influence of glide path on the screw-in effect and torque of nickel-titanium rotary files in stimulated resin root canals. *Restor Dent Endod* 2012; 37: 215-219.
- 18) Peters OA, Schönenberger K, Laib A. Effects of four Ni-Ti preparation techniques on root canal geometry assessed by micro computed tomography. *Int Endod J* 2001; 34: 221-230.
- 19) Huang Z, Quan J, Liu J, Zhang W, Zhang X, Hu X. A microcomputed tomography evaluation of the shaping ability of three thermally-treated nickel-titanium rotary file systems in curved canals. *J Int Med Res* 2019; 47: 325-334.
- 20) Pasqualini D, Alovisi M, Cemenasco A, Mancini L, Paolino DS, Bianchi CC, Roggia A, Scotti N, Berutti E. Micro-computed tomography evaluation of ProTaper Next and BioRace shaping outcomes in maxillary first molar curved canals. *J Endod* 2015; 41: 1706-1710.
- 21) Gagliardi J, Versiani MA, de Sousa-Neto MD, Plazas-Garzon A, Basrani B. Evaluation of the shaping characteristics of ProTaper Gold, ProTaper NEXT, and ProTaper Universal in curved canals. *J Endod* 2015; 41: 1718-1724.

Inhibition of Intracellular Glucose Metabolism by 2-deoxyglucose Suppresses Proliferation and Differentiation of Mouse Osteoblast-like Cells

Hirohito KATO, Yoichiro TAGUCHI, Runbo LI, Chiaki MANDAI, Masahiro NOGUCHI, Kei SHIOMI,
Hideki AKIMOTO, Sho MIZUTANI, Tomoko KANDA, Chizuko OGATA and Makoto UMEDA

Department of Periodontology, Osaka Dental University

Abstract

Purpose: Glucose metabolism plays a critical role in osteoblast differentiation and influences vital processes involved in bone formation and remodeling. This study explored the inhibitory effects of 2-deoxyglucose (2-DG) on glucose uptake by osteoblasts and its impact on cell differentiation.

Methods: Based on the structural similarity between 2-DG and glucose, the effects of glucose metabolism on osteoblast differentiation were examined by competitive inhibition of glucose uptake. MC3T3-E1 (mouse osteoblast-like cells) were cultured in media containing 10% FBS supplemented with 2-DG to evaluate cell proliferation and osteogenic differentiation.

Results: Inhibition of intracellular glucose metabolism by 2-DG inhibited MC3T3-E1 cell proliferation and mineralization. However, the gene expression of *Runx2* mRNA was enhanced in the 2-DG group. Moreover, there was a negligible difference in the osteocalcin production.

Conclusion: Decreased intracellular glucose metabolism inhibited osteoblast proliferation and differentiation.

Key words: glucose metabolism, osteoblasts, differentiation

Introduction

Bones play a crucial physiological role in supporting bodily movements, storing essential minerals such as calcium and phosphorus, and functioning as hematopoietic organs¹. Bone tissue constantly undergoes remodeling, with a continuous interplay between osteoblasts responsible for bone formation and osteoclasts responsible for bone resorption, ensuring the structural integrity and strength of the bones²⁻⁵. Therefore, it is important to elucidate the mechanisms regulating bone metabolism in periodontology. Alveolar bone regeneration is crucial in the success or failure of periodontal tissue regeneration therapy in periodontal treatment. Recent research has suggested that glucose metabolism plays a significant role in osteoblast differentiation⁶⁻⁸. Glucose serves as the primary substrate for cellular energy production and influences various cellular functions. Glucose uptake by osteoblasts has emerged as a critical regulatory checkpoint for osteoblast maturation and differentiation^{9,10}. Therefore, glucose metabolism may also be important in bone resorption in periodontitis and bone regeneration in periodontal tissue regeneration therapy.

2-Deoxyglucose (2-DG) shares structural similarities with glucose but cannot be metabolized intracellularly, competitively inhibiting glucose uptake. The characteristics of 2-DG are being researched for various applications, such as cancer therapy and immunotherapy¹¹⁻¹³. Therefore, it is important to investigate the effects of inhibiting glucose metabolism using 2-DG on osteoblast differentiation.

This study elucidated the importance of glucose metabolism in osteoblasts using osteoblast lineage cells, and the effect of 2-DG on osteoblast differentiation was clarified by inhibiting glucose uptake. The study may thus contribute to a better understanding of the regulatory mechanisms governing bone formation and metabolism by providing essential insights into glucose metabolism in osteoblasts.

Materials and Methods

1. Cell culture

MC3T3-E1 cells are immortalized mouse osteoblast-like cells that are commonly used for bone-related

culture studies. MC3T3-E1 cells were purchased from the Cell Engineering Division of RIKEN BioResource Research Center (Tsukuba, Japan), cultured in Modified Eagle's Medium (MEM; Nacalai Tesque, Kyoto, Japan), supplemented with 10% fetal bovine serum (FBS; HyClone, Thermo Fisher Scientific, MA, USA) and antibiotics (100 U/mL penicillin, 100 μ g/mL streptomycin, and 25 μ g/mL amphotericin B; Nacalai Tesque) at 37°C under 5% CO₂. The culture medium was changed every three days, and when the cells reached sub-confluence, they were harvested and subcultured. Cells were used between passages 3 and 6 for each experiment, according to our previous research methods¹⁴.

2. Conditions for culture medium with 2-DG solution

MC3T3-E1 cells were cultured in MEM supplemented with 10% FBS and a medium with a glucose concentration of 100 mg/dL was prepared with four 2-DG concentrations (0.05, 0.1, and 0.2 mM) dissolved in the medium. The concentration of 2-DG was selected by setting the highest concentration (0.2 mM) and diluting it two-fold with reference to the results of the cell proliferation. In this study, medium with a glucose concentration of 100 mg/dL was used as a positive control and medium with a glucose concentration of 0 mg/dL as a negative control. Osteogenic differentiation assays were performed using osteogenic medium containing 50 μ M L-ascorbic acid 2-phosphate (Nacalai Tesque), 10 mM β -glycerophosphate (Wako Pure Chemical Industries, Tokyo, Japan), and 10 nM dexamethasone (Wako Pure Chemical Industries) as previously described¹⁵.

3. Cell proliferation

The MC3T3-E1 cells were plated and adhered for 24 h. The medium was replaced with medium with or without 2-DG, and the cells were incubated for 24, 72, and 120 h. Cell proliferation was determined using Cell Count Reagent SF (Nacalai Tesque) by measuring the amount of formazan. The absorbance was measured at 450 nm and the data were analyzed using SoftMax Pro software (Molecular Devices, CA, USA).

4. Live cell staining

MC3T3-E1 cells were cultured in 24-well plates at a density of 2×10^3 cells/mL for 24 h. Subsequently, the medium was changed to a medium with or without 2-DG for 24, 72, and 120 h. At each time point, live cells were stained for 15 min at 37°C with 4 μ M Calcein-AM solution (Dojindo Molecular Technologies Inc., MD,

USA). Calcein-stained images were acquired using an all-in-one fluorescence microscope (BZ-9000, Keyence, Osaka, Japan), and the percentage of positively stained areas in the images was determined using ImageJ software (National Institutes of Health, MD, USA).

5. Cell migration assay

In this study, cell migration assay was performed using a wound repair assay kit (Ibidi GmbH, Martinsried, Germany). MC3T3-E1 cells were seeded at 3.5×10^4 cells/ $70 \mu\text{L}$ in a cell culture insert. After the cells reached confluence, the culture insert was removed and the medium was replaced with a serum-free medium containing 2-DG. Images of each wound were taken at 0, 12, and 24 h using a BZ-II all-in-one fluorescence microscope (Keyence). ImageJ software (National Institutes of Health) was used to measure the denuded area in each image. Data are presented as the percentage of healed wound area at 12 and 24 h compared with the initial wound at 0 h.

6. Alkaline phosphatase (ALP) staining

MC3T3-E1 cells were seeded in osteogenic Dulbecco's MEM (DMEM) with or without 2-DG and cultured for 1 or 2 weeks. To assess ALP activity, ALP staining was performed at each time point using an ALP staining kit (Sigma-Aldrich, MO, USA). In addition, staining intensity of ALP staining was evaluated using ImageJ software (National Institutes of Health).

7. Alizarin Red S (ARS) staining

MC3T3-E1 cells were cultured in osteogenic DMEM with or without 2-DG for 2 or 3 weeks. To assess the mineralization, the cells were stained with 1% ARS solution (Wako Pure Chemical Industries) for 3 min at room temperature and washed three times with phosphate-buffered saline. In addition, staining intensity of ARS staining was evaluated using ImageJ software (National Institutes of Health).

8. *Runx2* mRNA gene expression and osteocalcin (OCN) measurement

Whole-cell RNA was isolated using the RNeasy Mini Kit (Qiagen, Venlo, the Netherlands) and PrimeScript RT Reagent Kit (TAKARA Bio Inc., Kusatsu, Japan) according to the manufacturer's instructions. Gene expression was examined by real-time PCR assays (Thermo Fisher Scientific). mRNA expression of *Runx2* was evaluated using quantitative real-time PCR in accordance with standard protocols. Gene expression was normalized to the housekeeping gene glyceralde-

hyde phosphate dehydrogenase.

MC3T3-E1 cells were cultured in osteogenic DMEM, with or without 2-DG, for 3 weeks. The culture supernatant was collected and the quantity of OCN was quantified using an OCN detection kit (TAKARA Bio Inc.) according to the manufacturer's instructions.

9. Statistical analysis

Data are presented as the means \pm SD. One-way analysis of variance followed by Tukey's post hoc test was used to determine significance. p values < 0.05 were considered significant. Statistical analyses were performed using IBM SPSS Statistics Ver. 17 (IBM, IL, USA).

Results

1. Cell proliferation

The number of live cells stained with Calcein also decreased in the 2-DG group (Fig. 1A). According to the formazan test in the cell proliferation assay, the 2-DG group significantly suppressed the proliferative ability of MC3T3-E1 cells (Fig. 1B).

2. Cell migration

Cell migration was examined using a scratch assay; cell migration to the wound was significantly suppressed in the 2-DG (0.2 mM)-treated group compared to that in the control group (Fig. 2A). The migration ability showed a significant tendency to be gradually suppressed over time, and a concentration-dependent suppression tendency was observed in the 2-DG-added group after 24 h (Fig. 2B). There was a statistically significant difference in closure rates between the 0.05 mM test group and the other test groups, but no significant difference from the positive control of 100 mg/dL was identified.

3. ALP activity and mineralization

ALP staining intensity and activity were suppressed in the 2-DG-added group (Fig. 3). The number of calcifications stained with ARS was lower in the 2-DG-treated group (Fig. 4). ALP staining intensity at weeks 1 and 2 of incubation and ARS staining intensity at week 3 of incubation were lower than the negative control. This could be due to the strong inhibition of glucose metabolism by 2-DG.

4. *Runx2* mRNA gene expression and OCN production

The gene expression of *Runx2* significantly increased

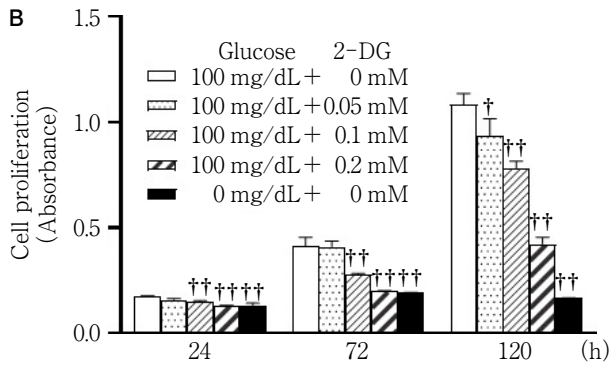
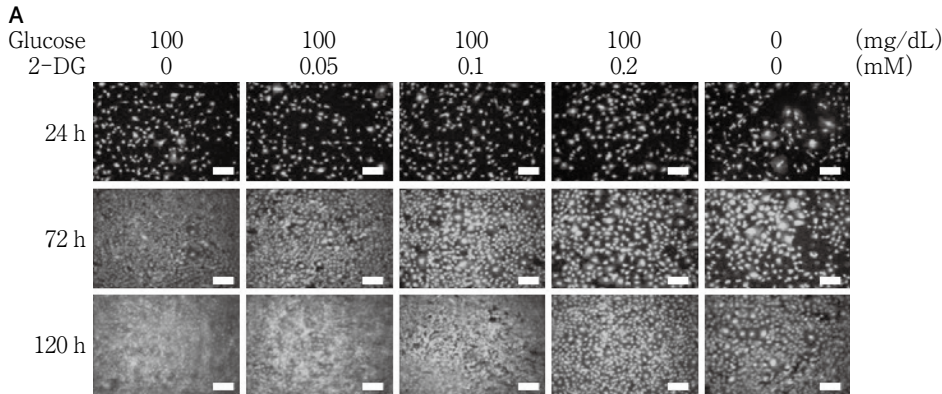


Fig. 1 Effect of 2-DG on cell proliferation in MC3T3-E1

(A) The number of viable cells (as detected through Calcein-AM staining) decreased in the 2-DG-added group and 0 mg/dL group (negative control). (B) The OD value of Cell Count Regent SF was assessed after culturing for 24, 72, and 120 h. Scale bars = 500 μ m. † : <0.05 versus control group. †† : <0.01 versus control group. Each experiment was performed three times for statistical analysis (n=3).

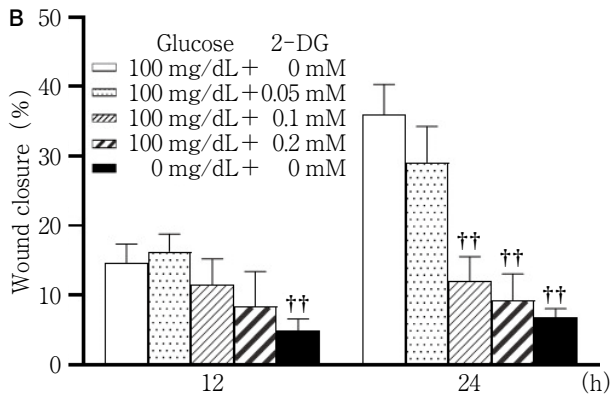
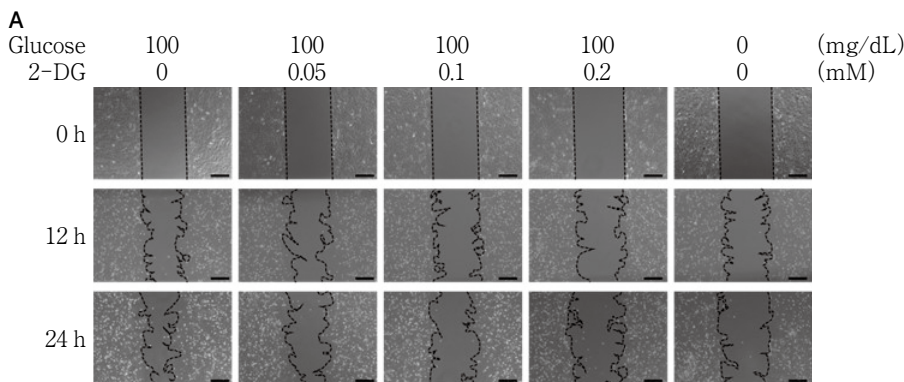


Fig. 2 Effect of 2-DG on cell migration in MC3T3-E1

(A) PDLCs were grown in a cell culture insert. After the cells reached confluence, the culture insert was removed and the medium was changed to a medium containing 2-DG. The final-to-initial wound size ratio represents the change in wound area. (B) The percentage of wound-healed area was measured after 0, 12, and 24 h. †† : <0.01 versus control group. Each experiment was performed three times for statistical analysis (n=3).

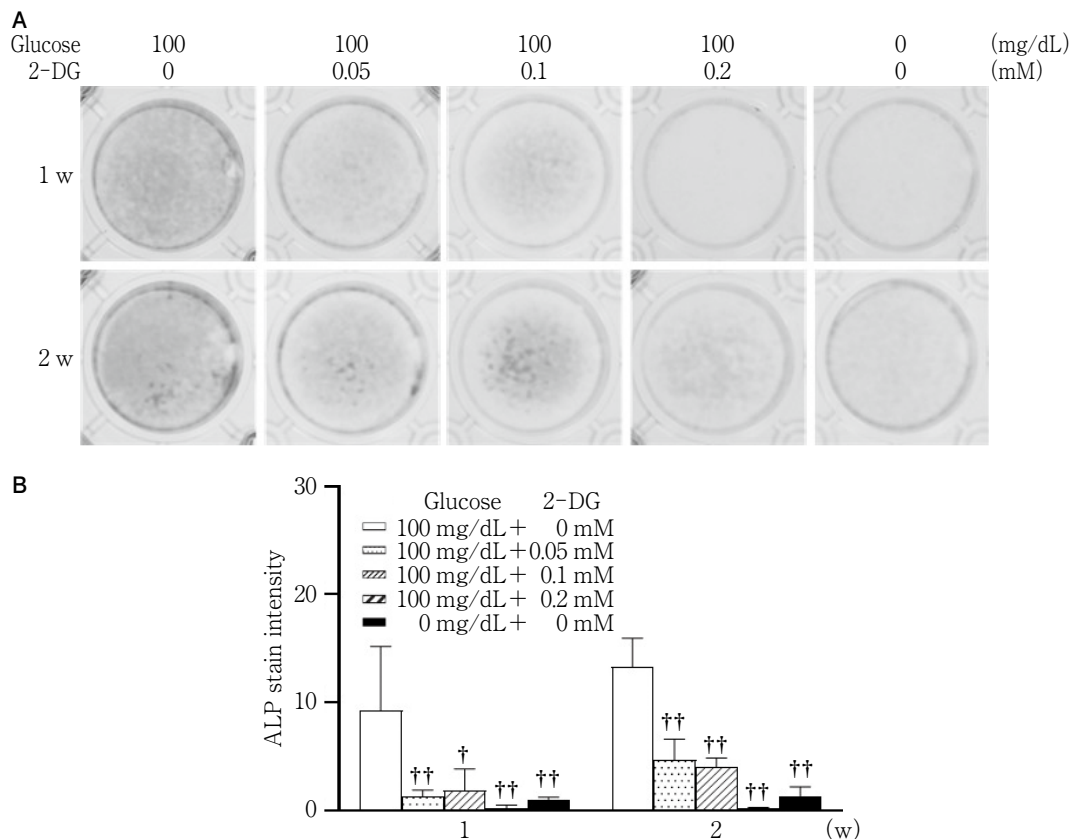


Fig. 3 Effect of 2-DG on ALP activity in MC3T3-E1

(A) The intensity of ALP staining was decreased in the 2-DG-added groups after 1 or 2 weeks. (B) Quantitative results were evaluated by Image J. † : <0.05 versus control group. †† : <0.01 versus control group. Each experiment was performed three times for statistical analysis (n=3).

in the 2-DG (0.2 mM) group (Fig. 5A). OCN production was slightly enhanced in the 2-DG-treated group; however, there was only a small difference in production (Fig. 5B).

Discussion

2-DG was used to investigate the effects of glucose metabolism on osteoblast differentiation. 2-DG is taken up by intracellular glucose transporters. Studies have reported that cells with a high glucose uptake capacity, such as osteoblasts and osteoclasts, are also characterized by a high 2-DG uptake capacity^{16,17}. The present study showed that the 2-DG-induced impairment of glucose metabolism suppressed the biological functions of mouse osteoblasts.

2-DG inhibited the proliferation and migration of mouse osteoblasts. Glucose metabolism regulates osteosarcoma cell growth¹⁸. In addition, our previous study showed that glucose metabolism was involved in the

migration of human gingival fibroblasts¹⁹. The observed inhibitory effects on cell proliferation and migration suggest that 2-DG could potentially interfere with the essential processes involved in bone formation and repair.

ALP is a specific marker of osteoblast differentiation and is expressed from early to mid-differentiation²⁰. The present study found that ALP activity was suppressed by the addition of 2-DG. The significant reduction in ALP activity in 2-DG-treated osteoblasts further supports the conjecture that 2-DG negatively affects mid-stage osteoblast differentiation. This is consistent with studies in other cell types, in which glycolysis inhibition has been associated with reduced ALP activity²¹. Thus, the inhibition of glucose metabolism may affect mid-stage osteoblast differentiation by suppressing ALP activity.

Mineralization has been evaluated as a marker of late osteoblast differentiation. Our results showed that the addition of 2-DG significantly suppressed mineralization.

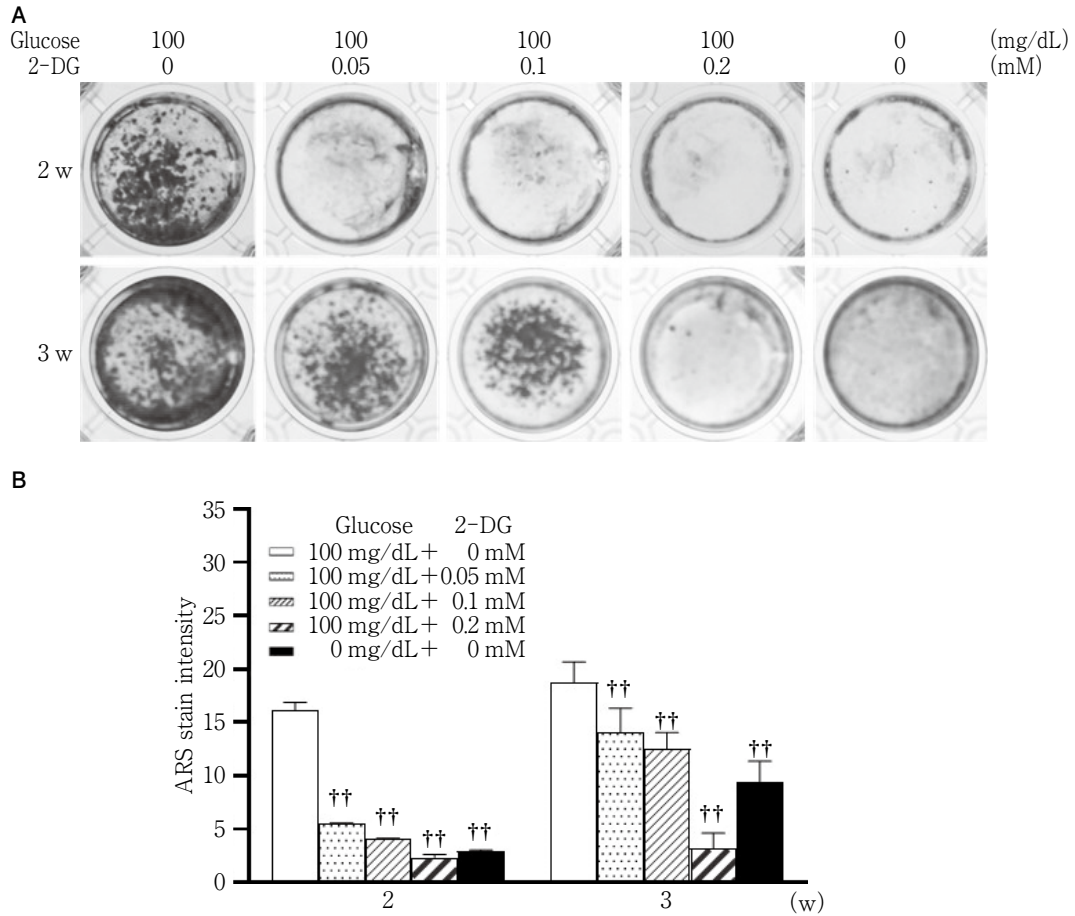


Fig. 4 Effect of 2-DG on mineralization in MC3T3-E1

(A) Calcified nodule formations stained with ARS were significantly decreased in the 2-DG-added groups. (B) Quantitative results were evaluated by Image J. ^{††} : <0.05 versus control group. Each experiment was performed three times for statistical analysis (n=3).

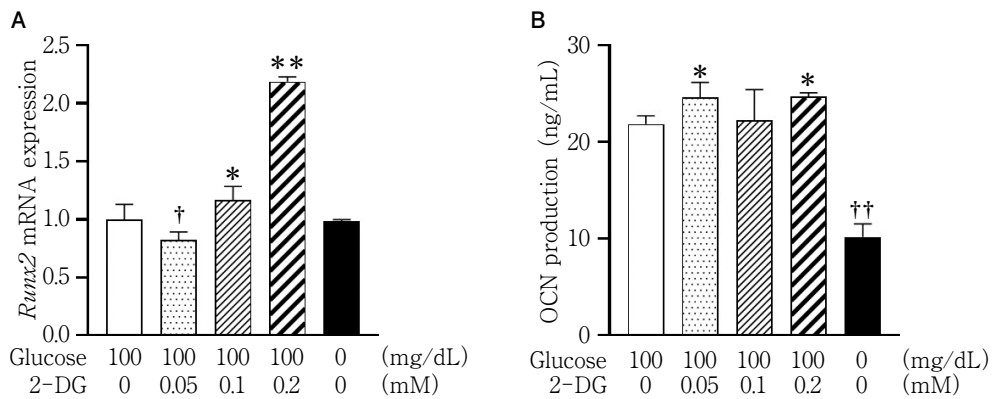


Fig. 5 Effect of 2-DG on *Runx2* mRNA expression and OCN production in MC3T3-E1

(A) *Runx2* mRNA expression in the 2-DG-added groups significantly increased or decreased depending on the concentration of 2-DG after 1 week. (B) Osteocalcin (OCN) production in the 2-DG-added groups increased after 3 weeks. A significant decrease compared with the control group is indicated by [†] : <0.05, ^{††} : <0.01. A significant increase compared with the control group is indicated by ^{*} : <0.05, ^{**} : <0.01. Each experiment was performed three times for statistical analysis (n=3). The expression of *Runx2* mRNA was evaluated as the ratio of expression at 100 mg/dL glucose concentration.

This result is similar to that of previous studies showing that bone formation is promoted by glucose transporters such as GLUT 1, 3, and 4²²⁾. Therefore, glucose metabolism is a key factor in bone mineralization.

Runx2 is a marker of early differentiation in osteoblast maturation and it is also an essential transcription factor in osteoblasts^{23,24)}. OCN is considered the most recently identified differentiation marker of osteoblasts among osteogenic markers²⁵⁾. The present study revealed unexpected results regarding *Runx2* and OCN. Although *Runx2* expression and OCN production were significantly enhanced in the 2-DG-added group, there was no particularly large difference in OCN production. The unexpected upregulation of *Runx2* gene expression in the 2-DG-treated group warrants further investigation. Inhibition of glucose metabolism by 2-DG may increase expression of *Runx2* as a result of the low degree of differentiation. Inhibition of early differentiation markers may indicate impaired osteoblast maturation, but 2-DG may not affect late osteoblast functionality, as there were significant but not large differences in OCN production. This observation suggests that the effects of 2-DG on osteoblast differentiation are selective and may vary at different stages of the differentiation process. *Runx2* is a gene that is expressed in osteoblasts in the early differentiated state. In this study, treatment with 0.2 mM 2-DG increased *Runx2* mRNA expression. We speculate that the increased expression of *Runx2* led to a low degree of differentiation and suppressed the formation of calcified nodules, which are an indicator of late differentiation. However, a detailed analysis using various molecular biological techniques would be required to demonstrate this phenomenon. We will examine the mechanisms involved in the increased mRNA expression of *Runx2* and OCN production in future research. The finding of the present study that 2-DG inhibits osteoblast proliferation and differentiation may lead to the discovery of a therapy through the regulation of glucose metabolism.

This study investigated the effects of 2-DG on osteoblast proliferation, migration and osteogenic differentiation. However, the role of glucose metabolism itself in osteoblasts remains to be elucidated. This study used 2-DG and osteoblasts to determine the importance of glucose metabolism in bone formation. However, further studies are required to elucidate the molecular mechanisms underlying these effects and explore the

potential clinical implications of these findings in relation to bone-related diseases and therapies.

Conclusions

The findings of this study suggest that inhibitory effects of 2-DG on osteoblast proliferation, migration, and osteogenic differentiation markers may have potential negative effects on bone formation.

Conflict of interest

The authors declare no conflicts of interest associated with this manuscript.

Acknowledgements

This study was partially supported by Grants-in-Aid for Scientific Research from the Japan Society for the Promotion of Science (C) (21K09946, 22K17084, and 22K09993) and the Osaka Dental University Research Promotion Grant (23-10).

References

- 1) Datta HK, Ng WF, Walker JA, Tuck SP, Varanasi SS. The cell biology of bone metabolism. *J Clin Pathol* 2008; 61: 577-587.
- 2) Boyle WJ, Simonet WS, Lacey DL. Osteoclast differentiation and activation. *Nature* 2003; 423: 337-342.
- 3) Parfitt AM. The coupling of bone formation to bone resorption: a critical analysis of the concept and of its relevance to the pathogenesis of osteoporosis. *Metab Bone Dis Relat Res* 1982; 4: 1-6.
- 4) Martin T, Gooi JH, Sims NA. Molecular mechanisms in coupling of bone formation to resorption. *Crit Rev Eukaryot Gene Expr* 2009; 19: 73-88.
- 5) Lee WC, Guntur AR, Long F, Rosen CJ. Energy metabolism of the osteoblast: implications for osteoporosis. *Endocr Rev* 2017; 38: 255-266.
- 6) Ning K, Liu S, Yang B, Wang R, Man G, Wang DE, Xu H. Update on the effects of energy metabolism in bone marrow mesenchymal stem cells differentiation. *Mol Metab* 2022; 58: 101450.
- 7) van Gestel N, Carmeliet G. Metabolic regulation of skeletal cell fate and function in physiology and disease. *Nat Metab* 2021; 3: 11-20.
- 8) Karner CM, Long F. Glucose metabolism in bone. *Bone* 2018; 115: 2-7.
- 9) Wei J, Shimazu J, Makinistoglu MP, Maurizi A, Kajimura D, Zong H, Takarada T, Lezaki T, Pessin JE, Hinoi E,

- Karsenty G. Glucose uptake and Runx2 synergize to orchestrate osteoblast differentiation and bone formation. *Cell* 2015; 161: 1576-1591.
- 10) Li W, Deng Y, Feng B, Mak KK. Mst1/2 kinases modulate glucose uptake for osteoblast differentiation and bone formation. *J Bone Miner Res* 2018; 33: 1183-1195.
 - 11) Zhang D, Li J, Wang F, Hu J, Wang S, Sun Y. 2-Deoxy-D-glucose targeting of glucose metabolism in cancer cells as a potential therapy. *Cancer Lett* 2014; 355: 176-183.
 - 12) Sottnik JL, Lori JC, Rose BJ, Thamm DH. Glycolysis inhibition by 2-deoxy-D-glucose reverts the metastatic phenotype in vitro and in vivo. *Clin Exp Metastasis* 2011; 28: 865-875.
 - 13) Christofi M, Le Sommer S, Mölzer C, Klaska IP, Kuffova L, Forrester JV. Low-dose 2-deoxy glucose stabilises tolerogenic dendritic cells and generates potent in vivo immunosuppressive effects. *Cell Mol Life Sci* 2021; 78: 2857-2876.
 - 14) Li R, Kato H, Nakata T, Yamawaki I, Yamauchi N, Imai K, Taguchi Y, Umeda M. Essential amino acid starvation induces cell cycle arrest, autophagy, and inhibits osteogenic differentiation in murine osteoblast. *Biochem Biophys Res Commun* 2023; 672: 168-176.
 - 15) Deng X, Kato H, Taguchi Y, Nakata T, Umeda M. Intracellular glucose starvation inhibits osteogenic differentiation in human periodontal ligament cells. *J Periodontal Res* 2023; 58: 607-620.
 - 16) Knowles HJ. Distinct roles for the hypoxia-inducible transcription factors HIF-1 α and HIF-2 α in human osteoclast formation and function. *Sci Rep* 2020; 10: 21072.
 - 17) Hollenberg AM, Smith CO, Shum LC, Awad H, Eliseev RA. Lactate dehydrogenase inhibition with oxamate exerts bone anabolic effect. *J Bone Miner Res* 2020; 35: 2432-2443.
 - 18) Feng Z, Ou Y, Hao L. The roles of glycolysis in osteosarcoma. *Front Pharmacol* 2022; 13: 950886.
 - 19) Li R, Kato H, Taguchi Y, Umeda M. Intracellular glucose starvation affects gingival homeostasis and autophagy. *Sci Rep* 2022; 12: 1230.
 - 20) Weinreb M, Shinar D, Rodan GA. Different pattern of alkaline phosphatase, osteopontin, and osteocalcin expression in developing rat bone visualized by in situ hybridization. *J Bone Miner Res* 1990; 5: 831-842.
 - 21) Takeno A, Kanazawa I, Tanaka KI, Notsu M, Sugimoto T. Phloretin suppresses bone morphogenetic protein-2-Induced Osteoblastogenesis and Mineralization via inhibition of phosphatidylinositol 3-kinases/Akt pathway. *Int J Mol Sci* 2019; 20: 2481.
 - 22) Arponen M, Jalava N, Widjaja N, Ivaska KK. Glucose transporters GLUT1, GLUT3, and GLUT4 have different effects on osteoblast proliferation and metabolism. *Front Physiol* 2022; 13: 1035516.
 - 23) Komori T. Runx2, a multifunctional transcription factor in skeletal development. *J Cell Biochem* 2002; 87: 1-8.
 - 24) Komori T. Runx2, an inducer of osteoblast and chondrocyte differentiation. *Histochem Cell Biol* 2018; 149: 313-323.
 - 25) García-Martín A, Reyes-García R, Avila-Rubio V, Muñoz-Torres M. Osteocalcin: a link between bone homeostasis and energy metabolism. *Endocrinol Nutr* 2013; 60: 260-263.

Risk of an Immediate-type Allergy to Minocycline Hydrochloride Ointment

Maki HOSOKI¹, Yoshifumi OKAMOTO², Toyoko TAJIMA¹, Mayu MIYAGI¹, Yoshiaki KUBO³,
Maiko SOGAWA³, Resmi RAJU⁴, Shaista AFROZ⁵ and Yoshizo MATSUKA¹

¹Department of Stomatognathic Function and Occlusal Reconstruction,
Tokushima University Graduate School of Biomedical Sciences

²Tokushima Prefecture Dental Association

³Department of Dermatological Science, Tokushima University Graduate School of Biomedical Sciences

⁴Eunice Kennedy Shriver National Institute of Child Health and Human Development (NICHD),
National Institutes of Health (NIH)

⁵Department of Prosthodontics and Dental Material, Aligarh Muslim University (India)

Abstract

Minocycline hydrochloride ointment is applied to periodontal pockets to treat periodontal disease. We encountered a case of an immediate-type allergy to minocycline hydrochloride dental ointment, despite the absence of a history of allergies to antibiotics.

Case report: The patient was a 72-year-old female, with no significant medical history. Systemic erythema and urticaria developed in June 2017. Similar symptoms occurred again in October and November 2017, for which she consulted for an internal medicine examination. However, the cause remained unknown. Because the symptoms always occurred after she received treatment for periodontal disease, we performed a prick test to diagnose any possible allergy caused by the materials used in her dental treatment. A positive reaction to the allergy test was reported for minocycline hydrochloride ointment. We informed her dentist and requested that periodontal maintenance treatment with minocycline hydrochloride ointment be ceased.

Course: She has not exhibited any allergic symptoms since the application of minocycline hydrochloride ointment was stopped.

Discussion: It was suspected that allergic symptoms could have developed during the course of periodontal maintenance treatment. Given that the incidence of allergic reactions is increasing, it is important to consider the possibility of allergic reactions to dental materials and medicaments.

Conclusion: An incremental application of a small amount of topical dental antibiotics into the periodontal pocket can result in immediate-type allergic reaction.

Key words: allergy, urticaria, minocycline hydrochloride ointment

Introduction

Minocycline is a semisynthetic, second-generation tetracycline derivative and is used worldwide for the treatment of acne. The mechanism of action is the inhibition of bacterial protein synthesis. It does not act on animal ribosome 80S, but specifically acts on bacterial ribosome 70S, so that the aminoacyl tRNA is inhibited from binding to the mRNA ribosome complex. The antibacterial spectrum is broad, and includes gram positive and negative bacteria, rickettsia, and chlamydia. The antibacterial activity is one to four times stronger than that of tetracycline. It has also been reported to be effective as an adjunct to scaling and root planing¹⁻³).

However, there are many reports of pigmentation as a side effect of minocycline⁴⁻¹¹). There are also some reports of anaphylaxis¹²⁻¹⁵). Additionally, minocycline is contraindicated in patients with a history of hypersensitivity to other drugs in the tetracycline group of antibiotics such as tetracycline and doxycycline^{15,16}). However, there have been fewer reported cases of allergy to minocycline than to other antibiotics such as penicillin and cephalosporin¹⁷).

We report a case of immediate-type allergy to minocycline hydrochloride dental ointment 2% (Periofeel Dental Ointment 2%, Showa Yakuhin Kako Co., Tokyo, Japan), used at the time of periodontal treatment, even though the patient had no history of allergy to any antibiotic.

Consent was obtained from the patient for publication. After obtaining consent, we inquired about treatment details from the internist.

Case Report

A 72-year-old Japanese female who developed recurrent allergic symptoms following each session of treatment for periodontal disease was referred for an allergy test, to rule out the possibility of allergic reactions to any dental materials, at Tokushima University Hospital in June 2017.

Her medical history was not significant except for insomnia and there was no history of allergic disease. History of dental treatments included dental implant surgery (bilateral mandibular molars) in 2003, treatments for intra-oral candidiasis in 2005, and temporo-

mandibular joint disorder in 2005. She had consulted several dentists for regular dental treatment over the years.

In February 2017, the patient consulted a new dental clinic for the treatment of periodontal disease. She received general periodontal maintenance treatment (scaling, root planing and polishing). A panoramic dental radiograph (Fig. 1) of the patient taken in February 2017 revealed five dental implants in the mandibular molar area. No significant pathological findings were observed around the implants. Alveolar bone resorption was observed around the molars, especially around the right lower second molar (Table 1).

The history of her present illness was as follows. In June 2017, she visited a dental clinic at around 16 : 00, where she received periodontal maintenance treatment. She returned home around 17 : 00. Later that day, the patient noticed urticaria all over her body, except for her face. Because the hospital was closed, she purchased over-the-counter medicine for local application and oral administration from a drugstore. Fortunately, her symptoms were relieved after taking the medicine. Similar symptoms recurred in the months of October and November 2017. At that time she consulted a physician and received an internal medicine examination. According to the physician, erythema and urticaria were observed throughout her body with the concomitant symptoms of nausea and diarrhea. The patient was treated with betamethasone sodium phosphate (RINDERON Injection, Shionogi Healthcare Co., Osaka, Japan) and metoclopramide hydrochloride (Primperan Injection, Nichi-Iko Pharmaceutical Co., Ltd., Toyama, Japan) drips, and was prescribed prednisolone (PREDONINE Tablets, Shionogi Healthcare Co.) 5 mg, Fexofenadine hydrochloride (Allegra Tablets, Sanofi K. K., Tokyo, Japan) 2T, and l-cysteine (HYTHIOL Tablets, Hisamitsu Pharmaceutical Co., Inc., Saga, Japan) 1T, and her symptoms seemed to subside. Her diagnosis was recorded as idiopathic urticaria. The patient noticed that the allergy recurred after each dental treatment and consulted her family dentist, who referred the patient to the dental metal allergy clinic of Tokushima University Hospital for allergy testing.

Allergy testing for the dental materials was planned and progress was monitored. There were seven dental medicaments that had been used in the dental clinic: six kinds of toothpaste and minocycline hydrochloride den-

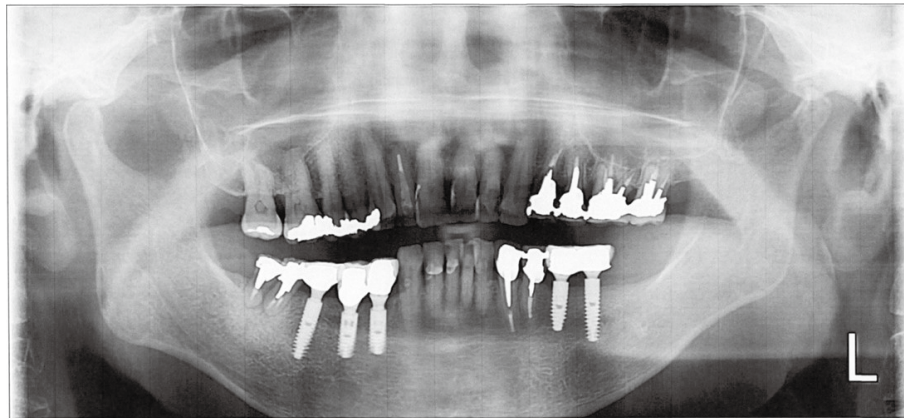


Fig. 1 Panoramic dental radiograph in February 2017

Alveolar bone resorption was observed around the molars, especially around the right lower second molar.

Table 1 Periodontal examination

2017 February	Mobility	0	0	0	0	0	0	0	0	0	0	0	0	0	0
	BOP	+	-	-	-	-	-	-	-	-	-	+	+	+	-
	EPP	4	4	3	3	3	3	3	3	3	3	4	5	4	4
		7	6	5	4	3	2	1	1	2	3	4	5	6	7
	EPP	6				3	3	3	3	3	3	4			/
	BOP	+				-	-	-	-	-	-	-			
	Mobility	0				0	0	0	0	0	0	0			
2017 March	Mobility	0	0	0	0	0	0	0	0	0	0	0	0	0	0
	BOP	-	+	-	-	-	-	-	-	-	-	-	-	+	+
	EPP	4	4	3	3	3	3	3	3	3	3	3	4	4	4
		7	6	5	4	3	2	1	1	2	3	4	5	6	7
	EPP	6				3	3	3	3	3	3	4			/
	BOP	+				-	-	-	-	-	-	-			
	Mobility	0				0	0	0	0	0	0	0			
2017 June	Mobility	0	0	0	0	0	0	0	0	0	0	0	0	0	0
	BOP	+	+	-	-	-	-	-	-	-	-	+	+	+	+
	EPP	4	4	3	3	3	3	3	3	3	3	3	3	4	4
		7	6	5	4	3	2	1	1	2	3	4	5	6	7
	EPP	7				3	3	3	3	3	3	3			/
	BOP	+				-	-	-	-	-	-	-			
	Mobility	0				0	0	1	1	0	0	0			
2017 October	Mobility	0	0	0	0	0	0	1	1	0	0	0	0	0	0
	BOP	-	-	-	-	-	-	-	-	-	-	-	-	-	-
	EPP	3	3	3	2	3	3	3	3	3	3	2	2	3	3
		7	6	5	4	3	2	1	1	2	3	4	5	6	7
	EPP	6				3	3	2	2	2	3	3			/
	BOP	-				-	-	-	-	-	-	-			
	Mobility	0				0	0	1	1	0	0	0			

Periodontal treatment reduced inflammation and periodontal pockets slightly.

Examination of Periodontal Pocket (EPP), Bleeding on Probing (BOP)

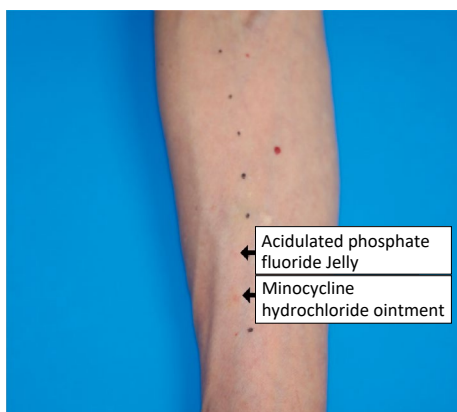


Fig. 2 The results of a prick test

The results of the prick test after 30 minutes are shown. Minocycline hydrochloride ointment showed a positive reaction. Eventually, acidulated phosphate fluoride jelly showed a negative reaction.

tal ointment which was applied to the gingival sulcus for treating periodontitis.

We conducted an open test for possible allergy to all the materials used for her dental treatment on the inner side of the patient's upper arm. The results were all negative after 15 minutes, 30 minutes and 60 minutes. A subsequent prick test showed a positive reaction to minocycline hydrochloride dental ointment. Eventually, acidulated phosphate fluoride jelly showed a negative reaction (Fig. 2). The family dentist and the patient were informed about the positive allergic reaction to minocycline hydrochloride. The dentist was advised to discontinue the usage of minocycline hydrochloride dental ointment for this patient.

Clinical Course

For the next six months, she received maintenance treatment by the family dentist on three occasions, but no subsequent allergic symptoms were observed.

Discussion

Drug allergy is an immune-mediated reaction. Most medicines have a small molecular weight, so antigenicity is low. However, they may become antigenic by binding with macromolecules such as protein *in vivo*. Antimicrobial and antifebrile agents are particularly

likely to cause drug allergy. Symptoms include itching, rash, fever, asthma, anaphylaxis, and severe forms of drug reactions such as Stevens-Johnson syndrome (SJS) and toxic epidermal necrolysis (TEN). Most drug allergies are classified as type I allergies. However, some drugs can also cause delayed allergic reactions, known as type IV allergies. In this case, based on the symptoms and test results, we concluded that a type I allergy was more likely than a type IV allergy. Diagnosis is established clinically by using a skin test. The first step following a positive allergic reaction test is to stop the use of any of the causative agents or drugs, followed by the administration of antihistamines and steroid drugs as needed¹⁷⁾.

Allergy to minocycline is less common than to penicillin and cephalosporin, in which the symptoms develop following oral administration rather than by topical administration as in minocycline hydrochloride ointment^{1,17)}. Minocycline hydrochloride ointment is a dental antibiotic formulation that is applied locally to periodontal pockets, usually once a week, for the treatment of periodontitis. Minocycline hydrochloride dental ointment 2% (Periofeel Dental Ointment 2%, Showa Yakuhin Kako Corp.) (1 syringe 0.5 g) contains 10 mg of minocycline hydrochloride. As of October 2022, the Pharmaceuticals and Medical Devices Agency (PMDA) has reported 12 cases of adverse reactions to minocycline hydrochloride ointment in Japan (Table 2). Minocycline hydrochloride ointment is contraindicated in patients with a history of hypersensitivity to the tetracycline group of antibiotics, and the risk of anaphylaxis or urticaria is naturally high when used in patients with any allergies to internal medicines. In the reported cases (Table 2), it is not clear whether there was a history of allergy to antibiotics in the past, and it is also not clear whether the onset occurred after multiple usage. In this case, there was no history of any allergic symptoms to antibiotics in the past, and there was no history of long-term administration of antibiotics such as minocycline hydrochloride (Minomycin, Pfizer Inc., New York, USA). A sleep-inducing drug, Zolpidem Tartrate (Myslee Tablets, Astellas Pharma Inc., Tokyo, Japan), was prescribed for insomnia by a family physician. She had no other significant medical history. Moreover, no allergic symptoms developed in February and March 2017 when periodontal treatment was performed without using minocycline hydrochloride oint-

Table 2 Side effect case list

No.	Year of occurrence	Sex	Age	Symptoms	Presence of suspected concomitant medication
1	2005	Female	60's	Vomiting, dyspnea, rash, erythema, pruritus	—
2	2006	Male	40's	Anaphylactic shock	—
3	2006	Male	50's	Anaphylactic shock (details unknown)	Ceftream Pivoxil, Loxoprofen Sodium Hydrate, Acrinol Hydrate
4	2009	Male	60's	Shock symptoms	Hydrogen Peroxide
5	2010	Male	60's	Laryngeal edema, whole body erythema	—
6	2014	Male	50's	Anaphylactoid reaction	—
7	2014	Female	60's	Drug eruption	Mecobalamin, Adenosine 5'-Triphosphate Disodium Hydrate, Isosorbide, Pitavastatin Calcium
8	2015	Female	20's	Shock symptoms	—
9	2018	Male	70's	Decreased level of consciousness, rash	—
10	2018	Male	70's	Anaphylactic shock	Pranoprofen, Teprenone, Amoxicillin Hydrate, Ethyl Aminobenzoate, Benzethonium Chloride, Lidocaine Hydrochloride/Adrenaline
11	2019	Female	60's	Hypersensitivity	—
12	2019	Female	50's	Anaphylactic shock	—

Twelve cases of side effects of minocycline hydrochloride ointment were reported to the Pharmaceuticals Medical Devices Agency of Japan.

ment. Although a prick test for minocycline hydrochloride was not conducted, it is possible that the additive in the dental ointment was the cause. However, current reports only suggest the possibility of diarrhea from high intake of such additives, and the likelihood of causing urticaria, as observed in this case, is considered to be low. Additionally, while the additive hypromellose is used in drug capsules, the patient had no recollection of an allergy to capsule-shaped medications. This suggests that the minocycline hydrochloride ointment used in the dental clinic resulted in sensitization/onset, causing her to develop allergic symptoms after her periodontal treatment in June. Minocycline hydrochloride ointment contains 10 mg of minocycline hydrochloride and, even if all the syringe is used, it is less than 1/10 of the dose of oral minocycline (100–200 mg). However, when it is used for periodontal maintenance, the duration of use is often long. Knowles et al. suggested that taking oral minocycline for more than 2 years increases the likelihood of allergies. We recommend that these risk factors be taken into account when minocycline hydrochloride

ointment is used over an extended period of time¹⁵⁾.

Conclusion

An incremental application of a small amount of topical dental antibiotics into the periodontal pocket can result in an immediate-type allergic reaction. It is important to document such cases so that dental practitioners can be aware of documented allergies to various dental materials for a proper diagnosis and to avoid such allergic reactions in the clinical practice.

Acknowledgements

We thank Helen Jeays, BSc AE, from Edanz Group (www.edanzediting.com/ac) for editing a draft of this manuscript.

Conflict of Interest

Conflict of Interest and Source of Funding:

This study was partly supported by “The initiative for Realizing Diversity in the Research Environment (Distinc-

tive Features Type and Collaboration Type)” of the Japanese Ministry of Education, Culture, Sports, Science and Technology and Grant-in-Aid for Scientific Research of Japan (20K10038). The authors state explicitly that there are no conflicts of interest in connection with this article.

References

- 1) Kassem AA, Ismail FA, Naggar VF, Aboulmagd E. Comparative study to investigate the effect of meloxicam or minocycline HCl in situ gel system on local treatment of periodontal pockets. *AAPS PharmSciTech* 2014; 15: 1021-1028.
- 2) Deng S, Wang Y, Sun W, Chen H, Wu G. Scaling and root planning, and locally delivered minocycline reduces the load of *Prevotella intermedia* in an interdependent pattern, correlating with symptomatic improvements of chronic periodontitis: a short-term randomized clinical trial. *Ther Clin Risk Manag* 2015; 11: 1795-1803.
- 3) Matthews D. Local antimicrobials in addition to scaling and root planing provide statistically significant but not clinically important benefit. *Evid Based Dent* 2013; 14: 87-88.
- 4) Ban M, Kitajima Y. Nail discoloration occurring after 8 weeks of minocycline therapy. *J Dermatol* 2007; 34: 699-701.
- 5) Cockings, JM, Savage NW. Minocycline and oral pigmentation. *Aust Dent J* 1998; 43: 14-16.
- 6) Geria AN, Tajirian AL, Kihiczak G, Schwartz RA. Minocycline-induced skin pigmentation: an update. *Acta Dermatovenerol Croat* 2009; 17: 123-126.
- 7) Haskes C, Shea M, Imondi D. Minocycline-induced scleral and dermal hyperpigmentation. *Optom Vis Sci* 2017; 94: 436-442.
- 8) Hung PH, Caldwell JB, James WD. Minocycline-induced hyperpigmentation. *J Fam Pract* 1995; 41: 183-185.
- 9) Krause W. Drug-induced hyperpigmentation: a systematic review. *J Dtsch Dermatol Ges* 2013; 11: 644-651.
- 10) Siller GM, Tod MA, Savage NW. Minocycline-induced oral pigmentation. *J Am Acad Dermatol* 1994; 30: 350-354.
- 11) Treister NS, Magalnick D, Woo SB. Oral mucosal pigmentation secondary to minocycline therapy: report of two cases and a review of the literature. *Oral Surg Oral Med Oral Pathol Oral Radiol Endod* 2004; 97: 718-725.
- 12) Okano M, Imai S. Anaphylactoid symptoms due to oral minocycline. *Acta Derm Venereol* 1996; 76: 164.
- 13) Hitchcock MG, Williford PM, Clayton BD. Minocycline hypersensitivity with respiratory failure. *Arch Dermatol* 1999; 135: 139-140.
- 14) Jang JW, Bae YJ, Kim YG, Jin YJ, Park KS, Cho YS, Moon HB, Kim TB. A case of anaphylaxis to oral minocycline. *J Korean Med Sci* 2010; 25: 1231-1233.
- 15) Knowles SR, Shapiro L, Shear NH. Serious adverse reactions induced by minocycline. Report of 13 patients and review of the literature. *Arch Dermatol* 1996; 132: 934-939.
- 16) Hamilton LA, Guarascio AJ. Tetracycline allergy. *Pharmacy (Basel)* 2019; 7: 104.
- 17) Baldo BA, Pham NH. *Drug Allergy: Clinical Aspects, Diagnosis, Mechanisms, Structure-Activity Relationships*. Springer: Berlin: 2013. 1-181, 245-313.

Submission Guidelines for *ODEP*

1. *ODEP* aims to develop conservative dentistry (operative dentistry, endodontology, and periodontology) through the publication of research and reviews on the following topics: (1) General dental medicine, clinical practice, and education on conservative dentistry; and (2) Conservative dentistry.
2. Papers are categorized into the following four types: (1) Original articles (reports on unique research discoveries); (2) Reviews (discussions on research questions and objectives to indicate future directions, or summaries of the contents of existing papers to propose new ideas); (3) Mini reviews (concise summaries of recent topics; mini reviews include papers awarded with prizes); and (4) Case and clinical reports (analysis of clinical records useful for dental care practice and development of the field of conservative dentistry). Reviews and mini reviews are categorized into the following: (1) Papers requested by the editorial board; and (2) Submitted papers.
3. Original articles and case and clinical reports are limited to the following: (1) Papers that have not been published in other journals; (2) Papers that are not presently submitted to another journal; and (3) Papers that are not presently scheduled for publication.
4. Acceptance or rejection of papers is determined through peer review (except for papers requested by the editorial board).
5. Submitted papers should be concisely written in English.
6. In principle, original articles should be organized as follows: (1) Abstract; (2) Introduction; (3) Materials and Methods; (4) Results; (5) Discussion; (6) Conclusion; (7) References; (8) Figure legend; (9) Figures and Tables. In principle, papers other than original articles should conform to the style format of original articles.
7. In principle, *ODEP* is published once a year in December. In addition, special issues are published when appropriate.
8. The Japanese Society of Conservative Dentistry provides a certain amount of support for the listing fees of papers. For cases in which the lead author is not a member of the Japanese Society of Conservative Dentistry, such support is not provided. For cases in which the lead author is a member, but the co-authors include a non-member, partial support is provided. The cost to be borne by the authors is determined based on the number of non-members. The costs for figures, tables and photographs, for dispatching and offprints, and for creating the J-STAGE registration data are borne by the authors. In the case of papers requested by the editorial board, such costs are exempted.
9. Date of submission is the date when the submitted manuscript arrives at the secretariat of the Japanese Society of Conservative Dentistry. Date of acceptance is the date when the reviewers determine that the submitted manuscript can be published.
10. The listing order is the order of acceptance. A certification of publication will be issued upon request.
11. Manuscripts are to be submitted via the Japanese Society of Conservative Dentistry's website, e-mail, or postal mail. Manuscripts submitted for publication should be addressed to the secretariat of the Japanese Society of Conservative Dentistry.
12. In principle, authors can proofread their manuscript a maximum of two times. Extensive changes, additions, or deletions made to the contents of the manuscript cannot be accepted. Proofs should be returned by the designated date. If the authors do not need to proofread their manuscript, they should mention this on the left side of the cover page.
13. The copyrights for articles published in *ODEP* belong to the Japanese Society of Conservative Dentistry.
14. Matters not mentioned in these guidelines will be independently determined by the editorial board.

Submission of your manuscript for publication must conform to the following "Submission Guidance" as well as "Submission Guidelines."

The publishing charge is 10,000 yen for a Journal page including tables and figures. Extra charges for such as figures and tables preparation, color printing of photographs will also be paid by the authors. If authors do not pay publishing charge, the article may be retracted.

Submission Guidance (applied as of the Issue 1 of Vol. 4)

Manuscript organization

1. In principle, original articles should be organized into the following sections: (1) cover page; (2) abstract; (3) Main text (Introduction, Materials and Methods, Results, Discussion, and Conclusion); (4) References; and (5) Figure and table captions. Page numbering should start with the cover page. In principle, manuscripts, such as reviews or case reports, other than original articles should be organized in the same format as that of original articles.
2. Manuscript sections
 - 1) Title: The title should concisely describe the contents of the manuscript. The subtitle should also clearly describe the contents, and should not consist of only numbers.
 - 2) Introduction: The introduction should clearly describe the background, novelty, purpose, and significance of the study.
 - 3) Materials and Methods: This section should provide detailed information on the materials, equipment, or methods used along with clear instructions so that the experiments can be reproduced by others. Parameter settings, number of specimens, extraction methods, statistics processing, and others should comply with the purpose of the study.
 - 4) Results: This section should simply present the findings without bias or interpretation. Measurement results should show characteristic values including mean values and standard deviations.
 - 5) Discussion: This section should carefully consider the materials and methods, results, and others referring to relevant literature. Please note that it should not be overly assertive and should avoid off-topic points. The discussion should stay focused on the study purpose and not digress into a general discussion.
 - 6) Conclusion: The section should precisely summarize the results obtained and relate them to the purpose of the study and hypothesis as presented in the Introduction.
3. Manuscripts should be prepared using A4-size paper. The suggested length of each typed page is 80 alphanumeric characters per line \times 25 lines per page using a 12-point font. Top/bottom/left/right margins should be approximately 25 mm. Non-Japanese names and places should be in their original names.
4. For the manuscript style, refer to the latest issue of the journal.

Ethics code

1. Each report on the result of clinical research (clinical trial or observational research) or research involving any specimen collected from a human body must include a clear statement that it was approved by the head of the affiliated institution or by the research ethics review board assigned by the institution's head, in order to expressly indicate that the research was conducted in compliance with all applicable guidelines and laws, including the Declaration of Helsinki and the medical research guidelines, etc. issued by the Ministry of Health, Labour and Welfare including the following:
 - 1) Ethical Guidelines for Life Science and Medical Research Involving Human Subjects;
 - 2) Guidelines for Gene Therapy and Other Clinical Research; and
 - 3) Clinical Trials Act.
2. Each report on the result of research on, or a case concerning, regenerative medicine technology, etc. as defined

in the Act on the Safety of Regenerative Medicine must include a clear statement that the technology was provided to the patients in compliance with the aforementioned Act.

3. Each report on a case of a therapeutic method involving any off-label drug or device, or any pharmaceutical, medical device, regenerative medicine, or other related product not domestically approved must include a clear statement that the use was approved by the committee concerned (research ethics review board, review board for unapproved new drugs, etc.) at the affiliated institution or that the case report was approved for publication by *ODEP's* Clinical and Epidemiological Ethics Committee.
4. In each instance of publication of an academic paper, all personal information must be thoroughly protected so that none of the research subjects (patients) can be identified from it.
5. In each instance where a patient's clinical photo or X-ray image is included in an academic paper for publication, a clear statement must be provided that the consent of each such patient (or a parent, guardian, or proxy if the patient is a minor or in case it is otherwise difficult to obtain consent from the patient) was duly obtained.
6. Each report on the result of research involving animal subjects must include a clear statement that the research was approved by the animal experiment committee, etc. at the affiliated institution.

Cover page

1. The title, authors' names, institutional affiliations, and corresponding author's contact address should be centered, with a new line for each item, on the cover page.
2. The title should be in upper and lowercase letters, where the first letter of each word is uppercased and the remaining letters are lowercased. Articles, prepositions, conjunctions, and commonly used technical terms are lowercased. For hyphenated compound words, the letters following the hyphen should be lowercased.
3. The corresponding author's contact details should include the following information: one author's name, institutional affiliation, postal address, telephone and fax numbers, and e-mail address.

Abstract

1. The abstract should be a maximum of 400 words organized into four sections with the following headings: Purpose, Methods, Results, and Conclusion. Approximately three keywords should be placed at the end of the abstract.
2. Contributors should put considerable effort into preparing the abstract as it may determine whether or not the reader continues with the manuscript. When necessary, abstracts should be checked by a native English reviewer (preferably with expertise in dental medicine).

Main text

1. Introduction, Materials and Methods, Results, Discussion, and Conclusion are the main headings and are not numbered.
2. Subparagraphs should be numbered in the following order: 1. 2. 3. ...; 1) 2) 3) ...; (1) (2) (3) ...; ① ② ③ ...; and a. b. c. ...
3. English characters should be written in the following manner:
 - 1) Generally, only the last name should be used to indicate a person.
 - 2) When the name of a product or manufacturer must be in the original language, the first letter of each word should be uppercased and the remaining letters lowercased.
In principle, "generic name (product name, company name, city [state in the case of U.S.], country)" should be used in English manuscripts. Trademark and registration symbols ® and ™ are not required.
 - 3) Regarding common nouns in German or Latin, the first letter should be uppercased and the remaining letters lowercased. For common nouns in English and French, all letters should be lowercased.
 - 4) Regarding binominal nomenclature, the first letter of the genus should be uppercased and the remaining letters lowercased. The names of all genera and species should be italicized. When the same genus

appears frequently, it is acceptable to replace the name with the initial after the first use.

Example: *Streptococcus mutans* → *S. mutans*

- 5) For nouns that must be in their original language, other than German, Latin, English or French, all letters should be lowercased, except for commonly used technical terms.
4. In principle, SI units are used for measurements.
5. Any conflicts of interests (COI) must be declared after the conclusions. When there is no COI, the statement “The authors declare no conflict of interest related to this paper” should be included.
6. Acknowledgments for all sources supporting this study including grant funds should be added after of COI.

References

1. References must be listed at the end of the main text, and numbered in the same order as they appear in the text.
 2. In the main text, a cited reference should appear with a superscript numeral and closing parenthesis. When two references are cited, a comma should be used to separate them; more than two references should be connected by an en dash between the first and last numeral.
Examples: “by authors³⁾”, “...is reported^{7,8)}”, “previous studies¹⁰⁻¹⁵⁾show”
 3. Examples of Reference
 - a. Journal articles
 - Number) Last name and first name of all authors with a comma separating each author. Title of paper. Name of journal and publishing year in the Christian era; Volume number: Inclusive page numbers of paper.
Example:
1) Clark AB, Erickson D, Hamilton FG. Tensile bond strength and modulus of elasticity of several composite resins. J Dent Res 1992; 37: 618-621.
 - b. Book
 - Number) Author (co-authors). Title of book. First/last volume. Edition. Publisher’s name: Publisher’s location (City); Publishing year in the Christian era. Cited pages.
Example:
2) Phillips RW. Skinner’s science of dental materials. 9th ed. WB Saunders: Philadelphia; 1991. 219-221.
 - c. Book with co-authors
 - Number) Contributor’s name. Title of contributed article. Name of editor (editor-in-chief). Book title. First/last volume. Edition. Publisher’s name: Publisher’s location (City); Publishing year in the Christian era. Cited pages.
Example:
3) Torneck CD. Dentin-pulp complex. Ten Cate AR. Oral histology. 5th ed. Mosby: St. Louis; 1998. 150-196.
For cases in which each author’s contribution is not separately indicated, the author’s name and the title of the contributed article should not be listed.
Number) Name of editor (editor-in-chief). Title of book. First/last volume. Edition. Publisher’s name: Publisher’s location (City); Publishing year in the Christian era. Cited pages.
 - d. Other writing styles
 - Abstracts of scientific meeting
 - Number) Presenter (all presenters should be cited. A comma should be used to separate the authors in the case of co-presentations.). Title of abstract. Name of journal and publishing year in the Christian era; Volume number: Inclusive page numbers, abstract number.
Example:
4) Marais JT. Cleaning efficacy of a new root canal irrigation material. J Dent Res 1998; 77: 669, Abst. No. 300.
 - Journal articles in press
- In principle, the same style as that of a regular journal article should be used; however, when the inclusive page

numbers are not known, they can be omitted. The statement “in press” should be shown at the end.

Example:

5) Sato K. Effect of toothbrushes on gingival abrasion. J Periodont Res 1994; 29: in press.

- Electronic journal

In principle, the same style as that of a regular journal article should be used; however, when the inclusive page numbers are not known, the DOI and other indicators should be shown. When papers are published in electronic journals before printing, the statement [Epub ahead of print] should be shown after the publishing year and month.

Example:

6) Sunada N, Ishii R, Shiratsuchi K, Shimizu Y, Tsubota K, Kurokawa H, Miyazaki M. Ultrasonic measurement of the effects of adhesive application and power density on the polymerization behavior of core build-up resins. Acta Odontol Scand; doi: 10.3109/00016357.2011.654252

- Internet website

Page publisher. Title of page. URL address. (Access date)

Example:

7) World Health Organization. Continuous improvement of oral health in the 21st century. http://www.who.int/oral_health/en/ (cited 2005. 10. 1)

4. In principle, journal names should be abbreviated in accordance with the format used by the journal.

Figures and tables

1. Figures, photographs, and tables are categorized into figures and tables, and then numbered. Paper size should be A4, and each figure and table should be printed on a separate page. The numbers allocated for the figures and tables should be consistent with those referred to in the text.
2. Figures and tables should be accompanied by explanations that are easily understandable. Explanations of figures/tables are presented as captions and explanations for tables/tables should be presented as footnotes.
3. If authors wish to have the figures shown in color, color data should be attached; if authors wish to have the figures shown in black and white, black-and-white data should be attached.

Notes on creating imaging data:

- The jpg data format should be used if possible.
 - Image size should correspond to the layout; image resolution should be at least 300 dpi for photographs and at least 1,200 dpi for line drawings.
4. If authors wish to reprint a figure from another publication, should be responsible for confirming whether permission is required from that publication, and obtaining permission if necessary. In addition, the source should be clearly stated in the explanatory text of each figure.

Sending manuscript intended for publication

1. The manuscript (cover page, abstract, main text, references, and figure and table captions are created as one file) should be formatted as a Microsoft Office Word (hereafter “Word”) document.
2. Figures should be provided in jpg or pdf format.
3. Tables should be provided in Microsoft Office Excel, jpg, pdf, or Word format.
4. File titles should be as follows: “author name”_“university name (name after department is not needed)”_“manuscript/figure/table/submission form”_“.filename extension (indicating file type)”.

Example) Nihon Tarou_Nihon University/manuscript.docx; Nihon Taro_Nihon University_Figure.jpg; Nihon Taro_Nihon Univesity_Table.xlsx; Nihon Taro_Nihon University_submission form.pdf

Also, pdf files with embedded fonts for all contents are acceptable for submission. In such cases, file names should be as follows: Nihon Taro_Nihon University_comprehensive manuscript.pdf

5. E-mail title (subject) should be “Submitted papers for ODEP”.

6. Submitted papers should be sent to the e-mail address of Oral Health Association of Japan: hensyu6@kokuhoken.or.jp. For safety, also send as a CC to hensyu5@kokuhoken.or.jp.
7. When e-mail submission is difficult for such reasons as the file size is too large, submission via an FTP server and other methods are acceptable. In such cases, the intent of submission should be informed by e-mail. In the e-mail, information regarding the site and other methods for downloading the file should be provided.
8. The submission form of *ODEP* provided on the Japanese Society of Conservative Dentistry's home page (<http://www.kokuhoken.or.jp/exterior/jscd/fileform/>) can be used for submission.

Reprographic Reproduction

The Japanese Society of Conservative Dentistry authorized Japan Academic Association For Copyright Clearance (JAC) to license our reproduction rights of copyrighted works. If you wish to obtain permissions of these rights, please refer to the homepage of JAC (<http://www.jaacc.org/en/>) and confirm appropriate organizations to request permission.

Thinking ahead. Focused on life.



Spaceline EX

スペースライン EXが iFデザイン賞の金賞を受賞

ドイツのiFデザイン賞は、50年以上の歴史を有し、各国から選ばれた審査員によって厳正に選考される世界的に権威のあるデザイン賞です。世界中から6,400以上のエントリーがあった中、最優秀デザインとして75件に授与される金賞（iF GOLD AWARD）をスペースライン EXが受賞しました。人間工学に基づき緻密に計算されたデザインは、患者さんだけでなく術者にも理想的で洗練されたデザインであると評価されました。



発売

株式会社 **モリタ**

大阪本社 大阪府吹田市垂水町3-33-18
〒564-8650 T 06. 6380 2525

東京本社 東京都台東区上野2-11-15
〒110-8513 T 03. 3834 6161

お問合せ お客様相談センター 歯科医療従事者様専用
T 0800. 222 8020 (フリーコール)

製造販売・製造

株式会社 **モリタ製作所**

本社工場 京都府京都市伏見区東浜南町680
〒612-8533 TEL 075-611-2141

久御山工場 京都府久世郡久御山町市田新珠城190
〒613-0022 TEL 0774-43-7594

販売名: スペースライン
一般的名称: 歯科用ユニット
機器の分類: 管理医療機器(クラスII)
特定保守管理医療機器
医療機器認証番号: 228ACBZX00018000

www.dental-plaza.com

シェードのない世界へようこそ

オムニクロマ

歯科充填用コンポジットレジン

保険適用

OmniCHROMA

オムニクロマ

形態付与したい症例にはペーストタイプ

OmniCHROMA Flow

オムニクロマフロー

汎用性の高いフロー性で、
前歯から臼歯までの幅広い症例に使用可能

OmniCHROMA Flow BULK

オムニクロマフローバルク

バルクタイプだから深い窩洞にも一括充填が可能
(硬化深さ3.5mm以上)



バルクタイプが
新登場!

1本でVITA16色に同化!

構造色を応用した オムニクロマシリーズの色調適合範囲

B1 A1 B2 D2 A2 C1 C2 D3 A3 D4 B3 A3.5 B4 C3 A4 C4

色付けはイメージ

オムニクロマ
特設ページはこちら



<https://www.tokuyama-dental.co.jp/omnichroma/>

オムニクロマ

標準医院価格¥4,000/1本4g(2.2mL) (管理医療機器) 認証番号: 230AFBZX00049000

オムニクロマフロー

標準医院価格¥4,900/1本3g(1.8mL) (管理医療機器) 認証番号: 302AFBZX00087000

オムニクロマフローバルク

標準医院価格¥4,900/1本3g(1.8mL) (管理医療機器) 認証番号: 305AFBZX00058000

株式会社トクヤマデンタル

お問い合わせ・資料請求
インフォメーションサービス

☎0120-54-1182

受付時間

9:00~12:00/13:00~17:00(土日祝日は除く)

Webにもいろいろ情報載っています!!

トクヤマデンタル

検索

Concept



急な引き込まれを大幅軽減



本来の根管から逸脱しづらい
刃部構造と柔軟性



I・II・IIIの3本で終了
簡単な手順、使用方法を採用



ホームページより
動画をご覧ください

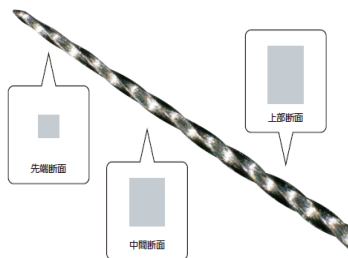


D ファインダー



- 過剰な切削・食い込みを軽減できる。
- 刃部強度を高め、穿通力を UP。
- 石灰化、狭窄した根管にも折れにくく有効。

グライドファインダー



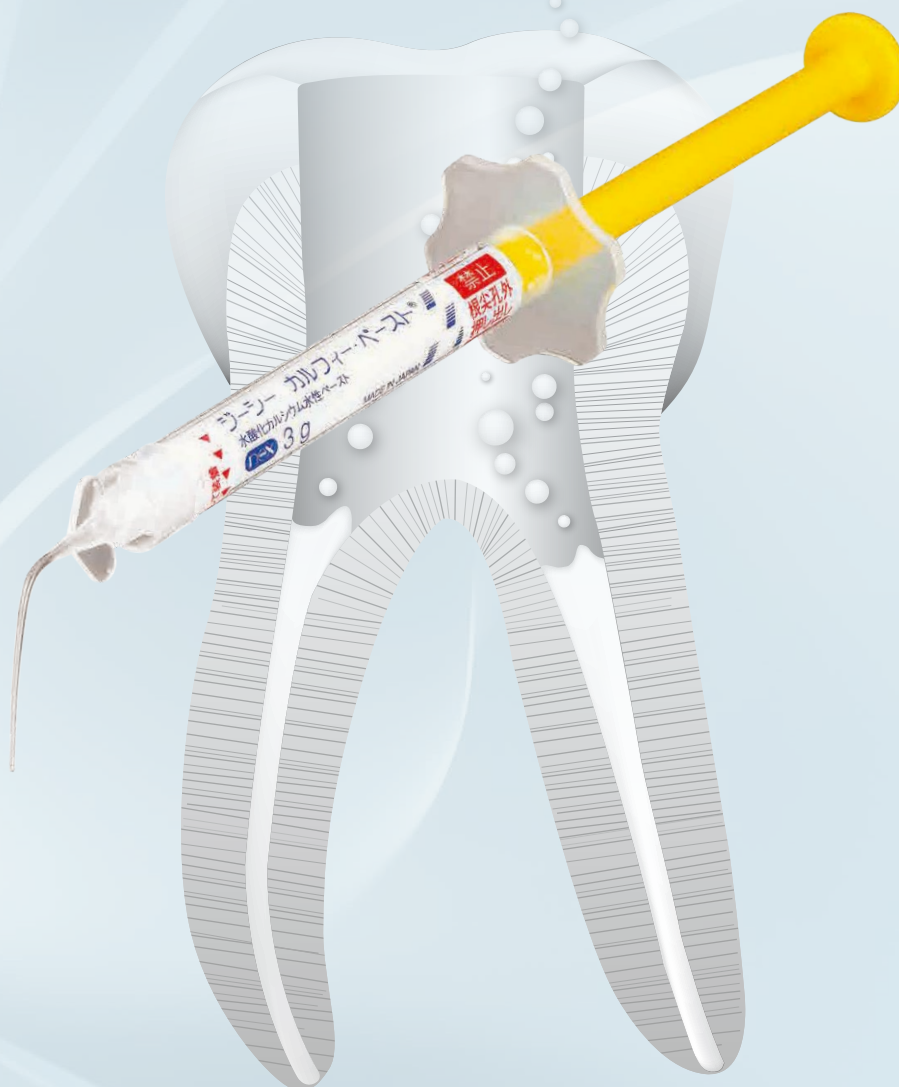
穿通性 + 切削性

- 先端部テーパを強化し力が伝わりやすい。
- 断面形状の変化による優れた切削性と柔軟性。
- 穿通のみならずグライドパス形成も可能。

医療機器届出番号 09B1X00006011050 一般医療機器 一般的名称：歯科用ファイル 販売名 マニー®D ファインダー
医療機器届出番号 09B1X00006011010 一般医療機器 一般的名称：歯科用ファイル 販売名 マニー®K ファイル



除去性に優れた 根管貼薬材



水酸化カルシウム濃度

36%

Tooth Pad.

製品動画はコチラ



× ジーシー 昭和薬品

水酸化カルシウム水性ペースト

NEW

カルフィー・ペースト

水酸化カルシウム系歯科根管充填材料 ジーシー カルフィー・ペースト
高度管理医療機器 21500BZZ00134000

発売元 株式会社 ジーシー / 製造販売元 株式会社 ジーシー 昭和薬品
東京都文京区本郷3丁目2番14号 東京都板橋区連沼町76番1号

※掲載情報は2023年6月現在のものです。 ※色調は印刷のため現品と若干異なることがあります。